UNIVERSIDAD DE SANTIAGO DE COMPOSTELA
DEPARTAMENTO DE BIOLOGÍA CELULAR Y ECOLOGÍA
ÁREA DE BIOLOGÍA CELULAR

"DESARROLLO DE LOS SISTEMAS GABAÉRGICO Y AMINÉRGICOS EN EL SISTEMA NERVIOSO CENTRAL DE PECES CARTILAGINOSOS"

MEMORIA

Que para optar al Grado de Doctor en Biología presenta

IVÁN M. CARRERA DE FIGUEIREDO

Santiago de Compostela, 2008

ISABEL RODRÍGUEZ-MOLDES REY, PROFESORA TITULAR DEL ÁREA DE BIOLOGÍA CELULAR DEL DEPARTAMENTO DE BIOLOGÍA CELULAR Y ECOLOGÍA DE LA UNIVERSIDAD DE SANTIAGO DE COMPOSTELA,

CERTIFICA,

Que la presente memoria titulada "Desarrollo de los sistemas gabaérgico y aminérgicos del sistema nervioso central de peces cartilaginosos", que para optar al Grado de Doctor en Biología presenta Don IVÁN M. CARRERA DE FIGUEIREDO, ha sido realizada bajo mi dirección. Y considerando que constituye trabajo de tesis, autorizo su presentación al Consejo de Departamento correspondiente.

Y para que así conste, expido el presente certificado en Santiago de Compostela, a 5 de Mayo de 2008.

El Doctorando — La Directora de la Tesis

Fdo.: Iván M. Carrera de Figueiredo — Fdo.: Isabel Rodríguez-Moldes Rey

Esta Tesis Doctoral forma parte de los siguientes Proyectos de Investigación:

1. – “Estúdio de la morfogénesis y regionalización del sistema nervioso central de peces elasmobranquios” Financiado por el Ministerio de Educación y Ciencia (BFU2004-03313).

2. – “Estudio da morfoxénese e rexionalización do sistema nervioso central en elasmobranquios” Incentivo Plan Nacional de la Xunta de Galicia (2005/PX009).

3. –“Formación del patrón del encéfalo en condrictios (peces cartilaginosos)” Financiado por el Ministerio de Educación y Ciencia (BFU2007-61154).

Parte de la realización de esta Tésis Doctoral ha sido posible gracias a la concesión de dos contratos asociado a los Proyectos de Investigación (BFU2004-03313) y (BFU2007-61154) durante los periodos 14/11/07-14/12/07 y 14/12/07-13/12/08.

Cinco años, dos canas y millones de horas delante de un ordenador que no siempre me entendía, es el saldo neto de esta tesis. Cabe ahora, mirar atrás y disfrutar del trabajo realizado y de los objetivos alcanzados, pero no sin antes destacar la aportación en distinta medida de aquellos que me ayudaron a concluir con éxito esta empresa.

Mi mayor y más sincero agradecimiento es para mi directora de tesis, Isabel Rodríguez-Moldes Rey, por haber creído en mí, por haberme acogido en su grupo de investigación, por guiarme en el universo de la Ciencia, y por ser esa gran persona a nivel humano y profesional que siempre estuvo ahí para apoyarme y darme ánimos en todo momento.

Gracias,

A ti Ramón Anadón, que siempre estuviste a un paso de distancia para solucionar, aconsejar y aportar esa otra visión tan necesaria.

A ti Pilar Molist, por "enseñarme los primeros pasos" en este largo camino.

También quiero dar las gracias a todas aquellas personas que han contribuido de alguna manera a la consecución de esta tesis doctoral.

En primer lugar a mis compañeros de laboratorio, con los que he compartido tantos buenos y malos momentos… y en especial a aquellos que a lo largo de los años se ganaron mi amistad incondicional:

A Verona, por ser la compañera y amiga que cualquiera desearía a su lado. Gracias por los innumerables buenos momentos que hemos compartido durante este viaje. Sé que siempre estarás ahí como hasta ahora.

A Antón, porque las juergas santiaguesas más divertidas las viví a tu lado. Todavía intento aprender de ti cómo compaginar la fiesta y el trabajo a esos niveles! A Pedro, ese gran amigo al que estoy irremediablemente unido por la buena comida y grandes juergas. A Sergio, por aportarme esa visión "freaky" del mundo, y animarme siempre con una buena carcajada. A Miguel Ángel, ese coruñés de monte alto que rompe todas las pistas de baile. Qué gran corazón tienes! A Chus, desde que te fuiste, esta ciudad es más tranquila aunque echo de menos tu compañía y esas pachangas a media mañana. A Fátima, por ese humor agrio pero tan adictivo. A Pablo, ese maestro del "éxito" que tan buenos momentos nos aportaba a todos. A Idoia y a Sol, por compartir mis últimos retoques "tesescos".

A mi familia, que siempre me apoyó y me dio más de lo que yo esperaba. Sois los pilares de mi persona.

Además, a todos los que compartieron conmigo esos momentos inolvidables durante todo este tiempo, Rui, Gerardo, Yago, Paula, Alberto, Pacho, Lula…

Y principalmente, a Mila (mi milonguita!), a la que Quiero, Amo y Adoro. Gracias por aguantar las interminables horas de mi tesis siempre con una sonrisa. Eres mi estrella y contigo estaré toda mi vida.

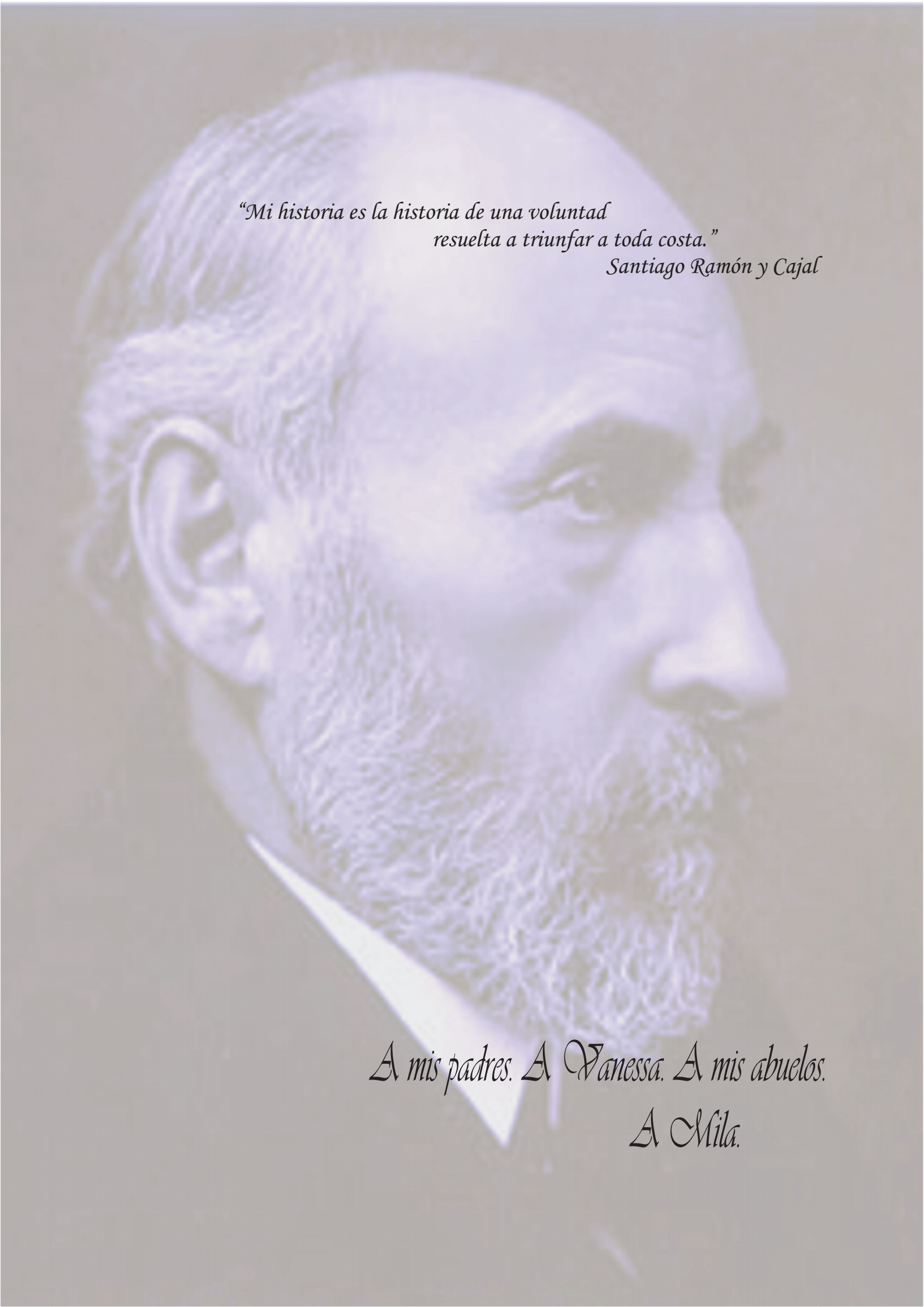

"Mi historia es la historia de una voluntad
resuelta a triunfar a toda costa."
Santiago Ramón y Cajal

A mis padres. A Vanessa. A mis abuelos.
A Mila.

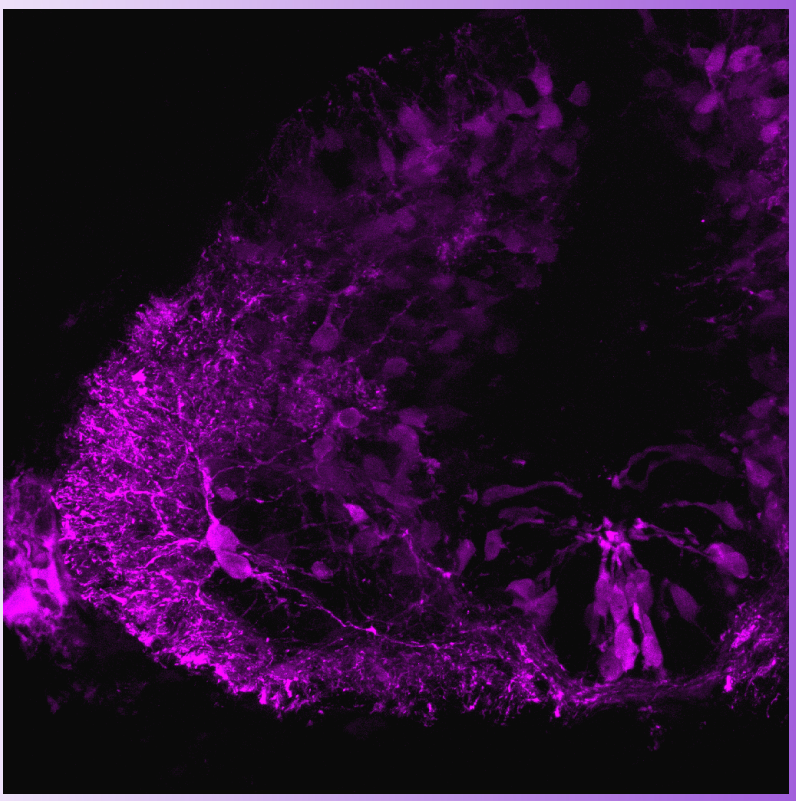

ÍNDICE

INTRODUCCIÓN

INTRODUCCIÓN

INTRODUCCIÓN

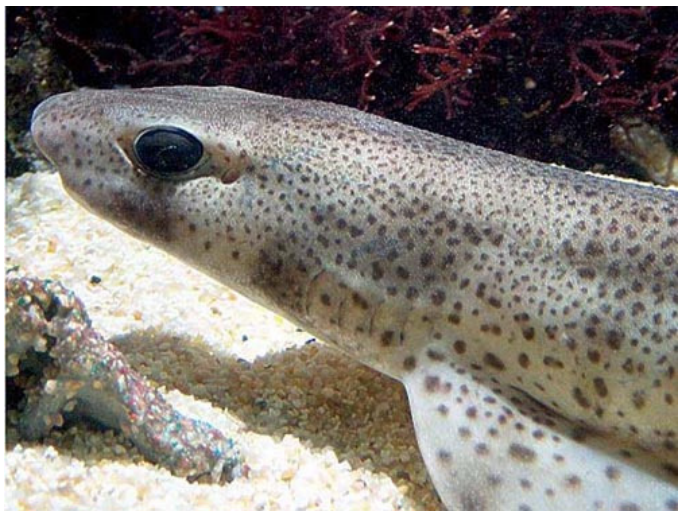

Los vertebrados evolucionaron en el agua a partir de antecesores cordados acuáticos. Todos los vertebrados originalmente acuáticos se reúnen bajo la denominación convencional de peces. Los peces son vertebrados poiquilotermos acuáticos, con agallas, se desplazan por medio de aletas y respiran oxígeno disuelto en el agua gracias a las branquias (sólo existe una clase de peces pulmonados). Constituyen casi la mitad del número total de vertebrados y se trata de un grupo muy heterogéneo. Los gnatóstomos o peces mandibulados se pueden englobar en dos líneas filogenéticas principales: los condrictios o peces cartilaginosos, y los actinopterigios o peces óseos. Los condrictios comprenden dos grupos actuales, los elasmobranquios (tiburones y rayas) y los holocéfalos (quimeras).

Como objeto de estudio hemos elegido una especie de elasmobranquio, la pintarroja o melgacho (*Scyliorhinus canicula*) por ser una especie muy accesible, ya que se encuentra a lo largo de toda la costa de Europa y es una de las pocas especies de elasmobranquios de la que se puede obtener cualquier estadio de desarrollo en cualquier época del año. Además, nuestro grupo de investigación lleva varios años estudiando

distintos aspectos de la anatomía del sistema nervioso de esta especie, siendo considerada un modelo representativo del grupo de elasmobranquios.

Nuestro interés se centra en el sistema nervioso de los condrictios porque a pesar de la importancia que tiene este grupo desde el punto de vista de la evolución de los gnatóstomos, se le ha prestado muy poca atención en comparación con los peces óseos. Tradicionalmente se ha considerado a los teleósteos, representantes de los peces óseos modernos y de todo el grupo de peces gnatóstomos. El presente estudio creemos que contribuye a demostrar que los condrictios presentan características neuroanatómicas específicas y que el análisis de las diferencias (y también de las similitudes) entre los peces óseos y cartilaginosos contribuye al conocimiento de la evolución de los vertebrados.

En este trabajo, estudiamos la distribución de una serie de neurotransmisores en el sistema nervioso central de la pintarroja durante el desarrollo. En general, los estudios comparativos acerca del sistema nervioso central entre vertebrados son objeto de enorme interés por posibles implicaciones en diversas afecciones neurodegenerativas, vasculares o tras algún tipo de trauma.

1. CARACTERÍSTICAS BIOLÓGICAS DE LA PINTARROJA

La pintarroja es un pleurotremado perteneciente a la Familia Scyliorhinidae (Fig. 1) que tiene un cuerpo largo y esbelto, y una cola relativamente corta. Tiene una cabeza ligeramente aplanada y unos grandes apéndices nasales que se proyectan hacia atrás, hasta el vértice de la boca. No presenta surcos labiales a los lados de la boca ni barbillones en las narinas, el cual es un carácter diagnóstico. Su color es gris rojizo de base con numerosas manchas pardas irregularmente distribuidas por el dorso, mientras que su vientre es blanquecino. Su talla máxima no suele sobrepasar los 70 cm de longitud. Vive en aguas templadas cerca de arrecifes rocosos, bahías arenosas y en plataformas continentales a unos 100 metros de la costa. Su alimentación consiste principalmente en invertebrados de fondo (moluscos y crustáceos) y pequeños peces. Cuando llega el momento del apareamiento se dirige a aguas más profundas. Las hembras, una vez fecundadas, regresan a aguas someras para poner sus huevos

formados por una cubierta córnea y provista de zarcillos que los enganchan a los arrecifes rocosos o a las masas de algas. El desarrollo embrionario es ovíparo, y el embrión sale de la cápsula después de un periodo que dura entre 5 y 12 meses, dependiendo de la temperatura media del agua exterior.

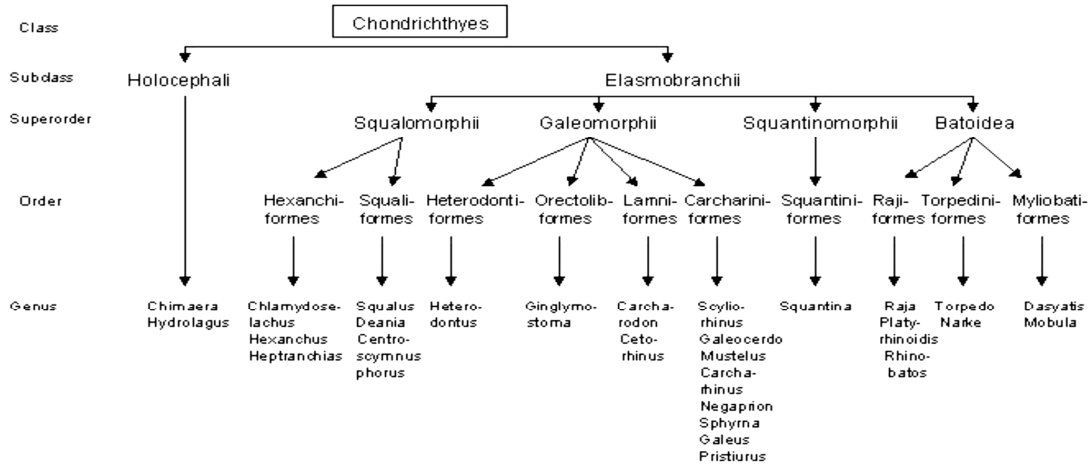

Figura 1. Clasificación de los peces cartilaginosos. Tomado de Compagno, 1977.

Las etapas de desarrollo embrionario de la pintarroja han sido caracterizadas por Ballard y colaboradores en 1993. Según estos autores, antes de la eclosión existen 34 estadios de desarrollo, durante los cuales el embrión sufre numerosos cambios cruciales para su estadificación, tales como el número de hendiduras branquiales abiertas, el tamaño de los filamentos branquiales, la densidad de pigmentación en retina, el número de somitas, la longitud total del embrión, la morfología del arco mandibular y el tamaño del saco vitelino. Para facilitar su comprensión, desglosaremos las características principales de los estadios clave en el desarrollo embrionario de la pintarroja. Hemos agrupado los distintos estadios embrionarios en tres principales etapas que buscan facilitar la posible equivalencia de estos estadios con las etapas de desarrollo conocidas y estudiadas en otros vertebrados acuáticos:

- *Etapa de desarrollo temprano*.

En la pintarroja, esta etapa engloba desde la fecundación hasta el estadio 25, caracterizado por la formación de 80 pares de somitas, la apertura de todas las hendiduras excepto los espiráculos, el alargamiento mandibular superior y la apreciación de filamentos primordiales. De esta etapa resulta la formación de las principales estructuras del embrión, siendo el estadio 25, que cierra esta etapa, comparable con el estadio 23 (1 día y 17 hrs) en medaka y 29 hpf en zebrafish.

- *Etapa de desarrollo intermedio*.

Esta etapa comprende desde el estadio 26 al 31. El embrión de pintarroja en el estadio 26 se caracteriza por la apertura de todas las hendiduras branquiales y los espiráculos, siendo correspondiente al estado filotípico de faríngula. El último estadio de esta etapa se destaca por la prominencia del rostro, el inicio de la regresión de los filamentos branquiales y de la pigmentación epidérmica. En esta etapa se alcanza la formación y organización definitiva del embrión así como una gran complejidad estructural. Este estadio 31 puede ser comparado con el estadio 35 (5 días y 12 hrs) en medaka y 48 hpf en zebrafish.

- *Etapa de desarrollo tardío*.

Esta última etapa abarca desde el estadio 32 al 34 (*prehatching*), caracterizado por la completa absorción del vitelo y pigmentación epidérmica, finalizando con la maduración del embrión y su posterior eclosión. El estadio 34 puede ser comparado con el estadio 39 (9 días) en medaka y más de 5 dpf en zebrafish.

Una vez fuera del huevo ó cápsula, el juvenil está plenamente capacitado para la exploración e interacción con su hábitat. El periodo de tiempo que transcurre desde que el juvenil (*posthatching*) abandona el huevo hasta que madura sexualmente, puede ser de un año, durante el cual se limita a incrementar su tamaño y masa corporal a fin de alcanzar los 60-70 cm de un ejemplar adulto. A continuación expondremos gráficamente los principales estadios de desarrollo embrionario que hemos estudiado, basándonos en la descripción de Ballard y colaboradores (1993);

Estadio 23 (S23)
- Se abren las hendiduras C1-C3
- Los arcos mandibulares se abren
- Aparecen las placodas óticas

Estadio 25 (S25)
- Se abren las hendiduras C1-C5
- Los arcos mandibulares se alargan
- Primordios de filamentos en C2-5

Estadio 26 (S26)
- Abiertas todas hendiduras C1-C6
- Filamentos branquiales en C2-C5
- Plexo capilar en mitad del vitelo

Estadio 28 (S28)
- Inicio pigmentación ocular
- Mandibulas en forma oval o elipse
- Se forma gl. Eclosión

Estadio 29 (S29)
- Circulo pigmentación ocular incompleto
- Mandibulas en forma de arco

Estadio 30 (S30)
- Circulo pigmentación ocular
- Filamentos de 4-5 cm
- 9-13 escamas en fila dorsal

Estadio 31 (S31)
- Rotación de 90º del rostro
- Entrada de agua en cápsula
- Filamentos alcanzan máx. longitud

Estadio 33 (S33)
- Disminución volumen saco vitelino
- Pigmento en toda epidermis

Estadio 34 (S34)
- Saco vitelino forma un botón
- Embrión ocupa totalmente el interior de la cápsula

2. EL SISTEMA NERVIOSO DE PECES CARTILAGINOSOS

Morfogénesis y organización del sistema nervioso

El primer estudio sobre el desarrollo del sistema nervioso central de elasmobranquios fue inicialmente realizado por Balfour (1878), aunque ha sido von Kupffer (1900) quien aportó una importante primera contribución al conocimiento de la morfogénesis de su sistema nervioso central. Posteriormente, estudios puntuales de ciertas regiones del encéfalo (telencéfalo: Holmgren 1922, *Squalus*; diencéfalo: Farner 1978a, *Scyliorhinus*; mesencéfalo: Farner 1978 b,c, *Scyliorhinus*) han supuesto pequeños avances en el conocimiento del desarrollo de este complejo sistema.

En la pintarroja, el desarrollo del sistema nervioso central sigue el patrón general de todos los vertebrados (Farner, 1978a-c; Ballard et al., 1993). En las primeras etapas del desarrollo embrionario, el vitelo es digerido y absorbido por las células del sincitio vitelino y es distribuido al embrión a través del sistema sanguíneo que rodea el vitelo. Las primeras células forman un disco embrionario (desarrollo meroblástico) que se invagina por su borde posterior formando un intestino primitivo. Por encima de este intestino primitivo, el ectodermo neural forma una placa que se pliega y se cierra, dando lugar al tubo neural (estadio 13; S13). Este tubo neural inmaduro, que contiene en su interior una cavidad (ventrículo) llena de líquido (líquido cefalorraquídeo), está formado por un par de placas interconectadas dorsalmente por la placa del techo, y ventralmente por la denominada placa del suelo (von Kupffer, 1900). Posteriormente, el disco embrionario recubre epibólicamente el vitelo en un proceso parcial de gastrulación, y se eleva por encima del vitelo (S16). A medida que el proceso de gastrulación avanza, el mesodermo desarrolla numerosos vasos sanguíneos que intercambiarán nutrientes y gases entre el saco vitelino y el embrión en desarrollo hasta la total absorción del vitelo. A partir de S23 el embrión en desarrollo se separa del saco vitelino, permaneciendo unido únicamente por un delgado pedúnculo, y se inicia una fase activa de morfogénesis y organogénesis que dará lugar al desarrollo de las estructuras morfológicas y estructurales del embrión, (Ballard et al., 1993).

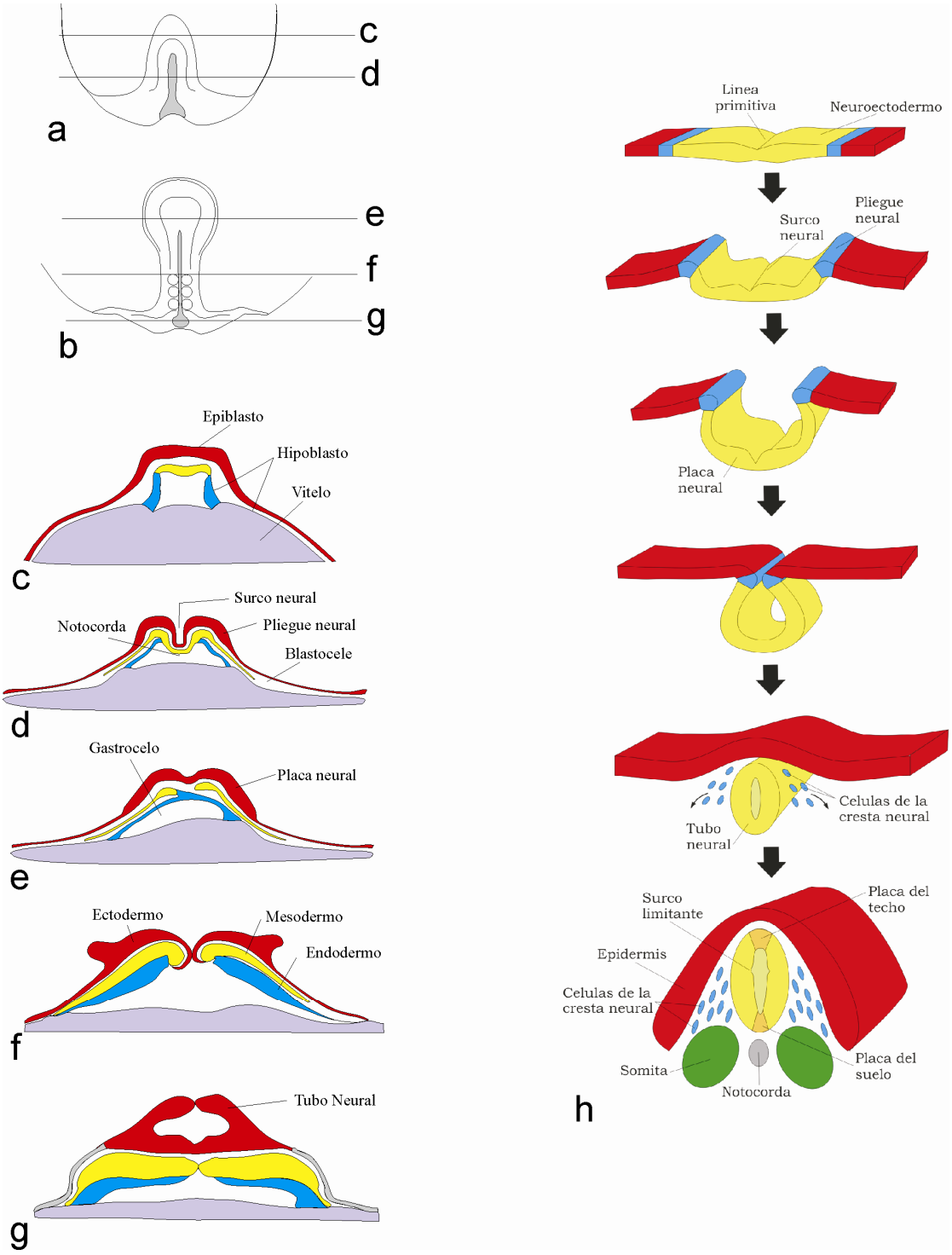

Figura 2. Formación del tubo neural. Representación esquemática de la formación del tubo neural y sus divisiones en elasmobranquios (*Scyliorhinus canicula*; a-g) y en tetrápodos (aves; h), modificado de Coolen y col. (2007); Gilbert, (2003); y Witschi, (1956).

Antes que se cierre la placa neural para formar el tubo, de sus bordes (cresta neural) se desprenden células que se distribuyen ampliamente por el cuerpo o permanecen próximas a la médula espinal como ganglios en disposición segmentaria. A continuación, en el tubo neural se distinguen dos partes; la porción encefálica (parte superior más voluminosa y de la que derivará el encéfalo) y la porción medular (parte más estrecha y larga, situada en el tronco del embrión y de la que derivará la médula espinal). La porción encefálica crece notablemente y de forma desigual dando lugar a tres dilataciones primarias denominadas vesículas encefálicas: el prosencéfalo, mesencéfalo y rombencéfalo. Los límites que separan estas tres vesículas primarias no están únicamente formados por constricciones, sino también por incipientes paquetes de fibras orientadas transversalmente, denominadas comisuras. Inmediatamente después, las tres vesículas primarias se subdividen en cinco principales vesículas: el prosencéfalo origina el telencéfalo y el diencéfalo, el mesencéfalo permanece como una única vesícula, mientras que el rombencéfalo se divide en metencéfalo y mielencéfalo.

A continuación tiene lugar la metamerización y la formación de los somitas (S17), iniciándose una serie de procesos morfogénicos tales como la flexión dorsal del tronco (S18), la flexión encefálica (curvatura del vértice, S19), el desarrollo de los primeros pares de bolsas faríngeas (S20), las placodas óticas, ópticas y olfativas (S21) y la apertura del primer par de hendiduras faríngeas (S22) que originarán los futuros espiráculos (Ballard y col., 1993).

En las fases tempranas del desarrollo del sistema nervioso central de peces cartilaginosos se distinguen tres vesículas prosencéfalo, mesencéfalo y rombencéfalo. Posteriormente, el prosencéfalo se diferencia en telencéfalo y diencéfalo, el mesencéfalo permanece igual y el rombencéfalo se subdivide en metencéfalo y mielencéfalo. A medida que el desarrollo avanza, las distintas partes del encéfalo se subdividen a su vez en distintas regiones:

- En el *telencéfalo* de pintarroja (o región alar del prosencéfalo secundario), se distinguen inicialmente (estadio 22-23) el palio (telencéfalo dorsal) y el subpalio (telencéfalo ventral), mientras que los bulbos olfatorios, las divisiones paliales (dorsal, medial y lateral) y subpaliales (septo, área superficial basal, área central

superficial y área periventricular ventrolateral) se distinguen en fases avanzadas del desarrollo embrionario (estadios 28-30).

- El *diencéfalo* de pintarroja se divide de forma clásica en epitálamo, tálamo dorsal/ventral e hipotálamo, aunque en la actualidad la visión neuromérica subdivide el diencéfalo en tres prosómeros: p1 (pretectum), p2 (tálamo dorsal y epitálamo) y p3 (tálamo ventral) y dos zonas sin división prosomérica (o región basal del prosencéfalo secundario) que serían el hipotálamo (área supraquiasmática, órgano paraventricular y órgano del receso posterior) y el área preóptica.
- El *mesencéfalo* se compone del tegmento mesencefálico y del techo óptico.
- El *rombencéfalo* está formado por el cerebelo y por un tegmento rombencefálico que se inicia rostralmente en el ístmo (límite entre mesencéfalo y rombencéfalo) y acaba caudalmente en el óbex (límite con la médula espinal). Siguiendo una división neuromérica, teniendo en cuenta los diferentes surcos, núcleos, salidas y entradas de nervios craneales, se pueden apreciar en el rombencéfalo entre 7 y 8 subdivisiones, los rombómeros.
- La *médula espinal* se puede a su vez subdividir a lo largo de su eje longitudinal en una región rostral, intermedia y caudal, teniendo en cuenta la densidad celular, y complejidad estructural. Dentro de cada región se distinguen dos zonas, una zona dorsal sensitiva y otra ventral motora.

La luz interna del tubo neural va adquiriendo diversas formas (sistema ventricular) a medida que se van formando las distintas vesículas del sistema nervioso central. Este sistema ventricular (que aloja el líquido cefalorraquídeo) está formado por cuatro ventrículos encefálicos (dos ventrículos telencefálicos, un ventrículo diencefálico o III ventrículo y un IV ventrículo presente en la cavidad rombencefálica) y un ventrículo cilíndrico que recorre toda la médula espinal que se denomina canal central. Las paredes de dichos ventrículos se desarrollan de forma desigual, y en la mayoría de las vesículas dan lugar a la formación de un surco longitudinal (el surco limitante de His), que permite diferenciar una placa basal (ventral) y una placa alar (dorsal). Las neuronas que se originan en las vecindades del surco limitante tendrán

una función visceral, mientras que aquellas que lo hacen de la región dorsal de la placa alar (aferente) y de la región ventral de la placa basal (eferente) serán somato-sensitivas y somato-motoras, respectivamente.

Dos modelos o teorías principales han sido propuestas para explicar la organización del sistema nervioso central: el modelo columnar o dorsoventral (Herrick, 1913; Nieuwehuys, 1998), y el modelo segmental o neuromérico (Gilland and Baker, 1993; Rubenstein y col., 1994; Puelles y Rubentein, 2003).

El modelo columnar sostiene que todo el sistema nervioso central (SNC) se puede dividir en dos zonas longitudinales, la placa alar y la basal, ambas separadas por el surco limitante de His. De esta manera, la parte alar es fundamentalmente sensorial, mientras que la parte basal es esencialmente motora. Este modelo divide la parte alar del rombencéfalo en una región somatosensorial y en una viscerosensorial, y la parte basal en una región visceromotora y en una somatomotora. Aunque esta división es clara en la médula espinal y en el rombencéfalo, tal no sucede en relación al mesencéfalo y prosencéfalo, en los cuales este surco limitante de His no se distingue claramente. Según este modelo, el mesencéfalo se divide en tres regiones columnares (tegmental medial, lateral y tectal) y el diencéfalo en cuatro zonas longitudinales (epitálamo, tálamo dorsal y ventral e hipotálamo) mientras que dentro del telencéfalo se diferencian dos zonas: una dorsal o palio y una ventral o subpalio. A su vez el palio se subdivide en palio lateral, medial y dorsal, mientras que el subpalio se subdivide en septo, estriado y área preóptica, (Nieuwehuys, 1998).

El modelo neuromérico, que surge a raíz de numerosos estudios de expresión de determinados marcadores neuronales y al patrón de expresión génica durante el desarrollo embrionario (ver Gilland y Baker, 1993; Rubenstein y col., 1994; Kuratani y Horigome, 2000; Puelles y Rubenstein, 2003), determina una subdivisión más específica (patrón de bandas) dentro de cada una de las vesículas encefálicas; estas bandas se denominan neurómeros. Los neurómeros son dilataciones del tubo neural que representarían centros de proliferación, diferenciación y migración. Los límites entre neurómeros se correlacionan con los límites de expresión de genes implicados en el desarrollo. Según esta teoría, el prosencéfalo se divide en prosencéfalo secundario (que origina el telencéfalo por un abombamiento dorsal, y el hipotálamo) y

en diencéfalo caudal. Puelles y Rubentein (2003) propusieron la existencia de tres prosómeros diencefálicos que serían el pretecho (p1), el tálamo (p2) y el pretálamo (p3). Sin embargo, los límites y las estructuras resultantes de estos segmentos transversales siguen estando todavía en discusión. Estos autores dividen el mesencéfalo en dos mesómeros, mientras que en el rombencéfalo se han diferenciado hasta ocho rombómeros, de los cuales el primero (región anterior) es el de mayor tamaño y cuya parte dorsal origina el cerebelo (Nieuwehuys, 1998; Gilland y Baker, 1993; Kuratani y Horigome, 2000).

Histogénesis del sistema nervioso

El patrón inicial de desarrollo del encéfalo de vertebrados es de tipo laminar, formado inicialmente por un epitelio pseudoestratificado (neuroepitelio) en el que las células de citoplasma alargado e irregular se extienden por todo el espesor del epitelio. Los núcleos de estas células neuroepiteliales poseen un alto grado de actividad mitótica, y una vez duplicado el DNA en las regiones basales (externas), emigran hacia la porción apical del citoplasma (ventricular) donde se dividen por mitosis. Los núcleos de las células hijas entonces regresan a la región basal donde vuelven a integrarse en el proceso de proliferación o bien comienzan a diferenciarse en neuroblastos. Este neuroepitelio primitivo se subdivide en una capa interna (ventricular o epéndima), que contiene células que continúan en el ciclo celular, convirtiéndose posteriormente en el epéndimo (epitelio que reviste el canal central y el sistema ventricular del sistema nervioso); una capa intermedia de células densamente aglomeradas, originada por los neuroblastos postmitóticos que abandonan el ciclo celular y la cual se transformará en la materia gris; y una capa externa de escasas células llamada capa marginal, derivando finalmente en la materia blanca del sistema nervioso central, (ver Nieuwenhuys, 1998; y Sanes y col., 2005 para revisión).

Anatomía del sistema nervioso central de la pintarroja

El sistema nervioso central de peces cartilaginosos en general presenta una gran similitud anatómica con el de los vertebrados más complejos y en especial con

los agnatos, anfibios y amniotas, en cuanto al desarrollo del telencéfalo se refiere, compartiendo así el mismo proceso de evaginación, inexistente en los demás peces gnatóstomos. Existen numerosas diferencias estructurales entre el telencéfalo de las distintas especies de peces condrictios, aunque la evaginación es el proceso morfogenético esencial de esta región. Dicho proceso de evaginación consiste en que las porciones dorsales y ventrales de las paredes laterales del telencéfalo embrionario se curvan hacia dentro y después sufren varios procesos de evaginación que resultan en la formación de un par de hemisferios que encierran a los ventrículos laterales (Northcutt y Braford, 1980; Butler y Hodos, 2005). Después de la evaginación (ver Fig. 3), la parte del palio que originalmente estaba en la posición más dorsal, respecto al ventrículo, se coloca en la parte más medial del telencéfalo dando lugar en el adulto al palio medial. En amniotas se organiza en esta región la formación hipocampal y el palio límbico, implicados en la memoria y emoción.

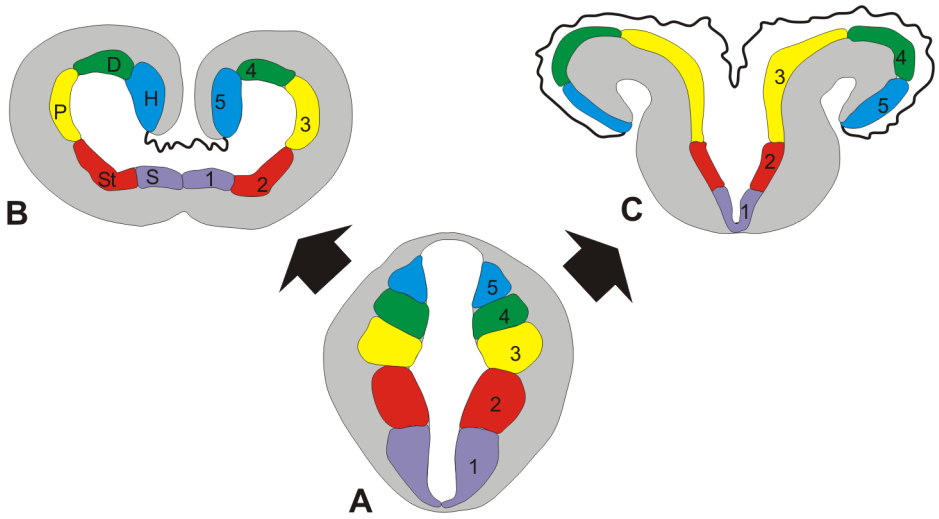

Figura 3. Procesos de desarrollo telencefálico en vertebrados: evaginación (B) y eversión (C). D, Palio dorsal; H, complejo hipocampal o palio medial; P, palio lateral; S, núcleo septal; St, estriado; 1-5, columnas o subdivisiones telencefálicas. Representación esquemática basada en la publicación de Northcutt y Braford, 1980.

El área palial originalmente situada en posición intermedia se convertirá en el palio dorsal, el cual formará las principales áreas paliales sensoriales y motoras del adulto mientras que el área palial originalmente más ventral se situará más lateralmente originando el palio lateral u olfatorio.

El estudio de Sterzi (1912) muestra que en tiburones los bulbos olfatorios se forman después de estos procesos de evaginación, a través del crecimiento hacia fuera de las paredes laterales de las porciones expandidas. Los bulbos olfatorios se comunican con los hemisferios telencefálicos mediante los pedúnculos olfatorios. Un detalle importante del encéfalo de tiburones es la conexión de las paredes mediales de los hemisferios en mayor o menor medida según las especies, siendo prácticamente total en el caso de *Scyliorhinus canicula*. En todos los peces cartilaginosos, el bulbo olfatorio es una estructura bien desarrollada pero que varía considerablemente de tamaño. Su superficie rostral o rostroventral se sitúa cerca de los órganos olfatorios lo que hace que el nervio olfatorio sea corto.

Según la descripción hecha por Smeets y colaboradores (1983), el diencéfalo de peces cartilaginosos adultos guarda la forma tubular del de embriones tempranos. Las espesas paredes laterales encierran un estrecho ventrículo que se expande ventrocaudalmente dentro del hipotálamo para formar el infundíbulo. El límite rostral del diencéfalo viene marcado por un plano que se extiende desde la zona lateral del velo transverso al quiasma óptico. Rostralmente al quiasma, la base del encéfalo se adelgaza y se engruesa de nuevo en la comisura anterior. Entre la comisura anterior y el quiasma óptico se localiza la región preóptica. El límite caudal de diencéfalo pasa por la comisura posterior hasta un profundo pliegue transverso exterior del suelo del encéfalo conocido como “plica encefálica ventral”. Rostral a este pliegue se observa una protusión intraventricular de las paredes encefálicas, el tubérculo posterior que constituye el techo del infundíbulo. Esta cavidad infundibular se expande caudalmente formando el receso posterior (receso mamilar), una cavidad ventricular dorsal que aparece caudalmente al tubérculo posterior, y también se expande lateralmente rodeándose por una densa masa neuronal que forman los lóbulos hipotálamicos inferiores. La placa del suelo del diencéfalo es delgada a excepción de su parte rostral, la cual contiene el quiasma óptico, la comisura postóptica y el núcleo medio

hipotálamico. Parte del suelo hipotálamico contribuye a la parte neural de la hipófisis. La parte epitelial de la hipófisis, la adenohipófisis, está pegada a la superficie ventrocaudal del diencéfalo.

Dos surcos externos son utilizados como referencias anatómicas. El primero es el surco tectodiencefálico, el cual marca el limite entre el techo y el diencéfalo y se continua caudalmente con el surco tectotegmental. El segundo es el surco talamohipotálamico, el cual separa externamente el tálamo del hipotálamo. El borde más dorsal del diencéfalo (parte rostral de epitálamo) contiene la glándula pineal y dos ganglios habenulares que conectan dorso-caudalmente entre sí por la comisura habenular. Rostral a esta comisura, el diencéfalo está cubierto por una estructura membranosa, la tela coroidea diencéfalica, la cual se continúa rostralmente con un profundo pliegue transversal, el velo transverso, que se encuentra anteriormente a la habenula. El punto de unión de ambas estructuras define el borde dorsal del límite telencéfalo-diencéfalo. El techo del diencéfalo se estrecha caudalmente a la comisura habenular formando una evaginación tubular, la epifísis. Más caudalmente, la comisura posterior marcará el borde dorsal del límite diencéfalo-mesencéfalo.

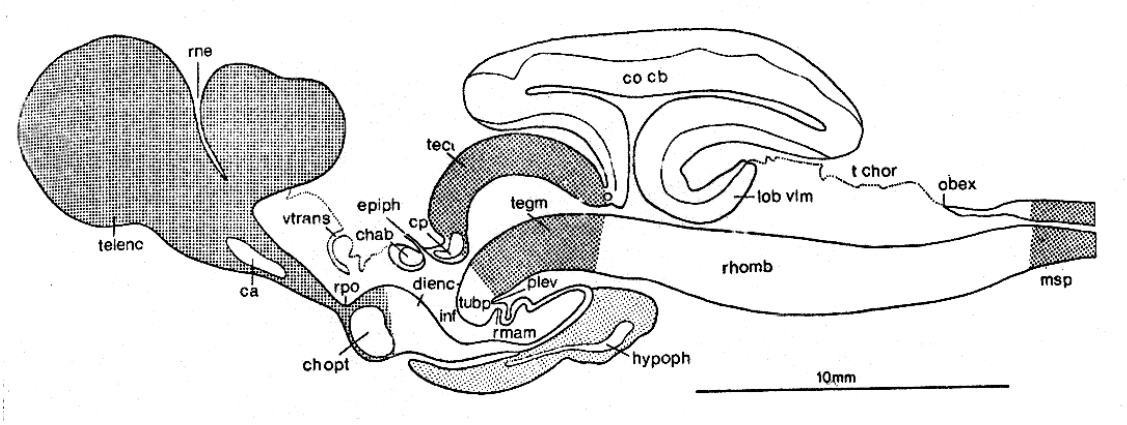

Figura 4. Encéfalo de pintarroja, *Scyliorhinus canicula*. Representación esquemática de un plano sagital del encéfalo de pintarroja (Smeets et al., 1983). Abreviaturas, rne: receso neuropórico; telec: telencéfalo; ca: comisura anterior; vtrans: velo transverso; rpo: receso preóptico; chopt: quiasma óptico; chab: comisura habenular; epiph: pineal; cp: comisura posterior; dienc: diencéfalo; inf: infundíbulo; rmam: receso posterior; hypoph: hipófisis; tubp: tubérculo posterior; plev: plica ventral; tegm: tegmento mesencefálico; tech: techo óptico; co cb: cuerpo cerebelar; lob vlm: lóbulo vestibulolateral; rhomb: rombencéfalo; t chor: tela coroidea; msp: médula espinal.

La parte más rostral del tallo encefálico, el mesencéfalo, comprende ventralmente el tegmento y dorsalmente el techo mesencefálico. Ambos se diferencian externamente por el surco tectotegmental. El techo es extenso y se organiza en dos lóbulos bilaterales que rodean sendas expansiones de la cavidad ventricular. Caudalmente, el techo se une al cuerpo cerebeloso vía el velo medular anterior. Rostralmente, el borde dorsal del mesencéfalo está marcado por la comisura posterior.

El rombencéfalo se extiende rostralmente desde el istmo hasta el óbex, rodeando el espacio romboide del cuarto ventrículo. Esta cavidad ventricular está formada ventralmente por la placa basal rombencefálica, mientras que las paredes laterales constituyen la placa alar. Este ventrículo está cubierto dorsalmente por un epitelio altamente vascularizado, la tela coroidea. Rostralmente, el cuarto ventrículo se extiende a ambos lados formando un receso lateral encerrado por la aurícula cerebelar, y disminuye gradualmente en la región más anterior del rombencéfalo, el istmo. Dorsalmente al tegmento rombencefálico se encuentra un cerebelo bien desarrollado formado por un largo cuerpo cerebeloso central y un par de aurículas laterales que encierran una gran cavidad ventricular que se extiende rostralmente sobre el techo mesencefálico y caudalmente sobre el cuarto ventrículo. Las aurículas pueden subdividirse en una lámina superior o rostromedial y otra inferior o caudolateral. Las láminas superiores de ambas aurículas contactan sobre el cuarto ventrículo mientras que caudolateralmente, se unen en su parte dorsal a las paredes laterales del rombencéfalo constituyendo el área octavolateral.

Caudalmente el rombencéfalo se continúa, mediante la región del óbex, con la médula o cordón espinal. La médula espinal de los elasmobranquios está constituida por cuatro regiones: cervical (3–6 segmentos), pectoral (16–18 segmentos), pélvica (34–36 segmentos) y caudal (60–80 segmentos; Smeets y col., 1983), siendo que cada región está formada por varios segmentos que aportan raíces dorsales (sensoriales) y ventrales (motoras).

3. MARCADORES DEL DESARROLLO TEMPRANO

En las últimas décadas, se han realizado numerosos estudios sobre la importancia funcional de los neurotransmisores en la interacción neuronal a nivel del sistema nervioso central de adultos. Sin embargo, durante el desarrollo neuronal temprano, se ha demostrado que algunos neurotransmisores clásicos (p.ej. ácido γ-aminobutírico, dopamina, serotonina) desempeñan una función como factor neurotrófico y/o morfogénico en vertebrados e invertebrados, mientras que en las etapas tardías del desarrollo pueden actuar funcionalmente induciendo procesos de sinaptogénesis (van Kesteren y Spencer, 2003). Además, la eliminación de estos neurotransmisores durante el desarrollo embrionario, resulta en un acentuado déficit del desarrollo encefálico en vertebrados (Lauder y col., 1981; Sivam y col., 1991; Yan y col., 1997; Durig y Hornung, 2000), indicando que dichos neurotransmisores pueden ser utilizados como marcadores de regiones encefálicas en desarrollo y fundamentales en estudios morfogénicos.

El sistema GABAérgico

El ácido γ-aminobutírico (GABA) es uno de los principales neurotransmisores, junto con la glicina, de acción inhibitoria en el SNC. Estudios de desarrollo en vertebrados han demostrado que tanto el GABA como su enzima de síntesis, la glutamato descarboxilasa (GAD), están entre los neurotransmisores y enzimas de síntesis de neurotransmisores que primero se expresan durante el desarrollo del SNC (Roberts y col., 1987; Aoki y col., 1989; Ekström y Ohlin, 1995; Barale y col., 1996; Obata, 1997; Katarova y col., 2000; Meléndez-Ferro y col., 2002, 2003). Estudios de las primeras fases del desarrollo en vertebrados también indican que el GABA puede desempeñar una importante función en procesos de sinaptogénesis (Madtes y Redburn, 1983), regulación neurotrófica y excitatoria (Madtes y Redburn, 1983; Cherubini y col., 1991; LoTurco y col., 1995; Liu y col., 1997; Barker y col., 1998; Obrietan y col., 2002; Fiszman y Schousboe, 2004), esencial para el inicio del desarrollo embrionario y que sería muy distinta a su posterior papel como principal neurotransmisor inhibitorio.

El GABA es un compuesto final, derivado del metabolismo de la glucosa. El α-cetoglutarato, formado por el ciclo de Krebs, sufre transaminación a aminoácido glutamato por la enzima GABA α-oxoglutarato transaminasa (GABA-T). En las células en las cuales el GABA es usado como neurotransmisor, la presencia de la enzima glutamato descarboxilasa permite la formación de GABA a partir del glutamato (Fig. 5). La GAD es necesaria para la síntesis del transmisor GABA, y por tanto se considera un marcador de neuronas gabaérgicas.

La liberación de GABA es dependiente de calcio y está relacionada con la despolarización de la terminal axónica. Sin embargo, también parece demostrada la existencia de una liberación independiente de calcio. La inactivación funcional primaria del GABA se lleva a cabo por sistemas de transporte de alta afinidad localizados en las neuronas gabaérgicas y especialmente en las células gliales circundantes. Su degradación, después de ejercida su función, se realiza por transaminación a nivel de las células gliales (GABA-transaminasa), para dar lugar finalmente al ácido succínico que es incorporado al ciclo de Krebs, (Alfonso y col., 2003).

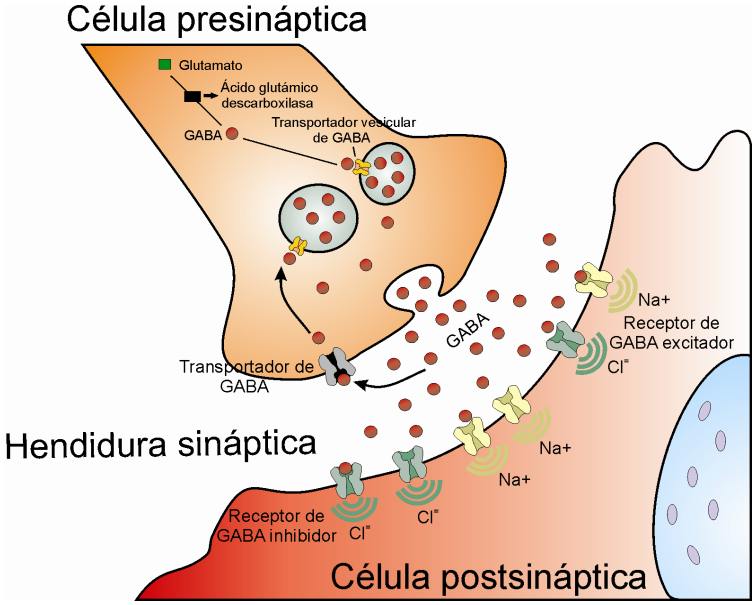

Figura 5. Esquema del metabolismo y liberación de GABA.

El receptor de GABA es una proteína de membrana que actúa como canal-receptor y está formado por varias subunidades. Dicho canal-receptor dispone de una zona de unión con afinidad por el GABA y, al menos, de otra zona de unión para las benzodiazepinas, grupo de fármacos con propiedades tranquilizantes y ansiolíticas. Es debido a este tipo de receptor molecular que el GABA actúa como neurotransmisor inhibitorio, produciendo una hiperpolarización en las neuronas postsinápticas. Dos tipos de GABA receptores, $GABA_A$ (postsináptico) y $GABA_B$ (presináptico), ejercen su función en la modulación de dicho transmisor. El receptor $GABA_A$ pertenece a la familia de receptores acoplados a canales iónicos, y diferencias en la expresión génica de sus subunidades pueden alterar las propiedades de este receptor, siendo este un mecanismo para la plasticidad sináptica. El receptor $GABA_B$ se encuentra en sinápsis axoaxónica tanto en el sistema nervioso central como periférico. Esta inhibición axoaxónica de la sinápsis GABAérgica bloquea o reduce considerablemente la liberación de dopamina (DA), serotonina (5-HT) o glutamato en la sinápsis neuronal.

El sistema catecolaminérgico

La tirosina hidroxilasa (TH) es la enzima encargada de la hidroxilación del aminoácido L-tirosina, siendo esta reacción enzimática el punto de regulación de la síntesis de catecolaminas (dopamina, DA; noradrenalina, NA; adrenalina, A) en el SNC. En consecuencia, la TH es la enzima limitante de la síntesis de catecolaminas y considerada como un marcador general de las células catecolaminérgicas. La distribución de células que expresan TH ha sido abordada en numerosos estudios del desarrollo del SNC (Spetcht y col., 1981a,b; Ekström y col., 1992; Manso y col., 1993; Foster, 1994; Puelles y Medina, 1994; Medina y col., 1994a,b; González y col., 1994a, 1995; Wallace y col., 1996; Marín y col., 1997; Pierre y col., 1997; Puelles y Verney, 1998; Rink y Wulliman, 2001, 2002; Sánchez-Camacho y col., 2002a,b; Pierre-Simons y col., 2002; McLean y Fetcho, 2004a,b; Abalo y col., 2005). Estudios ontogenéticos en vertebrados demuestran la importancia de las catecolaminas en la morfogénesis del SNC (di Porzio y col., 1990; Smeets y Reiner, 1994; Engele, 1998; Spencer y col., 1998, 2000), donde se cree que ejercen un papel como factor neurotrófico similar al descrito en relación a otros neurotransmisores como GABA.

La dopamina es un transmisor básico en el control de la actividad motora, y tiene también efectos sobre el comportamiento, por lo que en humanos se ha postulado que diversas alteraciones motoras (p.e. enfermedad de Parkinson) o del comportamiento (p.ej. la esquizofrenia), pueden ser debidas a modificaciones en la función dopaminérgica. También tiene efectos endocrinos, pues se ha establecido su participación en el control neuroendocrino de la función hipofisaria. Por su parte, la noradrenalina está principalmente relacionada con el ciclo sueño-vigilia y se ha postulado su participación en el control de las emociones y en el aprendizaje.

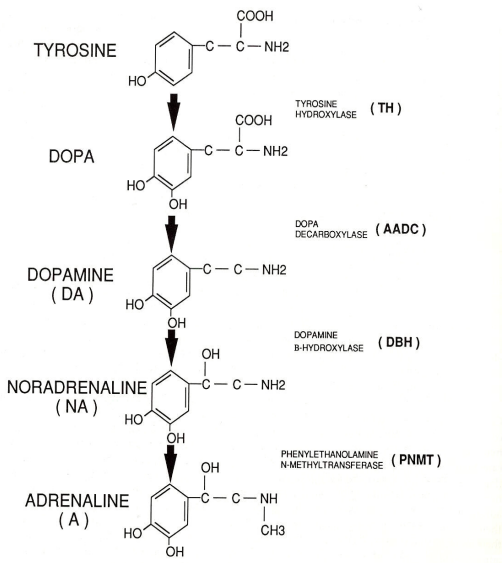

Figura 6. Esquema de la síntesis catecolaminérgica, (Smeets y Reiner, 1994).

El aminoácido tirosina es convertida en dihidroxifenilalanina (L-DOPA) por adición de un grupo hidroxilo al anillo catecol gracias a la actividad catalítica de la TH (Fig. 6). La L-DOPA es convertida en DA por carboxilación del grupo amino mediante la enzima DOPA carboxilasa (AADC). La DA ha sido considerada como uno de los productos terminales biológicamente activos en mayor cantidad de la síntesis de catecolaminas, mientras que L-DOPA se considera un precursor de DA, aunque estudios histoquímicas sugieren la posibilidad de que L-DOPA pueda ser una catecolamina terminal biológicamente activa, producida por algunas neuronas (Smeets y Steinbush, 1990; Vincent y Hope, 1990). Además de su función neuroquímica, la DA también es el precursor en la síntesis de noradrenalina (NA). Esta síntesis es llevada a cabo por la adición de un grupo hidroxilo al átomo de carbono próximo al anillo catecol de la DA, gracias al enzima dopamina β-hidroxilasa (DBH). Este enzima es un marcador de neuronas noradrenérgicas (y adrenérgicas). La NA es también un producto neuroquímico abundante en el SNC. Tanto en el SNC como en el sistema nervioso periférico, la NA

es convertida en adrenalina por metilación de un grupo amida terminal, mediante la enzima feniletanolamina N-metiltransferasa (PNMT).

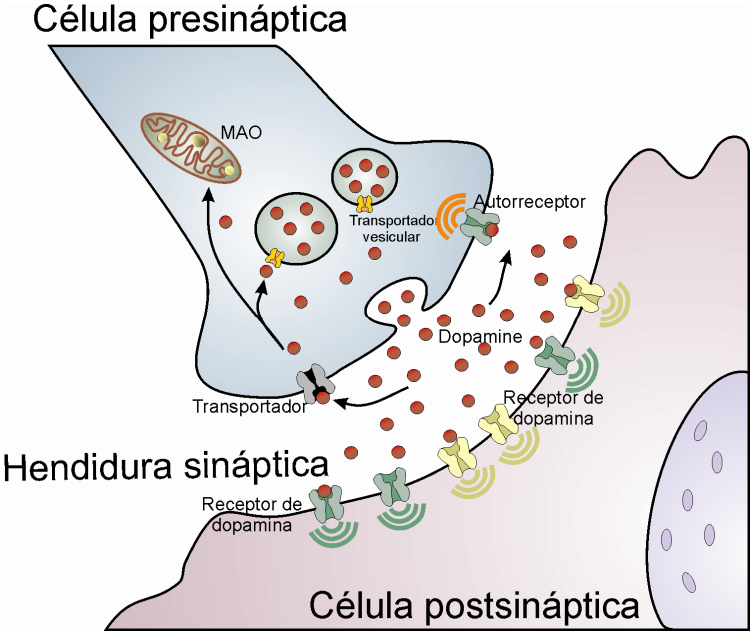

Figura 7. Esquema del metabolismo y liberación de dopamina.

La liberación de las catecolaminas se produce a partir de las vesículas sinápticas por un proceso de exocitósis dependiente del ión calcio en la terminal axónica por apertura de calcio. Una vez realizada su función, la inactivación de las catecolaminas tiene lugar bien por recaptación a la terminación presináptica o bien por degradación enzimática. La degradación de las catecolaminas es realizada por varias enzimas catalíticas, como la monoamina oxidasa (MAO) y la catecol-o-metiltransferasa (COMT). La MAO está presente intracelularmente y localizada en los terminales presinápticos y células de la glía; desarrollando la función de degradar dopamina después de ser capturada por las hendiduras sinápticas. Sin embargo, la COMT es de carácter postsináptico y está presente en la membrana celular.

La DA se une a receptores específicos para desencadenar sus acciones postsinápticas. Están caracterizados dos tipos de receptores dopaminérgicos (D1 y D2), atendiendo a sus propiedades farmacológicas. La NA, por otro lado, se une a receptores adrenérgicos de dos tipos: α y β. De ellos, los α-receptores tienen carácter inhibitório, mientras que los β-receptores son estimulatorios y están asociados al enzima adenil ciclasa, actuando a través del segundo mensajero AMP cíclico.

El sistema serotoninérgico

La serotonina o 5-hidroxitriptamina (5-HT) es una amina biogénica que presenta en su estructura un grupo indólico. Estudios de desarrollo en vertebrados han demostrado que al igual que los neurotransmisores o enzimas de síntesis antes mencionadas, la serotonina es uno de los primeros neurotransmisores que se expresan durante el desarrollo del SNC (Lidov y Molliver, 1982a,b; Wallace y Lauder, 1983; Wallace, 1985; Sako y col., 1986; Lauder, 1990; Okado y col., 1992). Estos estudios indican que la serotonina durante el desarrollo embrionario de vertebrados pude desempeñar un papel de molécula inductora de la neurogénesis (Lauder, 1990; Zhou y col., 2000; Buznikov y col., 2001; Branchereau y col., 2002; Pflieger y col., 2002; Petrova y Otellin, 2007) y diferenciación neuronal mediante la regulación de la división celular, migración, crecimiento axonal y sinaptogénesis (Lauder, 1993; Whitaker-Azmitia y col., 1996; Sodhi y Sanders-Bush, 2004; de Lucchini y col., 2005; Vitalis y col., 2007). En el SNC maduro, la 5-HT desempeña funciones importantes en el ámbito de la conducta, pudiendo su alteración provocar desórdenes conductuales como los que se presentan en el síndrome serotoninérgico asociado a la depresión en humanos. Además, entre otras acciones, la 5-HT interviene en un cierto control neuroendocrino a nivel del hipotálamo. El precursor de la serotonina es el aminoácido triptófano, que es captado por las neuronas serotoninérgicas de la circulación sanguínea. Una vez captado, el triptófano es transformado en 5-hidroxitriptófano por el enzima triptófano hidroxilasa y luego, éste es convertido en 5-HT por acción del ácido aromático L-amino descarboxilasa (AADC), un enzima análogo a la DOPA descarboxilasa en el caso de las catecolaminas (Fig. 8).

Los procesos de almacenamiento y liberación de la 5-HT son análogos a los que se producen en el caso de las catecolaminas, mediante la exocitosis del contenido de las vesículas sinápticas dependientes de ión. Una vez realizada su función, la inactivación de la 5-HT tiene lugar, bien por recaptación a la terminal presináptica o bien por degradación enzimática, que en este caso depende sólo del enzima MAO. Así, la MAO a partir de la 5-HT origina, por desaminación oxidativa el ácido 5-hidroxiindolacético, metabolito mayoritario de la 5-HT en el SNC.

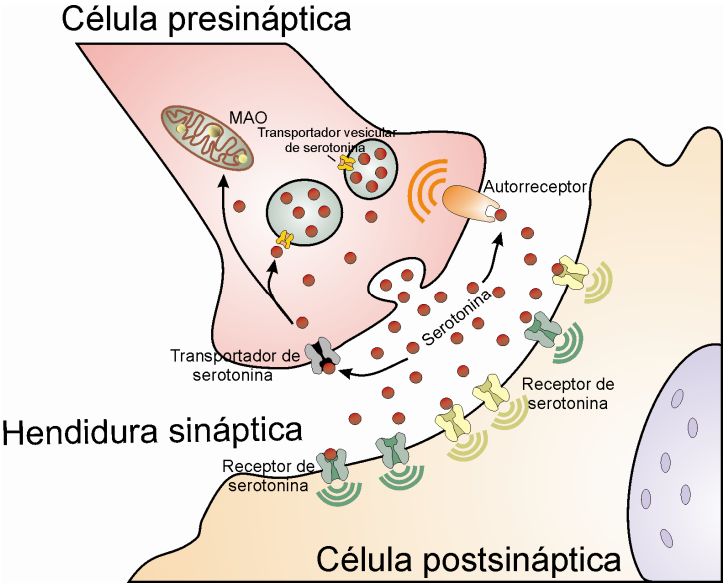

Figura 8. Esquema del metabolismo y liberación de serotonina.

A partir de estudios fisiológicos y farmacológicos en los que se han empleado diferentes antagonistas, se ha sugerido la existencia de varios subtipos de receptores a la serotonina. Se han descrito siete tipos principales de receptor (5-HT1-7), en base a sus características estructurales y funciones biológicas (Meneses, 1998). De ellos, la mayoría son postsinápticos, pero al menos dos de ellos (el 5-HT1B y el 5-HT1D) pueden ser autorreceptores, modulando la liberación del neurotransmisor.

4. Técnicas inmunohistoquímicas

Las técnicas inmunohistoquímicas son métodos de inmunolocalización y se basan en la unión específica de un anticuerpo a su antígeno en el tejido (Beesley, 1993). El lugar de la reacción antígeno-anticuerpo se visualiza añadiendo al final de la reacción el sustrato de la enzima más una sustancia denominada cromógeno. El producto originado al actuar la enzima sobre el sustrato, interacciona a su vez sobre el cromógeno y da lugar a un precipitado insoluble y coloreado. Como trazadores pueden emplearse distintos tipos de enzimas, siendo la más utilizada la peroxidasa (Del Moral, 1993).

Método de la peroxidasa-antiperoxidasa (PAP)

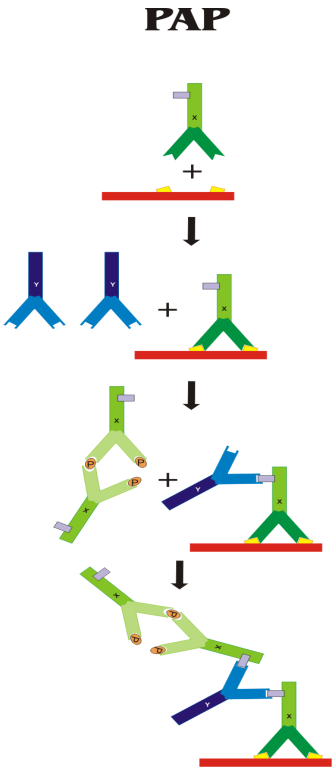

Figura 9. Representación gráfica del método PAP, modificado de Bolam, 1992.

Este procedimiento, desarrollado por Sternberger y colaboradores en 1970, utiliza un complejo preformado cíclico enzima-antienzima, que está compuesto por tres moléculas de enzima y dos moléculas de anticuerpo. En este método se utilizan tres anticuerpos, el primario dirigido a la molécula a visualizar, un anticuerpo secundario contra el anticuerpo primario, que a su vez hace de puente entre el anticuerpo primario y una tercera capa, que es un complejo peroxidasa-antiperoxidasa obtenido en la misma especie animal en la que se obtuvo el anticuerpo primario. La visualización se realiza mediante la aplicación de la DAB-peróxido de hidrógeno.

Las ventajas más relevantes de este método son:

- Con este método pueden demostrarse antígenos sin necesidad de marcar anticuerpos empleados para el procedimiento inmune, de forma que se evita su manipulación y la consiguiente pérdida de actividad.

- Por cada molécula de anticuerpo primario ligada al antígeno existen al menos tres moléculas de peroxidasa en el complejo final, lo cual incrementa considerablemente la sensibilidad de la técnica.

Método de streptavidina-biotina

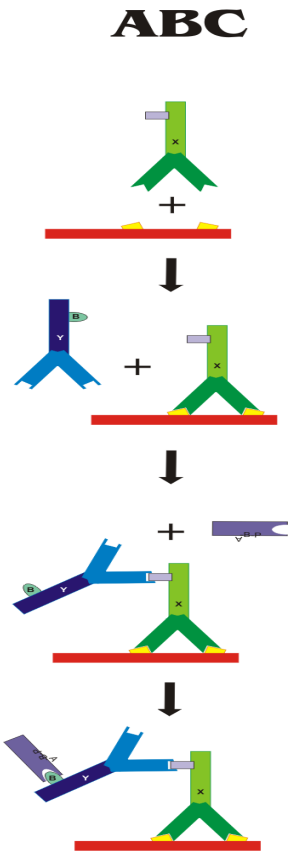

Figura 10. Representación gráfica del método ABC, modificado de Bolam, 1992.

El método de streptavidina-biotina (Hsu y col., 1981a, b) se trata de un procedimiento técnico muy sensible que utiliza anticuerpos marcados y se basa en la gran afinidad que entre sí poseen las moléculas de biotina y las de streptavidina, de forma que se genera un fuerte enlace no inmune. La biotina se puede acoplar a anticuerpos de forma que muchas moléculas de biotina se unen a una molécula de anticuerpo. Este anticuerpo biotinilado se une posteriormente a un gran número de moléculas de streptavidina (Jackson y Blythe, 1993). El tercer paso es la aplicación del complejo preformado streptavidina-biotina, acoplado por ejemplo a peroxidasa. Estos procedimientos son más sensibles que el método de PAP y además permiten una mayor dilución del anticuerpo primario a

utilizar. La visualización del complejo antígeno-anticuerpo se hace de la forma ya descrita anteriormente.

Método de inmunofluorescencia

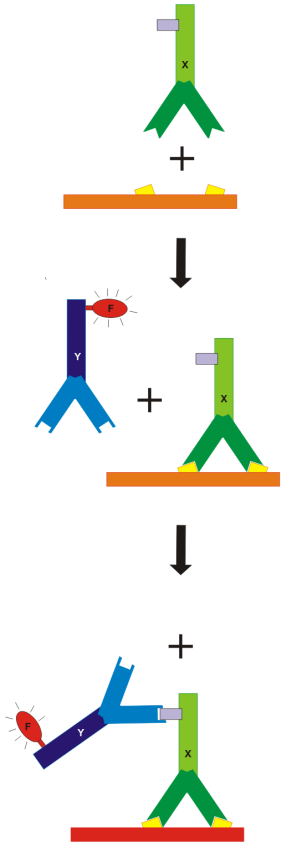

Figura 10. Representación gráfica del método de inmunofluorescéncia, modificado de Bolam, 1992.

El método de inmunofluorescencia presenta básicamente una metodología similar a los anteriores aunque con múltiples variaciones. En general el anticuerpo secundário se acopla a una molécula fluorescente para una fácil observación con un microscópio de flourescencia o un microscopio confocal. Este método permite multiples marcajes mediante el uso de anticuerpos primarios de diferentes especies animals a los que se acoplan diferentes anticuerpos secundários marcados con fluoróforos excitables por diferentes longitudes de onda. De esta forma, el método de inmunofluorescencia aplicado a la histología permite la detección de dos o más antígenos en la misma muestra de tejido histológico.

BIBLIOGRAFÍA

Abalo, X.M.; Villar-Cheda, B.; Anadón, R.; Rodicio, M.C. (2005) Development of the dopamine-immunoreactive system in the central nervous system of the sea lamprey. Brain Res Bull. 66:560-564.

Alfonso, M.; Andrade, M.A.; Durán, R.; García-Mayor, R.V. (2003) Neurotransmisión y Endocrinología. Tórculo (Eds), España.

Anadón, R.; Meléndez-Ferro, M.; Pérez-Costas, E.; Pombal M.A.; Rodicio, M.A. (1998) Centrifugal fibers are the only GABAergic structures of the retina of the larval sea lamprey: an immunocytochemical study. Brain Res. 782: 297-302.

Aoki, E.; Semba, R.; Kashiwamata, S. (1989) When does GABA-like immunoreactivity appear in the rat cerebellar GABAergic neurons? Brain Res. 502:245-51.

Balfour, F.M. (1878) The development of elasmobranch fishes. J Anat Physiol. 12:177-216.

Ballard, W.W.; Mellinger, J.; Lechenault, H. (1993) A series on normal stages for development of *Scyliorhinus canicula*, the lesser-spotted dogfish (Chondrichthyes: Scyliorhinidae). J. Exp. Zool. 267:318-336.

Barale, E.; Fasolo, A.; Girardi, E.; Artero, C.; Franzoni, M.F. (1996) Immunohistochemical investigation of γ-aminobutyric acid ontogeny and transient expression in the central nervous system of Xenopus laevis tadpoles. J. Comp. Neurol. 368:285-294.

Barker, J.L.; Behar, Y-X.; Li, Q-Y.; Ma, W.; Maric, D.; Maric, Y.; Schaffner, A.E.; Serafini, R.; Smith, S.V.; Somogyi, R.; Vautrin, J.Y.; Wen, X-L.; Xian, H. (1998) GABAergic cells and signals in CNS development. Perspect Dev Neurobiol. 5:305-322.

Beesley, J.E.; (1993) Immunocytochemical avenues. En "Immunocytochemistry. A practical approach" pp: 7-13. Beesley, J.E. (Ed). Oxford University Press. New York.

Bolam, J.; (1992) Experimental Neuroanatomy. A practical approach. Vol. 1. p: 115-120. IRL, Oxford.

Branchereau, P.; Chapron, J.; Meyrand, P. (2002) Descending 5-hydroxytryptamine raphe inputs repress the expression of serotonergic neurons and slow the maturation of inhibitory systems in mouse embryonic spinal cord. J Neurosci. 22:2598-2606.

Butler, A.B.; y Hodos, W. (2005) Comparative Vertebrate Neuroanatomy: Evolution and Adaptation. pp: 423-437, Wiley-Liss (2º Ed). New York.

Buznikov, G.A.; Lambert, H.W.; Lauder, J.M. (2001) Serotonin and serotonin-like substances as regulators of early embryogenesis and morphogenesis. Cell Tissue Res. 305:177-186.

Chiba, A.; Oka, S.; Saitoh, E. (2002) Ontogenetic changes in neuropeptide Y-immunoreactive cerebrospinal fluid-contacting neurons in the hypothalamus of the cloudy dogfish, *Scyliorhinus torazame* (Elasmobranchii). Neurosci Lett. 329:301-304.

Compagno, L.J.V. (1977) Phyletic relationships of living sharks and rays. Am. Zool. 17:303-322.

Coolen, M.; Sauka-Spengler, T.; Nicolle, D.; Le-Mentec, C.; Lallemand, Y.; et al. (2007) Evolution of axis specification mechanisms in jawed vertebrates: Insights from a Chondrichthyan. PLoS ONE 2:374.

Durig, J.; Hornung, J.P. (2000) Neonatal serotonin depletion affects developing and mature mouse cortical neurons. Neuroreport. 11:833-837.

Derobert, Y.; Plouhinec, J.L.; Sauka-Spengler, T.; Le Mentec, C., Baratte, B.; Jaillard, D.; Mazan, S. (2002) Structure and expression of three Emx genes in the dogfish *Scyliorhinus canicula*: functional and evolutionary implications. Dev Biol. 247:390-404.

Ekström, P.; Ohlin, L. M. (1995) Ontogeny of GABA-immunoreactive neurons in the central nervous system in a teleost, *Gasterosteus aculeatus L*. J. Chem. Neuroanat. 94: 271-288.

Ekström, P.; Honkanen, T.; Borg, B. (1992) Development of tyrosine hydroxylase-, dopamine- and dopamine beta-hydroxylase-immunoreactive neurons in a teleost, the three-spined stickleback. J Chem Neuroanat. 5:481-501.

Engele, J. (1998) Spatial and temporal growth factor influences on developing midbrain dopaminergic neurons. J Neurosci Res. 53:405-414.

Farner, H.P. (1978a) Embryonal development of the brain of the shark *Scyliorhinus canicula*. I. Formation of the shape of the brain, the migration mode and phase and the structure of the diencephalons. J Hirnforsch.19:313-332.

Farner, H.P. (1978b) Embryonal development of the brain of the shark *Scyliorhinus canicula*. II. The optic tectum and its stratification. J Hirnforsch.19:333-344.

Farner, H.P. (1978c) Embryonic development of the brain of *Scyliorhinus canicula*. III. The optical system and adjacent nuclei in the tegmentum mesencephali. J Hirnforsch. 19:405-414.

Fiszman, M.L.; Schousboe, A. (2004) Role of calcium and kinases on the neurotrophic effect induced by gamma-aminobutyric acid. J Neurosci Res.76:435-441.

Foster, G.A. (1994) Ontogeny of catecholaminergic neurons in the central nervous system ofmammalian species: general aspects, in: W.J.A.J. Smeets, A. Reiner (Eds.), Phylogeny and Development of Catecholamine Systems in the CNS of vertebrates, pp: 405-434; The Cambridge University Press, Cambridge.

Gilbert, Scott F. (2000) Developmental biology; Sinauer Associates, Inc., Sunderland, Massachusetts. 6th ed.

Gilland, E.; Baker, R. (1993) Conservation of neuroepithelial and mesodermal segments in the embryonic vertebrate head. Acta Anat (Basel). 148:110-123.

González, A.; Marín, O.; Tuinhof, R.; Smeets, W.J. (1994a) Ontogeny of catecholamine systems in the central nervous system of anuran amphibians: an immunohistochemical study with antibodies against tyrosine hydroxylase and dopamine. J Comp Neurol. 346:63-79.

González, A.; Marín, O.; Smeets, W.J. (1995) Development of catecholamine systems in the central nervous system of the newt *Pleurodeles waltlii* as revealed by tyrosine hydroxylase immunohistochemistry. J Comp Neurol. 360:33-48.

Herrick, C.J. (1913) Anatomy of the brain. En: "The reference handbook of the medical sciences". Vol. 2. pp: 274-342. Word (New York).

Holmgren, N. (1922) Points of view concerning forebrain morphology in lower vertebrales. J Comp Neurol. 34:391-459.

Hsu, S.M.; Raine, L.; Fanger, H. (1981a) Use of avidin-biotin-peroxidase complex (ABC) in immunoperoxidase techniques: a comparison between ABC and unlabeled antibody (PAP) procedures. J Histochem. Cytochem. 29:577-580.

Hsu, S.M.; Raine, L.; Fanger, H. (1981b) A comparative study of the peroxidase- antiperoxidase method and an avidin-biotin complex method for studying polypeptide hormones with radioimmunoassay antibodies. Am J Clin Pathol. 75:734-738.

Jackson, P.; Blythe, D. (1993) Immunolabelling techniques for light microscopy. En "Immunocytochemistry. A practical approach". pp: 15-41. Beesley, J.E. (Ed.). Oxford University Press. New York.

Katarova, Z.; Sekerkova, G.; Prodan, S.; Mugnaini, E.; Szabo, G**.** (2000) Domain-restricted expression of two glutamic acid decarboxylase genes in midgestation mouse embryos. J Comp Neurol. 424:607-627.

Kuratani, S.; Horigome, N. (2000) Developmental morphology of branchiomeric nerves in a cat shark, *Scyliorhinus torazame*, with special reference to rhombomeres, cephalic mesoderm, and distribution patterns of cephalic crest cells. Zoo Sci. 17:893-909.

Lauder, J.M. (1990) Ontogeny of the serotonergic system in the rat: serotonin as a developmental signal. NY Acad Sci. 600:297-313.

Lauder, J.M. (1993) Neurotransmitters as growth regulatory signals: role of receptors and second messengers. Trends Neurosci. 16:233-239.

Lauder, J.M.; Wallace, J.A.; Krebs, H. (1981) Roles for serotonin in neuroembryogenesis. Adv Exp Med Biol. 133:477-506.

Lidov, H.G.; Molliver, M.E. (1982a) Immunohistochemical study of the development of serotonergic neurons in the rat CNS. Brain Res Bull. 9:559-604.

Lidov, H.G.; Molliver, M.E.; (1982b) An immunohistochemical study of serotonin neuron development in the rat: ascending pathways and terminal fields. Brain Res Bull. 8:389-430.

Liu, J.; Morrow, A.L.; Devaud, L.; Grayson, D.R.; Lauder, J.M. (1997) GABAA receptors mediate trophic effects of GABA on embryonic brainstem monoamine neurons in vitro. J Neurosci. 17:2420-2428.

LoTurco, J.J.; Owens, D.F.; Heath, M.J.; Davis, M.B.; Kriegstein, A**.**R. (1995) GABA and glutamate depolarize cortical progenitor cells and inhibit DNA synthesis. Neuron. 15:1287-1298.

de Lucchini, S.; Ori, M.; Cremisi, F.; Nardini, M.; Nardi, I. (2005) 5-HT2B-mediated serotonin signaling is required for eye morphogenesis in *Xenopus*. Mol Cell Neurosci. 29:299-312.

McLean, D.L.; Fetcho, J.R. (2004a) Ontogeny and innervation patterns of dopaminergic, noradrenergic, and serotonergic neurons in larval zebrafish. J Comp Neurol. 480:38-56.

McLean, D.L.; Fetcho, J.R. (2004b) Relationship of tyrosine hydroxylase and serotonin immunoreactivity to sensorimotor circuitry in larval zebrafish. J Comp Neurol. 480:57-71.

Madtes, P.Jr.; Redburn, D.A. (1983) GABA as a trophic factor during development. Life Sci. 33:979-984.

Manso, M.J.; Becerra, M.; Molist, P.; Rodriguez-Moldes, I.; Anadón, R. (1993) Distribution and development of catecholaminergic neurons in the brain of the brown trout. A tyrosine hydroxylase immunohistochemical study. J Hirnforsch. 34:239-60.

Marín, O.; González, A.; Smeets, W.J. (1997) Basal ganglia organization in amphibians: afferent connections to the striatum and the nucleus accumbens. J Comp Neurol. 378:16-49.

Medina, L.; Puelles, L.; Smeets, W.J. (1994a) Ontogenesis of catecholamines systems in the brain of the lizard *Gallotia galloti*, in: W.J.A.J. Smeets, A. Reiner (Eds.), Philogeny and Development of Catecholamine Systems in the CNS of vertebrates, pp: 361-377; The Cambridge University Press, Cambridge.

Medina, L.; Puelles, L.; Smeets, W.J. (1994b) Development of catecholamine systems in the brain of the lizard *Gallotia galloti*. J Comp Neurol. 350:41-62.

Meléndez-Ferro, M.; Pérez-Costa, E.; Villar-Cheda, B.; Abalo, X.M.; Rodríguez-Muñoz, R.; Rodicio, M.C.; Anadón, R. (2002) Ontogeny of γ-aminobutyric acid-immunoreactive neuronal populations in the forebrain and midbrain of the sea lamprey. J Comp Neurol. 446:360-376.

Melendez-Ferro, M.; Perez-Costas, E.; Villar-Cheda, B.; Rodriguez-Munoz, R.; Anadón, R.; Rodicio, M.C. (2003) Ontogeny of gamma-aminobutyric acid-immunoreactive neurons in the rhombencephalon and spinal cord of the sea lamprey. J Comp Neurol. 464:17-35.

Meneses, A. (1998) Physiological, pathophysiological and therapeutic roles of 5-HT systems in learning and memory. Rev Neurosci. 9:275-89.

del Moral, G. (1993) Técnicas inmunohistoquímicas. En "Laboratorio de anatomía patológica". Vol. 1. pp: 343-348. McGraw-Hill (Eds.), Interamericana, Madrid.

Nieuwenhuys, R. (1998) Histogenesis. En "The central nervous system of vertebrates" (Nieuwenhuys, R.; Donkelaar, H.J.; Nicholson, C., Editores) pp: 229-271. Springer-Verlag, Berlin Heilderberg.

Northcutt, R.G.; Braford, M.R. (1980) New observations on the organization and evolution of the telencephalon of actinopterygian fishes. En: Comparative neurology of the telencephalon, S.O.E. Ebbesson, (ed). pp: 41-98 Plenum Press, New York.

Obata, K. (1997) Excitatory and trophic action of GABA and related substances in newborn mice and organotypic cerebellar culture. Dev Neurosci. 19:117-119.

Obrietan, K.; Gao, X.B.; Van Den Pol, A.N. (2002) Excitatory actions of GABA increase BDNF expression via a MAPK-CREB-dependent mechanism-a positive feedback circuit in developing neurons. J Neurophysiol. 88:1005-1015.

Okado, N.; Sako, H.; Homma, S.; Ishikawa, K. (1992) Development of serotoninergic system in the brain and spinal cord of the chick. Prog Neurobiol. 38:93-123.

Petrova, E.S.; Otellin, V.A. (2007) Serotonin is involved in the regulation of histogenetic processes in rat embryonic neocortex. Bull Exp Biol Med. 143:372-375.

Pflieger, J.F.; Clarac, F.; Vinay, L. (2002) Postural modifications and neuronal excitability changes induced by a short-term serotonin depletion during neonatal development in the rat. J Neurosci. 22:5108-5117.

Pierre, J.; Mahouche, M.; Suderevskaya, E.I.; Reperant, J.; Ward, R.; (1997) Immunocytochemical localization of dopamine and its synthetic enzymes in the central nervous system of the lamprey *Lampetra fluviatilis*. J Comp Neurol. 380:119-135.

Pierre-Simons, J.; Reperant, J.; Mahouche, M.; Ward, R. (2002) Development of tyrosine hydroxylase-immunoreactive systems in the brain of the larval lamprey *Lampetra fluviatilis*. J Comp Neurol. 447:163-176.

di Porzio, U.; Zuddas, A.; Cosenza-Murphy, DB.; Barker, JL. (1990) Early appearance of tyrosine hydroxylase immunoreactive cells in the mesencephalon of mouse embryos. Int J Dev Neurosci. 8:523-532.

Puelles, L.; Medina, L. (1994) Development of neurons expressing tyrosine hydroxilase and dopamine in the chicken brain: a comparative segmental analysis, in: W.J.A.J. Smeets, A. Reiner (Eds.), Philogeny and Development of Catecholamine Systems in the CNS of vertebrates, pp: 381-404; The Cambridge University Press, Cambridge.

Puelles, L.; Verney, C. (1998) Early neuromeric distribution of tyrosine-hydroxylase-immunoreactive neurons in human embryos. J Comp Neurol. 394:283-308.

Puelles, L.; Rubenstein, J.L. (2003) Forebrain gene expression domains and the evolving prosomeric model. Trends Neurosci. 26:469-476.

Rink, E.; Wullimann, M.F. (2001) The teleostean (zebrafish) dopaminergic system ascending to the subpallium (striatum) is located in the basal diencephalon (posterior tuberculum). Brain Res. 889:316-330.

Rink, E.; Wullimann, M.F. (2002) Development of the catecholaminergic system in the early zebrafish brain: an immunohistochemical study. Brain Res Dev. 137:89-100.

Rubenstein, J.L.; Martinez, S.; Shimamura, K.; Puelles, L**.;** (1994) The embryonic vertebrate forebrain: the prosomeric model. Science 266:578-580.

Roberts, A.; Dale, N.; Ottersen, O.P.; Storm-Mathisen, J. (1987) The early development of neurons with GABA immunoreactivity in the CNS of *Xenopus laevis* embryos. J Comp Neurol. 261:435-449.

Sako, H.; Kojima, T.; Okado, N. (1986) Immunohistochemical study on the development of serotoninergic neurons in the chick: I. Distribution of cell bodies and fibers in the brain. J Comp Neurol. 253:61-78.

Sánchez-Camacho, C.; Marín, O.; López, J.M.; Moreno, N.; Smeets, W.J.; ten Donkelaar, H.J.; González, A. (2002a) Origin and development of descending catecholaminergic pathways to the spinal cord in amphibians. Brain Res Bull. 57:325-330.

Sánchez-Camacho, C.; Martín, O.; Ten Donkelaar, H.J.; González, A. (2002b) Descending supraspinal pathways in amphibians: III. Development of descending projections to the spinal cord in *Xenopus laevis* with emphasis on catecholaminergic inputs. J Comp Neurol. 446:11-24.

Sanes, D.H.; Reh, T.A.; Harris, W.A., eds. (2005) Birth and migration. En "Development of the nervous system", pp:76-105. Academic Press, S. Diego. 2nd ed.

Schuske, K.; Beg, A.A.; Jorgensen, E.M. (2004). The GABA nervous system in *C. elegans*. Trends Neurosci. 27:407-414.

Sivam, S.P.; Krause, J.E.; Breese, G.R.; Hong, J.S. (1991) Dopamine-dependent postnatal development of enkephalin and tachykinin neurons of rat basal ganglia. J Neurochem. 56:1499-1508.

Smeets, W.J.A.J.; Nieuwenhuys, R.; Roberts B.L. (1983) The central nervous system of cartilaginous fishes. Structure and functional correlations. Springer-Verlag, Berlin.

Smeets, W.J.; Steinbusch, H.W. (1990) New insights into the reptilian catecholaminergic systems as revealed by antibodies against the neurotransmitters and their synthetic enzymes. J Chem Neuroanat. 3:25-43.

Smeets, W.J.; Reiner, A. (1994) Phylogeny and development of catecholamine systems in the CNS of vertebrates. Cambridge University Press.

Smeets, W.J.; González, A. (2000) Catecholamine systems in the brain of vertebrates: new perspectives through a comparative approach. Brain Res Rev. 33:308-379.

Sodhi, M.S.; Sander-Bush, E. (2004) Serotonin and brain development. Int Rev Neurobiol. 59:111-174.

Specht, L.A.; Pickel, V.M.; Joh, T.H.; Reis, D.J. (1981a) Light-microscopic immunocytochemical localization of tyrosine hydroxylase in prenatal rat brain. II. Late ontogeny. J Comp Neurol. 199:255-276.

Specht, L.A.; Pickel, V.M.; Joh, T.H.; Reis, D.J. (1981b) Light-microscopic immunocytochemical localization of tyrosine hydroxylase in prenatal rat brain. I. Early ontogeny. J Comp Neurol. 199:233-253.

Spencer, G.E.; Klumperman, J.; Syed, N.I. (1998) Neurotransmitters and neurodevelopment. Role of dopamine in neurite outgrowth, target selection and specific synapse formation. Perspect Dev Neurobiol. 5:451-467.

Spencer, G.E.; Lukowiak, K.; Syed, N.I. (2000) Transmitter-receptor interactions between growth cones of identified Lymnaea neurons determine target cell selection in vitro. J Neurosci. 20:8077-8086.

Sternberger, L.A.; Ardí, P.H.; Cuculis, J.J.; Meyer, H.G. (1970) The unlabeled antibody enzyme method of immunocytochemistry: Preparation and properties of soluble antigen-antibody complex (horseradish peroxidase-antiperoxidase) and its use in identification of spirochetes. J Histochem Cytochem. 18:315-333.

Sterzi, G. (1912) Il sistema nervoso centrale dei vertebrati. Presci, vol. II. Draghi, pp 473. Padova.

van Kesteren, R.E.; Spencer, G.E. (2003) The role of neurotransmitters in neurite outgrowth and synapse formation. Rev Neurosci. 14:217-231.

Vincent, S.R.; Hope, B.T. (1990) Tyrosine hydroxylase containing neurons lacking aromatic amino acid decarboxylase in the hamster brain. J Comp Neurol. 295:290-298.

Vitalis, T.; Cases, O.; Passemard, S.; Callebert, J.; Parnavelas, J.G. (2007) Embryonic depletion of serotonin affects cortical development. Eur J Neurosci. 26:331-344.

von Kupffer, C. (1900) Studien zur vergleichenden Entwicklungsgeschichte des kopfes der kranioten. Verlag von JF Lehmann, München & Leipzig, pp 1-86.

Wallace, J.A. (1985) An immunocytochemical study of the development of central serotoninergic neurons in the chick embryo. J Comp Neurol 236:443-453.

Wallace, J.A.; Lauder, J.M; (1983) Development of the serotonergic system in the rat embryo: an immunocytochemical study. Brain Res Bull. 10:459-479.

Wallace, J.A.; Romero, A.A.; Gabaldon, A.M.; Roe, V.A.; Saavedra, S.L.; Lobner, J. (1996) Tyrosine hydroxylase-containing neurons in the spinal cord of the chicken. I. Development and analysis of catecholamine synthesis capabilities. Cell Mol Neurobiol. 16:625-648.

Whitaker-Azmitia, P.M.; Druse, M.; Walker, P.; Lauder, J.M. (1996) Serotonin as a developmental signal. Behav Brain Res. 73:19-29.

Witschi, E. (1956) Development of vertebrates, Saunders Company eds. New York. Chap.13:202-208.

Yan, W.; Wilson, C.C.; Haring, J.H. (1997) Effects of neonatal serotonin depletion on the development of rat dentate granule cells. Dev Brain Res. 98:177-184.

Zhou, F.C.; Sari, Y.; Zhang, J.K. (2000) Expression of serotonin transporter protein in developing rat brain. Dev Brain Res. 119:33-45.

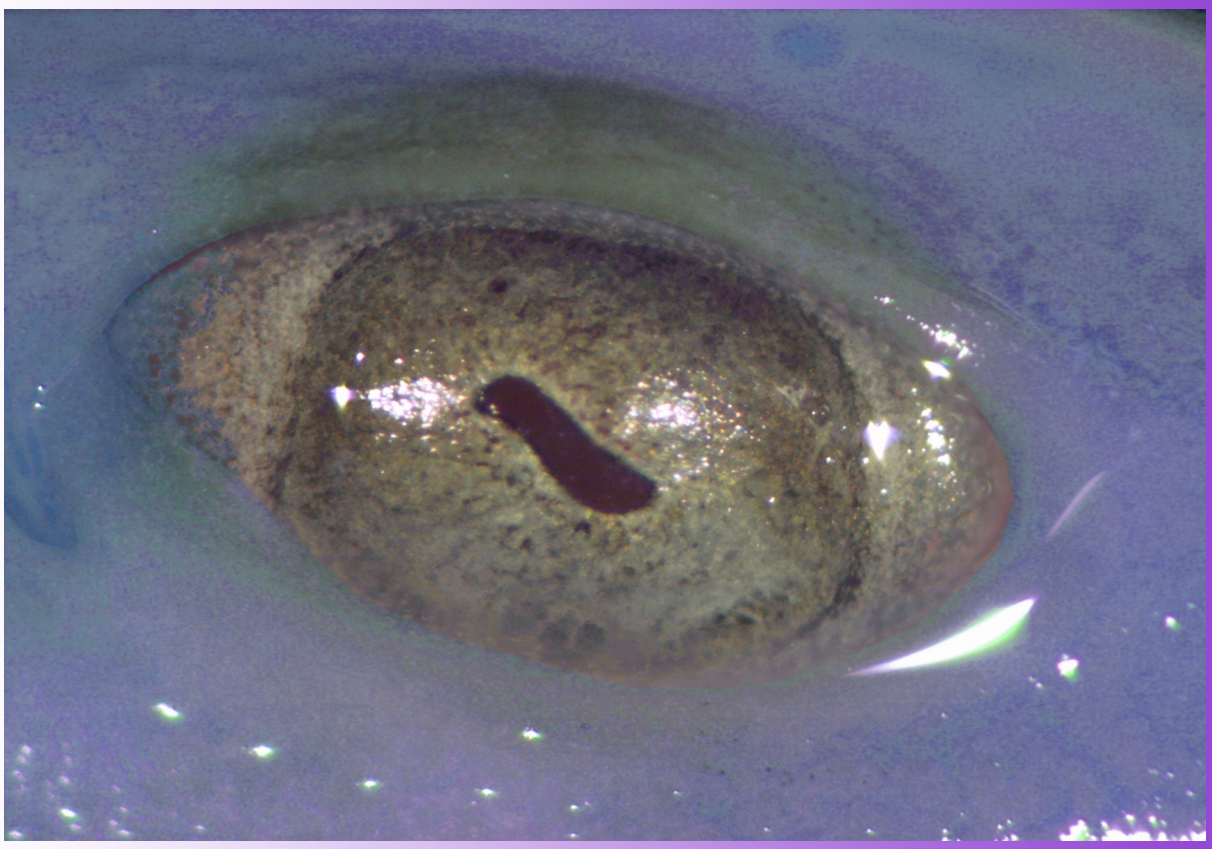

PLANTEAMIENTO Y OBJETIVOS

PLANTEAMIENTO Y OBJETIVOS

El sistema nervioso central de los condríctios, y en especial el de la pintarroja (*Scyliorhinus canicula*) ha sido objeto de numerosos estudios hodológicos e inmunohistoquímicos (ver introducción) debido a su estratégica posición filogenética (emparentado con los osteíctios), siendo también un grupo relacionado evolutivamente con actinopterígios, anfíbios y amniotas. Dicha posición filogenética les proporciona un crucial patrón morfológico para el estudio comparado entre los varios modelos de vertebrados, fundamental para caracterizar la evolución del sistema nervioso central. Por todo ello, la pintarroja se afianza como el mejor modelo para estudios neuroanatómicos en elasmobranquios. Sin embargo, son muy escasos los estudios de desarrollo en peces cartilaginosos (Farner, 1978a-c; Chiba et al., 2002; Derobert et al., 2002; Coolen et al., 2007), a pesar de que son claves tanto para el conocimiento de la organización de los diferentes sistemas de neurotransmisores, como también para su estudio a lo largo de la evolución de vertebrados.

Las técnicas inmunohistoquímicas constituyen una metodología muy extendida en la caracterización de los distintos sistemas neuroquímicos en vertebrados, siendo una herramienta fundamental para reconocer los patrones básicos de dichos sistemas, identificando así los rasgos filogenéticos que se han conservado a lo largo de la evolución. Sin embargo, en la actualidad, poco se conoce sobre el desarrollo de los sistemas de neurotransmisores clásicos como el sistema gabaérgico, catecolaminérgico y serotoninérgico, a pesar de que estas sustancias neuroquímicas están ampliamente difundidas en las estructuras nerviosas tanto de invertebrados como de cordados.

Por ello, los objetivos planteados en este estudio han sido:

1º. Objetivo: (*capítulo 1*) Analizar la organización espacio-temporal y neuromérica del **sistema gabaérgico** en el SNC de la pintarroja durante el desarrollo embrionario y etapa juvenil, utilizando como marcadores neuroquímicos el ácido γ-amino butírico (GABA) y su enzima de síntesis, la glutamato descarboxilasa (GAD).

2º. Objetivo: (*capítulo 2*) Analizar la organización espacio-temporal y neuromérica del **sistema catecolaminérgico** en el SNC de la pintarroja durante el desarrollo embrionario y etapa juvenil, utilizando como marcador neuroquímico la tirosina hidroxilasa (TH).

3º. Objetivo: (*capítulo 3*) Analizar la organización espacio-temporal y neuromérica del **sistema serotoninérgico** en el SNC de la pintarroja durante el desarrollo embrionario y etapa juvenil, utilizando como marcador neuroquímico la serotonina (5-HT).

4º. Objetivo: (*capítulo 4*) Analizar comparativamente las distintas estructuras gabaérgicas, catecolaminérgicas y serotoninérgicas presentes en el SNC de la pintarroja, en estadios tardíos del desarrollo embrionario (S30, S31) y en la etapa juvenil, tratando de caracterizar la relación entre la organización de los tres sistemas de neurotransmisores estudiados y su posible efecto en el desarrollo y maduración del sistema nervioso central de pintarroja. Para llevarlo a cabo hemos utilizado dobles y triples marcajes con los marcadores anteriores, que fueron observados en el microscopio de barrido confocal.

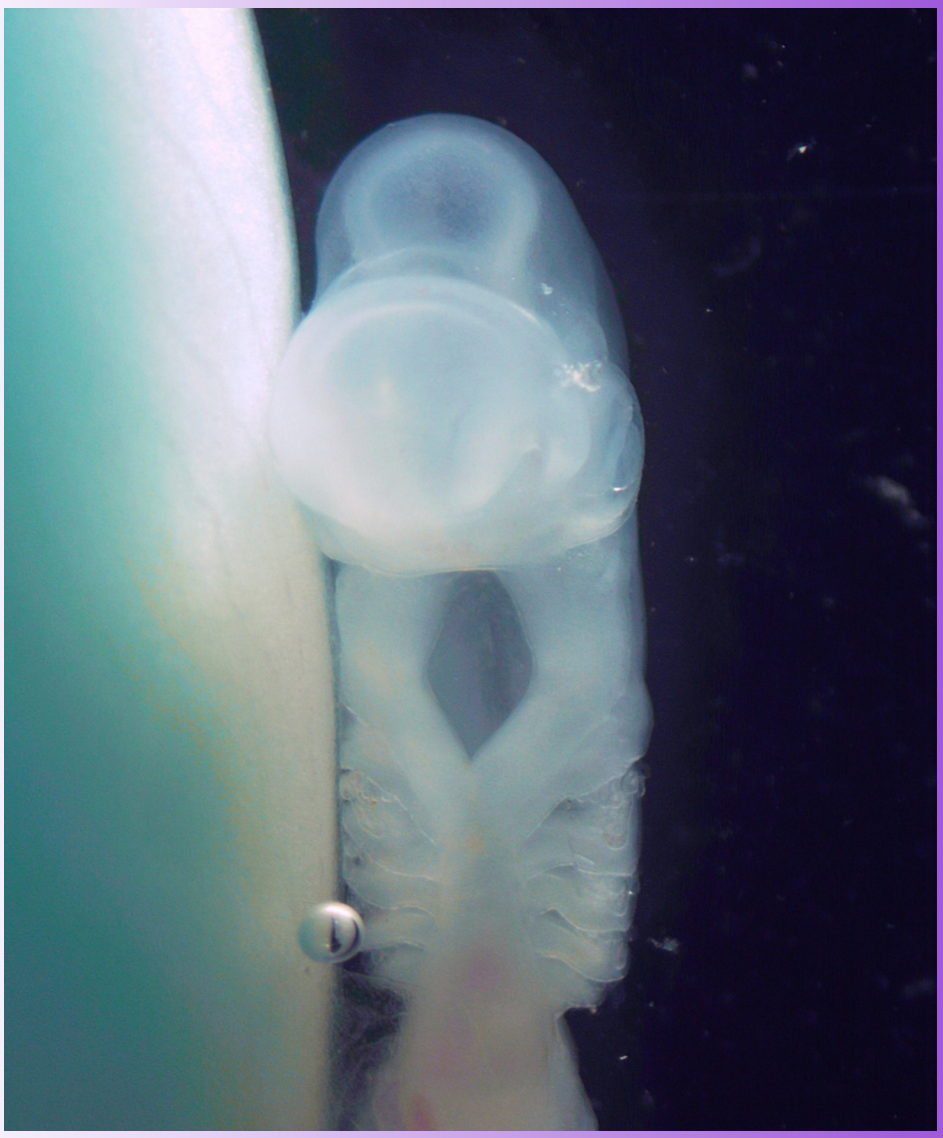

RESULTADOS Y DISCUSIÓN

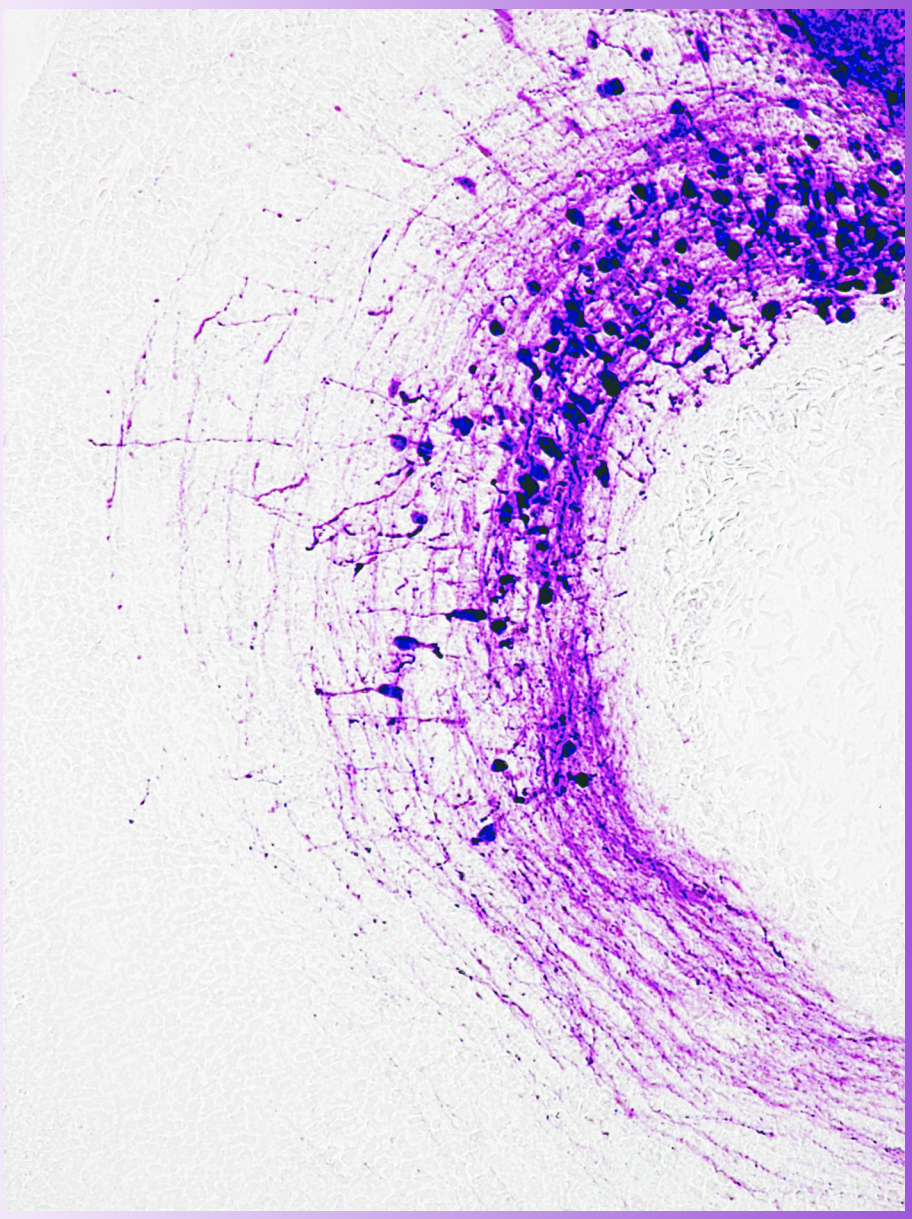

CAPÍTULO 1

Development of GABAergic Cells and Fibres in the Central Nervous System of the dogfish (*Scyliorhinus canicula*): An Immunohistochemical Study with Antibodies against GABA and GAD

CAPÍTULO 1

Development of GABAergic Cells and Fibers in the Central Nervous System of the dogfish (*Scyliorhinus canicula*): An Immunohistochemical Study with Antibodies against GABA and GAD

Some results of the present work appear published in the following articles:

- Sueiro, C; **Carrera**, **I**; Molist, P; Rodríguez-Moldes, I; Anadón, R. (2004) Distribution and development of glutamic acid decarboxylase immunoreactivity in the spinal cord of the dogfish *Scyliorhinus canicula* (elasmobranchs). J Comp Neurol. 478:189-206.

- **Carrera**, **I**; Sueiro, C; Molist, P; Holstein, GR; Martinelli, GP; Rodríguez-Moldes, I; Anadón, R. (2006) GABAergic system of the pineal organ of an elasmobranch (*Scyliorhinus canicula*): a developmental immunocytochemical study. Cell Tissue Res. 323:273-281.

- Sueiro, C; **Carrera**, **I**; Ferreiro, S; Molist, P; Adrio, F; Anadón, R; Rodríguez-Moldes, I. (2007) New insights on saccus vasculosus evolution: a developmental and immunohistochemical study in elasmobranchs. Brain Behav Evol. 70:187-204.

- Rodríguez-Moldes, I; Ferreiro-Galve, S; **Carrera, I**; Sueiro, C; Candal, E; Mazan, S; Anadón, R. (2008) Development of the cerebellar body in sharks: Spatiotemporal relations of Pax6 expression, cell proliferation and differentiation. Neurosci Lett. 432:105-110.

- **Carrera, I**; Ferreiro-Galve, S; Sueiro, C; Anadón, R; Rodríguez-Moldes, I. (2008) Tangentially migrating GABAergic cells of subpallial origin invade massively the pallium in developing sharks. Brain Res Bull. 75:405-409.

- Ferreiro-Galve, S; **Carrera, I**; Candal, E; Villar-Cheda, B; Anadón, R; Mazan, S; Rodríguez-Moldes, I. (2008) The segmental organization of the developing shark brain based on neurochemical markers, with special attention to the prosencephalon. Brain Res Bull. 75:236-240.

INTRODUCTION

γ -Aminobutyric acid (GABA), probably the most widely distributed inhibitory neurotransmitter in the central nervous system (CNS) of vertebrates, is one of the earliest neurotransmitters synthesized by the embryonic CNS. GABA is synthesized by enzymes of the glutamic acid decarboxylase (GAD) family and appears to be directly or indirectly involved in most if not all of the physiological functions of the nervous system, through control of the excitable state of neurons (see Barker et al., 1998). In addition to its role as a neurotransmitter (activating $GABA_A$ receptors), GABA has been shown to exert trophic actions during development (Lauder et al., 1998; Behar et al., 2001; Nguyen et al., 2001; Owens et al., 2002; Demarque et al., 2002; Represa and Ben-Ari, 2005), being one of the first neurotransmitters to be detected in the embryonic brain and spinal cord. Although the mechanisms regulating the GABA expression in developing systems are fairly unknown, there are some developmental studies in amniotes (*in situ* and *in vitro*) that show the trophic effect of GABA on the neurite growth before synapse formation (see Represa and Ben-Ari, 2005 for revision). These studies have shown that GABA is the first neurotransmitter to become functional in developing networks and mediates the formation of functional synaptic contacts, providing an example of the multiple actions that this molecule can exert at different developmental stages. To acquire knowledge about the trophic role of GABA in the developing brain is essential to know the spatial organization of GABAergic cells. These cells can be identified by their capability to synthesize GABA using glutamic acid decarboxylase (GAD) as biosynthetic enzyme. Antibodies against GABA and GAD have been largely used in mammals as markers for GABAergic cells in studies about development of different brain regions, particularly the cerebral cortex and the cerebellum (see for revision, Fairén et al., 1998; Barker et al., 1998; Takayama and Inoue, 2004; Huang et al., 2007), which contrast with the scarcity of similar studies in the entire vertebrate brain of mammals and non-mammalian vertebrates (*mammals:* Katarova et al., 2000; *reptiles:* Naujoks-Manteuffel et al., 1994; *amphibians:* Roberts et

al., 1987; Barale et al., 1996; *teleosts:* Doldán et al., 1999; Ekström and Ohlin, 1995; Higashijima et al., 2004; *cyclostomes:* Meléndez-Ferro et al., 2002, 2003).

As far as we are aware there are no studies of the ontogeny of the GABAergic system in the brain of cartilaginous fishes, and those related with the adult organization are very scarce (Álvarez-Otero et al., 1995; Sueiro, 2003). Therefore, the aim of the present study was to provide the first description of the development of the GABAergic system in the CNS of an elasmobranch, on the basis of the labelling with immunocytochemical markers against GABA and GAD. This study reveals the early appearance, migration and segmental organization of the GABAergic cell groups as well as the development of the early scaffold of GABAergic axon tracts. A further aim was to compare the development of the GABAergic system in elasmobranchs with that of other vertebrate groups, to achieve a better understanding of the developmental evolution of this system.

MATERIAL AND METHODS

Experimental animals

Embryos of the lesser-spotted dogfish (*Scyliorhinus canicula*) were kindly provided by the "Aquário Vasco da Gama", the "Oceanário" of Lisbon (Portugal) and "Aquarium Finisterrae" of Coruña, (Spain). The embryos were staged according to Ballard and colleagues (1993). The following embryonic stages were analysed: stage 22 (S22; two pairs of pharyngeal clefts open), S23 (three pairs of pharyngeal clefts open), S24 (diamond-shaped mouth), S25 (four pairs of open pharyngeal clefts), S26 (five pairs of pharyngeal clefts open, simple gill bars), S27 (some gill filaments show on the pharyngeal arches), S28 (transverse oval mouth, gills with external filaments), S29 (mandibular arches crowded into the mouth opening), S30 (embryo with a detectable rostrum), S31 (long branchial filaments), S32 (regression of the external gill filaments and the skin pigmentation begins), S33 (shinkage of the external yolk sac) and S34 (development of the hatching gland and digestive secretions). In addition, we used juveniles (of 9-12 cm in length) and some adult dogfish (40-60 cm in length).

Tissue preparation

Embryos were anaesthetized with 0.05% tricaine methane sulphonate (MS-222; Sigma, St. Louis, MO) in seawater and separated from the yolk before fixation. Prehatching, juvenile and adult specimens were deeply anaesthetized with MS-222 and then perfused intracardially with elasmobranch Ringer's solution (1.7% NaCl, 0.024% KCl, 0.031% CaCl2, 0.044% MgCl2, 0.113% Na2SO4, 0.049% NaCO3H, and 2.7% urea) followed by the appropriate fixative. Adequate measures were taken to minimize pain or discomfort. All procedures conformed to the guidelines established by the Spanish Royal Decree 223/1998 for animal experimentation and were approved by the ethical committee of the University of Santiago de Compostela.

For GAD immunohistochemistry, the embryos were separated from the yolk and fixed by immersion (embryos: S22, two specimens; S23, two embryos; S24, four embryos; S25, three embryo; S26, five embryos; S27, four embryos; S28, four embryos; S29, two embryos; S30 and S31, five embryos each; S32, six embryos; S33 four embryos) or perfusion (prehatching embryos: four specimens; juveniles: two specimens; adults: two specimens) in 4% paraformaldehyde in elasmobranch phosphate buffer (EPB: 0.1M phosphate buffer containing 670mM urea, pH 7.4). For GABA immunocytochemistry, specimens were fixed by immersion after separation from the yolk (embryos: S25, S28 and S29 two embryos each stage; S30 and S31 one specimen each stage) or perfusion (prehatching embryos: one specimen; juveniles: two specimens, adults: one specimen) in 5% glutaraldehyde in EPB with 1% sodium metabisulphite added, and postfixed in the same fixative.

Embryos and brains and spinal cords of juveniles and adults were postfixed for 4 hours, cryoprotected with 30% sucrose in phosphate buffer (PB), embedded in OTC compound (Tissue Tek, Torrance, CA), and frozen with liquid nitrogen-cooled isopentane. Parallel series of sections (14-18 μm thick) were cut in sagittal or transverse planes on a cryostat, and mounted on Superfrost Plus (Menzel-Glasser®) slides.

GAD immunocytochemistry

For GAD immunocytochemistry, the sections were pretreated with H_2O_2 to eliminate endogenous peroxidase, rinsed twice in 0.05M Trizma-buffered saline containing 0.1% Tween-20 at pH 7.4 (TBS-T) for 10 minutes each, before being processed by the ABC method with a sheep anti-GAD65/67 polyclonal antiserum (1440-4) as primary antibody (kindly provided by Dr. E. Mugnaini; dilution 1:50,000) raised against GAD partially purified from rat brain synaptosomes (Oertel et al., 1981). The sections were then rinsed in TBS-T (two 10-min rinses), incubated in biotinylated rabbit anti-sheep antiserum (Vector; 1:200) for 1 hour, rinsed in TBS-T, and incubated in StreptABComplex/HRP (Vector) for 30 min. The endogenous biotin was blocked before incubation with a biotin blocking system (Vector). The immunoreaction was developed with 0.005% diaminobenzidine (DAB; Sigma) and 0.003% H2O2. All dilutions were made with TBS-T containing 15% rabbit preimmune serum (Chemicon), and all incubations were carried out in a humid chamber at room temperature. Finally, the sections were dehydrated, mounted and coverslipped. The antibody has been used in different vertebrate groups, including fishes (Mugnaini and Maler, 1987; Maler and Mugnaini, 1994) and details about its specificity have been recently published by MacLeod and colleagues (2006). Moreover, its specificity in the dogfish brain was tested by western blot of brain extracts of adult dogfish and rat (Sueiro et al., 2004). As negative controls, the primary, secondary or tertiary antibodies were omitted. In these control sections, no immunostaining was observed.

GABA tissue preparation and immunocytochemistry

GABA immunocytochemistry was performed on sections of embryos and brains and spinal cords of juvenile and adults. The endogenous peroxidase was eliminated as above and sections were then processed by the PAP method, with a rabbit anti-GABA polyclonal antiserum raised by immunizing albino rabbits with a GABA glutaraldehyde-bovine serum albumin complex (Affiniti, Mamhead, UK; diluted 1:1000) as primary antibody. Goat anti-rabbit IgG (Dako; 1:100) and rabbit PAP

complex (Sigma, 1:500) were used as secondary and tertiary antibodies respectively. All dilutions were made with TBS-T containing 15% goat serum and 1% sodium metabisulphite. The immunoreaction was developed as above and the sections dehydrated and coverslipped accordingly. Negative controls were performed as above. No immunostaining was observed in control sections.

Imaging

The sections were photographed with an Olympus microscope equipped with a color digital camera. The photographs were adjusted for brightness and contrast with Corel Photo Paint (Corel, Ottawa, Canada), and photos were composed with Corel Draw.

RESULTS

The chronological development of the GABAergic cell groups is summarized in Table I. GAD-immunoreactive (ir) cells were observed at very early developmental stages indicating their implication in the synthesis of GABA, hence being GABAergic cells. Since that GAD-ir and GABA-ir cells have shown the same distribution pattern in the CNS of embryos (S25, S28-S31, S34), juveniles and adults, we considered that both immunomarkers reveal the presence of GABAergic cells. Therefore, we use the term GABAergic to refer to GAD-ir and GABA-ir structures.

Results have been grouped in three developmental periods or phases (early, intermediate and late). The *early developmental period* (S22-S25) is characterized by the establishment of first GABAergic populations in relation with main neuromeric boundaries. GABAergic cell populations were observed in the postoptic area and basal plate of the caudal prosencephalon, rhombencephalon and rostral spinal cord (S22); ventral telencephalon (S23); ventral hypothalamus and ventral thalamus (S24) and at the

alar plate [posterior commissure and isthmal regions (S23), pretectum (S24) and optic tectum (S25)]. Some of these GABAergic populations were located in relation with neuromeric boundaries. The *intermediate developmental period* (S26-S31) is characterized by the establishment of the mature laminar GABAergic architecture in the walls of the dogfish CNS and the formation of the main GABAergic fiber tracts of the axonal scaffold. The "mature" GABAergic organization was established at the *late developmental period* (S32-S34) being characterized by an extensive distribution of GABAergic structures throughout the entire dogfish CNS, similar to that reported in adults (Sueiro, 2003).

Distribution of GABAergic cells and fibers during embryonic development

The distribution of GABAergic cells and fibers in the CNS of the developing dogfish is schematically represented in Fig. 1. The GABAergic cell groups of the dogfish brain were tentatively related to a segmental organization pattern described in the forebrain of vertebrates (Puelles and Rubenstein, 2003) and in the rhombencephalon of dogfish (Gilland and Baker, 1993; Kuratani and Horigome, 2000), using cranial nerves and external anatomical brain morphology as mainly recognizable marks.

Early developmental period (S22-S25)

Stage 22 (S22)

GABAergic cells were first observed at the postoptic area (rostral diencephalon), synencephalic tegmentum (caudal diencephalon), rhombencephalon and rostral spinal cord (Fig. 1a). In the rostral diencephalon (Figs. 2A,B), GABAergic cells were observed at the ventral walls of the postoptic area, and these few weak stained GABAergic cells showed a short process to the preoptic recess (Fig. 2B). Some weak stained GABAergic cells with large somata and short processes were observed in the synencephalic basal plate (Fig. 2C), forming the primordium of the nucleus of the medial longitudinal fascicle (nMLF). In the rhombencephalon, large GABAergic cell bodies were observed sparsely distributed along the marginal zone of the entire

tegmental extension (Fig. 2D) being continuous with those of the rostral spinal cord, although a few faintly GABAergic cells were also seen at the intermediate zone, presenting ventral processes (Fig. 2D). The GABAergic cells of the primordial nmlf (Fig. 2C), were sending long caudal GABAergic axonal processes through the ventral zone, to form later the medial longitudinal fascicle, whose fibers will intermingle with the short ventral processes of the GABAergic cells at caudal tegmentum (Fig. 2D) and rostral spinal cord.

Stages 23-24 (S23-S24)

At these stages (Figs. 1b,c; 2E-N), the density of GABAergic cells in the basal prosencephalon increased and first populations appeared at the telencephalic basal plate (subpallium), and prosencephalic alar plate (posterior commissure), which together with the isthmic population, marked the rostral and caudal mesencephalic boundaries. The subpallial GABAergic cells showed weak immunoreactivity (Fig. 2E) and the density of the postoptic group notably increased from S23 to S24 (Figs. 2F,I,J). A hypothalamic GABAergic population appeared at S24 being formed by small and intense stained cells, some of them CSF-c cells located at the medial ventricular zone, and also by large moderate to intense labelled somata (Figs. 2I,J) laterally located. At thalamic regions, some round and moderate stained GABAergic cells were first observed at S24 forming a thin band (Fig. 2I) that corresponds to the primordium of the ventral thalamus. Intensely stained cells were observed at the prosencephalic, mesencephalic and rhombencephalic tegmenti (Figs. 2E,G,I,K). In the alar plate of the prosencephalon, some ventricular GABAergic cells were grouped in the marginal region of the posterior commisure area (Fig. 2G, I,L), showing processes ending in a growth cone-like dilatation and oriented ventrally. At these stages, large GABAergic cell bodies with long processes oriented dorsoventrally were observed at the isthmic level, forming a dense medial columnar cell cluster (Figs. 2E,H,M). From S24, the rhombencephalic GABAergic cells were gathered in several conspicuous groups related directly with the boundaries between rhombomeres (Figs. 2I,M,N). Most of these cells showed long

ventral processes towards the marginal zone (Figs. 2M,N), compatible with a vertical migration. In the rostral spinal cord, a few GABAergic perikarya were observed at S24 in the mantle/marginal layer at middle levels. These cells were pear-shaped with processes coursing ventrally and often exhibiting irregular profiles. Numerous GABAergic processes coursed from both rhombencephalic and rostral spinal cord cells to join the basal GABAergic fibers of the medial longitudinal fascicle, whose fibers coursed throughout the entire tegmentum (Figs. 2M,N) to the spinal cord.

Stage 25 (S25)

This stage is characterized by the appearance of GABAergic cells in the optic tectum, by the increased density of most GABAergic brain populations and by the patterning of the rhombencephalic GABAergic groups. Most of GABAergic cells in the basal telencephalon occupied the marginal zone (MZ; Figs. 3A,B,F) while others in the intermediate zone (IZ; Figs. 3A,B,F), showed apical prolongations to the ventricular surface. At the postoptic area some round and moderate stained GABAergic cells formed a thin band extending from the ventral postoptic marginal walls (suprachiasmatic nucleus) to the primordium of the ventral thalamus (Fig. 3C). GABAergic cells with ventricular processes were observed both at marginal locations in the ventral postoptic region and at the lateral infundibular walls (Fig. 3C). Except at the rostral area (slightly dorsal to the zona limitans intrathalamica), GABAergic cells and fibers were lacking in the dorsal thalamus. In the hypothalamus, the density of the GABAergic cells at the lateral and ventral infundibular walls slightly increased, extending through all layers (Figs. 3C,F). At this stage, both the basal GABAergic population of the prosencephalic/mesencephalic tegmentum (Figs. 3D-G) and the posterior commissure group (Figs. 3F,G) increased notably their cell density. The GABAergic cells of the basal prosencephalic band extended rostrally towards the caudal hypothalamic population (Figs. 3D,E,F). Some scattered GABAergic cells were observed along the marginal zone of the optic tectum (Fig. 3D) and a small group was also located just rostral to the cerebellar primordium (Figs. 3D,H), forming a short

dorso-ventral column at the isthmus. In the rest of the rhombencephalic tegmentum, GABAergic cells were packed in clusters related to the different rhombomeric bulges (Figs. 3I,J). Within these groups, apical GABAergic cells showed a short dorsal process with a radial migration-like morphology (Figs. 3I,J), while the rest of GABAergic cells at the intermediate layer sent long ventral process to the marginal layer, increasing the density of the GABAergic fibers of the medial longitudinal fascicle (Figs. 3J, 6).

Intermediate developmental period (S26-S31)

Stages 26-27 (S26-27)

From S26 (Fig. 1d) onwards, the layering of the GABAergic cells was apparent in most brain regions, being mainly observed at the intermediate and ventricular zone, while their prolongations extended throughout the marginal zone. At these middle-early developmental stages, GABAergic cells firstly appeared at the preoptic area, saccus vasculossus, cerebellum and spinal cord (CSF-c cells; S26) and at the posterior recess organ, posterior tubercle, habenula and viscerosensory column (S27).

In the subpallial walls, GABAergic cells at the ventricular zone showed a bipolar morphology with apical prolongations contacting the ventricular surface and basal prolongation directed toward the intermediate zone (Figs. 4A,B,C), where abundant immunoreactive cells extended their prolongations to the marginal zone. The rostral and lateral extensions of GABAergic cells form a sharp limit that separates the thicker (three layered) walls of the ventral (subpallial) telencephalon from the thinner (neuroblastic) walls of the dorsal (pallial) telencephalon (Figs. 4A,B). This limit probably represents the pallial/subpallial boundary. Interestingly, at this stage (S26) some longitudinal fibers extended rostrally beyond this limit to course transversely toward to the ventricle (Fig. 4B). In the preoptic area (S26), a population of GABAergic cells with ventricular process, continuous with the subpallial groups, was observed at both rostral and caudal preoptic recess walls (Figs. 4A,C,D). More caudally, the postoptic GABAergic cells were arranged in a very wide ventro-dorsal column (Fig. 4D), continuous with the ventral thalamic GABAergic group, which formed a wedge between p3 (ventral

thalamus) and p2 (dorsal thalamus), following the zona limitans intrathalamica (Figs. 4C,D,F). GABAergic cells with ventricular process were located at the marginal walls of the dorsal and ventral thalamus domains (Figs. 4C,F,G), just rostrally to the posterior commissure. GABAergic CSF-c cells were observed at the ventricular and intermediate zones of the ventral and lateral infundibular walls of the hypothalamus (Figs. 4A,C,D) and at the marginal walls of the posterior recess organ and posterior tubercle (Fig. 4E). A few faint oval GABAergic cells were observed in the walls of the primordial neurohypophysis and saccus vasculossus. In the habenula, a few GABAergic cells (some of them with ventricular process) were seen at S27 near the habenular commisssure (Figs. 4C,G). Numerous GABAergic cells were observed in the posterior commissure, forming a wide alar band between the rostral optic tectum and the area slightly rostral to the fasciculus retroflexus (Figs. 4A,C,H,J), and at the marginal zone of the pretectum. In the basal forebrain tegmentum, in a saggital section at the midline, the GABAergic cell band of the basal plate was seen extended from the rostral mesencephalic tegmentum (slightly caudal to the oculomotor nerve root level) to the caudal hypothalamus, being continuous with the GABAergic hypothalamic cell population (Figs. 4C,D) and the wedge thalamic groups (the dorsal GABAergic cell group of the ventral thalamus; Figs. 4C,H).

Numerous GABAergic cells of the optic tectum were seen along the entire marginal zone (Figs. 4A,C,H,I), while some GABAergic cells were also seen at the intermediate zone, exhibiting a ventral process towards the ventricle (Fig. 4I). In the rhombencephalon, two different GABAergic cell organization patterns were observed, formed by two GABAergic groups from the isthmus to the caudal level of acusticofacial nuclei nerve root (VII-VIII), and five small groups from this level to the rostral spinal cord. The rostral groups were formed by moderate to strongly stained GABAergic cells densely packed along the tegmentum (Figs. 4A,K,L). These GABAergic cells were gathered at both sides of the floor plate, some of them extended contacting processes to the ventricle (Fig. 4L), and at the marginal and intermediate layers (Fig. 4L). In contrast, from the level of VII-VIII nuclei nerve root to the rostral spinal cord,

GABAergic cells tended to segregate into five smaller groups (Fig. 4M). In a transverse section, these five clusters of GABAergic cells extended from both sides of the floor plate to almost the dorsal tegmental region, being located at the marginal and intermediate zones (Fig. 4M). The dorsalmost GABAergic cell group formed the viscerosensory column (S27), extended at the alar plate of the caudal rhombencephalic tegmentum. Some GABAergic cells and fibers were seen at the floor plate, mainly at its ventral zone (Figs. 4L,M). Some GABAergic cells were observed at the ventral region of the rostral cerebellar plate, continuous with the dorsoventral GABAergic cell column of the isthmus (Fig. 4K). In the rostral spinal cord, the dorsal and ventral walls were thin, exhibited some GABAergic cells at the mantle layer and a few CSF-c GABAergic cells in the floor plate.

At S26 and S27, the density of the medial longitudinal fascicle increased notably at the basal plate of the prosencephalic (Figs. 4D,G,J; 6), mesencephalic and rhombencephalic (Figs. 4J-N; 6) tegmenti. From the GABAergic cells of the postoptic area, fibers were observed coursing through the rostral hypothalamus to join the GABAergic fibers of the medial longitudinal fascicle (Figs. 4C,D; 6). This conspicuous prosencephalic longitudinal GABAergic fiber tract may correspond to the postoptic commissure tract (TPOC). Some of these longitudinal GABAergic fibers also innervated the GABAergic cell groups of the posterior tubercle nucleus and the dorsal hypothalamic walls (Figs. 4C,D; 6). At these stages, a dense longitudinal bundle of GABAergic fibers were also seen at the alar plate, coursing rostrally from the posterior commissure nucleus, through the dorsal thalamus and turning ventrally to the zona limitans intrathalamica (Figs. 4C,F,G; 6), probably corresponding to the dorsoventral diencephalic tract (DVDT). Some GABAergic fibers were also observed coursing through the dorsal walls of the proximal habenular region (Figs. 4G; 6). From the the posterior commissure, thick transverse bundles of GABAergic fibers were seen coursing towards the basal plate (Figs. 4J; 6), surrounding the fasciculus retroflexus (absent of GABAergic fibers), probably corresponding to the tract of the posterior commissure (TPC). In the entire rhombencephalic tegmentum, the several GABAergic cell groups

extended GABAergic fibers that form at the alar plate a dorsal longitudinal tract (Figs. 4J,L,M; 6) or join to the lateral and ventral medial longitudinal fascicle (Figs. 4K,L,M,N; 6), increasing notably their fiber density.

Stages 28-31 (S28-S31)

The main features of these mid-late developmental stages were the massive invasion of tangential migrating GABAergic cells into the pallium, the layered distribution of the GABAergic cells at most regions of the dogfish CNS and the establishment of the mature GABAergic fiber tracts. At S28 (Fig. 1e), subpallial GABA-ir cell processes were extended rostrally along the intermediate zone reaching the dorsal telencephalon (Figs. 5A,B). GABAergic cells with the morphology of tangentially migrating cells were seen in two dome-shaped protrusions of the rostrolateral subpallial walls and extending laterodorsally and rostrodorsally to take a superficial location (Figs. 5C,D). At subsequent stages (S29-S31; Fig. 1f), these GABAergic cells were seen migrating tangentially toward lateral and dorsal pallial regions (Figs. 5E-G; 6), most of them forming "strings of cells" periventricularly (Fig. 5G), extending in pallial superficial layers or towards the primordial olfactory bulb. In the hypothalamus (S28), GABAergic cells were observed at the intermediate and ventricular layers (Figs. 5H,I,J), exhibiting a long and intense immunoreactive process that contacts the ventricle. From S28, GABAergic cells at both postoptic and thalamic areas (Figs. 5H,I) were moderate to faintly stained, and their density begin to decrease from S31 onwards, as well as the relative size of the GABA immunonegative dorsal thalamus domain (Figs. 5A,H,I). Most of the GABAergic cells observed at the saccus vasculossus walls were located at the proximal ventricular zone exhibited at least two conspicuous processes: a short apical process that often ended as a small intraventricular protusion (Figs. 5H-J) and a long basal process that extended to the marginal zone, increasing the marginal GABAergic fiber network density. In the alar plate, the pineal organ (S30) exhibited two to five GABAergic cells per section (transverse to the stalk), showing triangular or bipolar somata, often with a short apical process and several basal

processes. At these stages (S28-S31), the distribution of the GABAergic cells through the different tegmental zones of the optic tectum was similar along its entire extension (Figs. 5H,I,L). In the caudal prosencephalic/mesencephalic basal plate, the tegmental GABAergic cells bands were absent at the isthmus level, emphasizing the isthmic boundary between the mesencephalon and rhombencephalon (Figs. 5I,K,M).

In the rhombencephalic tegmentum at S28, GABAergic cells formed a variable number of groups that have grown by addition of immunoreactive cells along the tegmentum. In a transverse section, the isthmic level showed four separated periventricular GABAergic cell groups (Fig. 5N), a ventral group at both sides of the midline, a dorsal group extended through the alar plate near the ventricle, and two small groups located in a medial position just ventral to the sulcus limitans of His. However, at the VII-VIII nuclei nerve root level, the same five periventricular groups described at previous stages were observed (Figs. 5O,P). At the obex level, the rhombencephalic tegmentum showed three conspicuous GABAergic cell groups with a similar process orientation observed in rostral levels (Figs. 5Q,R). In the basal plate, two small GABAergic cell groups were observed at the ventricle and dorsal intermediate zone, while at the alar plate an enlarged GABAergic cell group was observed in almost the entire area being absent at the dorsalmost zone (Fig. 5R). The dorsalmost GABAergic cells of the viscerosensory column have increased considerably their density at this stage (Figs. 5Q,R). In saggital sections, extending throughout the viscerosensory lobe at the level of the facial nerve entrance, a large number of GABAergic cells exhibited round darkly stained somata with long ventral processes that together with the visceromotor column-associated cell groups formed a columnar GABAergic pattern (Fig. 5S). In the cerebellum (S29), a band of GABAergic cells were seen at the thick intermediate zone extended throughout most of the cerebellar plate, probably mostly consisting of Purkinje cells, although some GABAergic cells were also observed at the ventricular zone. In transverse sections through the lateral walls of the rostral spinal cord (S28), despite of the GABAergic CSF-c cells at the ventral region, two main groups of non-CSF-c pear-shaped GABAergic cells were observed extending along the

cord, one ventrolateral and the other dorsolateral, with a thin band of negative cells separating them (Fig. 5T).

In saggital sections at these stages (S28-S31), the diencephalon and mesencephalon presented a dense network of both longitudinal and transverse GABAergic fibers mainly at lateral levels (Figs. 5A,G,H,I). Some transverse GABAergic fibers were observed coursing between the postoptic area through the ventral preoptic area and the subpallium (Figs. 5H,I; 6). Longitudinal GABAergic fibers were also observed coursing through the dorsal postoptic region, connecting the rostral diencephalic GABAergic nuclei with those of the caudal telencephalon, probably representing the supraoptic tract (SOT; Figs. 5A,H; 6), or coursing caudally through the ventral marginal walls of the rostral and medial hypothalamus, representing the hypothalamic-hypopheseal tract (hht; Figs. 5H,I,J; 6). Some longitudinal GABAergic fibers of the medial longitudinal fascicle were observed innervating the caudal hypothalamus (paraventricular organ and posterior recess organ; Figs. 5H,I; 6). Also in the caudal hypothalamus (S31), a conspicuous GABAergic fiber tract connected the hypothalamic ventral walls with the saccus vasculosus (Figs. 5J; 6) through the hypothalamic commissure. At these middle-late stages, the main transverse and longitudinal GABAergic fiber pathways were observed at the prosencephalon (Figs. 5A,G,H,I; 6).

Along the rhombencephalic tegmentum, a dense network of transverse GABAergic fibers were sent from the dorsalmost GABAergic groups to the ventral intermediate zone of the tegmentum, that together with the dorsal intermediate and the entire marginal zone exhibited numerous small longitudinal GABAergic fiber bundles (Figs. 5M-S). Three main longitudinal GABAergic fiber clusters were seen located in the intermediate and marginal layers adjacent to the GABAergic cell groups, two at the basal plate (ventral and lateral medial longitudinal fascicle; Figs. 5N,O,Q,S; 6) and one at the ventral region of the alar plate (dorsal longitudinal tract; Figs. 5M,N,O,Q; 6). The marginal zone also showed numerous transversal GABAergic fibers that together with some apical processes of the GABAergic cell groups cross the midline ventrally and dorsally respectively (Figs. 5N,O,Q). In the spinal cord, GABAergic cells of the

ventrolateral column (mostly cells of the ventral subgroup) gave rise to commissural axons coursing in a conspicuous ventral commissure (Fig. 5T). At later stages (S29-S31) GABAergic fibers were mainly distributed in the lateral and ventrolateral regions, while the dorsal region of the spinal cord lacked a marginal layer with GABAergic fibers. These fiber regions are the probable primordia of the lateral and ventral funiculi, respectively.

Late developmental period (S32-S34)

Stages 28-31 (S28-S31)

The GABAergic cells and fibers distribution in the prosencephalon, rhombencephalon and spinal cord at these late stages might represent the mature organization of the GABAergic system in the dogfish CNS (Fig. 1g), similar to that seen later in adults. At S32, the general organization pattern of GABAergic cells in the telencephalon (Fig. 7A) is basically similar to that observed in later stages (S34; Figs. 7B,D), being this "mature" organization characterized by an abundant GABAergic cells at the dorsal (pallial) telencephalon and scarce GABAergic cells and abundant fibers at the ventral (subpallial) telencephalon. From S32, some faintly GABAergic cells were observed in the granule layer of the olfactory bulbs (Figs. 7B,C) and at the subpallial region of the basal superficial area (Figs. 7B,D). At these stages, a few faintly stained GABAergic CSF-c cells were observed in the preoptic area and at the basal hypothalamus, spreaded along the ventral and lateral periventricular walls (Figs. 7E,F). Similar to these faintly stained GABAergic cells at the hypothalamus were also observed at the postoptic area, posterior tubercle, posterior recess organ, pineal organ and saccus vasculosus (Figs. 7E,F). At these late stages (S32-S34), a few GABAergic cells were observed the basal layers of the optic tectum densely innervated by GABAergic fibers (Fig. 7G). In the lateral intermediate zone of the cerebellar body (Fig. 7H), GABAergic cells were seen in three layers: forming a thin transient band that lay below a negative fiber layer, a thick Purkinje cell layer mostly consisting of faint GABAergic perikarya and a thin primordial molecular layer that contains densely

grouped small highly GABAergic cells, presumptively stellate cells, and thin GABAergic processes. The primordial granular layer was broader close to the thick dorsomedial ventricular zone and contained faintly GABAergic cells (putative Golgi cells) and GABAergic synaptic buttons associated to primordial glomeruli (not shown).

In S32-S34 GABAergic cells were gathered in several groups along the rhombencephalic tegmentum, diminished in density and staining intensity (Figs. 7H-K), being mainly observed in transverse sections at the periventricular region of the dorsolateral basal plate from the isthmus to the caudal trigeminal nuclei nerve root level (Figs. 7H-J). The distribution of GABAergic perikarya in the spinal cord (S32-S34) showed two groups of non-CSF-c GABAergic perikarya (dorsal and ventral to Stieda's fascicle) and also showed GABAergic CSF-c cells whose perikarya were located at different ependymal levels surrounding the central canal (Figs. 7L,M) and in the most ventral region of the dorsal walls (Fig. 7L). In addition to these cells, faintly GABAergic neurons were observed in the ventral and dorsal horns (Figs. 7L,M).

In the olfactory bulbs, some GABAergic fibers were observed in S33 at the inner olfactory layers (granular and mitral cell layers) while at S34 the glomeruli were innervated by a GABAergic dendritic arborization pattern (Figs. 7B,C), also observed at juveniles and adults. At S34 and in contrast with the previous stages the entire hypothalamic regions were intensely innervated by a dense network of thin GABAergic longitudinal and transverse fibers and boutons similar to adult (Figs. 7E,F). At S32 and on the basis of GABAergic fiber pattern observed at this region, we could recognize the different layers seen later in the adult optic tectum (Fig. 7G): the stratum medullare externum contained numerous GABAergic fibers that form longitudinal bundles; the stratum cellulare externum showed scarce GABAergic fibers; the stratum cellulare internum contained abundant transverse beaded GABAergic fibers; the stratum medullare internum was almost absent of GABAergic fibers; the stratum cellulare internum (periventricular) contained numerous GABAergic fibers that exhibit an intense immunoreactivity; and the stratum fibrosum showed no GABAergic fibers. From the rhombencephalic GABAergic cell populations, long commissural GABAergic

transverse bundle fibers were seen coursing medially through the tegmentum and crossing dorsally the midline. Although some transverse GABAergic fibers were also seen at the dorsal region of the alar plate and marginal areas, most of them were packed in conspicuous longitudinal bundles located all over the tegmentum, being mainly abundant in the alar plate and in the viscerosensory lobe (Figs. 7H-K). The midline region was absent of GABA immunoreactivity apart from the commissural fibers that crossed it dorsally and ventrally (Figs. 7I,J). At the area postrema level, longitudinal GABAergic fibers were located mainly at the marginal areas of the tegmentum (Fig. 7K). In the granular layer of the cerebellar body (Fig. 7H), numerous intensely GABAergic boutons and fibers were observed among small cell bodies as well as in the fiber region below the Purkinje cell layer. In the spinal cord (S32-S34), the densest GABAergic innervation was observed in the dorsal horns and at the marginal nucleus (Fig. 7L), which contained compact bundles of GABAergic fibers. In sagittal sections, numerous GABAergic fibers could be observed coursing longitudinally, often forming compact bundles as in the dorsal horn and lateral funiculus, or being more homogeneously distributed as in the ventral funiculus (Fig. 7L).

Distribution of GABAergic cells and fibers in juveniles and adults

In juveniles, as in adults, the GABAergic system was completely developed, and therefore the dense GABAergic innervation observed in the brain and spinal cord makes difficult the somata identification. Although, the mature GABAergic cell and fiber distribution pattern observed in juveniles was similar to adults, these structures showed a high density and immunostained in juveniles (Figs. 8A-S).

In the olfactory bulbs, some GABAergic cells were observed at both granular and glomerular layers of juveniles (Figs. 8A,B). In the pallium, GABAergic cells were abundant in the dorsal and medial pallium but absent in the lateral pallium (Figs. 8A-C). In the subpallium, GABAergic cells were relatively scarce in the area periventricularis ventrolateralis, basal superficial area and olfactory bulb, being absent from septal regions. Interestingly, the basal superficial area contained abundant immunonegative

cells with their somata and dendrites densely covered by GABAergic boutons (Fig. 8C). The organization of the GABAergic cells in the rostral diencephalon of juveniles was roughly similar to that described at previous stages. The preoptic area, postoptic area, posterior recess organ, the posterior tubercle and the optic tectum showed some scattered GABAergic cells at juveniles (Figs. 8C-H) but not in adults. However, GABAergic cells were observed in juveniles at the habenula (Fig. 8E), pineal organ (Fig. 8E), hypothalamus (Figs. 8F-H) and mesencephalic tegmentum (Figs. 8H,I). In the rhombencephalic tegmentum of juveniles, two GABAergic cell groups were observed caudally to the acusticofacial nerve nucleus level. These GABAergic cells were arranged in several subgroups and exhibited a weak positivity, being located at the basal plate (reticular formation; Figs. 8M-Q), while at the viscerosensory lobe (Figs. 8M-O) a conspicuous GABAergic cell group exhibited a moderate to intense immunoreactivity. In the cerebellum (Figs. 8J-N), GABA immunoreactivity was absent from the ventricular zone of the granular eminences, weak in Purkinje cells, moderate in Golgi cells of the granular layer and in stellate cells of the molecular layer. In the juvenile spinal cord, GABAergic neurons were observed in the dorsal horns, around the central canal, in the ventral horns, and in interstitial location in the white matter (Figs. 8R,S).

In the olfactory bulb, GABAergic fibers were observed in all the olfactory layers except the marginal olfactory fiber layer, although the richest GABAergic innervations was observed in the granular layer and at the glomeruli (Figs. 8A,B). Within the telencephalon, GABAergic fibers were mainly innervating the superficial dorsal pallium, the olfactory tract nucleus described in elasmobranchs by Smeets (1983), and the basal superficial area (Figs. 8A-C). In this subpallial region at caudal levels, numerous GABAergic boutons were observed surrounding immunonegative cells (Fig. 8C). In the preoptic area (Fig. 8D), numerous GABAergic fibers and terminals were observed at the entopeduncular and preopticomagnocelular nucleus. These longitudinal fibers formed the main tracts between the telencephalic and the diencephalic nuclei. In the hypothalamic floor, some longitudinal GABAergic fibers formed the faint hypothalamic-hypopheseal tract (Figs. 8F-I) that innervates the neurointermediate lobe

with numerous GABAergic fiber terminals and boutons. Moreover, GABAergic fibers and terminals were mainly seen at the hypothalamic lobes, infundibular walls, lateral and posterior recess. The dense network of GABAergic fibers found in the mesencephalon and diencephalon of juveniles was similar to that observed in S32, being the lateral region of the thalamus one of the most GABAergic innervated regions of the prosencephalon together with the infundibular walls of the hypothalamus (Figs. 8F-I). The epithalamus presented two relatively dense innervated neuronal systems by GABAergic fibers and boutons that are the pineal organ and the habenula (Fig. 8E). The pineal organ showed some smooth GABAergic fibers that coursed longitudinally along the pineal stalk (Fig. 8E), while GABAergic boutons were observed contacting massively some cells of the pineal. The distribution of the GABAergic fibers through the different layer of the optic tectum resembles that observed at previous stages, being the extratum medullare externum and internum the denser layers (Figs. 8F-I).

The entire extension of the rhombencephalic tegmentum exhibited GABAergic fibers (Figs. 8J-Q) and they were mainly located in the central grey and lateral to the interpeduncular nucleus at the isthmus level, in the viscerosensory column caudally to the trigeminal nerve nucleus level, in the vagal lobe nucleus and in the oliva inferior at the area postrema. In the cerebellum (Figs. 8J-N), an intense immunoreactivity to GABA was seen in Golgi cell terminals around glomeruli of the granular layer, in fibers of the molecular layer and in synaptic boutons contacting somata and dendrites of Purkinje cells. The juvenile spinal cord was richly innervated by GABAergic fibers (Figs. 8R,S), being the pattern of GABAergic innervation roughly similar to that observed in S33, although the number of GABAergic boutons in dorsal areas of the dorsal horn was increased considerably and boutons were scattered throughout a wider region.

DISCUSSION

The development of the GABAergic cells and fibers was investigated in the CNS of dogfish, which represents the first study of the development of the GABAergic system in the entire brain of an elasmobranchs. One major finding was the labeled GABAergic cells observed in early stages, indicating that GABA is synthesized in some of the earliest neuronal types. Other remarkable features in the dogfish GABAergic system development are: a) the palliopetal tangential migration displayed by subpallial GABAergic neurons, similar to that reported in mammals; b) the segmental distribution of the GABAergic cell populations exhibiting a clear neuromeric pattern, and c) the early establishment of the GABAergic axonal scaffold that will constitute the complex neuronal networks characteristic of the mature brain.

Chronology of the development of the GABAergic populations in dogfish: comparison with other vertebrates

In the present study we have compared the relative order of appearance of the various GABAergic groups in the dogfish CNS with those reported in other vertebrates, as shown in Table II. This comparison, especially with other fish groups, has shown some interesting differences and many similarities.

The main similarity with other developing vertebrates was that the first GABAergic cells identified were observed at very early stages of development. In dogfish, some GABAergic cells were already observed in several brain areas at S22, when the early organogenesis is taking place. Although we have not studied earlier embryonic stages, the scarcity and weak immunoreactivity of the GABAergic cells observed at S22 suggest they represent the earliest differentiating brain GABAergic cells. Clusters of GABAergic cells have also been observed in the early brain of cyclostomes (*Petroyzon marinus*: Meléndez-Ferro et al., 2002, 2003; E11), teleosts (*Gasterosteus aculeatus*: Ekström and Ohlin, 1995; 51 hours postfertilization-hpf-); *Danio rerio*: Doldán et al., 1999; 16 hpf), amphibians (*Xenopus laevis:* Barale et al., 1996; stages 35/36) and

mammals (mouse: Katarova, 2000; E10.5), indicating that the early differentiation of brain GABAergic cells is a common feature among vertebrates.

The order of appearance of the different GABAergic populations in dogfish is roughly similar to that reported in other vertebrate groups, as indicated in table II. The GABAergic cells located in the basal plate of the prosencephalon (postoptic area, nucleus of the medial longitudinal fascicle), rhombencephalon and rostral spinal cord were the earliest populations observed both in dogfish (S22) and most vertebrate groups (see table II). After this early stage, new GABAergic groups were added in the dogfish prosencephalon (S23), being observed at the ventral telencephalon (subpallium), caudal prosencephalic tegmentum, and the posterior commissure. GABAergic cells have been reported in the posterior commissure nucleus (pretectum) of other vertebrates at middle-early developmental stages (*cyclostomes:* Meléndez-Ferro et al., 2002, 2003; *teleosts:* Ekström and Ohlin, 1995; *amphibians:* Barale et al., 1996), while it is one of the first to appear in mammals (Katarova et al., 2000). At the end of the first third of the total dogfish embryonic period, GABAergic cells were seen in the hypothalamus and ventral thalamus (S24), in the optic tectum (S25) and at the preoptic area, saccus vasculosus, cerebellum and spinal cord (GABAergic CSF-c cells) at S26. From all of these GABAergic populations, the postoptic groups have been reported in all vertebrates as one of the first to appear, except in mouse (Katarova et al., 2000) where it develops late in development (see table II). In dogfish, from S27, GABAergic cells appeared in the habenula, caudal hypothalamus (posterior tubercle nucleus, posterior recess organ) and at the dorsal rhombencephalon (the viscerosensory column). In other vertebrate embryos, the GABAergic populations of the posterior recess walls and viscerosensory area have been also reported in middle stages of development (middle-appearing populations) although in mammals and amphibians, GABAergic cells of viscerosensory, were seen in early stages (Barale et al., 1996; Katarova et al., 2000). Moreover, while the caudal hypothalamic GABAergic cells (posterior tubercle nucleus) were first observed in middle dogfish stages, as reported in teleosts (Ekström and Ohlin., 1995), in cyclostomes GABAergic cells in similar location appeared very early (Meléndez-Ferro

et al., 2002). In the dogfish telencephalon, pallial GABAergic cells were first observed at S28 (probably after migrating tangentially from the subpallium, see below) and also in most vertebrate studied pallial GABAergic cells were also observed at middle-late embryonic stages (table II). The later GABAergic cells to appear in dogfish were located at the pineal organ (S30) and at the olfactory bulb (S32). GABAergic cells have being also reported at later stages in the olfactory bulb of cyclostomes (*Petroyzon marinus:* Meléndez-Ferro et al., 2002), teleosts (*Danio rerio:* Doldán et al., 1999) and amphibians (*Xenopus laevis:* Barale et al., 1996), while in mammals (mouse: Katarova et al., 2000) GABAergic cells were observed in the olfactory placode from early stages (E10.5).

However, large temporal differences among vertebrates were noted in the chronological appearance of the GABAergic cells at the ventral thalamus and optic tectum. Whereas in dogfish the ventral thalamic cells appeared at middle-early stages (S24), as in amphibians (Barale et al., 1996) and mammals (Katarova et al., 2000), they were observed later in other fish groups (*cyclostomes:* Meléndez-Ferro et al., 2002; *teleosts:* Ekström and Ohlin, 1995). Moreover, the middle-early appearance of the GABAergic cells of the dogfish optic tectum was in contrast to that reported in the rest of embryonic vertebrates studied, where this population developed rather late (table II).

In dogfish the major density of GABAergic cells was observed at S30, when numerous populations expanded along the entire CNS. However, from S31 to adults, most of these populations have decreased drastically in density and in juveniles very few GABAergic cell clusters were observed in the dogfish brain and spinal cord, similar to that reported in adults (Sueiro, 2003). Therefore, these results point to a transient GABA expression in some brain regions such as the pre- and postoptic areas, hypothalamus (except in the saccus vasculosus and in some CSF-c cells of the paraventricular organ), epithalamus, mesencephalic and rhombencephalic tegmenti, viscerosensory column, cerebellum and spinal cord (table I). A transient GABA expression has been also reported in some cells of the amphibian hypothalamus (Barale et al., 1996), in chick motoneurons (Von Bartheld and Rubel, 1989) and in retinal

horizontal cells of mammals (Versaux-Botteri et al., 1989). The mechanisms underlying this transient GABA expression are thought to be the programmed cell death (apoptosis) or a phenotypic switch (Barale et al., 1996).

In general, the relative order of appearance of the different GABAergic populations observed in the dogfish CNS is roughly similar to that reported in most vertebrate embryos, which indicates either the importance of the early functional maturation of the different brain regions during development and also the conserved expression of the main GABAergic centers at the CNS among vertebrates.

Neurogenesis and migration of GABAergic neurons: the dogfish telencephalon as model

In the telencephalic hemispheres, GABAergic cells were observed at very early stages (S23) in ventral areas (subpallium), increasing in density progressively through the subsequent stages until reaching the maximum density at S30. From S31 to juveniles, the subpalial GABAergic cells decreased progressively in density and remained restricted to some conspicuous clusters at the lateral subpallium, basal superficial area and ventrolateral periventricular area. In the pallium, however, the first GABAergic cells were observed very late (S28) with respect to the subpallial ones and their morphology and location (extended along the rostral superficial zone) is compatible with a tangential migration from the subpallial walls (see below). The mature organization of GABAergic pallial cells was observed from S33 onwards.

At early stages of development, the neuroepithelial walls of the dogfish neural tube yielded three distinct layers from pial to ventricular surface: the marginal zone (MZ), the intermediate zone (IZ), and the germinal layer also named the ventricular zone (VZ). Over the past century, studies on developing telencephalic regions of brain have provided evidence for a radial migration pathway, responsible of the primary mechanism in layering formation. A similar layering process can be distinguished in dogfish following the spatiotemporal distribution of GABAergic cells in the brain walls, especially in those of the ventral telencephalon. It begins when early differentiated GABAergic cells of the neuroepithelial walls appear subventricularly and farest (S23),

apparently leaving the VZ, to turn radially to the IZ and even to the MZ (S25). This predominant direction of movement is evident later (S26), when the density of GABAergic cells increased in the three layers but specially in the IZ and abundant fibers were packed in the IZ and MZ. This radial migration process of GABAergic cells was also observed at the dome-shaped protrusions located at the laterorostral walls of the ventral telencephalon, clearly evident at S28-S31 (see Figs. 5D,G), from where GABAergic cells seemed to begin a tangential migration (see below). We consider that these lateral eminences of the dogfish ventral telencephalon may be the possible homologous of the lateral ganglionic eminences of mammals. From these mammalian structures, GABAergic cells migrate radially into the region of the striatal mantle (Wichterle et al., 2001; Anderson et al., 2001), before taking the tangential route to the future cortex (De Carlos et al., 1996; Tamamaki et al., 1997; Tanaka et al., 2006).

From S28, a tangential migration process was displayed by some GABAergic neurons observed first in the subpallial eminences and then in the marginal and intermediate zones of the pallium, similar to those of well-characterized tangentially migrating cells in the cortex of mammals (Anderson et al., 1997; Tamamaki et al., 1997; Lavdas et al., 1999; Anderson et al., 2001; Marín and Rubenstein, 2001; Jiménez et al., 2002). GABAergic cells with branched leading processes directed towards the ventricle were also observed, as in mammals (Nadarajah et al., 2002). In dogfish, these cells are most frequent just in the border of the subpallium, suggesting that they are seeking for the migration pathways. In this study we have demonstrated two tangential migration pathways of subpallial-derived neurons in the developing dogfish telencephalon (superficial and intermediate), similar to those reported in mammals (de Carlos et al., 1996; Tamamaki et al., 1997; Marín and Rubenstein, 2001; Jiménez et al., 2002; Tanaka et al., 2006). The superficial pathway starts at S28, when some GABAergic subpallial cells extend medially throughout the pallium margin. The intermediate pathway of tangential migration starts also at S28 when GABAergic cells pass through the dome-shaped protrusion. Palliopetal migrating GABAergic cells continue dorsalward into the ventral, lateral, dorsal and medial pallial subdivisions (S28-S32).

The tangential migration pathways reported in mammals appear to have distinct telencephalic origins, including the medial (Chapouton et al., 1999; Sussel et al., 1999; Lavdas et al., 1999; Wichterle et al., 1999; Anderson et al., 2001; Polleux et al., 2002; Valcanis and Tan, 2003), lateral (de Carlos et al., 1996; Tamamaki et al., 1997; Anderson et al., 2001; Jiménez et al., 2002), or caudal (Nery et al., 2002; Xu et al., 2004; Yozu et al., 2005) ganglionic eminences, showing the complex nature of the mammalian cortex. At the end of the mammalian development, a multidirectional tangential migration seemed to take place in all laminar zones of the pallium (for reviews, see Parnavelas, 2000; Marín and Rubenstein, 2001, 2003; Tanaka et al., 2006), and interestingly a similar process appears to occur at later stages of dogfish development (from S32).

In the pallium of mammals, the GABAergic interneurons are known to populate the cortical layers with a radial inside-out neurogenesis gradient of migration (Luskin et al., 1993; Mione et al., 1994; Tan et al., 1998; Parnavelas, 2000; Marín and Rubenstein, 2001, 2003; Anderson et al., 2001; Ang et al., 2003; Valcanis and Tan, 2003; Hevner et al., 2004; Yozu et al., 2005), oriented by radial glial cells. As in mammals (E17), the radial migration of the dogfish pallial GABAergic cells was observed at later stages of development (from S32). This radial migration in the pallium seemed to work as a structural process in the neuronal diversity, being also observed in most regions of the dogfish SNC (i.e. hypothalamus, optic tectum, rhombencephalic tegmentum, cerebellum and spinal cord), in order to stratify the future GABAergic system (for review, see Marin and Rubenstein, 2001, 2003).

The GABAergic cell groups in the developing CNS in dogfish

Prosencephalic GABAergic populations

Olfactory bulb

During middle-to-late development (S29-S32), some GABAergic cells of ventral telencephalon appeared to invade the olfactory bulb through a lateral migration route. Several studies in other vertebrates have shown that the ventral telencephalon,

probably the striatum, is the source of these GABAergic olfactory cells (*cyclostomes*: Meléndez-Ferro et al., 2002; *teleosts:* Adolf et al., 2006; Grandel et al., 2006; *birds*: Cobos et al., 2001; *mammals*: Anderson et al., 2001; Stenman et al., 2003; Vergano-Vera et al., 2006). In dogfish, the number of GABAergic cells and the intensity of immunoreaction in the olfactory bulb diminished dramatically after S33, suggesting that GABA expression in these cells may be related to the maturation of olfactory centres.

Telencephalic hemispheres

In the telencephalic hemispheres, the organization of the GABAergic system during development turned to be notably complex, as it was explained in the layering processes section. Moreover, our present results show that the ontogeny of GABAergic systems in dogfish may provide valuable information on the organization of forebrain territories and boundaries, as also seen in other vertebrate groups (Roberts et al 1987; Martinoli et al., 1990; Bennis et al., 1991; Naujoks-Manteuffel et al., 1994; Ekström and Ohlin, 1995; Barale et al 1996; Katarova et al., 2000; Meléndez-Ferro et al., 2002). As observed in teleosts (Ekström and Ohlin, 1995; Martin et al., 1998) and lampreys (Meléndez-Ferro et al., 2002), in mid-early dogfish embryos (S26-S28) GABAergic cells are only found in the subpallium, indicating that GABA/GAD are subpallial markers during early development stages. In these stages (S26-S28), the rostral subpallium at lateral levels was characterized by the sharp limit between the region containing GABAergic cells and the remainder telencephalon, defining the pallio-subpallial boundary. These results show that the sulcus limitans (the rostral sulcus of the telencephalic neuroepithelium; Smeets et al., 1983) in the lamina terminalis was not a precise morphological landmark to define the pallio-subpallial boundary, since that boundary (rostral GABAregic limit at S26) was observed slightly caudal to this sulcus.

Preoptic area and diencephalon

From S26 to S33, numerous GABAergic cells occupied the walls of the preoptic area but its density and the intensity of immunoreaction diminished dramatically after S33. Preoptic GABAergic cells also appeared at middle developmental stages in cyclostomes (*Petroyzon marinus:* Meléndez-Ferro et al., 2002; Reed et al., 2002), teleosts (*Gasterosteus aculeatus:* Ekström and Ohlin, 1995; *Danio rerio:* Doldán et al., 1999) and amphibians (*Xenopus laevis:* Barale et al., 1996) although in mouse they were already observed from early stages (Katarova et al., 2000). In dogfish, the preoptic GABAergic population was continuous with that of the subpallium (rostrally) and postoptic area (caudally).

The GABAergic postoptic group (suprachiasmatic population) developed from S22 to S32, while at subsequent stages their density and the intensity of immunoreaction diminished. A similar GABAergic cell location was reported in other vertebrate embryos (*cyclostomes:* Meléndez-Ferro et al., 2002; *teleosts:* Ekström and Ohlin, 1995; Doldán et al., 1999; *amphibians:* Barale et al., 1996 and *mammals:* Behar et al., 1994; Katarova et al., 2000). Interestingly, postoptic GABAergic cells were observed at very early stages of dogfish development, as in most vertebrate embryos studied but in mouse (Katarova et al., 2000). Although little is known about the functional implication of GABA in the CNS of elasmobranchs, in other fish GABAergic neurons of the postoptic group of fish are related with the processing of visual information (Anglade et al., 1999; Médina et al., 1994) and receive primary afferents from the retina (Pinganaud and Clairambault, 1979; Wullimann and Northcutt, 1988), enhancing the probable involvement of GABA at this area in the processing of the visual information.

In dogfish embryos, hypothalamic GABAergic cells were seen from S24, increasing their density during subsequent stages until forming a conspicuous population of CSF-c cells in the ventral and lateral infundibular walls (S26) to diminish gradually in density and staining intensity at later stages. In other vertebrate embryos, hypothalamic GABAergic cells were also reported at middle developmental stages in cyclostomes (Reed et al., 2002; Meléndez-Ferro et al., 2002), teleosts (Ekström and

Ohlin, 1995; Doldán et al., 1999), amphibians (Barale et al., 1996) and mammals (Katarova et al., 2000). In the caudal hypothalamus of dogfish, a few GABAergic cells were seen in the posterior tubercle and posterior recess walls at S27, these cells showing long processes that contact the ventricle. In other fish, GABAergic neurons appeared earlier in the posterior tubercle nucleus than in the posterior recess organ (*cyclostomes:* Meléndez-Ferro et al., 2002; *teleosts:* Ekström and Ohlin, 1995; Doldán et al., 1999), while in dogfish both populations appeared simultaneously during development (S27).

GABAergic cells appeared in the dogfish thalamus at S24, probably corresponding to the ventral thalamus. Later on (S26), these thalamic GABAergic cells were forming a band that also occupies the basal region of dorsal thalamus following the zona limitans intrathalamica. This thalamic GABAergic population increased in density during the subsequent stages of development, being continuous with the caudal GABAergic tegmental group, and rostrally with the postoptic populations. From prehatching stages, this distribution of GABAergic cells was sustained although their immunostaining intensity diminished notably, being absent in juveniles. In other fish, GABAergic cells were reported in the ventral thalamus at relative late stages of development (*cyclostomes:* Meléndez-Ferro et al., 2002, 2003; *teleosts:* Ekström and Ohlin, 1995; Doldán et al., 1999; Muller et al., 2006), while in tetrapods these GABAergic cells appeared very early (*amphibians:* Naujoks-Manteuffel et al., 1994; Barale et al., 1996; *mammals:* Behar et al., 1994; Katarova et al., 2000), similar to that observed in dogfish.

Synencephalon and mesencephalon

In the dogfish pretectum, GABAergic cells formed a packed cluster in the ventricular walls at the level of the posterior commissure from early development (S23). In the next stages (S24-S26), most of these cells exhibited a large process that losted the ventricular contact, apparently taking a dorsoventral migration route to form a conspicuous dorsoventrally enlongated pretectal group. This cell group formed a continuous band with the prosencephalic/mesencephalic tegmental group (see below).

At subsequent stages, the numerous pretectal GABAergic cells were intermingled with the profuse dorsoventral GABAergic fibers that coursed through the same region to form part of the posterior commissure tract. Mid-early appearing GABAergic cells were also reported in the posterior commissure area of other vertebrate embryos (*cyclostomes:* Meléndez-Ferro et al., 2002; *teleosts:* Ekström and Ohlin, 1995; Doldán et al., 1999; *amphibians:* Barale et al., 1996; *mammals:* Behar et al., 1994; Katarova Katarova et al., 2000), thus being a shared feature of the development of the GABAergic system among vertebrates.

From S23, GABAergic cells appeared in the synencephalic tegmentum (primordium of the nucleus of the medial longitudinal fascicle) to later (S26) extended to the rest of the ventral prosencephalon forming a continuous longitudinal band with the GABAergic hypothalamic cell population rostrally. This basal longitudinal band of GABAergic cells of the prosencephalon was still seen at the mature stages, although diminishing gradually their intensity in the posthatching phase (juveniles). In cyclostomes (Meléndez-Ferro et al., 2002), teleosts (Ekström and Ohlin, 1995; Doldán et al., 1999) and mammals (Katarova et al., 2000), GABAergic cells of the nucleus of the medial longitudinal fascicle were one of the first populations to appear, similar to that observed in dogfish, while in amphibians (Barale et al., 1996) they appeared slightly later in development (table II).

In dogfish embryos, some of the GABAergic cells of the posterior commissure (S23), just rostral to the optic tectum, were seen extending their processes through the external layers of the rostral optic tectum, to form a GABAergic cell band along the external tectal layer at later stages (S25), probably indicating a migration process. On the other hand, at S26 GABAergic cells occupied all the tectal walls showing processes crossing the IZ to reach the VZ (radial migrating morphology). These observations suggests that the optic tectum of dogfish, presents both tangential (earlier) and radially (later) migration processes, similar to that observed in the telencephalon (see above). At mid-late stages (S29-S30), GABAergic cells were mainly located at the tectal periventricular zone with a long apical process extending towards the ventricular zone,

which was absent of GABAergic somata. This GABAergic organization was roughly similar to that observed in juveniles, but differs with adults where no GABAergic cells were reported (Sueiro, 2003). GABAergic cells were also observed at the optic tectum of other vertebrates, appearing relatively late in development (Behar et al., 1994; Ekström and Ohlin, 1995; Barale et al., 1996; Doldán et al., 1999; Katarova et al., 2000; Meléndez-Ferro et al., 2002, 2003), in contrast to that observed in dogfish. This striking difference in the order of appearance of the tectal GABAergic population could represent a characteristic feature in the development of the dogfish GABAergic system in this region.

Rhombencephalic GABAergic populations

The first rhombencephalic GABAergic neurons appeared very early (S22) in the IZ of the isthmic region and also sparsely distributed along the MZ of the entire rhombencephalic tegmentum. The presence of rhombencephalic GABAergic cells from very early stages of development appear to be common in vertebrates (Roberts et al., 1987; Naujoks-Manteuffel et al., 1994; Ekström and Ohlin, 1995; Martín et al., 1998; Doldán et al., 1999; Katarova et al., 2000; Meléndez-Ferro et al., 2003), thus indicating these cells are playing a key role in the rhombencephalic development. In dogfish embryos from S23 to S26, numerous GABAergic cells formed a dorso-ventral column in the isthmic region, which may correspond to the GABAergic cells observed in the early rostral rhombencephalon of other vertebrates (*cyclostomes:* Meléndez-Ferro et al., 2003; *teleosts:* Ekström and Ohlin, 1995; Martin et al., 1998; Doldán et al., 1999; *amphibians:* Roberts et al., 1987; Naujoks-Manteuffel et al., 1994; Barale et al., 1996; *mammals:* Lauder et al., 1986; Katarova et al., 2000). In the rest of the dogfish rhombencephalic tegmentum, as in the isthmus, GABAergic cells also exhibited a dorso-ventral orientation complatible with a possible dorso-ventral/radial migration. These GABAergic cells were gathered in several repetitive conspicuous groups, setting in a segmental organization related with the rhombomeric boundaries described in

Scyliorhinus embryos by Kuratani and Horigome (2000) (see below). In teleosts, GABAergic cells of the rhombencephalon were also grouped in clusters (Ekström and Ohlin, 1995; Doldán et al., 1999), being three (periventricular, medial, and lateral) the GABAergic groups reported in cyclostomes (Meléndez-Ferro et al., 2003) and two (medial and ventral) that of amphibians and mammals (Roberts et al., 1987; Naujoks-Manteuffel et al., 1994; Katarova et al., 2000). This spatial repetitive organization of GABAergic cells in conspicuous clusters along the vertebrate rhombencephalon was taken as evidence for a rhombomeric organization of the rhombencephalon, as observed in dogfish (present results).

The numerous GABAergic cell groups observed at different rhombencephalic levels in early dogfish embryos formed longitudinal columns along the tegmentum. From S28 to S31, three main longitudinal columns were clearly distinghised, while a fourth column was formed caudally by the GABAergic cells of the viscerosensory column. These four longitudinal GABAergic columns correspond to the four sensory-motor columns: somatosensory, viscerosensory, visceromotor, and somatomotor columns. From S31 to juveniles, GABAergic cells were almost absent from the rostral rhombencephalic tegmentum, being restricted to the reticular (basal plate) and to the viscerosensory column (alar plate), showing a close relation with the branchiomotor nuclei distribution. GABAergic cells have been also described in the developing viscerosensory lobe and associated nuclei of other vertebrates (Roberts et al., 1987; Naujoks-Manteuffel et al., 1994; Ekström and Ohlin, 1995; Martín et al., 1998; Doldán et al., 1999; Katarova et al., 2000; Meléndez-Ferro et al., 2003), whereas three longitudinal bands of rhombencephalic GABAergic cells (ventral alar, dorsal basal and ventral basal bands) exist in lamprey (late prolarvae: Meléndez-Ferro et al., 2003), salamander (stage 34: Naujoks-Manteuffel et al., 1994) and mouse (E11.5: Katarova et al., 2000). It has been suggested that this columnar organization of GABAergic cells, arranged in several longitudinal bands throughout the rhombencephalic tegmentum, has a multineuromeric origin (Meléndez-Ferro et al., 2003). Our present results also support this idea, on the basis of the observation of discreet GABAergic groups at mid-early

stages (S26-S28) that grow in density and merged between them, which led to the formation of these continuous longitudinal columns. The chronological appearance of dogfish rhombencephalic GABAergic cell groups, firstly in the isthmic region followed by the caudal and intermediate tegmental regions, also reported in the sea lamprey (Meléndez-Ferro et al., 2003), together with the formation of the longitudinal bands later, reinforce the idea of a multineuromeric origin of the fish GABAergic groups differentiated by dorsoventral pattern clues (Liu and Fetcho, 1999; Gahtan et al., 2002; Meléndez-Ferro et al., 2003). Moreover, in amphibians GABAergic interneurons are thought to develop along these longitudinal GABAergic cell columns (Naujoks-Manteuffel et al., 1994), probably indicating the functional maturation of sensory and motor systems at these developmental stages in vertebrates.

The early GABAergic cells observed in the cerebellum during dogfish development were located at the rostral portion at S26, probably coursing from the isthmic dorso-ventral GABAergic cell column observed at the previous stage. At late stages (S31-S32), the mature GABAergic organization reported in the adult cerebellum (Álvarez-Otero et al., 1995, 1996; Sueiro, 2003) was already recognized, and GABAergic cells were occupying the molecular layer (stellate cells), the Purkinje cell layer and the granular layer (Golgi cells). The GABAergic Purkinje cells, Golgi cells and stellate cells seemed to originate from the cerebellar body ventricular zone, although the order of appearance could not be assessed. Moreover, taking the position of GABAergic cells with perikarya or processes included in the ventricular zone as a marker of the origin of these cells, in the cerebellar body the GABAergic cells originate from an intermediate-lateral longitudinal region of the cerebellar plate, and not from the thick medial ventricular zone which at later stages gives rise to most granular cells. In mammals, the cerebellar GABAergic interneurons originate from a common pool of precursors (Leto et al., 2006), which reminds our observations in the dogfish cerebellar body. The differential origin of neurons of molecular/Purkinje cell layers appears clearly related to the topographical segregation between the granular and the molecular/Purkinje cell layers observed in dogfish cerebellum. Late-appearing GABAergic cells were also

reported during cerebellar development in teleosts (*Gasterosteus:* 114h embryo; Ekström and Ohlin, 1995) and mammals (rat: E17; Behar et al., 1994; mouse: E11.5; Katarova et al., 2000). GABAergic cells were present in the different cerebellar layers of all gnathostomes, and appeared rather late in development, which represent a common feature of the cerebellar GABAergic system.

Spinal GABAergic populations

In the embryonic rostral spinal cord of dogfish, GABAergic cells were observed in the earliest stage studied (S22), in which the spinal cord presents an almost neuroepithelial appearance, reinforcing the idea that GAD/GABA is expressed in some of the earliest cell types. At S26, dorsal and ventral groups of GABAergic perikarya were present in the mantle layer throughout most of the spinal cord length, being the CSF-c GABAergic cells restricted to the ventral wall (floor plate). Later in development (S28), GABAergic cells increased in density and formed two well-defined longitudinal columns along the lateral wall (ventrolateral and dorsolateral columns) of the spinal cord. At late stages (S32-S34) GABAergic cells were observed surrounding the central canal (CSF-c), at the dorsal peryependymal region and in the ventral and dorsal horns, resembling the mature (juveniles and adults) GABAergic cell organization in the spinal cord. The developmental pattern of GABAergic cell organization observed in dogfish spinal cord is similar to those reported with anti-GABA antibodies in other fish embryos (*cyclostomes:* Meléndez-Ferro et al., 2003; *teleosts:* Ekström and Ohlin, 1995; Martin et al., 1998). Moreover, GABAergic CSF-c cells (Kolmer-Aghdur cells) have been also reported in other vertebrate spinal cord at early stages (*cyclostomes:* Meléndez-Ferro et al., 2003; *teleosts:* Bernhardt et al., 1992; Ekström and Ohlin, 1995; Martin al., 1998; *amphibians:* Dale et al., 1987a,b; Roberts et al., 1987; Barale et al., 1996; Binor and Heathcote, 2001), similar to that observed in dogfish (S26), although they were not observed in mammal embryos (Phelps et al., 1999). Taken together, observations in the spinal cord of different vertebrate groups reveal a rather well-conserved developmental pattern as regards the GABAergic system.

The roles of GABA in the early developing brain

The early development of GABAergic neurons and the sequential appearance of the several GABAergic neuronal clusters observed in the dogfish CNS is compatible with the idea that GABA is one of the first neurotransmitters to appear in the brain of vertebrates (Roberts et al., 1987; Aoki et al., 1989; Ekström and Ohlin, 1995; Meléndez-Ferro et al., 2002, 2003). It is though that GABA play a relevant role as an excitatory transmitter in the immature CNS, acting as a trophic factor for developing neurons, controlling cell proliferation, neuroblast migration and dendritic maturation during vertebrate brain development (Madtes and Redburn, 1983; Meier et al., 1991; Cherubini et al., 1991; Lauder et al., 1993, 1998; LoTurco et al., 1995; Barker et al., 1998; Ji et al., 1999; Katarova et al., 2000; Takayama and Inoue, 2004; Represa and Ben-Ari, 2005). Studies on cultured cerebellar cells of primates have demonstrated that GABAergic axons innervate migrated cells prior to the appearance of $GABA_A$ receptors and its subsequent GABA immunoreactivity (Meinicke and Rakic, 1992). This data indicated that the trophic effects of GABA on early migrated neurons enhanced the expression of $GABA_A$ receptor in those migrating cells and that is thought to play an important role in cell proliferation, migration, or the onset of neuronal differentiation during early embryogenesis (Ma and Barker, 1995; Lauder et al., 1998). In the present study we have observed that the first GABAergic cells of the early positive clusters (i.e. the rhombencephalic GABAergic cell groups) project axons that innervate regions where the subsequent GABAergic groups appear, suggesting a role on the control of the onset of differentiation processes of GABAergic cells during the dogfish CNS development.

As described in other vertebrates (Lo Turco and Kriegstein, 1991; Ekström and Ohlin, 1995; Martín et al., 1998; Doldán et al., 1999; Katarova et al., 2000; Meléndez-Ferro et al., 2003), in dogfish embryos from S23 to S31, GABAergic neuroblasts formed columnar clusters within the ventricular zone in the posterior commissure, ventral thalamus, postoptic area, infundibular walls, optic tectum, basal prosencephalon, rhombencephalon, cerebellum and spinal cord. This GABAergic neuroblasts exhibited a

bipolar morphology resembling a CSF-c cell type, with one thick process contacting the ventricle and a long apical process. The idea that this GABAergic neuroblast of the ventricular zones migrate to the definitive sites of terminal differentiation to form the mature GABAergic cell populations, has been proposed by Behar and colleagues (1994) and is consistent with our present results in dogfish. Moreover, at late stages (S32-34), GABA was detectable in all brain regions that have been reported in the adult dogfish, supporting the idea of Behar and colleagues (1994) that at late stages of brain development, many cells may already presented the mature GABAergic phenotype, releasing GABA as inhibitory neurotransmitter.

Segmental organization of the GABAergic populations in the dogfish brain

GABAergic pattern and prosomeric model

During development, GABAergic cell populations of the dogfish prosencephalon form discrete domains, alternatively with regions devoid of labelled cells, as also reported in other vertebrate groups (*cyclostomes*: Meléndez-Ferro et al., 2002; *teleosts*: Ekström and Ohlin, 1995; Doldán et al., 1999; Higashijima et al., 2004; *amphibians*: Roberts et al., 1987; Naujoks-Manteuffel et al., 1994; Barale et al., 1996; *mammals*: Katarova et al., 2000). The organization of these domains in the dogfish forebrain follows the simplified prosomeric model proposed by Puelles and Rubenstein (2003) that subdivided the caudal diencephalon of mouse in three segments or prosomeres (p1-p3). According to this model, the secondary prosencephalon comprises the telencephalon, the preoptic area and the hypothalamus (the rostral diencephalon), being considered a complex protosegments not subdivided into prosomeres in vertebrates. Our present results also support this observation since GABAergic cells of the ventral telencephalon, preoptic area and rostral diencephalon (postoptic groups), although firstly being separated populations, eventually formed a continuous cellular band, without conspicuous boundaries. In the caudal prosencephalon, the alar plate of the third prosomere (p3) corresponds to the ventral thalamus, where two adjacent GABAergic populations, dorsal and ventral, were distinguished, the dorsal group being

formed by GABAergic cells with ventricular process. The zona limitans intrathalamica is considered the limit between p2 and p3 (Puelles and Rubenstein, 1993). In dogfish, a conspicuous tract of GABAergic fibers were also seen coursing through this area, connecting the GABAergic medial longitudinal fascicle (basal plate) with the dorsal diencephalic tract (alar plate). Shortly caudal to the zona límitans intrathalamica, a thin GABAergic cell band was seen, probably representing the immunopositive cell band of the dorsal thalamus, although most extension of this p2 domain is immunonegative. The absence of GABAergic cells in part of the dorsal thalamus has been also reported in other vertebrates (*lampreys*: Meléndez-Ferro et al., 2002 *teleosts*: Martinoli et al., 1990; Ekström et al., 1995; Doldán et al., 1999; Higashijima et al., 2004; *amphibians*: Naujoks-Manteuffel et al., 1994; Barale et al., 1996; *mammals*: Katarova et al., 2000), and can be interpreted as a conservative characteristic of the vertebrate developing GABAergic system. The alar plate of the prosomere 1, which contains the posterior commissure and the pretectum, was largely populated in dogfish by GABAergic cells with ventricular process at the marginal region (posterior commissure) and migrated cells adjacent to this region, forming together the pretectal GABAergic population of the posterior commissure. This population extends caudal to the fasciculus retroflexus, which probably corresponds with the caudal limit of p1 (the synencephalon-mesencephalon boundary), which at basal level matches with the exit of the oculomotor nerve root (Kuratani and Horigome, 2000). Our results support previous observations in other fish showing that the homogeneity of GABAergic pretectal population precludes any subdivision in these domain (*lamprey:* Meléndez-Ferro et al., 2000; *teleosts:* Ekström and Ohlin, 1995; Hauptmann and Gerster, 2000a,b), although using different cell markers, Pombal and Puelles (1999) have divided the p1 alar plate domain of lamprey in several portions (precommissural, commissural, and postcommissural). As reported in other vertebrate groups (*lampreys*: Meléndez-Ferro et al., 2002 *teleosts*: Martinoli et al., 1990; Ekström et al., 1995; Doldán et al., 1999; Higashijima et al., 2004; *amphibians*: Naujoks-Manteuffel et al., 1994; Barale et al., 1996; *mammals*: Katarova et al., 2000), during dogfish development this pretectal population is

characterized by a great density of GABAergic cells in the ventricular zone (posterior commissure cells) that probably migrate ventrally to originate the pretectal GABAergic population.

GABAergic pattern and rhombomeres

During mid-late embryonic stages (S28-S31), GABAergic cells of the dogfish rhombencephalon were organized in several discreet clusters, alternatively with regions devoid of GABA immunoreactivity, resembling the rhombomeric pattern of GABAergic cells observed in other vertebrate embryos (*teleosts:* Ekström et al., 1995; Higashijima et al., 2004; *mammals:* Katarova et al., 2000). The organization of these repetitive rhombencephalic domains in dogfish respects the rhombomeric model proposed for elasmobranchs (Gilland and Baker, 1993; Kuratani and Horigome, 2000) subdividing this region in eight segments (r1-r8). In zebrafish, studies of the expression of several genes in the rhombencephalon have revealed a striking similar segmental pattern (Higashijima et al., 2004). In the dogfish, the rhombomeric domains can be approximately identified on the basis of fixed external or internal landmarks, such as the cranial nerve roots or characteristic cytoarchitectural entities (Kuratani and Horigome, 2000). Our results showed that in dogfish GABAergic cells develop in different rhombencephalic segments, but the rhombomeric boundaries could only be tentatively traced by comparing the distribution of GABAergic cells with the rhombomeric limits proposed in elasmobranchs (Gilland and Baker, 1993; Kuratani and Horigome, 2000). So, the first GABAergic cluster (S23) appeared in the rostral rhombencephalon extending through the isthmic region, probably corresponding to the extension of rhombomere (r) 1. Later (S24-S28), numerous GABAergic cell clusters were distributed in a close relation with the external bulges that is thought to define externally the rhombomeres. From the rostral level of the trigeminal nerve root to the level of the vagal nerve root, we observed five external bulges that contained one conspicuous GABAergic cell cluster each, probably corresponding to the next five rhombomeres (r3-r7). In dogfish, the non-segmental region of the caudal rhombencephalon, which

extends from the vagal nerve root level to the rostral spinal cord, probably correspond to the caudal rhombomere (r8). In the late developmental embryos (S32-S34), the caudal rhombencephalon showed a dense GABAergic cell groups extended in a segmentary pattern throughout the viscerosensory column in close relation with the reticular GABAergic cells of the basal plate. In vertebrates, this segmentary pattern was related to the branchiomeric nerve motor nuclei (i.e. glossofaringeal and vagal nerve nuclei) that characteristically develop on even-numbered rhombomeres (see Gilland and Baker, 1993). Therefore, we assumed in dogfish that these dorsocaudal rhombencephalic GABAergic population related to the branchial nerves were extended from r6 to r8. Thus, GABAergic system in elasmobranch embryos exhibit the same dorsoventral and longitudinal GABAergic cell migration pattern and the same conserved relationship with rhombomeres as reported in amniote embryos (see Bronner-Fraser, 1995).

Spatial and temporal patterns of GABAergic innervation in the dogfish CNS

Studies on the development of axonal pathways in vertebrates have evidenced that early GABAergic neurons emit thin axons that would contribute to the initial regionalization of the brain (Ba-Charvet et al., 1998) and constitute the early axonal scaffold, in close association with the early pattern of axonal organization of the developmental brain (Wilson et al., 1990; Chitnis and Kuwada, 1990; Kimmel et al., 1995). In this study, we assumed that the GABAergic axonal tracts observed at early stages (S23-S26) are likely to be one of the first truly 'pioneering' axons that give rise to the early axonal scaffold, as reported in other vertebrates (Lauder et al., 1986; Ekström and Ohlin, 1995). This assumption is based on the fact that in dogfish, GABA is synthesized in neuronal processes at very early stages of development (S22) and, since the GABAergic processes follow the early scaffold development, is reasonable to assume that they are pioneering axons that contribute to the formation of the early axonal scaffold. Moreover, our present results show that the early GABAergic populations observed (at the primordial nucleus of the medial longitudinal fascicle, posterior commissure area, postoptic area and rhombencephalic tegmentum), are

equivalent to the clusters of cells that originated the early axonal scaffold described with specific axogenesis markers in other vertebrates (*cyclostomes:* Barreiro-Iglesias et al., 2008; *teleosts:* Wilson et al., 1990; *mammals:* Easter et al., 1993; Mastick and Easter, 1996). Although we have observed how the GABAergic innervation develops in almost the entire central nervous system, we could not discern between different developmental phases because the processes of axonal elongation and development of axon terminal fields were often intermingled at any developmental stage. Therefore, we restrict the discussion to the formation of the axonal scaffold in the dogfish CNS and its evolutionary context.

In studies of axogenesis made in different vertebrate species, different names have been applied to similar tracts of the early axonal scaffold. Below, we will use the terminology adopted in the cat shark (*Scyliorhinus torazame*; Kuratani and Horigome, 2000) when possible, or the most common names used for tracts in other vertebrates. The first GABAergic axonal tract to be observed in dogfish brain (S22) was the medial longitudinal fascicle (MLF), which was also the first GABAergic tract to appear in the brain of cyclostomes (Meléndez-Ferro et al., 2002, 2003), teleosts (Ekström and Ohlin, 1995; Doldán et al., 1999), amphibians (Roberts et al., 1987) and mammals (Lauder et al., 1986; Katarova et al., 2000). Moreover, using axonal markers (HNK-1, α/β-tubulin), labelling techniques as the horseradish peroxidase (HRP) and DiI, the MLF was also the first axonal tract to differentiate in elasmobranchs (Kuratani and Horigome, 2000) as in all vertebrate groups studied (*cyclostomes:* Kuratani et al., 1998; Barreiro-Iglesias et al., 2008; *teleosts:* Wilson et al., 1990; Ross et al., 1992; Doldán et al., 2000; Ishikawa et al., 2004; *amphibians:* Key and Anderson, 1999; *birds:* Covell and Noden, 1989; *mammals:* Easter et al., 1993; Mastick and Easter, 1996). In dogfish, the earliest GABAergic fibers in the MLF arise from the GABAergic cells located at the basal region of the synencephalon that could correspond to the nucleus of the medial longitudinal fascicle (nMLF). At these early embryonic stages (S22-S24), GABAergic axons from the reticular rhombencephalic cells and ventral spinal cord cells join the

MLF pioneer tract, as it has also been reported with axonal markers in other anamniotes (Ross et al., 1992; Barreiro-Iglesias et al., 2008).

The next early GABAergic tract in dogfish was observed at S24 rostrally to the isthmic level, intermingled with the dorsoventrally columnar cluster of GABAergic cells. Interestingly, this transverse dorsoventral fiber tract was observed only during very early embryonic stages (S24-S25), being almost absent from S26 onwards. This transverse tract at the isthmus was also reported with antibodies against tubulin in the *cat shark* (Kuratani and Horigome, 2000) and in mouse (Mastick and Easter, 1996), representing one of the earliest fiber tracts seen in vertebrates.

From S24, GABAergic fibers coursing from the GABAergic cells of the posterior commissure group, formed a dorsoventral fiber bundle that corresponds to the posterior commissure tract (TPC) also reported during early development in other vertebrates with GABA markers (Lauder et al., 1986; Roberts et al., 1987; Ekström and Ohlin, 1995; Doldán et al., 1999; Katarova et al., 2000; Meléndez-Ferro et al., 2002). This early tract has also been showed with axonal markers in the cat shark (Kuratani and Horigome, 2000).

The tract of the postoptic commissure (TPOC) of dogfish was first observed at S25, coursing from the GABAergic cells of the postoptic group through the diencephalic basal plate to join the MLF. A similar longitudinal tract was described in the basal diencephalon of the cat shark using HNK-1 as axonal marker (Kuratani and Horigome, 2000). In other vertebrates, a similar GABAergic TPOC was recognized at middle-early developmental stages in cyclostomes (Meléndez-Ferro et al., 2002), teleosts (Ekström and Ohlin, 1995; Doldán et al., 1999), amphibians (Roberts et al., 1987) and mammals (Lauder et al., 1986; Katarova et al., 2000). The TPOC has been described as part of a lateral longitudinal system that courses through the ventral and dorsal thalamus (Mastick and Easter, 1996), and together with the MLF formed the TPOC/MLF longitudinal tract system also described in cyclostomes (Barreiro-Iglesias et al., 2008), teleosts (Wilson et al., 1990; Ross et al., 1992; Doldán et al., 2000; Ishikawa et al., 2004) and amphibians (Key and Anderson, 1999; Easter and Taylor, 1989).

At S26, most of the GABAergic fiber tracts that form the early axonal scaffold in dogfish were already recognized. In the diencephalic alar plate, GABAergic cells of the posterior commissure group (a part from being the origin of the TPOC) give also rise to a bundle of GABAergic fibers that courses through the dorsal thalamus and turning ventrally through the zona limitans intrathalamica (dorsoventral diencephalic tract) to join the longitudinal GABAergic fibers of the TPOC at the basal plate. This transverse GABAergic fiber tract, is probably homologous to the dorsoventral diencephalic tract described with axonal markers in developing *cat shark* (Kuratani and Horigome, 2000), and to the habenular commissure tract in zebrafish (Wilson et al., 1990; Ross et al., 1992). Interestingly, this GABAergic tract was not observed in other vertebrate developmental study except in mammals (Katarova et al., 2000).

Within the dogfish rhombencephalic tegmentum, despite of the MLF in the basal plate, a longitudinal GABAergic fiber tract was observed at the alar plate (S26), probably homologous to the dorsolateral longitudinal fascicle (DLL) described with axonal markers in the cat shark (Kuratani and Horigome, 2000) and in other vertebrates (Ross et al., 1992; Mastick and Easter, 1996; Ishikawa et al., 2004; Barreiro-Iglesias et al., 2008).

At later stages (S26-S30), GABAergic fibers also coursed in rostral tracts connecting the telencephalon and the diencephalon. A thin bundle of GABAergic fibers was observed coursing longitudinally through the ventral walls of the preoptic recess connecting the subpallium and the postoptic area nuclei, probably corresponding with the course of fasciculus basalis telencephali (fbt; S26). Whereas the fbt arches ventrally the preoptic area with scarce density of longitudinal GABAergic fibers, the supraoptic tract (SOT; S30), probably corresponding with the medial forebrain bundle, arches dorsally the preoptic area and connects the TPOC with the telencephalon. This conspicuous longitudinal bundle is the last GABAergic fiber tract to appear during dogfiah development, similar to the late appearing GABAergic supraoptic fibers reported in teleosts (Ekström and Ohlin, 1995; Doldán et al., 1999), amphibians (Roberts et al., 1987) and mammals (Lauder et al., 1986; Katarova et al., 2000). This

supraoptic tract was also reported using axonal markers in most vertebrates (Ross et al., 1992; Kuratani et al., 1998; Anderson and Key, 1999; Doldán et al., 2000; Murakami et al., 2001; Ishikawa et al., 2004; Nural and Mastick, 2004).

Finally at mid-late stages (S27-S31) of dogfish development, some GABAergic fibers were observed at the habenula and caudal hypothalamus, forming three different tracts: coursing through the dorsal walls of the habenula, coursing through the hypothalamic floor (the hypothalamo-hypophyseal tract) and GABAergic fibers coursing from the MLF through the dorsal walls of the posterior recess organ (probably corresponding to the mammillotegmental tract reported in mammals; Mastick and Easter, 1996), although these conspicuous GABAergic tracts do not appear to contribute with fibers to the early dogfish GABAergic axonal scaffold.

The similarity of the early tracts that constitutes the axonal scaffold in most vertebrate classes and the GABAergic fiber tracts observed in dogfish development suggest that these early GABAergic tracts represent the axonal scaffold in elasmobranchs, and also that GABA has an important role in the formation of the initial axonal scaffold of the CNS in vertebrates. Moreover, after the analysis of the origin and development of the dogfish GABAergic tracts, two remarkable features emerge: the early establishment of the main GABAergic fiber pathways (MLF, TPOC, SOT, TPC) is in close relation with the early development of GABAergic neurons, as observed in zebrafish (Wilson et al., 1990; Chitnis and Kuwada, 1990), and the spatio-temporal organization of these dogfish GABAergic fiber tracts matches with that reported in other vertebrates, indicating a conserved feature of the GABAergic fiber scaffold development.

BIBLIOGRAPHY

Adolf, B.; Chapouton, P.; Lam, C.S.; Topp, S.; Tannhäuser, B.; Strähle, U.; Götz, M.; Bally-Cuif, L. (2006) Conserved and acquired features of adult neurogenesis in the zebrafish telencephalon. Dev Biol. 295:278-293.

Álvarez-Otero, R.; Pérez, S.E.; Rodríguez, M.A.; Adrio, F.; Anadón, R. (1995) GABAergic neuronal circuits in the cerebellum of the dogfish *Scyliorhinus canicula* (Elasmobranchs): an immunocytochemical study. Neurosci Lett. 187:87-90.

Álvarez-Otero, R.; Perez, S.E.; Rodriguez, M.A.; Anadón, R. (1996) Organisation of the cerebellar nucleus of the dogfish, *Scyliorhinus canicula* L.: a light microscopic, immunocytochemical, and ultrastructural study. J Comp Neurol. 368:487-502.

Anderson, R.B.; Key, B. (1999) Role of acetylcholinesterase in the development of axon tracts within the embryonic vertebrate brain. Int J Dev Neurosci. 17:787-793.

Anderson, S.A.; Eisenstat, D.D.; Shi, L.; Rubenstein, J.L.R. (1997) Interneuron migration from basal forebrain to neocortex: dependence on Dlx genes. Science 278:474-476.

Anderson, A.S.; Marín, O.; Horn, C.; Jennings, K.; Rubenstein, J.L.R. (2001) Distinct cortical migrations from the medial and lateral ganglionic eminences. Development 128:353-363.

Ang, E.S.; Haydar, T.F.; Gluncic, V.; Rakic, P. (2003) Four-dimensional migratory coordinates of GABAergic interneurons in the developing mouse cortex. J Neurosci. 23:5805-5815.

Anglade, I.; Mazurais, D.; Douard, V.; Le Jossic-Corcos, C.; Mañanos, E.L.; Michel, D.; Kah, O. (1999) Distribution of glutamic acid decarboxylase mRNA in the forebrain of the rainbow trout as studied by in situ hybridization. J Comp Neurol. 410:277-289.

Aoki, E.; Semba, R.; Kashiwamata, S. (1989) When does GABA-like immunoreactivity appear in the rat cerebellar GABAergic neurons? Brain Res. 502:245-251.

Ba-Charvet, K.T.; Boxberg, Y.; Guazzi, S.; Boncinelli, E.; Godement, P. (1998) A potential role for the OTX2 homeoprotein in creating early 'highways' for axon extension in the rostral brain. Development 125: 4273-4282.

Ballard, W.W.; Mellinger, J.; Lechenault, H.; (1993) A series on normal stages for development of *Scyliorhinus canicula*, the lesser-spotted dogfish (Chondrichthyes: Scyliorhinidae). J Exp Zool. 267:318-336.

Barale, E.; Fasolo, A.; Girardi, E.; Artero, C.; Franzoni, M.F.; (1996) Immunohistochemical investigation of γ-aminobutyric acid ontogeny and transient expression in the central nervous system of *Xenopus laevis* tadpoles. J Comp Neurol. 368:285-294.

Barker, J.L.; Behar, T.; Li, Y.X.; Liu, Q.Y.; Ma, W., Maric, D.; Maric, I.; Schaffner, A.E.; Serafini, R.; Smith, S.V.; Somogyi, R.; Vautrin, J.Y.; Wen, X.L.; Xian, H. (1998) GABAergic cells and signals in CNS development. Perspect dev neurobiol. 5:305-322.

Barreiro-Iglesias, A.; Villar-Cheda, B.; Abalo, X.M.; Anadón, R.; Rodicio, M.C. (2008) The early scaffold of axon tracts in the brain of a primitive vertebrate, the sea lamprey. Brain Res Bull. 75:42-52.

Behar, T.N.; Schaffner, A.E., Colton, C.A.; Somogyi, R.; Olah, Z.; Lehel, C.; Barker, J.L. (1994) GABA-induced chemokinesis and NGF-induced chemotaxis of embryonic spinal cord neurons. J Neurosci. 14:29-38.

Behar, T.N.; Smith, S.V.; Kennedy, R.T.; McKenzie, J.M.; Maric, I.; Barker, J.L. (2001) GABA(B) receptors mediate motility signals for migrating embryonic cortical cells. Cereb Cortex. 11:744-753.

Bennis, M.; Calas, A.; Geffard, M.; Gamrani, H. (1991) Distribution of GABA immunoreactive systems in the forebrain and midbrain of the chameleon. Brain Res Bull. 26:891-898.

Bernhardt, R.R.; Patel, C.K.; Wilson, S.W.; Kuwada, J.Y. (1992) Axonal trajectories and distribution of GABAergic spinal neurons in wildtype and mutant zebrafish lacking floor plate cells. J Comp Neurol. 326:263-272.

Binor, E.; Heathcote, R.D. (2001) Development of GABA-immunoreactive neuron patterning in the spinal cord. J Comp Neurol. 438:1-11.

Bronner-Fraser, M. (1995) Patterning of the vertebrate neural crest. Perspect Dev Neurobiol. 3:53-62.

Chapouton, P.; Gärtner, A.; Götz, M. (1999) The role of Pax6 in restricting cell migration between developing cortex and basal ganglia. Development 126:5569-5579.

Cherubini, E.; Gaiarsa, J.L.; Ben-Ari, Y. (1991) GABA: an excitatory transmitter in early postnatal life. Trends Neurosci. 14:515-519.

Chitnis, A.B.; Kuwada, J.Y. (1990) Axonogenesis in the brain of zebrafish embryos. J Neurosci. 10:1892-1905.

Cobos, I.; Puelles, L.; Martínez, S. (2001) The avian telencephalic subpallium originates inhibitory neurons that invade tangentially the pallium (dorsal ventricular ridge and cortical areas). Dev. Biol. 239:30-45.

Covell, D.A. Jr.; Noden, D.M. (1989) Embryonic development of the chick primary trigeminal sensory-motor complex. J Comp Neurol. 286:488-503.

Dale, N.; Roberts, A.; Ottersen, O.P.; Storm-Mathisen, J. (1987a) The development of a population of spinal cord neurons and their axonal projections revealed by GABA immunocytochemistry in frog embryos. Proc R Soc Lond B Biol Sci. 232:205-215.

Dale, N.; Roberts, A.; Ottersen, O.P.; Storm-Mathisen, J. (1987b) The morphology and distribution of 'Kolmer-Agduhr cells', a class of cerebrospinal-fluid-contacting neurons revealed in the frog embryo spinal cord by GABA immunocytochemistry. Proc R Soc Lond B Biol Sci. 232:193-203.

De Carlos, J.A.; López-Mascaraque, L.; Valverde, F. (1996) Dynamics of cell migration from the lateral ganglionic eminence in the rat. J Neurosci. 16:6146-6156.

Demarque, M.; Represa, A; Becq, H.; Khalilov, I.; Ben-Ari, Y.; Aniksztejn, L. (2002) Paracrine intercellular communication by a Ca2C and SNARE independent release of GABA and glutamate prior to synapse formation. Neuron 36:1051-1061.

Doldán, M.J.; Prego, B.; Holmqvist, B.I.; De Miguel, E. (1999) Distribution of GABA-immunolabeling in the early zebrafish (*Danio rerio*) brain. Eur J Morphol. 37:126-129.

Easter, S.S. Jr.; Taylor, J.S. (1989) The development of the *Xenopus* retinofugal pathway: optic fibers join a pre-existing tract. Development 107:553-573.

Easter, S.S. Jr.; Ross, L.S.; Frankfurter, A. (1993) Initial tract formation in the mouse brain. J Neurosci. 13:285-299.

Ekström, P.; Ohlin, L.M. (1995) Ontogeny of GABA-immunoreactive neurons in the central nervous system in a teleost, *Gasterosteus aculeatus L*. J Chem Neuroanat. 9:271-288.

Fairén, A.; Álvarez-Bolado, G.; De Diego, I.; Smith-Fernández, A. (1998) GABA-immunoreactive cells of the cortical primordium contribute to distinctly fated neuronal populations. Perspect Dev Neurobiol. 5:159-173.

Gahtan, E.; Sankrithi, N.; Campos, J.B.; O'Malley, D.M. (2002) Evidence for a widespread brain stem escape network in larval zebrafish. J Neurophysiol. 87:608-614.

Gilland, E.; Baker, R. (1993) Conservation of neuroepithelial and mesodermal segments in the embryonic vertebrate head. Acta Anat (Basel). 148:110-123.

Grandel, H.; Kaslin, J.; Ganz, J.; Wenzel, I.; Brand, M. (2006) Neural stem cells and neurogenesis in the adult zebrafish brain: Origin, proliferation dynamics, migration and cell fate. Develop Biol. 295:263-277.

Hauptmann, G.; Gerster, T. (2000a) Regulatory gene expression patterns reveal transverse and longitudinal subdivisions of the embryonic zebrafish forebrain. Mech Dev. 91:105-18.

Hauptmann, G.; Gerster, T. (2000b) Combinatorial expression of zebrafish Brn-1- and Brn-2-related POU genes in the embryonic brain, pronephric primordium, and pharyngeal arches. Dev Dyn. 218:345-58.

Hevner, R.F.; Daza, R.A.; Englund, C.; Kohtz, J.; Fink, A. (2004) Postnatal shifts of interneuron position in the neocortex of normal and reeler mice: evidence for inward radial migration. Neuroscience 124:605-618.

Higashijima, S.; Mandel, G.; Fetcho, J.R. (2004) Distribution of prospective glutamatergic, glycinergic, and GABAergic neurons in embryonic and larval zebrafish. J Comp Neurol. 480:1-18.

Huang, Z.J.; Di Cristo, G.; Ango, F. (2007) Development of GABA innervation in the cerebral and cerebellar cortices. Nat Rev Neurosci. 8:673-686.

Ishikawa, Y.; Kage, T.; Yamamoto, N.; Yoshimoto, M.; Yasuda, T.; Matsumoto, A.; Maruyama, K.; Ito, H. (2004) Axonogenesis in the medaka embryonic brain. J Comp Neurol. 476:240-253.

Ji, F.; Kanbara, N.; Obata, K. (1999) GABA and histogenesis in fetal and neonatal mouse brain lacking both the isoforms of glutamic acid decarboxylase. Neurosci Res. 33:187-194.

Jiménez, D.; Lopez-Mascaraque, L.M.; Valverde, F.; De Carlos, J.A. (2002) Tangential migration in neocortical development. Dev Biol. 244:155-169.

Katarova, Z.; Sekerkov, G.; Prodan, S.; Mugnaini, E.; Szabo, G. (2000) Domain-restricted expression of two glutamic acid decarboxylase genes in midgestation mouse embryos. J Comp Neurol. 424:607-627.

Key, B.; Anderson, R.B. (1999) Neuronal pathfinding during development of the rostral brain in Xenopus. Clin Exp Pharmacol Physiol. 26:752-754.

Kimmel, C.B.; Ballard, W.W.; Kimmel, S.R.; Ullmann, B.; Schilling, T.F. (1995) Stages of embryonic development of the zebrafish. Dev Dyn. 203:253-310.

Kuratani, S.; Horigome, N.; Ueki, T.; Aizawa, S.; Hirano, S. (1998) Stereotyped axonal bundle formation and neuromeric patterns in embryos of a cyclostome, *Lampetra japonica*. J Comp Neurol. 391:99-114.

Kuratani, S.; Horigome, N. (2000) Developmental morphology of branchiomeric nerves in a cat shark, *Scyliorhinus torazame*, with special reference to rhombomeres, cephalic mesoderm, and distribution patterns of cephalic crest cells. Zoo Sci. 17:893-909.

Lavdas, A.A.; Grigoriou, M.; Pachnis, V.; Parnavelas, J.G. (1999) The medial ganglionic eminence gives rise to a population of early neurons in the developing cerebral cortex. J Neurosci. 19:7881-7888.

Lauder, J.M. (1993) Neurotransmitters as growth regulatory signals: role of receptors and second messengers. Trends Neurosci. 16:233-240.

Lauder, J.M.; Han, V.K.; Henderson, P.; Verdoorn, T.; Towle, A.C. (1986) Prenatal ontogeny of the GABAergic system in the rat brain: an immunocytochemical study. Neuroscience 19:465-493.

Lauder, J.M.; Liu, J.; Devaud, L.; Morrow, A.L. (1998) GABA as a trophic factor for developing monoamine neurons. Perspect Dev Neurobiol. 5:247-259.

Leto, K.; Carletti, B.; Williams, I.M.; Magrassi, L.; Rossi, F. (2006) Different types of cerebellar GABAergic interneurons originate from a common pool of multipotent progenitor cells. J Neurosci. 26:11682-11694.

Liu, K.S.; Fetcho, J.R. (1999) Laser ablations reveal functional relationships of segmental hindbrain neurons in zebrafish. Neuron 23:325-335.

Lo Turco, J.J.; Kriegstein, A.R. (1991) Clusters of coupled neuroblasts in embryonic neocortex. Science 252:563-566.

LoTurco, J.J.; Owens, D.F.; Heath, M.J.; Davis, M.B.; Kriegstein, A.R. (1995) GABA and glutamate depolarize cortical progenitor cells and inhibit DNA synthesis. Neuron 15:1287-1298.

Luskin, M.B.; Parnavelas, J.G.; Barfield, J.A. 1993 Neurons, astrocytes, and oligodendrocytes of the rat cerebral cortex originate from separate progenitor cells: an ultrastructural analysis of clonally related cells. J Neurosci. 13:1730-1750.

Ma, W.; Barker, J.L. (1995) Complementary expressions of transcripts encoding GAD67 and GABAA receptor alpha 4, beta 1, and gamma 1 subunits in the proliferative zone of the embryonic rat central nervous system. J Neurosci. 15:2547-2560.

MacLeod, K.M.; Soares, D.; Carr, C.E. (2006) Interaural timing difference circuits in the auditory brainstem of the emu (*Dromaius novaehollandiae*). J Comp Neurol. 495:185-201.

Madtes, P.; Redburn, D.A. (1983) GABA as a trophic factor during development. Life Sci. 33:979-984.

Maler, L.; Mugnaini, E. (1994) Correlating gamma-aminobutyric acidergic circuits and sensory function in the electrosensory lateral line lobe of a gymnotiform fish. J Comp Neurol. 345:224-252.

Marín, O.; Rubenstein, J.L.R. (2001) A long, remarkable journey: tangential migration in the telencephalon. Nat Rev Neurosci. 2:780-790.

Marín, O.; Rubenstein, J.L.R. (2003) Cell migration in the forebrain. Annu Rev Neurosci. 26:441-483.

Martín, S.C.; Heinrich, G.; Sandell, J.H. (1998) Sequence and expression of glutamic acid decarboxylase isoforms in the developing zebrafish. J Comp Neurol. 396:253-266.

Martinoli, M.G.; Dubourg, P.; Geffard, M.; Calas, A.; Kah, O. (1990) Distribution of GABA immunoreactive neurons in the forebrain of the goldfish, *Carassius auratus*. Cell Tissue Res. 260 77-84.

Mastick, G.S.; Easter, S.S. Jr. (1996) Initial organization of neurons and tracts in the embryonic mouse fore- and midbrain. Dev Biol. 173:79-94.

Médina, M.; Repérant, J.; Dufour, S.; Ward, R.; Le Belle, N.; Miceli, D. (1994) The distribution of GABA-immunoreactive neurons in the brain of the silver eel (*Anguilla anguilla L.*). Anat Embryol. 189:25-39.

Meier, H.; Hertz, L.; Schousboe, A. (1991) Neurotransmitters as developmental signals. Neurochem Int. 19:1-15.

Meinecke, D.L.; Rakic, P. (1992) Expression of GABA and GABAA receptors by neurons of the subplate zone in developing primate occipital cortex: evidence for transient local circuits. J Comp Neurol. 317:91-101.

Meléndez-Ferro, M.; Pérez-Costa, E.; Villar-Cheda, B.; Abalo, X.M.; Rodríguez-Muñoz, R.; Rodicio, M.C.; Anadón, R. (2002) Ontogeny of γ-aminobutyric acid-immunoreactive neuronal populations in the forebrain and midbrain of the sea lamprey. J Comp Neurol. 446:360-376.

Meléndez-Ferro, M.; Pérez-Costas, E.; Villar-Cheda, B.; Rodríguez-Muñoz, R.; Anadón, R.; Rodicio, M.C. (2003) Ontogeny of gamma-aminobutyric acid-immunoreactive neurons in the rhombencephalon and spinal cord of the sea lamprey. J Comp Neurol. 464:17-35.

Nadarajah, B.; Alifragis, P.; Wong, RO.; Parnavelas, J.G. (2002) Ventricle-directed migration in the developing cerebral cortex. Nat Neurosci. 5:218-224.

Mione, M.C.; Danevic, C.; Boardman, P.; Harris, B.; Parnavelas, J.G. 1994 Lineage analysis reveals neurotransmitter (GABA or glutamate) but not calcium-binding protein homogeneity in clonally related cortical neurons. J Neurosci. 14:107-123.

Mugnaini, E.; Maler, L. (1987) Cytology and immunocytochemistry of the nucleus of the lateral line lobe in the electric fish *Gnathonemus petersii* (Mormyridae): evidence suggesting that GABAergic synapses mediate an inhibitory corollary discharge. Synapse 1:32-56.

Muller, E.; Le Corronc, H.; Triller, A.; Legendre, P. (2006) Developmental dissociation of presynaptic inhibitory neurotransmitter and postsynaptic receptor clustering in the hypoglossal nucleus. Mol Cell Neurosci. 32:254-273.

Murakami, Y.; Ogasawara, M.; Sugahara, F.; Hirano, S.; Satoh, N.; Kuratani, S. (2001) Identification and expression of the lamprey Pax6 gene: evolutionary origin of the segmented brain of vertebrates. Development 128:3521-3531.

Naujoks-Manteuffel, C.; Himstedt, W.; Gläsener-Cipollone, G. (1994) Distribution of GABA-immunoreactive neurons in the brain of adult and developing salamanders (*Pleurodeles waltli*, *Triturus alpestris*). Cell Tissue Res. 276:485-501.

Nery, S.; Fishell, G.; Corbin, J.G. (2002) The caudal ganglionic eminence is a source of distinct cortical and subcortical cell populations. Nat Neurosci. 5:1279-1287.

Nguyen, L; Rigo, JM; Rocher, V; Belachew, S; Malgrange, B; Rogister, B; Leprince, P; Moonen G. (2001) Neurotransmitters as early signals for central nervous system development. Cell Tissue Res. 305:187–202.

Nural, H.F.; Mastick, G.S. (2004) Pax6 guides a relay of pioneer longitudinal axons in the embryonic mouse forebrain. J Comp Neurol. 479:399-409.

Oertel, W.H.; Schmechel, D.E.; Tappaz, M.L.; Kopin, I.J. (1981) Production of a specific antiserum to rat brain glutamic acid decarboxylase by injection of an antigen-antibody complex. Neuroscience 6:2689-2700.

Owens, D.F.; Kriegstein, A.R. (2002) Is there more to GABA than synaptic inhibition? Nat. Rev. Neurosci. 3:715-727.

Parnavelas, J.G. (2000) The origin and migration of cortical neurones: new vistas. Trends Neurosci. 23:126-131.

Phelps, P.E.; Alijani, A.; Tran, T.S. (1999) Ventrally located commissural neurons express the GABAergic phenotype in developing rat spinal cord. J Comp Neurol. 409:285-298.

Pinganaud, G.; Clairambault, P. (1979) The visual system of the trout Salmo *irideus Gibb*. A degeneration and radioautographic study. J Hirnforsch. 20:413-431.

Polleux, F.; Whitford, K.L.; Dijkhuizen, P.A.; Vitalis, T.; Ghosh, A. (2002) Control of cortical interneuron migration by neurotrophins and PI3-kinase signalling. Development 129:3147-3160.

Pombal, M.A.; Puelles, L. (1999) Prosomeric map of the lamprey forebrain based on calretinin immunocytochemistry, Nissl stain, and ancillary markers. J Comp Neurol. 414:391-422.

Puelles, L.; Rubenstein, J.L. (1993) Expression patterns of homeobox and other putative regulatory genes in the embryonic mouse forebrain suggest a neuromeric organization. Trends Neurosci. 16:472-479.

Puelles, L.; Rubenstein, J.L. (2003) Forebrain gene expression domains and the evolving prosomeric model. Trends Neurosci. 26:469-476.

Reed, K.L.; MacIntyre, J.K.; Tobet, S.A.; Trudeau, V.L.; MacEachern, L.; Rubin, B.S.; Sower, S.A. (2002) The spatial relationship of gamma-aminobutyric acid (GABA) neurons and gonadotropin-releasing hormone (GnRH) neurons in larval and adult sea lamprey, *Petromyzon marinus*. Brain Behav Evol. 60:1-12.

Represa, A.; Ben-Ari, Y. (2005) Trophic actions of GABA on neuronal development.Trends Neurosci. 28:278-283.

Roberts, A.; Dale, N.; Ottersen, P.; Storm-Mathisen, J. (1987) The early development of neurons with GABA immunoreactivity in the CNS of *Xenopus laevis* embryos. J comp neurol. 261:435-449.

Ross, L.S.; Parrett, T.; Easter, S.S. Jr. (1992) Axonogenesis and morphogenesis in the embryonic zebrafish brain. J Neurosci. 12:467-482.

Rubenstein, J.L.; Puelles, L. (1994) Homeobox gene expression during development of the vertebrate brain. Curr Top Dev Biol. 29:1-63.

Smeets, W.J.A.J.; Nieuwenhuys, R.; Roberts, B.L. (1983) The central nervous system of cartilaginous fishes. Berlin: Springer-Verlag.

Stenman, J.; Toresson, H.; Campbell, K. (2003) Identification of Two Distinct Progenitor Populations in the Lateral Ganglionic Eminence: Implications for Striatal and Olfactory Bulb Neurogenesis. J Neurosci. 23:167-174.

Sueiro, C. (2003) Estudio inmunohistoquímico de los sistemas gabaérgicos del sistema nervioso central de peces elasmobranquios y su relación con sistemas catecolaminérgicos y peptidérgicos. Doctoral Thesis. University Santiago de Compostela. Spain.

Sueiro, C.; Carrera, I.; Molist, P.; Rodríguez-Moldes, I.; Anadón, R. (2004) Distribution and development of glutamic acid decarboxylase immunoreactivity in the spinal cord of the dogfish *Scyliorhinus canicula* (elasmobranchs). J Comp Neurol. 478:189-206.

Sussel, L.; Marín, O.; Kimura, S.; Rubenstein, J.L.R. (1999) Loss of Nkx2.1 homeobox gene function results in a ventral to dorsal molecular respecification within the basal telencephalon: evidence for a transformation of the pallidum into the striatum. Development 126:3359-3370.

Takayama, C.; Inoue, Y. (2004) GABAergic signaling in the developing cerebellum. Anat Sci Int. 79:124-136.

Tamamaki, N.; Fujimori, K.E.; Takauji, R. (1997) Origin and route of tangentially migrating neurons in the developing neocortical intermediate zone. J Neurosci. 17:8313-8323.

Tan, S.S.; Kalloniatis, M.; Sturm, K.; Tam, P.P.; Reese, B.E.; Faulkner-Jones, B. (1998) Separate progenitors for radial and tangential cell dispersion during development of the cerebral neocortex. Neuron 21:295-304.

Tanaka, H.D.; Maekawa, K.; Yanagawa, Y.; Obata, K.; Murakami, F. (2006) Multidirectional and multizonal tangential migration of GABAergic interneurons in the developing cerebral cortex. Development 133:2167-2176.

Valcanis, H.; Tan, S.S. (2003) Layer specification of transplanted interneurons in developing mouse neocortex. J Neurosci. 23:5113-5122.

Vergano-Vera, E.; Yusta-Boyo, M.J.; De Castro, F.; Bernad, A.; De Pablo, F.; Vicario-Abejón, C. (2006) Generation of GABAergic and dopaminergic interneurons from endogenous embryonic olfactory bulb precursor cells. Development 133:4367-4379.

Versaux-Botteri, C.; Pochet, R.; Nguyen-Legros, J. (1989) Immunohistochemical localization of GABA-containing neurons during postnatal development of the rat retina. Invest Ophthalmol Vis Sci. 30:652-659.

Von Bartheld, C.S.; Rubel, E.W. (1989) Transient GABA immunoreactivity in cranial nerves of the chick embryo. J Comp Neurol. 286:456-471.

Wichterle, H.; Turnbull, D.H.; Nery, S.; Fishell, G.; Álvarez-Buylla, A. (2001) In utero fate mapping reveals distinct migratory pathways and fates of neurons born in the mammalian basal forebrain. Development 128:3759-3771.

Wilson, S.W.; Ross, L.S.; Parrett, T.; Easter, S.S. (1990) The development of a simple scaffold of axon tracts in the brain of the embryonic zebrafish, *Brachydanio rerio.* Development 108:121-45.

Wullimann, M.F.; Northcutt, R.G. (1988) Connections of the corpus cerebelli in the green sunfish and the common goldfish: a comparison of perciform and cypriniform teleosts. Brain Behav Evol. 32:293-316.

Xu, Q.; Cobos, I.; De La Cruz, E.; Rubenstein, J.L.R.; Anderson, S.A. (2004) Origins of cortical interneuron subtypes. J Neurosci. 24:2612-2622.

Yozu, M.; Tabata, H.; Nakajima, K. (2005) The caudal migratory stream: a novel migratory stream of interneurons derived from the caudal ganglionic eminence in the developing mouse forebrain. J Neurosci. 25:7268-7277.

ABBREVIATIONS

AC	cerebellar auricula
ACS	central superficial area
APV	ventrolateral periventricular area
ASB	basal superficial area
Cb	cerebellum
cc	central canal
CN	cerebellar nucleus
CSF-c	cerebrospinal fluid contacting cell
Dh	dorsal horn
Di	diencephalon
DLL	dorsolateral longitudinal fascicle
DVDT	dorsoventral diencephalic tract
fbt	basal telencephalic fascicle
fr	retroflexus fascicle
GR	cerebellar granular layer
H	hypophysis
Ha	habenula
hht	hypothalamic-hypopheseal tract
Hyp	hypothalamus
IHL	inferior hypothalamic lobe
IP	interpeduncular nucleus
IS	isthmus
LNI	neurointermediate lobe
ME	median eminence
Mes	mesencephalon
MesTg	mesencephalic tegmentum
MLF	medial longitudinal fascicle
MOL	cerebellar molecular layer
mtt	mammillotegmental tract
OB	olfactory bulb
Optp	optic placode
OS	optic stalk
OT	optic tectum
P	pallium
Pc	posterior commissure
Pi	pineal organ
Po	preoptic area
Pon	postoptic nucleus
Pr	posterior recess
Pret	pretectum
Pro	posterior recess organ
PTN	posterior tubercle nucleus
PVO	paraventricular organ
R	Rathke's pouch
r1-r8	rhombomeres
Ret	tegmental reticular groups
Rh	rhombencephalon
Rpo	preoptic recess
S	septum
SCN	suprachiasmatic nucleus
Si	infundibuli saccus
SOT	supraoptic tract
Sp	subpallium
Spc	spinal cord
SV	saccus vasculosus
Syn	synencephalon
Td	dorsal thalamus
TPC	posterior commissure tract
TPOC	postoptic commissure tract
Tv	ventral thalamus
Vh	ventral horn
VMC	visceromotor column
VSC	viscerosensorial column
VTA	ventral tegmental area
III	oculomotor nucleus
IIIr	oculomotor nerve root
IV	trochlear nucleus
Vr	trigeminal nerve root
Vm	trigeminal motor nucleus
VI	abducens nucleus
VII	facial nucleus
VIIIm	magnocellular octaval nucleus

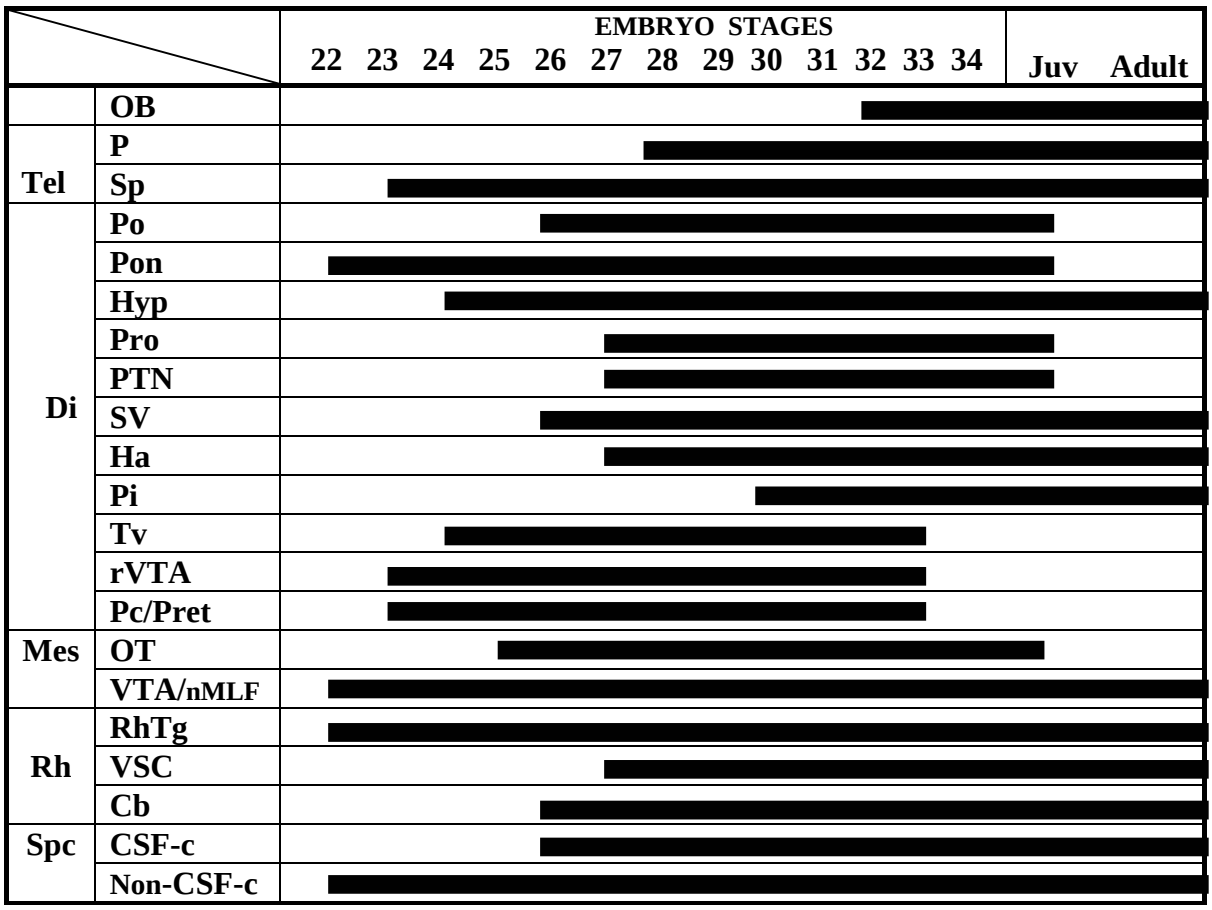

Table I. Timetable showing the sequence of appearance of GABAergic cell groups in the dogfish brain during development and posthatching periods.

	Tel			Di				Mes		Rh	Spc
	OB	**P**	**Sp**	**Pon**	**Tv**	**Hyp**	**PC**	**Mes Tg**	**OT**	**RhTg**	**Spc**
S. canicula (present study)	6th	5th	2nd	1st	3rd	2nd	2nd	1st	4th	1st	1st
Petromyzon marinus (Meléndez-Ferro et al., 2002, 2003)	4th	5th	3rd	1st	4th	2nd	3rd	1st	3rd	1st	3rd
Danio rerio (Doldán et al., 1999)	3rd	3rd	1st	1st	3rd	2nd	2nd	1st	3rd	1st	1st
Gasterosteus aculeatus (Ekström & Ohlin, 1995)	-	4th	2nd	1st	4th	3rd	3rd	1st	4th	2nd	1st
Xenopus laevis (Barale et al., 1996)	4th	3rd	3rd	1st	1st	2nd	3rd	2nd	3rd	1st	1st
mouse (Katarova et al., 2000)	1st	3rd	1st	2nd	2nd	2st	1st	1st	3rd	1st	1st

Table II. Comparison of the timetable appearance of CNS GABAergic cell groups among vertebrates.

Figure 1. Schematic representations of sagittal sections of dogfish embryo brains at S22 (a), S23 (b), S24 (c), S26 (d), S28 (e), S31 (f) and S33 (g) showing the distribution of GABAergic cells (circles) and fibers (thin lines). The diencephalic-mesencephalic and mesencephalic-rhombencephalic boundaries are represented by broken lines. The exit of some cranial nerve roots (III,V,VII,VIII) is also represented. Scale bars: 100µm (a-f) and 250µm (f).

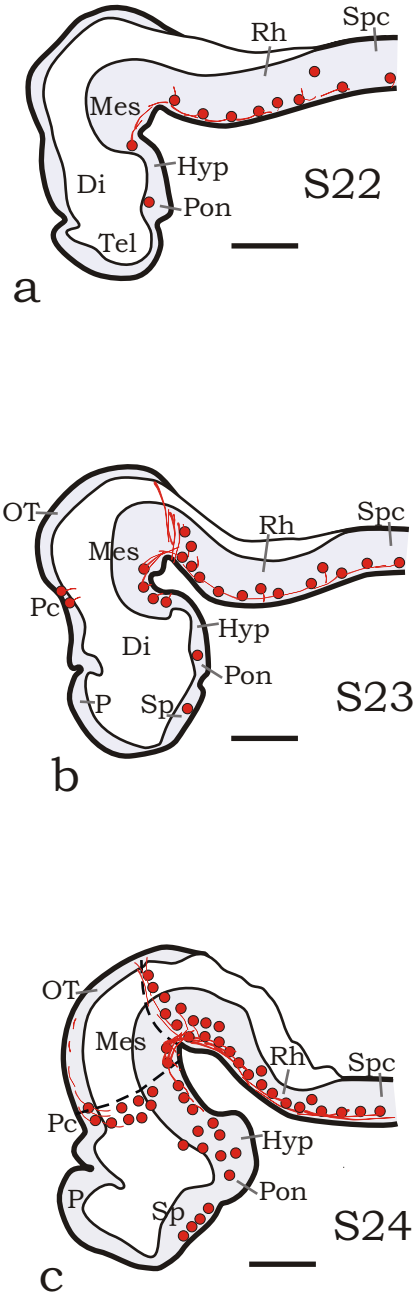
Rh
Spc
Mes
Hyp
Di
Pon
Tel
S22
a
OT
Rh
Spc
Mes
Pc
Hyp
Di
Pon
P
Sp
S23
b
OT
Mes
Rh
Spc
Pc
Hyp
P
Sp
Pon
S24
c

Fig. 1

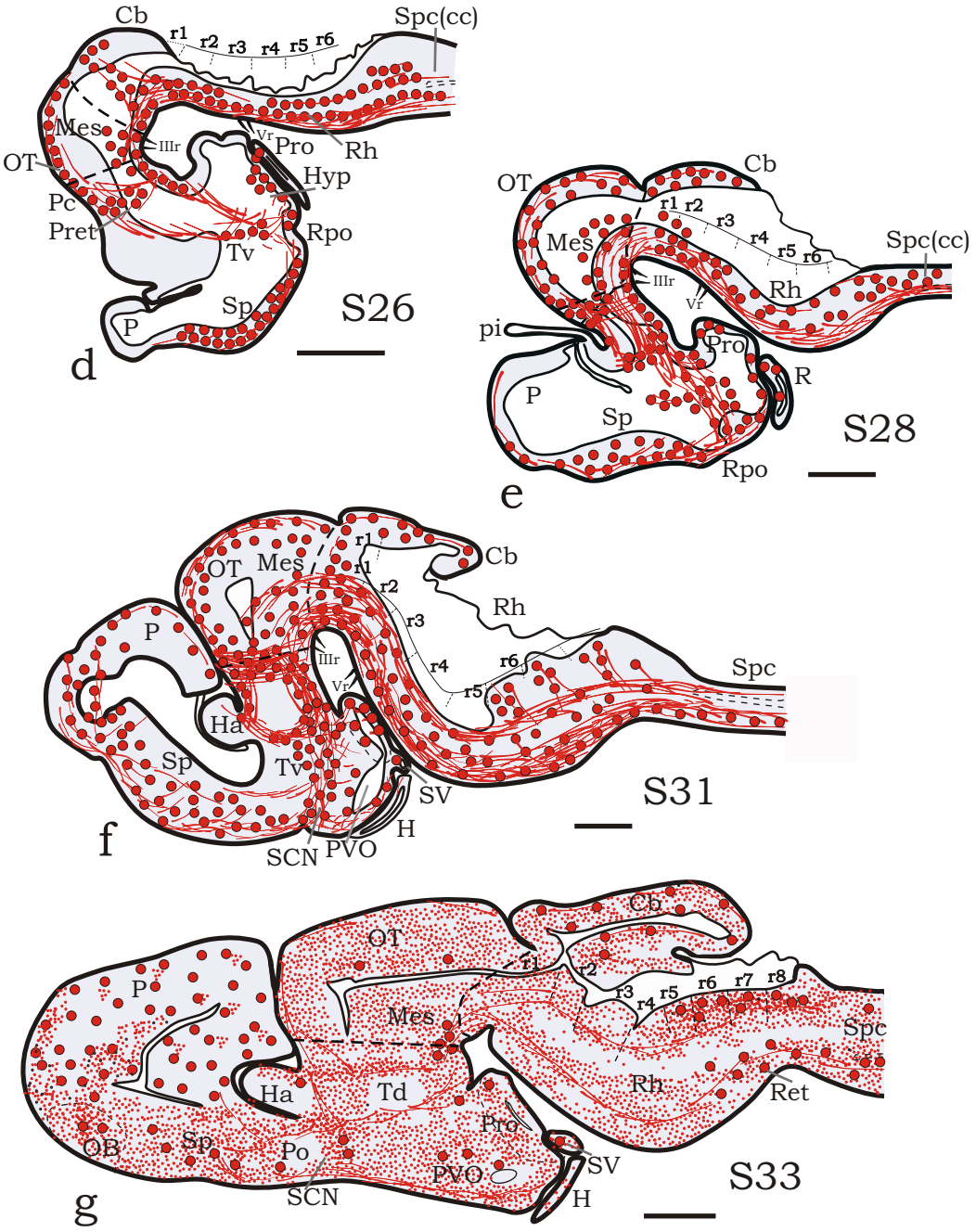
Cb
r1 r2 r3 r4 r5 r6
Spc(cc)
Mes
IIIr
Vr
Pro
Rh
OT
Hyp
Pc
Pret
Rpo
Tv
Sp
P
S26
d
OT
Cb
r1 r2
r3
r4
r5 r6
Spc(cc)
Mes
IIIr
Vr
Rh
pi
Pro
R
P
Sp
S28
Rpo
e
r1
OT
Mes
r1
Cb
r2
Rh
r3
P
IIIr
r4
r6
Spc
Vr
r5
Ha
Sp
Tv
SV
S31
f
H
SCN
PVO
Cb
OT
r1
r2
P
r3
r4
r5
r6
r7
r8
Mes
Spc
Rh
Ret
Ha
Td
Pro
OB
Sp
Po
PVO
SV
S33
SCN
H
g

Fig. 1 (cont.)

Figure 2. Sagittal (**A-N**) sections throughout the brain of embryos of *Scyliorhinus canicula* showing the distribution of GABAergic cells and fibers at S22 (**A-D**), S23 (**E-H**) and S24 (**I-N**). **A.** Panoramic view of a paramedian section of the S22 brain to show faint GABAergic cells at the postoptic area (arrowheads). Rostral is to the left. **B** Detail of the postoptic area, parallel to the squared area in A, showing a faint GABAergic cells with ventricular process (arrowhead). **C.** Section of the rostral mesencephalon to show some GABAergic cells (arrowhead) at the ventral tegmental zone (nmlf) extending long processes (arrow) caudally, representing the first GABAergic fibers of the mlf. **D.** Section to show some faintly GABAergic cell bodies at the intermediate zone (arrowhead) and at the marginal zone extending long processes (arrows) at rostral rhombencephalic levels. **E.** Panoramic section of S23 to show faint GABAergic cells at the caudal subpallium. Inset; Detail of the GABAergic subpallial cell showing a big round perykarion, squared in E. **F.** Section showing a weak stained GABAergic cell (arrowhead) at the ventral walls of the postoptic area. **G.** Detail of the caudal prosencephalon, parallel to the squared area in E, showing GABAergic cells at the primordium of the basal prosencephalic tegmentum (arrowheads) and at the marginal zone of the posterior commissure (arrow). **H.** Detail of the GABAergic cell group at the isthmus, extending their long processes dorsoventrally (arrowhead). Note also some GABAergic cells at the alar plate of the isthmus (arrow). **I.** Panoramic section of S24 to show the distribution of the GABAergic cells in the main brain regions. **J.** Detail of the postoptic area, parallel to the squared area in I, showing GABAergic cells (arrowheads) forming a ventral longitudinal band at the postoptic area. **K.** Detail of the mesencephalic and synencephalic tegmentum, parallel to the squared area in I, showing GABAergic cell band at the basal tegmental area formed by GABAergic cells at medial levels (arrowheads). **L.** Detail of the pretectal region, parallel to the squared area in I, showing GABAergic cells with ventricular process at the posterior commissure (arrowheads) showing also dorsoventrally processes towards the GABAergic cells of the pretectum (arrows). **M.** Sagittal rhombencephalic secction to show GABAergic cells mainly located at the basal plate. **N.** Detail section of the squared area in M, showing rhombencephalic tegmental GABAergic cells (arrowheads) with ventral processes that intermingled with the longitudinal GABAergic fibers (arrows) at the marginal zone. Scale bars: 250µm (A,E,I) ; 50µm (B,D,J,K,L,N); 100µm (C,G,H,M); 25µm (F).

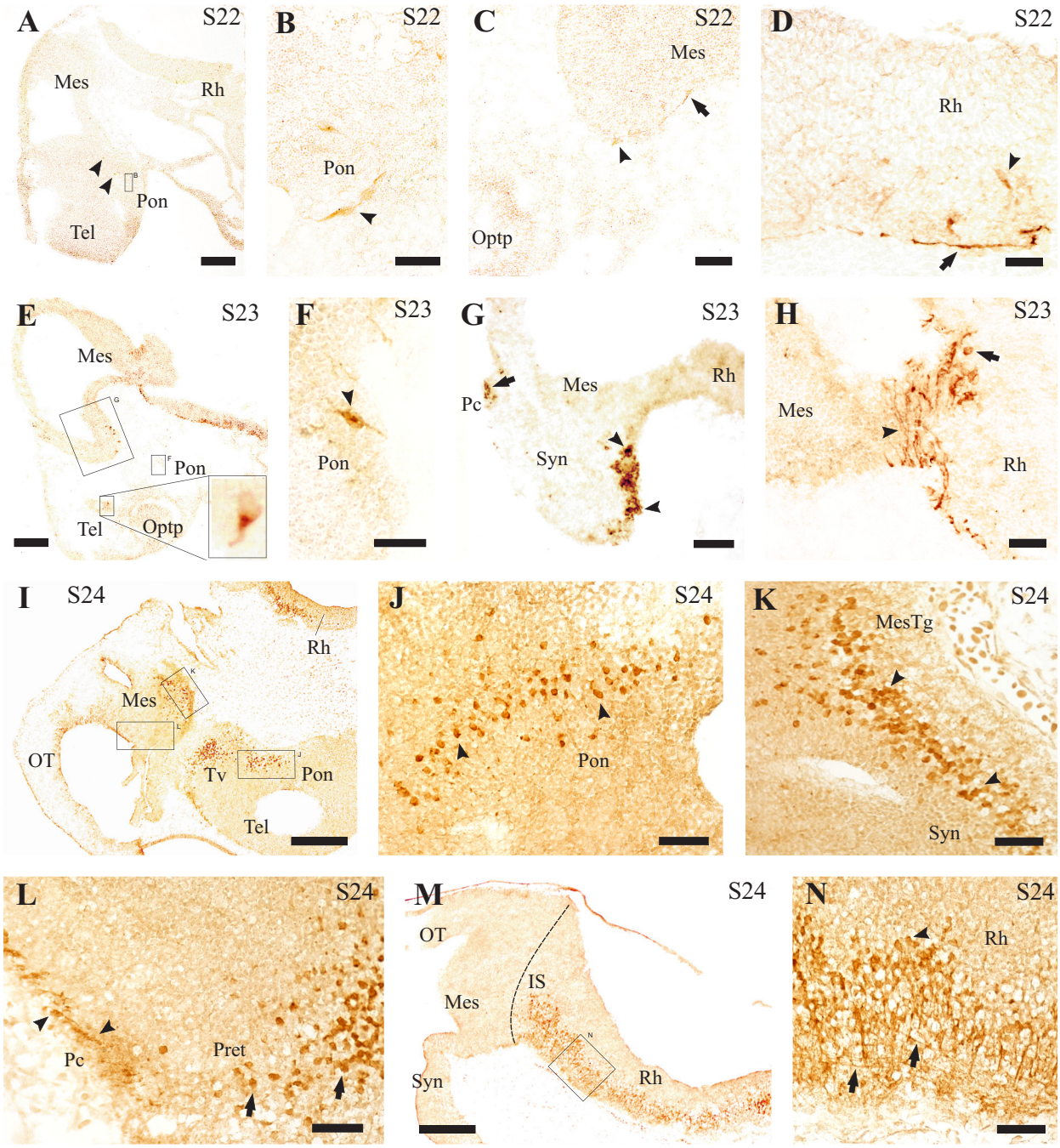
A
S22
Mes
Rh
Pon
Tel
B
S22
Pon
C
S22
Mes
Optp
D
S22
Rh
E
S23
Mes
Pon
Tel
Optp
F
S23
Pon
G
S23
Pc
Mes
Rh
Syn
H
S23
Mes
Rh
I
S24
Rh
Mes
OT
Tv
Pon
Tel
J
S24
Pon
K
S24
MesTg
Syn
L
S24
Pc
Pret
M
S24
OT
IS
Mes
Syn
Rh
N
S24
Rh

Fig. 2

Figure 3. Sagittal (**A-J**) sections throughout the brain of embryos of *Scyliorhinus canicula* showing the distribution of GABAergic cells and fibers at S25. **A.** Panoramic section of GABAergic cells in the basal telencephalon (arrowheads) at S25. **B.** Detail of the squared area in A, showing GABAergic cells in the ventral telencephalon located in the mantle (arrows) and intermediate (arrowheads) zones. **C.** Detail of the rostral diencephalon, parallel to the squared area in A, showing some GABAergic cells forming a thin band (arrows) from the ventral postoptic marginal walls to the primordium of the ventral thalamus. Note GABAergic cells with ventricular process at the lateral infundibular walls (thick arrow). Note also some GABAergic CSF-c cells at hypothalamic ventral walls (doble arrow). **D.** Panoramic view of a paramedian section to show the distribution of GABAergic cells in the prosencephalon, mesencephalon and rostral rhombencephalon at S25. **E.** Detail section of the rostral rhombencephalon, parallel to the squared area in D, to show the extension of the basal GABAergic cell column (arrowheads) to reach the isthmus level. **F.** Panoramic view of a paramedian section of the prosencephalon showing GABAergic cells at the synencephalon, hypothalamus and ventral telencephalon. **G.** Detail at lateral level of the pretectum, squared area in F, showing GABAergic cells at the posterior commissure extending long processes (arrowhead) towards the pretectal population. **H.** Detail of the isthmus, squared area in D, to show GABAergic cells with a migrating morphology (arrowhead) at the rostral level of the cerebellar primordium. Note the rostral rhombencephalic GABAergic cell band at the ventral tegmentum (arrows). **I** and **J.** Sagittal section of the rhombencephalic tegmentum to show conspicuous GABAergic cell groups formed by radial migrating GABAergic cells (arrowheads in I) that match with the possible rhombomeric boundaries (arrowheads in J). Note the profuse GABAergic longitudinal fiber tract (mlf; arrows in J) that course through the ventral tegmentum. Scale bars: 100µm (A,C,E,G-J); 50µm (B); 250µm (D,F).

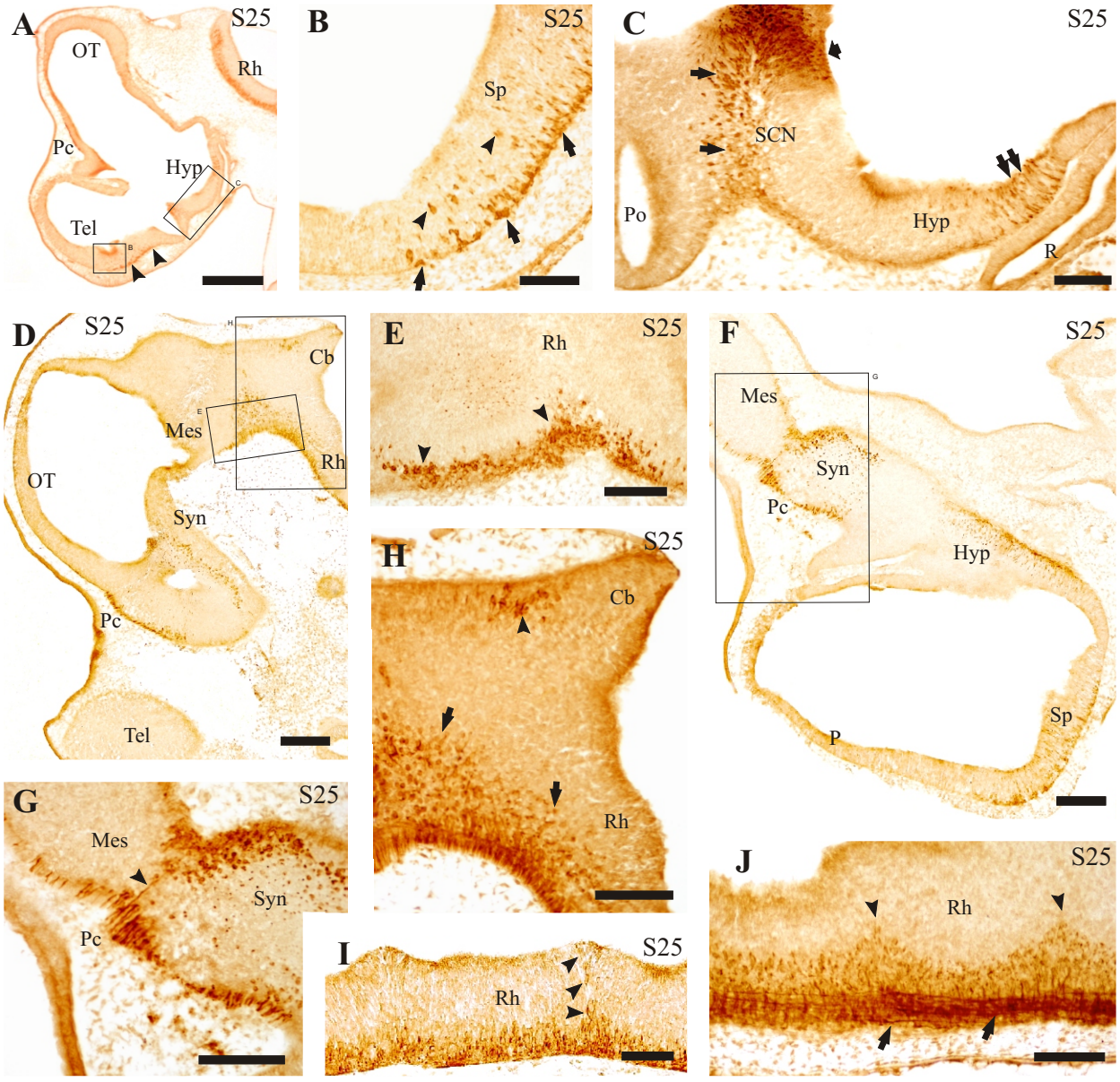
A
S25
OT
Rh
Pc
Hyp
Tel
B
S25
Sp
C
S25
SCN
Po
Hyp
R
D
S25
Cb
Mes
Rh
OT
Syn
Pc
Tel
E
S25
Rh
F
S25
Mes
Syn
Pc
Hyp
Sp
P
G
S25
Mes
Syn
Pc
H
S25
Cb
Rh
I
S25
Rh
J
S25
Rh

Fig. 3

Figure 4. Sagittal (A-H,J,K,N) and transverse (I,L,M) sections throughout the brain of embryos of *Scyliorhinus canicula* showing the distribution of GABAergic cells and fibers at S26 (A-C,F,I,L,M) and S27 (D,E,G,H,J,K,N). **A.** Panoramic brain section at S26 to show the GABA positivity of the subpallium (arrowheads). Note its sharp limit (dotted line) with the pallium. Note also the early organization of the main GABAergic cell groups such as the hypothalamus, optic tectum and rhombencephalon. **B.** Detail of the subpallium, squared area in A, showing bipolar GABAergic cells in the VZ with a process contacting the ventricle (arrowheads). Note GABAergic fibers (arrows) coursing rostrally to the pallial/subpallial boundary (dotted line), some of them taking a radial course (thick arrow). **C.** Sagittal section of the prosencephalon and mesencephalon to show the GABAergic cell organization at lateral levels. Note the increased density of the pretectal and tegmental GABAergic cell bands continuous with the GABAergic thalamic and hypothalamic cell population, respectively. **D.** Detail of the hypothalamus to show GABAergic cell column (arrowheads) between the postoptic commissure and the ventral thalamus. Note the CSF-c cells at the lateral and ventral infundibular walls (arrows), and GABAergic fibers at the marginal layer (thick arrows). Note the dense bundle of longitudinal GABAergic fibers that reach the caudal hypothalamus (doble arrow), and the thin fiber tract (thin arrow) that course ventrally the preoptic recess to the subpallium. **E.** GABAergic cells at the PTN (arrow) and at the Pro (arrowhead). Note the long process contacting the ventricle (arrowhead) of the Pro GABAergic cell. **F.** Detail of the thalamic region, parallel section squared in C, showing GABAergic cells at the ventral thalamus (arrow) and at the rostral portion of the dorsal thalamus (arrowheads). Note the GABAergic cells at the marginal zone of the posterior comissure (thick arrow). **G.** Detail of the proximal region of the habenula, parallel section squared in C, to show a few GABAergic cells (arrow) at the dorsal ependymal layer. Note also some longitudinal GABAergic fibers (arrowheads) coursing along the dorsal layer. **H.** Detail of the pretectal region and rostral optic tectum, parallel section squared in C, to show GABAergic cell densely located at the marginal zone (thick arrows) and the GABAergic cell longitudinal pretectal population (arrow). Note the longitudinal GABAergic cell bands at the synencephalic tegmentum (arrowhead). **I.** Transverse section of the optic tectum showing GABAergic cells at the external layer (arrowhead) and a few occupying the intermediate layer (arrow). **J.** Section at the synencephalon, to show the dorso-ventral posterior commissure bundles of GABAergic fibers (arrowheads) and the longitudinal GABAergic fibers (arrows) that coursed dorsally and ventrally the tegmentum. **K.** Section of the rostral rhombencephalon to show the dorsoventral GABAergic cell band (arrowheads) at the isthmic level (isthmic limit marked with dotted line), the cerebellar GABAergic cell band (arrow) located dorsally and the GABAergic fibers at the basal rhombencephalic tegmentum (mlf; thick arrows). Note the absence of GABAergic cells at the isthmus. **L.** Transverse section at isthmic level to show two main GABAergic groups, at the ventral plate (arrowheads) and at the dorsal plate (arrow). Note that the GABAergic cells of the ventral group sending long commissural processes that cross the floor plate (doble arrow). **M.** Transverse section at caudal level of acusticofacial nuclei nerve root to show five packed GABAergic cell groups (arrowheads) that extended from both sides of the floor plate to the dorsal tegmental region, occupying the marginal and intermediate zones. Note that the GABAergic cells of the several groups sent short processes towards the ventricle and also the ventral commissural GABAergic fiber tract that cross the floor plate (thick arrow). **N.** Sagittal detail of the rhombencephalon at the caudal level to show GABAergic cells of the several tegmental groups (arrowheads) as well as the longitudinal GABAergic fiber tracts (arrows) that run through the basal plate. Note the numerous horizontal GABAergic fibers that intermingle with the vertical GABAergic cell processes. Scale bars: 25µm (E); 50µm (G,I,N); 100µm (B,D,F,H,J-M); 250µm (A,C).

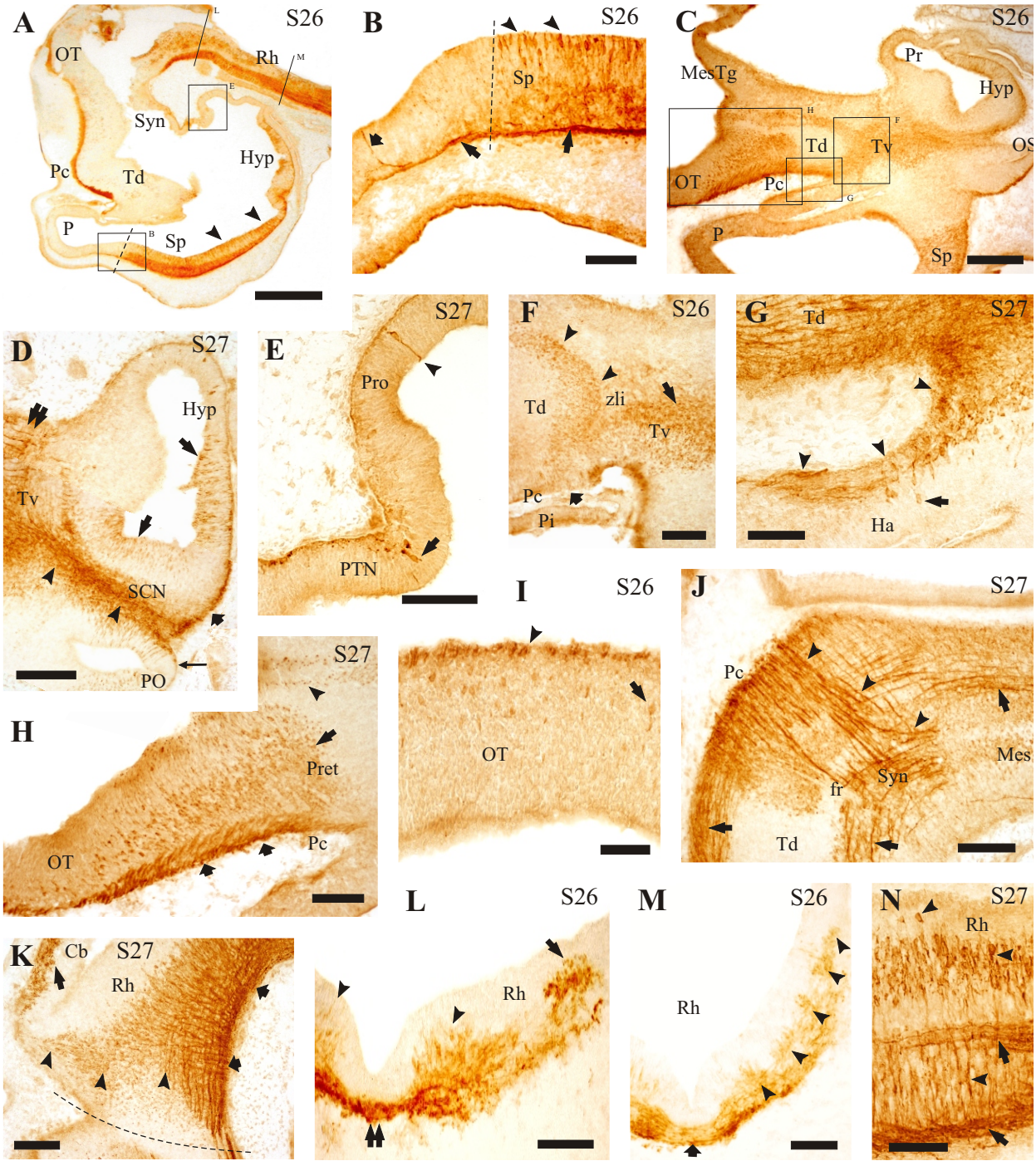
A
S26
OT
Rh
Syn
Hyp
Pc
Td
P
Sp
B
S26
Sp
C
S26
MesTg
Pr
Hyp
Td
Tv
OT
Pc
P
Sp
D
S27
Hyp
Tv
SCN
PO
E
S27
Pro
PTN
F
S26
Td
zli
Tv
Pc
Pi
G
Td
S27
Ha
H
S27
Pret
OT
Pc
I
S26
OT
J
S27
Pc
Mes
fr
Syn
Td
K
Cb
S27
Rh
L
S26
Rh
M
S26
Rh
N
S27
Rh

Fig. 4

Figure 5. Sagittal (A-D,F-M,S) and transverse (E,N-R,T) sections throughout the brain (A-S) and spinal cord (T) of embryos of *Scyliorhinus canicula* showing the distribution of GABAergic cells and fibers at S28 (A-D,I-K,N-T), S29 (E,F) and S31 (G,H,L,M). **A.** Sagittal section of the prosencephalon to show the GABAergic distribution at S28, (isthmic limit marked with broken line). **B.** Detail of the rostral telencephalon to show numerous GABAergic cells in the subpallium (arrow) and some GABAergic fibers (arrowheads) coursing towards the pallium. **C.** Lateral section of the telencephalon to show the radial migration morphology of the GABAergic cells (thick arrow) of the subpallium and some GABAergic cells migrating tangentially (arrow) towards the pallium. **D.** Detail of the dome-shaped protusions of the rostrolateral subpallial walls to show palliopetal GAD-ir cells (arrowheads) squared in C. Note the several directions taken by the tangentially migrating cells with growth cone-like leading processes at this region. **E.** Transverse section at the lateral telencephalon to show numerous GABAergic cells (arrowheads) migrating tangentially towards the pallium. Note the superficial "stripe" (thick arrow) of GABAergic tangentially migrating cells. **F.** Sagittal telencephalic section to show the morphology of the GABAergic tangential migrating cells extending rostrodorsally (arrows) towards the pallium. Inset; Detail of a characteristic leading growth cones (arrowhead) of the tangentially migrating cell squared in F. **G.** Sagittal section of the rostral prosencephalon at S31 to see the increased density of GABAergic tangentially migrating cells through the lateral (arrowhead) and dorsal (thick arrows) pallial regions. **H.** Sagittal section at lateral level of the diencephalon to show the GABAergic fiber tracts that inervate the prosencephalic tegmentum. **I.** Panoramic section of the prosencephalon to show the GABAergic domains. (isthmic limit marked with broken line). **J.** Detail of the ventral walls of the caudal hypothalamus, parallel section squared in I, to show CSF-c GABAergic cells (arrowheads) at the proximal ventricular zone of the saccus vasculossus. **K.** Detail of the mesencephalic tegmantum at the midline, showing numerous GABAergic cells with ventral processes (arrowheads). **L.** Sagittal section of the S31 optic tectum to show weak GABAergic cells mainly at the intermediate layers. **M.** Sagittal section at the isthmic level to show the different mesencephalic (arrow) and rhombencephalic (thick arrow) GABAergic cell group distribution. Note the intense density of the longitudinal GABAergic fiber tracts (arrowheads) at the alar plate. (broken line marks the isthmic limit). **N.** Transverse section at the isthmic level (marked in A), showing four periventricular GABAergic cell groups (arrowheads). GABAergic cells with thin apical process coursing to the ventricle. Note the numerous GABAergic fibers sent from the three dorsalmost GABAergic groups (thick arrow) and some GABAergic commissural fibers crossing the ventral midline (arrows). **O.** Transverse section at the acusticofacial nuclei nerve root level (marked in A), to show five periventricular GABAergic cell groups (arrowheads). Note the long basal processes (thick arrows) to the basal region sent mainly by the alar GABAergic cell groups. **P.** Detail of the ventricular zone at the alar rhombencephalic plate, parallel section squared in O, to show GABAergic cells sending a short apical process (arrowheads) that contact the ventricle. **Q.** Transverse section at the obex level showing three conspicuous GABAergic cell groups (arrowheads). **R.** Transverse detail section of the alar tegmental GABAergic cell groups at caudal level. Note the dense GABAergic cells of the viscerosensory group (arrow), the dorsalmost tegmental group. **S.** Sagittal section at the caudal rhombencephalon to show GABAergic viscerosensory and visceromotor column-associated cells (arrowheads) packed in a columnar GABAergic pattern. Note the long ventral GABAergic processes (thich arrows) send by dorsal GABAergic cells (arrow). **T.** Transverse section at the rostral spinal cord to show two main groups of GABAergic cells at the ventrolateral (arrow) and dorsolateral (arrowhead) regions. Note a few GABAergic CSF-c bipolar cells at the floor plate (thick arrow). Scale bars: 250µm (A,G,); 100µm (B,C,E,F,H,I,L-O,Q,S); 50µm (D,K,R,T); 25µm (J,P).

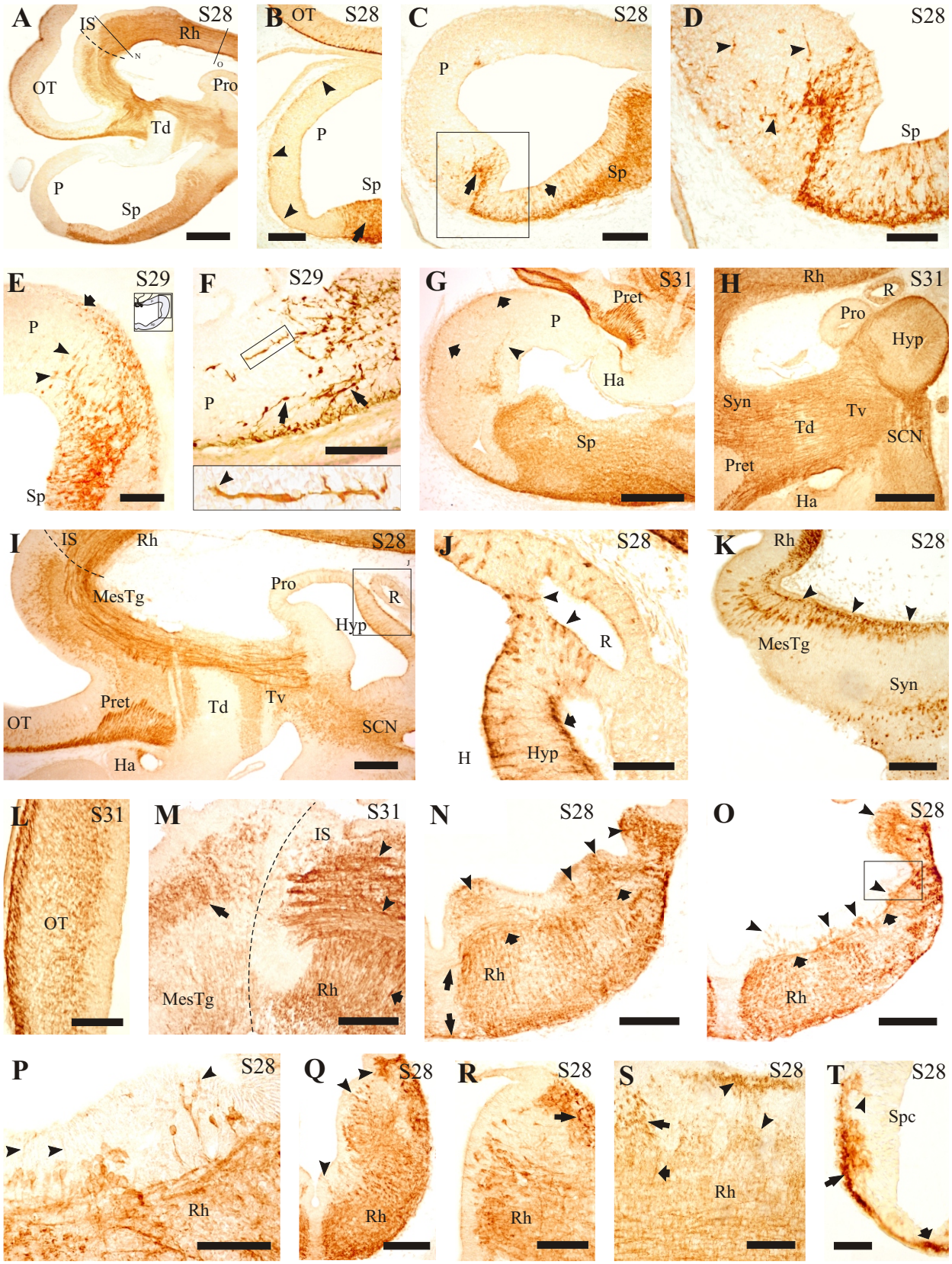
A
S28
IS
Rh
N
O
OT
Pro
Td
P
Sp
B
OT
S28
P
Sp
C
S28
P
Sp
D
S28
Sp
E
S29
P
Sp
F
S29
P
G
S31
Pret
P
Ha
Sp
H
Rh
S31
R
Pro
Hyp
Syn
Tv
Td
SCN
Pret
Ha
I
IS
Rh
S28
MesTg
Pro
R
Hyp
Pret
Td
Tv
OT
SCN
Ha
J
S28
R
H
Hyp
K
Rh
S28
MesTg
Syn
L
S31
OT
M
S31
IS
MesTg
Rh
N
S28
Rh
O
S28
Rh
P
S28
Rh
Q
S28
Rh
R
S28
Rh
S
S28
Rh
T
S28
Spc

Fig. 5

Figure 6. Drawing of a parasagittal section of the dogfish brain that schematically represents the main GABAergic fiber pathways at S31. Scale bar: 100 μm.

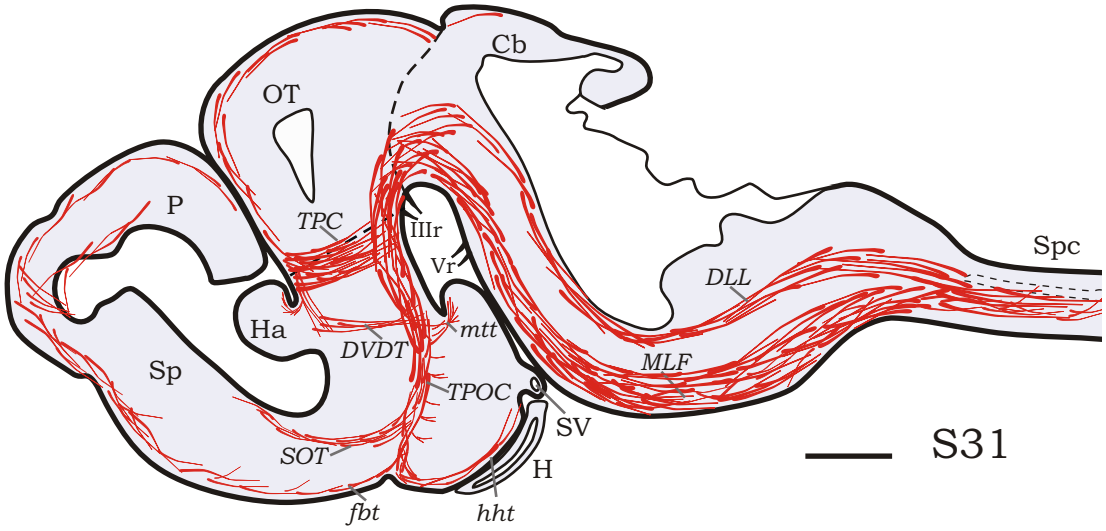
Cb
OT
P
TPC
IIIr
Vr
Spc
DLL
Ha
DVDT
mtt
MLF
Sp
TPOC
SV
S31
SOT
H
fbt
hht

Fig. 6

Figure 7. Sagittal (A,E,H) and transverse (B-D,F,G,I-M) sections throughout the brain (A-K) and spinal cord (L,M) of embryos of *Scyliorhinus canicula* showing the distribution of GABAergic cells and fibers at S32 (A,G,I-L), S33 (E,H) and S34 (B-D,F,M). **A.** Sagittal section at S32 showing some stripes of GABAergic cells in the pallium (arrowheads) and numerous GABAergic cells and fibers in the subpallium. **B.** Transverse section of the subpallium to show the distribution of GABAergic cells and fibers. Note that the density of GABAergic fibers and boutons was especially dense at the ventral basal superficial area, central superficial area and at the pallial/subpallial border (the region ventral to the lateral pallium and dorsolateral to the basal superficial area). **C.** Transverse section at the olfactory bulb, parallel section squared in B, showing intense stainly GABAergic fibers innervating the glomeruli (arrowheads). **D.** Detail of the squared area in B showing some GABAergic cells (arrowheads) at the dorsal basal superficial area. Note the intense GABAergic fiber innervations of the ventral portion of the central superficial area (thick arrows). **E.** Sagittal section of the caudal hypothalamus at S33 to show a few faintly stained GABAergic CSF-c cells (arrowheads) in the periventricular zone. Note the dense GABAergic fiber innervation of the lateral and ventral regions of the paraventricular organ. **F.** Transverse section of the caudal hypothalamus at S34 showing the "mature" GABAergic fiber innervation seen later in adults. **G.** Transverse section of the optic tectum at S32 to show the layered of GABAergic fibers. **H.** Sagittal section of the caudal rhombencephalon at S33 to show the "mature" GABAergic cell and fiber organization. Note the columnar GABAergic cell and fiber disposition at the viscerosensory and motor columns (thick arrows). **I.** Transverse section of S32 at the isthmic level to show scarce GABAergic cells (arrowhead) at the periventricular region of the dorsolateral basal plate. Note the intense density of GABAergic innervation at the central grey region (thick arrow). **J.** Transverse section caudal to the trigeminal nerve nucleus level to show numerous longitudinal GABAergic bundles of fibers located all over the tegmentum, being mainly abundant in the dorsolateral alar plate (thick arrow) and in the viscerosensory lobe (arrowhead). **K.** Transverse section at the obex level to show longitudinal GABAergic fiber bundles throughout the tegmentum, mainly located at the dorsolateral region (arrowhead) of the alar plate. **L.** Transverse section at the rostral level of the spinal cord to show GABAergic CSF-c cells at the ventral (arrowhead) and dorsolateral (thick arrow) ventricular walls of the central canal. Note the numerous non-CSF-c GABAergic perikarya located at the intermediate zone, being densest at the lateral marginal region (arrow) of the ventral horn. **M.** Transverse section of the rostral spinal cord to see some faintly GABAergic CSF-c cells (arrowheads) surrounding the central canal and a few periependymal GABAergic cells (arrow) in the ventral horn. Scale bars: 250µm (A,B,F,H); 50µm (C,D,K,L); 100µm (E,G,I,J); 25µm (M).

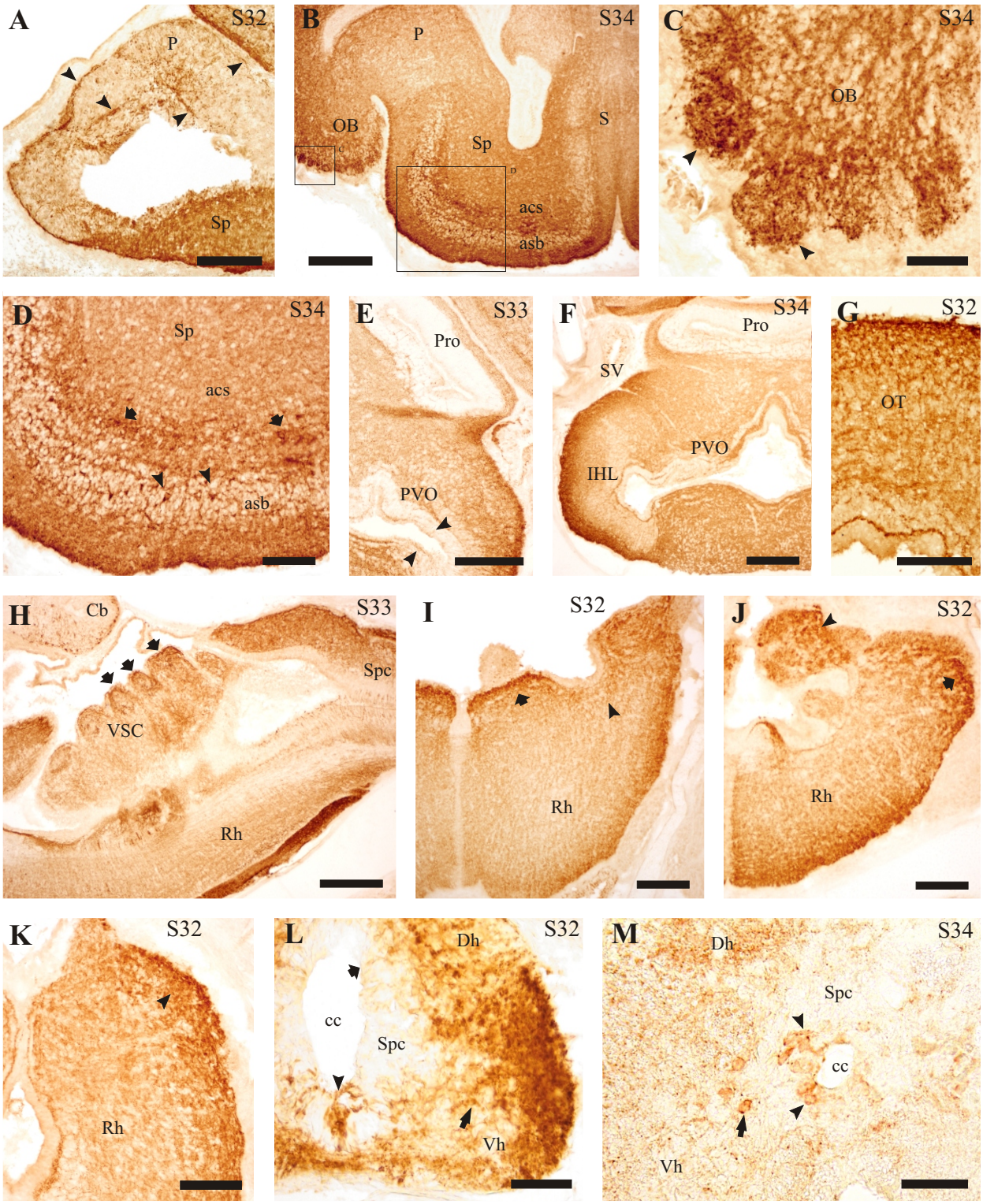
A
S32
P
Sp
B
S34
P
OB
Sp
S
acs
asb
C
S34
OB
D
S34
Sp
acs
asb
E
S33
Pro
PVO
F
S34
Pro
SV
PVO
IHL
G
S32
OT
H
Cb
S33
Spc
VSC
Rh
I
S32
Rh
J
S32
Rh
K
S32
Rh
L
Dh
S32
cc
Spc
Vh
M
Dh
S34
Spc
cc
Vh

Fig. 7

Figure 8. Schematic drawings of transverse sections through the brain and rostral spinal cord of a juvenile dogfish, showing at the right the distribution of GABAergic perikarya and fibers and at the left the anatomical landmarks. Upper drawing represents a sagittal section of the brain showing the level of transverse sections. See abbreviation list. Scale bars: 2 mm.

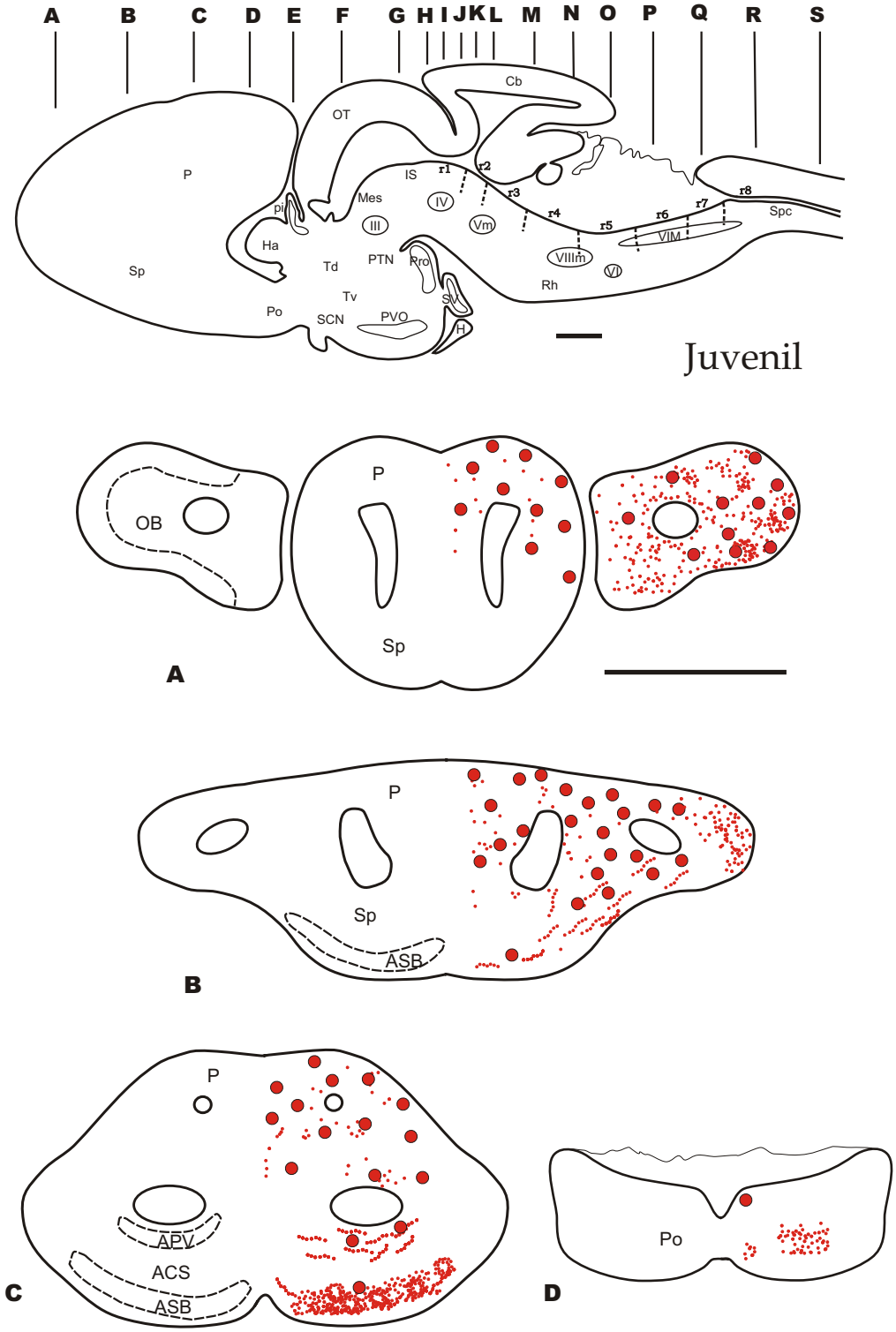
A B C D E F G H I J K L M N O P Q R S
Cb
OT
P
IS
r1
r2
r3
r4
r5
r6
r7
r8
Spc
Mes
pi
IV
III
Vm
VIM
Ha
Sp
Td
PTN
Rro
VIIIm
VI
Rh
Tv
Po
SCN
PVO
H
Juvenil
OB
P
Sp
A
P
Sp
ASB
B
P
APV
ACS
ASB
C
Po
D

Fig. 8

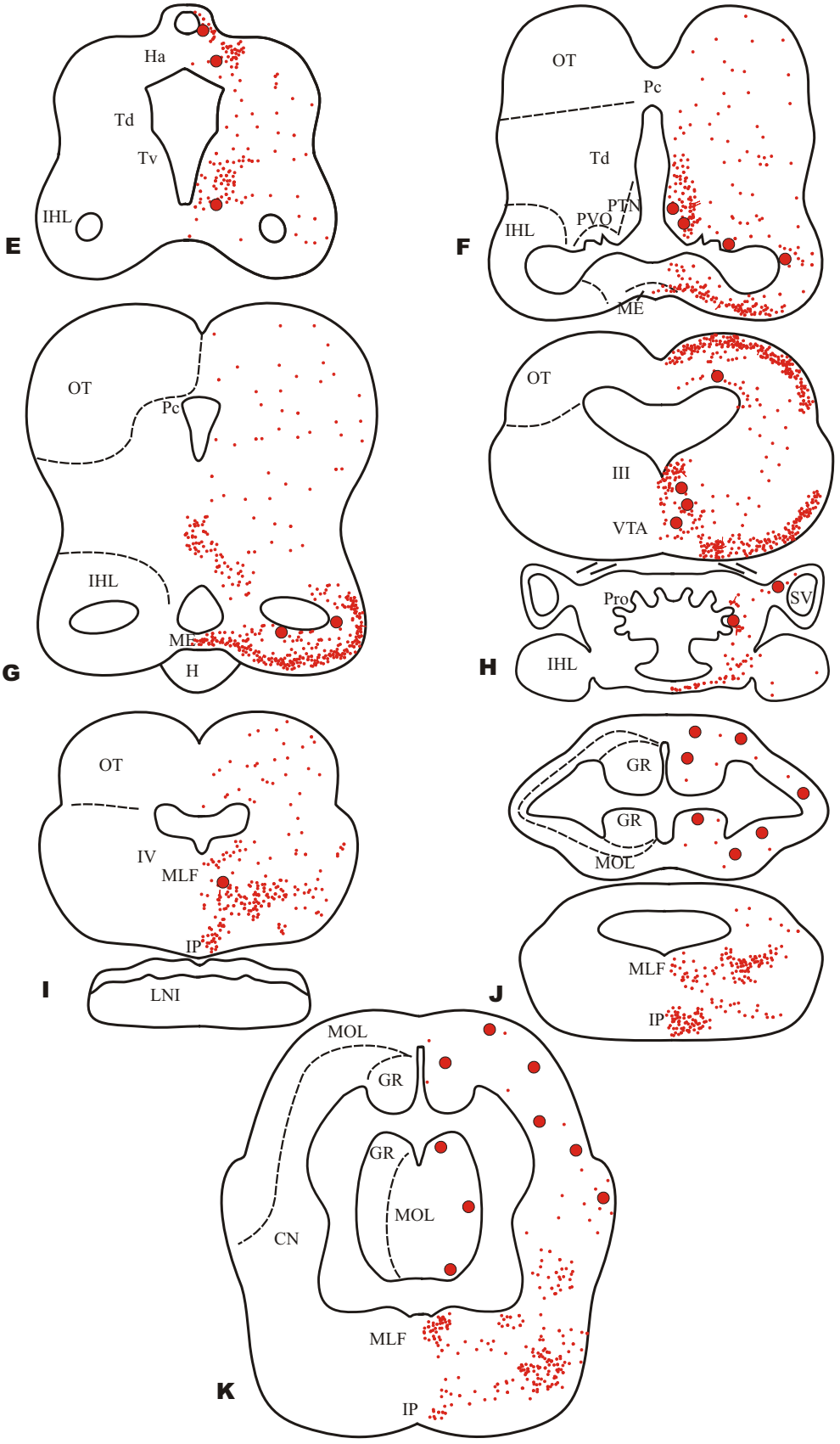
E
Ha
Td
Tv
IHL
F
OT
Pc
Td
PTN
PVO
IHL
ME
G
OT
Pc
IHL
ME
H
H
OT
III
VTA
Pro
SV
IHL
I
OT
IV
MLF
IP
LNI
J
GR
GR
MOL
MLF
IP
K
MOL
GR
GR
MOL
CN
MLF
IP

Fig. 8 (cont. I)

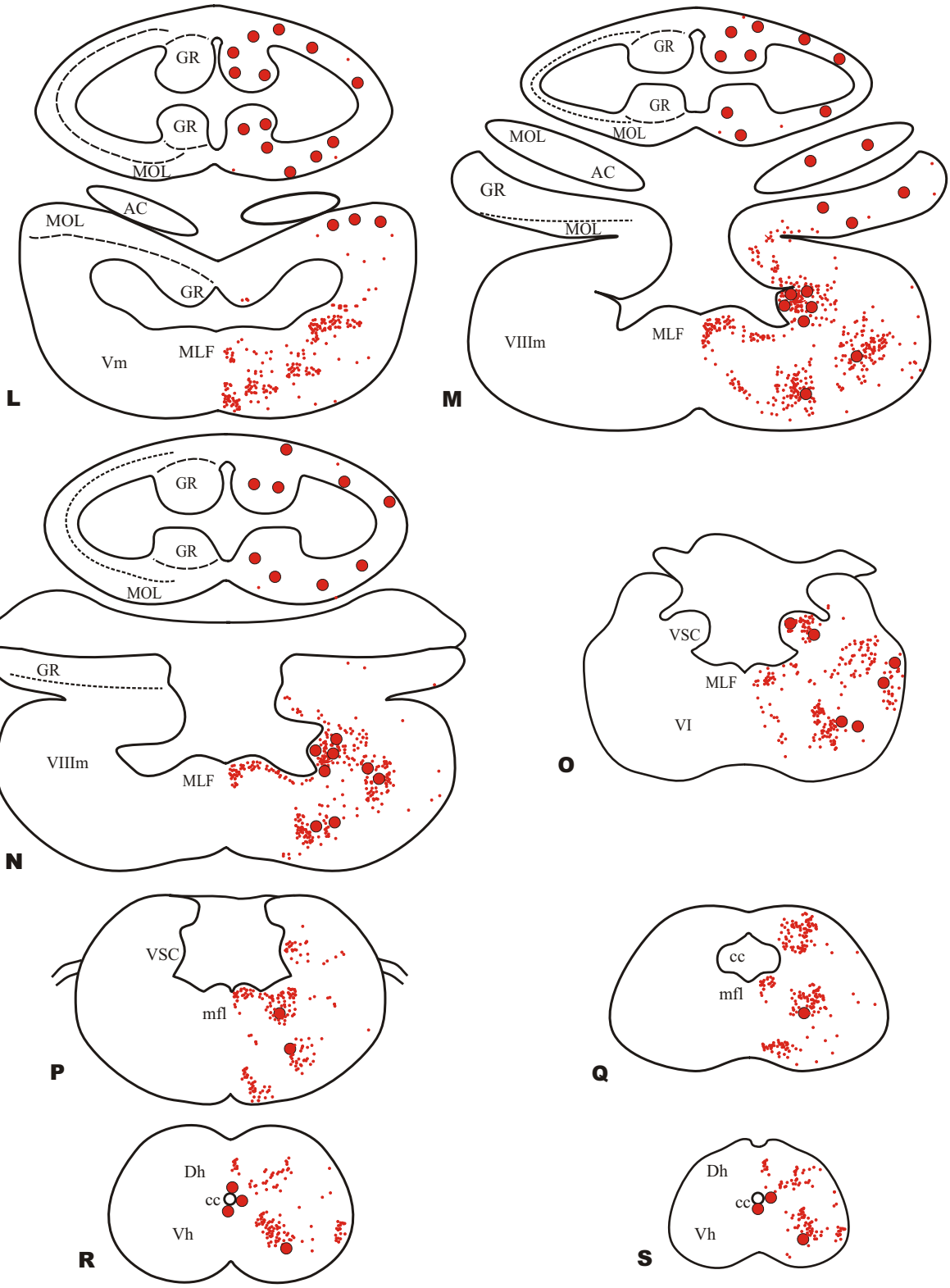
GR
GR
MOL
AC
MOL
GR
Vm
MLF
L
GR
GR
MOL
MOL
AC
GR
MOL
VIIIm
MLF
M
GR
GR
MOL
GR
VIIIm
MLF
N
VSC
MLF
VI
O
VSC
mfl
P
cc
mfl
Q
Dh
cc
Vh
R
Dh
cc
Vh
S

Fig. 8 (cont. II)

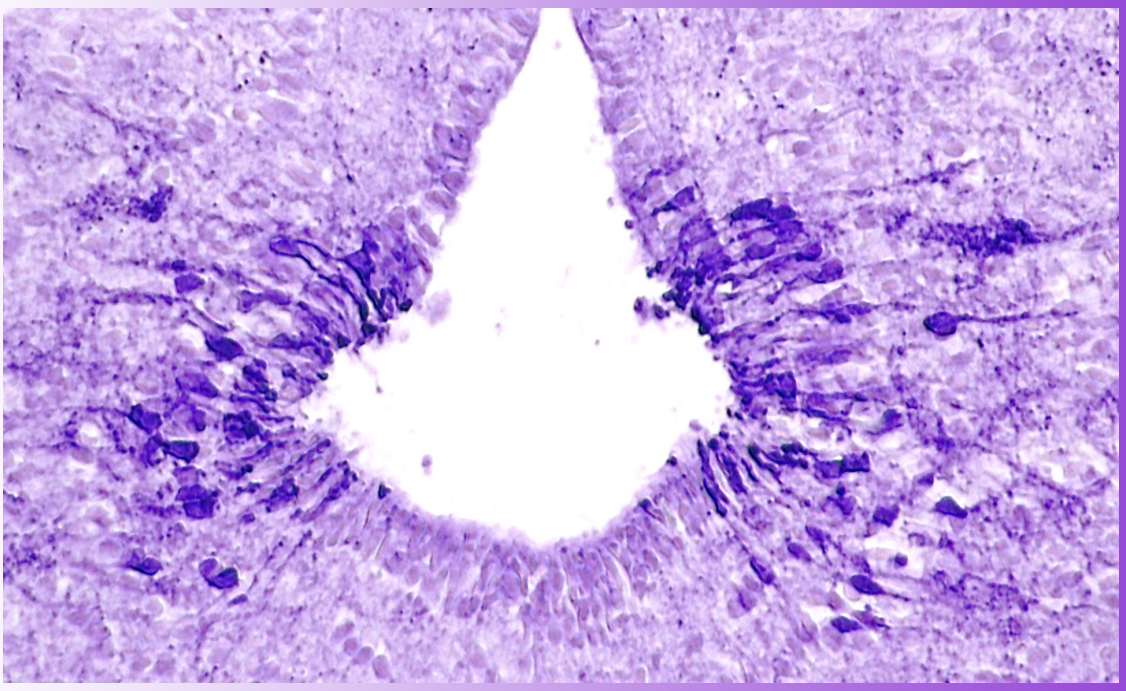

CAPÍTULO 2

Development of the Catecholaminergic System in the Central Nervous System of the lesser-spotted dogfish (*Scyliorhinus canicula*) revealed by Tyrosine Hydroxylase Immunohistochemistry

CAPÍTULO 2

Development of the Catecholaminergic System in the Central Nervous System of the lesser-spotted dogfish (*Scyliorhinus canicula*) revealed by Tyrosine Hydroxylase Immunohistochemistry

Some results of the present work appear published in the following articles:

- Sueiro, C; **Carrera**, **I**; Rodríguez-Moldes, I; Molist, P; Anadón, R. (2003) Development of catecholaminergic systems in the spinal cord of the dogfish *Scyliorhinus canicula* (Elasmobranchs). *Dev. Brain Res*. 142:141-150.

- **Carrera**, **I**; Sueiro, C; Molist, P; Ferreiro, S; Adrio, F; Rodríguez, M.A; Anadón, R; Rodríguez-Moldes, I. (2005) Temporal and spatial organization of tyrosine hydroxylase-immunoreactive cell groups in the embryonic brain of an elasmobranch, the lesser-spotted dogfish. *Brain Res. Bull*. 66:541–545.

- Sueiro, C; **Carrera**, **I**; Ferreiro, S; Molist, P; Adrio, F; Anadón, R; Rodríguez-Moldes, I. (2007) New insights on Saccus vasculosus evolution: a developmental and immunohistochemical study in elasmobranchs. *Brain Behav Evol*. 70:187-204.

- Ferreiro-Galve, S; **Carrera**, **I**; Candal, E; Villar-Cheda, B; Anadón, R; Mazan, S; Rodríguez-Moldes, I. (2008) The segmental organization of the developing shark brain based on neurochemical markers, with special attention to the prosencephalon. Brain Res Bull. 75:236-240.

INTRODUCTION

Catecholamines (dopamine, noradrenaline and adrenaline) are synthesized from the aromatic amino acid tyrosine by a series of enzymes from which, tyrosine hydroxylase (TH) is the first and rate-limiting step and catalyzes the conversion of L-tyrosine to 3,4-dihydroxy-L-phenylalanine (L-DOPA). Knowledge about the roles of catecholamines in the nervous system of vertebrates came in part from immunohistochemical studies, which allow knowing the location and cytological characteristics of the catecholamine-containing neurons.The use of antibodies against the different catecholamines, TH and other synthesis enzymes (aromatic L-amino acid decarboxylase, dopamine-b-hydroxylase and phenyl-ethanolamine-N-methyltransferase) has enabled detailed studies about catecholaminergic (CA) systems. Knowledge about the organization of this system in vertebrates are mostly based on TH immunohistochemistry since antibodies against this enzyme have been extensively and successfully applied to the brains of representative of each major class while data about the other enzymes and about catecholamines are still sparse or absent in many groups (for a review, see Smeets and González, 2000).

The study of catecholamines has become particularly important in relation to research on mechanisms regulating dopaminergic phenotype and their involvement in neurological disorders (i.e. Parkinson´s disease). To know the localization of catecholamines is essential to understand the basic functions of CA system and then try to find new pharmacological approaches in human neurological disorders. Also important is to know how CA systems have evolved. To this, comparative studies about the organization of CA in the central nervous system (CNS) of vertebrates are crucial (for revision, see Smeets and González, 2000). This approach has led to reconsider the classical view of the evolution of vertebrate central CA systems by an increase in complexity from anamniotes to amniotes and, instead, it has been proposed that anamniotes contain CA groups of which the counterparts in amniotes have lost the capacity to produce catecholamines (Smeets and González, 2000).

Comparative studies about the brain development of CA system are also essencial to better understand its evolution, however, such studies are scarce in tetrapods (Specht et al., 1981a,b: Foster, 1994; Puelles and Medina, 1994; Medina et al., 1994a,b; González et al., 1994a, 1995; Wallace et al., 1996; Marín et al., 1997; Sánchez-Camacho et al., 2002a,b) and fish (Ekström et al., 1992; Manso et al., 1993; Pierre et al., 1997; Rink and Wulliman, 2001, 2002; Pierre-Simons et al., 2002; McLean and Fetcho, 2004a,b; Abalo et al., 2005) and they are lacking in some other vertebrate groups as chondrychthyans. Development studies have revealed that the organization of CA system is highly conserved among vertebrates, being thus especially suitable for the identification of boundaries and, accordingly, for the identification of homologies. The neuromeric approach has shown to be extremely useful for this since it enables the comparative study of the brain distribution of neurons according their neurochemical contents and their topographical relationships, contributing to a better understanding of the evolution of specific brain features (Puelles, 1995). Assuming an identical segmental pattern in the brain of all vertebrates, the organization and development of the CA cell groups with respect to the segmental plan of brain organization facilitate direct comparison between different species (Smeets and González, 2000). The TH antibody has become a crucial CA marker for developmental studies in vertebrates and specially in those following a neuromeric approach (Medina et al., 1994a,b; Puelles and Medina, 1994; Puelles and Verney, 1998; Vitalis et al., 2000; Marín et al., 2005).

Elasmobranchs posses well developed CA systems, whose organization in the adult brain has been studied in several species and shows a rather consistent pattern among them (Meredith and Smeets, 1987; Northcutt et al., 1988; Stuesse et al., 1990; Stuesse and Cruce, 1992; Stuesse et al., 1994). In the adult dogfish, however, only the CA systems of the hypothalamus have been studied in detail (Molist et al., 1993) and there are no developmental studies on the CA systems of the brain of cartilaginous fish. For this, the aim of the present study was to analyze the expression of the TH in the brain and spinal cord of developing dogfish, in order to know the sequence of appearance and distribution of the different CA cells groups and main axonal pathways. The results obtained have been analyzed from a segmental approach. We believe that the present

study results would get more insight into developmental comparative aspects of CA systems in the CNS of vertebrates.

MATERIAL AND METHODS

Experimental animals

Embryos of the lesser-spotted dogfish (*Scyliorhinus canicula*) were kindly provided by the Aquarium 'Vasco de Gama', the Oceanarium of Lisbon (Portugal) and Aquarium "Finisterrae" of A Coruña (Spain). The embryos were staged according to Ballard et al. (1993). The following stages were used: stage 25 (S25 four pairs of open pharyngeal clefts; two embryos), stages 26 and 27 (S26-S27, five pairs of open pharyngeal clefts, simple gill bars; three embryos of each stage), stage 28 (S28, transverse oval mouth, gills with external filaments; five embryos), stage 29 (S29, mandibular arches crowded into the mouth opening; three embryos), stages 30 (S30, eyeballs circled with black pigment; five embryos) and stage 31 (S31, detectable rostrum and long branchial filaments; five embryos), stage 32 (S32, regression of branchial filaments and initial eye pigmentation; six embryos), stages 33 (S33) and 34 (S34, prehatching; four embryos of each stage). Five small juvenile (between 9 and 12 cm in length), and four adult dogfish (40-60 cm of total length; provided by a local fisherman) were also used.

Tissue preparation

The embryos were separated from the yolk sac and fixed by immersion in 4% paraformaldehyde in 0.1 M elasmobranch phosphate buffer (0.1 M phosphate buffer containing 670 mM urea, pH 7.4). Young and adult dogfish were deeply anesthetized with 1% tricaine methane sulfonate (Sigma) in sea water, and intracardially perfused with elasmobranch Ringer solution containing 1% procaine (3–5 min) followed by the same fixative used for embryos. Then, the brains and spinal cords were dissected out and immersed in the same fixative for 4 h. All procedures for animal experimentation

conformed to the guidelines of the European Community and were approved by the ethical committee of the University of Santiago.

Immunohistochemistry

For immunocytochemistry, the embryos and the juvenile and adult brains and spinal cords were cryoprotected with 30% sucrose in phosphate buffer (PB), embedded in OTC compound (Tissue Tek, Torrance, CA), and frozen with liquid-nitrogen-cooled isopentane. Sagittal or transverse sections of 14–16-mm thick were obtained on a cryostat and mounted on gelatin-coated slides or Superfrost Plus (Menzel-Gläser®) slides. The sections were pretreated with H_2O_2 to eliminate endogenous peroxidase, and then sequentially treated with 10% normal goat serum for 1 h, TH antibody (mouse monoclonal, Chemicon, Temecula, CA; MAB318, dilution 1:1000) overnight, phosphate-buffered saline (PBS) at pH 7.4 (two 10-min rinses), goat anti-mouse Ig serum (Dakopatts, Glostrup, Denmark, dilution 1:50) for 1 h, PBS (two 10-min rinses), mouse PAP complex (Dakopatts, dilution 1:250) for 1 h, and PBS (two 10-min rinses). The immunoreaction was developed with 0.005% diaminobenzidine (DAB; Sigma) and 0.003% H_2O_2. All dilutions were made in PBS containing 0.2% Triton X-100, and incubations were made in a humid chamber at room temperature. Finally, the sections were dehydrated, mounted and coverslipped. According to the technical information supplied by the manufacturer, the TH antiserum was raised against denatured TH from rat pheochromocytoma and it recognizes an epitope on the outside of the regulatory N-terminus of TH. Its specificity has been assessed by Western blot; it recognizes a single protein band of approximately 59-63 kD and does not cross-react with dopamine-beta-hydroxylase, phenylalanine hydroxylase, tryptophan hydroxylase, dehydropteridine reductase, sepiapterin reductase and phenethanolamine-N-methyl transferase. Moreover, the antibody has wide species cross-reactivity and was used for demonstrating the catecholaminergic systems in a number of species (Melander et al., 1986; Rolletschek et al., 2001; Chu and Wilczynski, 2002; Jakobsson et al., 2004). In the adult dogfish brain, the TH antibody yielded results comparable to those described previously in distribution maps of this substance in the elasmobranch brain (Northcutt et al., 1988; Stuesse et al.,

1990; Stuesse and Cruce, 1991; Stuesse and Cruce, 1992; Stuesse et al., 1992). In addition, in negative controls performed by omitting the primary, secondary or tertiary antibodies, no immunostaining was observed.

Imaging

The sections were photographed with an Olympus microscope equipped with a color digital camera. The photos were adjusted for brightness and contrast with Corel Photo Paint (Corel, Ottawa, Canada), and composed with Corel Draw.

RESULTS

The chronological development of the TH-ir cell groups is summarized in Table I. The first TH-immunoreactive (TH-ir) cells appeared in the diencephalon (suprachiasmatic, posterior tubercle and posterior recess nuclei) and rostral spinal cord at S26. At S28, TH-ir cells occupied the ventral thalamus/dorsal hypothalamus while at S30-S31 a great number of TH-ir cell groups appeared in the telencephalon (pallium), synencephalon (sustantia nigra/rostral ventral tegmental area), mesencephalon (caudal ventral tegmental area) and rhombencephalon (locus coeruleus/subcoeruleus, viscerosensory column and reticular formation). From S32 to S33, TH-ir cells were observed at the olfactory bulb, preoptic area and paraventricular organ while the latest TH-ir cells appeared in the subpallium and saccus vasculosus at juveniles and in the central grey region at adults. The first TH-ir fibers were observed in the posterior tubercle of S28 and at S31 the main ascending and descending fiber pathways were established. At S32, TH-ir fibers reached most of CNS areas and the active phase of maturation of the catecholaminergic system started. The organization of TH-ir cells and fibers observed in postembryonic stages (juveniles and adults) could be roughly recognized at S33. This “mature” organization was featured by the high density of TH-ir neurons in the main catecholaminergic nuclei (suprachiasmatic nucleus, posterior tubercle, sustantia nigra/ventral tegmental area, viscerosensory column and spinal cord)

and their profuse TH-ir innervation, being the main TH-ir pathways also recognized at this stage (S33).

Distribution of TH-ir cells and fibers during embryonic development

The distribution of TH-ir cells and fibers in the CNS of the developing dogfish is schematically represented in Figure 1.

Stages 26-27 (S26-S27)

The first TH-ir cells were detected in the diencephalon of S26 (Fig. 1A). Most of them appeared in the posterior tubercle, although a few weak labelled TH-ir cells were also in the caudal walls of the posterior recess (Fig. 2A) and at postchiasmatic levels, just caudally to the preoptic recess (Figs. 1A). These diencephalic TH-ir populations formed the primordia of the posterior tubercle nucleus, posterior recess organ and the suprachiasmatic nucleus (PTN, Pro and SCN), respectively. Moreover, in the rostral spinal cord some TH-ir cerebrospinal fluid-contacting (CSF-c) cells were observed in the floor plate (Figs. 1A, 2B).

Stages 28-29 (S28-S29)

From S28, two types of TH-ir cells were identified in the posterior recess organ on the basis of their relation with the ventricle. Some cells showed a ventricular process, being CSF-c cells, while others were located superficially and extended processes parallel to the outer surface (Fig. 2C). At these stages, the density of TH-ir cells in the PTN (Figs. 2C,D) and the SCN (Fig. 2D) increased, and a few weakly TH-ir cells were also observed dorsocaudally to the SCN and ventrorostrally to the PTN, extending between these two TH-ir nuclei (Figs. 1B, 2D,E). These weakly stained TH-ir cells were placed in a region extended between the ventral thalamus (Tv) and the dorsal hypothalamus. We have termed this TH-ir group as the ventral thalamus/dorsal hypothalamus group. Moreover, the number of TH-ir CSF-c cells per section of the rostral spinal cord increased notably in relation with previous stages (Fig. 2F).

Stage 30 (S30)

The density of diencephalic TH-ir cells and fibers in the PTN and SCN increased notably with respect to previous stages (Figs. 1C, 2G-K). At this stage, the TH-ir cells and fibers of the ventral thalamus/dorsal hypothalamus showed higher cell density and intensity of immunostaining than previously (Figs. 2H,I). As in previous stages, these TH-ir cells extended through the ventral (rostral) part of the ventral thalamus and dorsal hypothalamus forming an apparently continuous TH-ir population with those of the PTN and the SCN (Figs. 2H,I). In contrast, the number of TH-ir cells in the posterior recess organ did not increase appreciably with development (Fig. 2J). Also at this stage, a few weakly TH-ir cells appeared in subventricular position at the rostral rhombencephalon representing the locus coeruleus primordium (LC; Table I; Fig. 1C). In addition, a few weakly stained TH-ir cells were seen in the caudal tegmentum (Figs. 1C, 2M), representing the primordial catecholaminergic cells of the caudal reticular formation (Ret; Table I). In the spinal cord, the CSF-c TH-ir cells were numerous along the floor of the central canal. On the basis of their size, shape, immunostaining intensity and relative position to the ventricle, these TH-ir cells appeared to form a heterogeneous population (Fig. 2N).

Thick prolongations of the ventral thalamus/dorsal hypothalamus TH-ir cells showing terminal dilatations with the appearance of growth cones were observed longitudinally oriented between the PTN and SCN groups (Figs. 2H,I). No TH-ir fibers were observed rostrally to the SCN and, in consequence, no ascending tracts were observed at this stage, being the rostral forebrain absent of any TH immunoreactivity. At this stage, some thin and scarce TH-ir fibers clearly arising from SCN TH-ir cells coursed throughout the hypothalamic floor forming part of the primordial hypothalamo-hypophyseal tract (Fig. 2G). Thin descending longitudinal fibers (Figs. 2K,L) that arise from PTN TH-ir cells were seen along the basal plate throughout the synencephalon and mesencephalon without reaching the rostral rhombencephalon (isthmus). Longitudinal TH-ir fibers were not observed in the rhombencephalon. Within the spinal cord, TH-ir

fibers were present in the the ventral region (Fig. 2N), while at rostral levels TH-ir longitudinal fibers were densely gathered in the ventral funiculum.

Stage 31 (S31)

At this stage, a few weakly stained TH-ir neurons appeared in the dorsal part of the caudal telencephalon (Figs. 1D, 3A). These TH-ir neurons were scattered and presented small oval perikarya with thin processes not showing any particular orientation. At this stage, further TH-ir cell groups appeared in the synencephalon, mesencephalon and rhombencephalon (Fig. 1D; Table I). In early S31, a few weakly TH-ir cells were observed rostrally to the basalmost extension of the fasciculus retroflexus (Fig. 3B). Later, two clearly separated groups of weakly stained TH-ir cells, rostral and caudal, were recognized in the synencephalic and mesencephalic tegmenti: the rostral group was located around the basis of the fasciculus retroflexus (synencephalon), whereas the caudal group was located at the level of the oculomotor nerve root (midbrain; Fig. 1D). The rostral group gave rise to conspicuous medial and lateral TH-ir populations, the rostral ventral tegmental area (rVTA; Figs. 1D, 3B), and the substantia nigra (SN), respectively. The midbrain group only originated the faintly stained TH-ir cell group corresponding to the caudal ventral tegmental area (cVTA), located at the level of the oculomotor root. Thus, the weakly TH-ir cells that appeared in the synencephalon of early S31 (Fig. 3B), constituted the primordium of the ventral tegmental area/substantia nigra cell groups (VTA/SN). In the rostral rhombencephalic tegmentum (isthmic level) of late S31, TH-ir cells were gathered in two groups located dorsally in the tegmentum and laterally to the walls of the fourth ventricle (Fig. 1D). The somata of these neurons were ellipsoid with processes extending ventrolaterally away from the ventricle. On the basis of its neuroanatomical position, the most dorsal group, already observed at S30, corresponded to the locus coeruleus (LC; Figs. 1D, 3E), while the ventralmost group extended more laterocaudally, corresponding to the reticular nucleus subcoeruleus (Sc; Fig. 1D). In the rhombencephalon, extending throughout the viscerosensory lobe (between the level of the facial nerve root and the

vagal nucleus), a number of TH-ir cells exhibited a round darkly stained somata surrounded by a dense network of processes (Fig. 1D). Some TH-ir cells were also seen extended in a periventricular position just ventral to the sulcus limitans, forming the visceromotor column-associated cell group. In the caudal rhombencephalon, medium-sized to small TH-ir perikarya belonging to the reticular formation extended at the caudalmost region of the rhombencephalon, from the caudal level of the abducens motor nucleus to the obex level. They appeared grouped in two populations on the basis of their position and orientation. The most dorsal group, located just lateral to the viscerosensory lobe, contained TH-ir cells with dorsolaterally oriented processes while the second group, located slightly more ventrocaudally (Fig. 3F), showed their processes lateroventrally oriented.

In the posterior recess organ, some thin TH-ir fibers were observed coursing along the external walls, probably arising from the PTN (Figs. 3B, 4). In this stage, the density of TH-ir fibers that coursed along the hypothalamic floor from the SCN increased. No ascending fibers from the diencephalon were observed. However, in the caudalmost rhombencephalon, just rostrally to the area postrema level, some longitudinal ascending TH-ir fibers were observed coursing in the ventromedial region of the tegmentum (Fig. 3G), reaching the caudal level of the abducens motor nucleus. These ascending TH-ir fibers showed a typical migrating pattern (Figs. 3G,H). The main origin of these ascending TH-ir fibers seemed to be the spinal cord TH-ir CSF-c cells located ventrally to the central canal (Fig. 3G). Longitudinal, probably ascending, TH-ir fibers were also observed along the entire extension of the spinal cord, except in its caudal part. The stage 31 was also characterized by the development of the main descending TH-ir fiber tracts that ran from the diencephalon to the rostral rhombencephalic tegmentum (caudally to the isthmic level; Figs. 1D, 3C,D, 4). As seen in S30, the origin of the main TH-ir descending tracts seemed to be the PTN. These tracts coursed longitudinally throughout the synencephalic and mesencephalic tegmenti among the weakly TH-ir cells of the VTA/SN and further, reaching the isthmic tegmentum (Figs. 3C,D, 4). The straight course of these TH-ir fibers, the absence of branching and the presence of

abundant axon-ending bulbous dilatations (growth cones), revealed a clear migrating pattern (Fig. 3D).

Stage 32 (S32)

At S32, the number of TH-ir cells increased considerably in most already established nuclei (Table I; Figs. 5A-L), although further TH-ir populations appeared in the olfactory bulbs and preoptic area (Figs. 5A,C). In the olfactory bulb, TH-ir cells and fibers were located in the primordial granule cell layer, close to the olfactory recess, (Fig. 5A). In the dorsal telencephalon (pallium), TH-ir cells increased considerably their density, and TH-ir cells formed a scattered population that extended from caudal to rostral pallial levels (Fig. 5B). In the preoptic region, small scattered periventricular TH-ir cells were observed at the preoptic recess walls (Fig. 5C). In the diencephalon, the TH-ir cells of the SCN (Figs. 5E,F), PTN (Figs. 5D,E) and ventral thalamus/dorsal hypothalamus (Figs. 5D,E,F) increased considerably their density and remained forming a continuous band (Fig. 5E), although different subpopulations were distinguished by the cell size, processes orientation, cell density and staining intensity. This continuous diencephalic band of TH-ir cells and fibers seemed to be adjacent to the TH-ir cell groups of the VTA and SN (Figs. 5E,G). At the isthmus level, the locus coeruleus and subcoeruleus TH-ir cells (Figs. 5H) reached their highest density at this stage. In the rhombencephalon, the TH-ir cells associated to the viscerosensorial and visceromotor columns increased considerably their density in relation to the previous stage, as well as their intrinsic TH-ir fibers (Figs. 5I,J). Also at this stage, the density of TH-ir reticular cells and fibers in the caudal rhombencephalon increased notably (Fig. 5K). Intense staining TH-ir CSF-c cells were observed almost throughout the entire length of the spinal cord (Fig. 5L).

At this stage, the first TH-ir fibers were observed in the telencephalon. They were located at the granule cell layer of the olfactory bulbs (Fig. 5A) and in the pallium (Fig. 5B). As at this stage ascending TH-ir fibers extended just slightly rostral from the preoptic area (Fig. 4), we have considered that the scarce telencephalic innervation has

an intrinsic origin (Fig. 5B). Within the ventral diencephalon it was clearly observed that the profuse TH-ir tract that ran along the hypothalamic floor (Figs. 5M,N) through the median eminence finally reached the neurointermediate lobe of the hypophysis thus forming part of the hypothalamo-hypophyseal tract. At this stage, a few smooth TH-ir fibers coursed through the external surface of the saccus vasculosus epithelium close to the vascular walls, and small TH-ir bundles were observed in its lateral pouches (Fig. 5N). In early S32, two different descending TH-ir fibers tracts were observed from the diencephalon (Figs. 4; 5D,E,G) coursing throughout the alar and basal regions of the tegmentum. The PTN seemed to be the main origin of both the basal (Figs. 5D,E) and the alar denscending tract, although TH-ir cells of the ventral thalamus/dorsal hypothalamus (Fig. 5G) may also contribute to the alar tract. At caudal rhombencephalic levels both tracts seemed to blend with the TH-ir spinal cord ascending fibers (Figs. 4, 5D,O,P). A conspicuous TH-ir innervation (formed by both longitudinal and intrinsic TH-ir fibers) was observed at the viscerosensory column, in the dorsal region of the caudal tegmentum, tangled with the TH-ir cell bodies (Figs. 5I,J). In the rostral half of the spinal cord, the distribution of the TH-ir fibers was similar to the previous stage, but the density of the innervation in the ventromedial region increased notably. Also at this stage, some TH-ir fibers were observed gathered at the lateral and ventrolateral regions of the rostral half of the spinal cord.

Stages 33- 34 (S33-S34)

In the olfactory bulb of S33 we already recognized the two TH-ir cell types (granular and periglomerular cells) described in adults on the basis of their location and morphology (Sueiro, 2003). At the granular cell layer, many oval TH-ir cells were observed extending processes in several directions (Figs. 6A,B). These granular neurons were in higher density than the TH-ir cells also found near the glomerulii (periglomerular cells) (Figs. 6A,B). No TH-ir cells were observed in the ventral telencephalon (subpallium) and in the lateral pallium, while in the dorsal pallium the density of TH-ir cells increased notably (Figs. 1E, 6C). In the preoptic region of S34

(prehatching embryos), scattered TH-ir periventricular neurons were observed ventrally to the preoptic recess and a few CSF-c cells were noted in its walls. From rostral levels of the optic chiasm, the numerous TH-ir cells of the SCN formed a tight cluster with dorsoventrally oriented processes that did not contact the ventricle. As in preceeding stages, this group was continuous with the TH-ir cells of the ventral thalamus/dorsal hypothalamus and PTN (Figs. 1E, 6D-G), which showed a high cell density. In the posterior recess organ, TH-ir cells showed similar density than in previous stages (Figs. 6D,E,G). In S33, a few TH-ir cells were observed in the dorsal walls of the paraventricular organ (PVO; Figs. 6F,G), and some of them were CSF-c cells (Fig. 6G). Just caudally to the PTN, the TH-ir cells of the ventral tegmental area formed a tight medial cluster that extended throughout the synencephalic and rostral mesencephalic tegmenti until the caudal level of the interpeduncular nucleus (rostral rhombencephalic level) (Figs. 1E, 6D,F). From S33 onwards, these TH-ir neurons were highly stained and their processes were predominantly oriented dorsoventrally (Figs. 6D,F). The fasciculus retroflexus divides this major TH-ir cell group in two subgroups (Fig. 6D), a rostral (synencephalic) and caudal (mesencephalic) VTA subgroups (rVTA and cVTA, respectively) (Fig. 1E). A small cluster of TH-ir neurons, the substantia nigra (SN), was observed laterally to the rVTA (Fig. 6F). This lateral synencephalic population presented darkly stained somata with large processes always oriented mediolaterally (Fig. 6F). At these late stages, the rhombencephalic TH-ir cell groups showed almost no variation in density with respect to previous stages, although the TH-ir cells of the viscerosensory lobe, mainly at S34, increased notably their immunoreactivity, size and density (Fig. 6H). From S33, a second type of TH-ir cells was observed in the rostral spinal cord (Fig. 6I). While most of the TH-ir cells observed in previous stages were CSF-c cells located ventral to the central canal, a few moderately TH-ir stained cells with fairly irregular perikarya were located ventromedially in the rostral spinal cord. In transverse sections, these TH-ir cells exhibited a bipolar or multipolar appearance, with rather irregular, frequently branched dendrites extended in the grey matter or into the adjacent white matter, but never contacted the ventricle (Fig. 6I).

In the olfactory bulb of S33 and prehatching stages, a dense amount of thin TH-ir fibers was observed in the granular layer being scarce in the glomerular layer and absent in the olfactory fibre layer (Figs. 6A,B). Within the telencephalic hemispheres, the only innervated regions (intrinsic TH-ir fiber innervation) were the dorsal pallium pars superficialis (Fig. 6C) and the lateral pallium. The most densely innervated areas in the diencephalon were the preoptic area, SCN, dorsal walls of the PVO, posterior tubercle (Figs. 6D-G), ventral thalamus (Figs. 6D,E) and synencephalic tegmentum (Figs. 6D-F). A moderate to scarce density of TH-ir fibers was observed in the rest of the diencephalic areas, while no TH-ir innervation was observed in the habenula and dorsal thalamus. The distribution of TH-ir fibers observed in the SV in these late embryonic stages (Fig. 6J) was similar to S32 but the density of fibers coursing along the hypothalamic floor to the neurointermediate lobe of the hypophysis was higher in prehatching embryos. In the mesencephalon and rhombencephalon, TH-ir fibers were mainly observed in the locus coeruleus region, cerebellar peduncle and in the viscerosensory lobe (Fig. 6H) while no TH-ir fibers were seen at the optic tectum or cerebellum.

A few thin scattered axons were observed emerging rostrally from the preoptic area probably corresponding to a TH-ir ascending axonal pathway to the telencephalon (Fig. 4). At S33 and S34, the density of the two longitudinal TH-ir tracts descending from the diencephalon increased considerably (Fig. 6E) and they were observed along the mesencephalic and rhombencephalic tegmenti, intermingled with the TH-ir ascending rhombencephalic fibers (Fig. 4). The distribution of the TH-ir fibers in the spinal cord of S33 was much more complex than in previous stages (Fig. 6I). Despite of the increased density of the TH-ir fibers at the ventral and lateral funiculi, a small TH-ir fiber tract was developed in the dorsal funiculus at the dorsal horn. In sagittal sections, these TH-ir tracts consisted of thin beaded fibers mainly observed in the rostral half of the spinal cord.

Distribution of TH-ir cells and fibers in juveniles and adults

The distribution of TH-ir cells and fibers in the juvenile CNS is schematically represented in figure 7. This distribution was roughly similar to adults although the TH-ir cell groups were less conspicuous in juveniles and the density of TH-ir fibers and bouttons was lower.

Telencephalon

TH-ir cells. The distribution of the TH-ir structures in the juvenile olfactory bulbs was similar to the previous stages (S33-S34) but showing higher density (Figs. 7A,B; 8A,B). Juvenile olfactory bulbs showed bipolar TH-ir cells near the glomerulii (Figs. 7A; 8A,B) with processes that surrounded them, as reported in adults (Sueiro, 2003). In the telencephalic hemisphere, the caudal pallium pars dorsalis showed high density of TH-ir cells (Figs. 7A-C; 8C) of different subtypes depending on the soma morphology (granular, monopolar, bipolar and triangular cells), as described in adults by Sueiro (2003). The lateral pallium also contained some round TH-ir cells (Fig. 8D) surrounded by a moderate TH-ir fiber network. Although not observed in embryos, some scattered TH-ir cells were found in the caudal subpallium of juveniles (Figs. 7B,C; 8E), mainly located at caudal levels of the basal superficial area and ventral septum. Most of these TH-ir cells were round in shape and in general faintly stained. In the adult subpallium, the TH-ir cells were scarce at rostral regions of the basal superficial area and ventral septum but more abundant caudally.

TH-ir fibers. In the telencephalic hemispheres of juveniles, and observed previously in adults (Sueiro, 2003), the density of TH-ir fibers in the pallium was higher than in the subpallium, being especially high at the medial pallium. In spite of the abundant TH-ir innervation observed in the ventral telencephalon of juveniles, the presence of longitudinal TH-ir fibers, could be well discerned specially in the caudal part of mature juveniles (one month after hatching) were they appeared to course along with the medial forebrain bundle (Fig. 8F). These longitudinal TH-ir fibers extending between telencephalon and diencephalon could be also distinguished in adult (Fig. 8G).

More rostrally, these TH-ir fibers appeared to densely innervate the basal superficial area and the periventricular ventrolateral regions of the subpallium contrasting with the scarce TH-ir innervation in the striatum and septum. Its origin could be in the diencephalic TH-ir neurons (preoptic, suprachiasmatic, ventral thalamus and posterior tubercle groups) (Figs. 8F,G).

Preoptic area

TH-ir cells. A few scattered TH-ir cells were still observed in the preoptic area of posthatching stages, being mainly periventricular cells without contacting the ventricle (Figs. 7D; 8F).

TH-ir fibers. In spite of the weak to moderate TH-ir innervation observed at preoptic levels it was possible to discern, especially in juveniles, thick longitudinal TH-ir process that coursed longitudinally between the diencephalon and telencephalon as mentioned above.

Hypothalamus and posterior tubercle

TH-ir cells. In juveniles and adults, numerous small TH-ir cells of the suprachiasmatic nucleus were spreaded out occupying a wider region than that observed at previous stages (Figs. 7E; 8F,I). The density and the staining intensity of the TH-ir cells of the ventral thalamus/dorsal hypothalamus, posterior tubercle and posterior recess organ were roughly similar to that observed at the prehatching stage, presenting the same continuous TH-ir cell distribution (Figs. 7E,F; 8H,I), although the highest cell density was still observed at the posterior tubercle. A few faintly TH-ir perikarya were noted in the dorsal walls of the paraventricular organ of juveniles and adults. Also in the walls of the saccus vasculosus, scarce TH-ir cells, generally grouped in pairs showed a short ventricular process, being mainly located at the proximal regions, near the neurointermediate lobe.

TH-ir fibers. A dense TH-ir intrinsic innervation was observed at the posterior tubercle of juveniles and adults (Figs. 7F; 8H-J), being moderate to weak in the external walls of the posterior recess organ and saccus vasculosus (Figs. 7H; 9G). The

longitudinal TH-ir fibers observed along the hypothalamic floor were in high density at proximal levels (Figs. 7F,G; 9F), but moderate in the median eminence and neurointermediate lobe. Abundant longitudinal TH-ir fibers appeared to course connecting the posterior tubercle with the telencephalon (Figs. 8F,G) and with the synencephalon (Fig. 8J), although at the adult their density decreased considerably.

Epithalamus and thalamus

TH-ir cells. No TH-ir neurons were found in the epithalamus, in either the pineal organ or the habenula of juveniles and adults. Dorsally (caudally) to the suprachismatic nucleus, abundant TH-ir neurons were observed in the ventral thalamus/dorsal hypothalamus region (Figs. 7E,F; 8F-I), with their processes laterally oriented.

TH-ir fibers. Moderate TH-ir innervation was mainly observed in the ventral thalamus/dorsal hypothalamus (Figs. 7E; 8F-I) and at the habenular dorsolateral nucleus (Figs. 7E; 9E), being gathered in a mass that extended to the dorsolateral area. A few TH-ir fibers were also seen in the posterior commissure but not in the pineal organ and in the subcommissural organ. Although a bundle of TH-ir fibers were observed coursing in the habenular commissure, the main longitudinal TH-ir fibers appeared to course throughout the ventral thalamus/dorsal hypothalamus TH-ir cell group, extending between the rostral and the caudal prosencephalon (Figs. 8F,G,I).

Synencephalon and mesencephalon

TH-ir cells. Both in juveniles and adults, the TH-ir cell density of the extense band along the synencephalic (SN/rVTA) and mesencephalic tegmentum (cVTA) slightly decreased (Figs. 7G,H; 8H,I,K,L), although in transverse sections their large and rounded TH-ir perikarya showed an intense immunoreactive staining and exhibited a thick long processes extended mediolaterally between the SN and the rVTA TH-ir cells (Fig. 8K) or rostro-caudally between both VTA subgroups (Figs. 8H,L).

TH-ir fibers. The TH-ir innervation of the synencephalon was less dense than in the diencephalon and, although there were widely spread fibers within this region,

they were concentrated close to the midline (Figs. 7G,H; 8J). This network of TH-ir fibers was extended between the synencephalon and the mesencephalon tegmentum, arching around the corresponding TH-ir neuronal groups. In the mesencephalic tegmentum, a moderate to scarce innervation of TH-ir fibers was observed in the dorsal periventricular region (Figs. 7H,I; 8J), surrounding the interpeduncular nucleus and in the remaining regions of the mesencephalic tegmentum. In the optic tectum a moderate amount of TH-ir fibers innervated the periventricular walls being scarce or absent in the superficial tectal layers (Fig. 9H).

Rhombencephalon

TH-ir cells. The TH-ir cells of the locus coeruleus (Figs. 7K; 8M,N; 9A) and subcoeruleus (Figs. 7K; 8N) groups observed at the rostral rhombencephalon showed almost no variation in density with that observed in prehatching stages, although their staining intensity decreased slightly in postembryonic stages. Interestingly, in adults a group of few small weak oval TH-ir cells were observed in the central grey at medial subependymal regions between the caudal level of locus coeruleus/subcoeruleus groups and the rostral level of the trigeminal motor nucleus (Fig. 9B). More caudally, numerous TH-ir neurons were grouped in the periventricular region of the facial and vagal lobes of juveniles and adults although in a lesser density than in late embryos (Figs. 7M-P; 9C). In contrast to the previous stages, the intensity of immunolabelling in the TH-ir ventrally oriented reticular cells was moderate in juveniles and adults (Figs. 7M-Q; 9D). No TH-ir cells were observed in the cerebellum of juveniles or adults.

TH-ir fibers. At the isthmus level, a moderate density of TH-ir fibers was present in the region located between the trochlear nucleus (recognizable by the ChAT-immunoreactivity of its cells) and the fourth ventricle while this innervation was scarce surrounding the interpeduncular nucleus. At slightly caudal levels, abundant TH-ir fibers innervate the lateral walls to the interpeduncular nucleus (Figs. 7I-K), the surroundings of the locus coeruleus (Figs. 7K; 8M; 9A), the dorsal periventricular zone (central grey region; Figs. 7L; 9B) and laterally to the midline (Figs. 7L-O; 9I) while at caudal levels moderate to abundant density of TH-ir fibers was seen in the dorsal part of

the viscerosensory column (Figs. 7M-P; 9C). A few scattered TH-ir fibers were also observed laterally to the inferior olivary nucleus (Figs. 7P,Q). In the remaining rhombencephalic areas TH-ir fibers were scarce or absent.

Spinal cord

TH-ir cells. In juveniles and adults, CSF-c TH-ir neurons were located ventrally to the central canal from the rostral to medial levels of the spinal cord (Figs. 7R,S; 9J), and a few TH-ir cells were also observed at the ventral horn of the rostral spinal cord (Figs. 7R,S).

TH-ir fibers. In both juveniles and adults the TH-ir fibers were observed along the whole extension of the spinal cord, and although they occupied both white and grey matter, they were preferentially located in the dorsal horn, especially in the dorsal funiculus on both sides of the dorsal midline glial septum and in the marginal nucleus region (Figs. 7R,S).

DISCUSSION

The development of TH-immunoreactive cells and fibers was investigated in the CNS of the lesser-spotted dogfish, which represents the first study of the development of the catecholaminergic system in elasmobranchs. In the interpretation of the dogfish developmental data obtained in this study, three remarkable features emerge. First, when comparing the timetable of development of catecholaminergic systems in dogfish with that of other vertebrates, especially mammals, the relative early appearance of this system in the dogfish development together with its distribution pattern in mature stages, which show great similarities with other vertebrates, specially mammals. However, some wide variations between TH-ir groups were noticed among elasmobranchs, and also with other vertebrate groups. The second feature is the neuromeric organization of most TH-ir structures in the brain of dogfish. The

expression of TH-ir structures in the embryonic dogfish brain showed a conspicuous localization according to the neuromeric pattern advocated by Puelles and Rubenstein (2003). Another interesting finding was that the establishment of the "mature-like" pattern of the catecholaminergic innervation and its relation to the functional maduration of the corresponding centers was set at middle-late stages (S32).

Chronology of the development of the serotoninergic populations in dogfish: comparison with other vertebrates

We have associated the relative order of appearance of the various CA groups in the CNS of the dogfish with the timetable of its development reported by Ballard and colleagues (1993) and we have also compared it with those reported in other vertebrates. This comparison, especially that made with other fish groups, has shown some interesting differences and many similarities as shown in Table II.

The main similarity with other fish groups was noted in the timing of development of the TH-ir groups in relation with the length of embryonic period. In *S. canicula*, TH-ir cells were observed for the first time at about the first third of the total embryonic period (S26), being this early appearance similarly to that reported in teleosts (*Gasterosteus aculeatus:* Ekström et al., 1992; *Salvelinus fontinalis:* Bolliet and Ali, 1992; *Salmo trutta fario:* Manso et al., 1993; *Danio rerio:* Guo et al., 1999; McLean and Fetcho, 2004a,b), where first CA populations were observed about the 25-30% of the total embryonic period. A similar early appearance was reported in cyclostomes development, both in TH-ir cells (*Lampetra fluviatilis:* Pierre-Simons et al., 2002) and DA-ir cells (*Petroyzon marinus:* Abalo et al., 2005). However, differences were noted in the order of appearance of the different TH-ir populations (see Table II). In dogfish, as in amphibians, first CA groups to differentiate are those of the diencephalon, followed by the rombencephalon and then by the mesencephalic groups. However, cyclostomes and teleosts never develop CA cells in the mesencephalon while in reptiles and mammals these cells are the earliest to differentiate.

In dogfish, the earliest TH-ir population was located in the posterior tubercle. This tubercular CA group is well developed in all vertebrates studied (Smeets and González,

2000), being also the first to differentiate, excepting in reptiles and mammals in which it develops just after the mesencephalic CA populations (see Table II). Thus, the early development of posterior tubercle CA cell groups appears to be rather general in vertebrates. It also seems to be common in vertebrates that the different diencephalic (thalamic and hypothalamic) CA populations develop concurrently or just after the tuberclar CA populations. In dogfish, the development of the TH-ir cells of the suprachiasmatic nucleus and posterior recess organ is simultaneous to those of the posterior tubercle and just preceed that of ventral thalamus. In most vertebrates studied, as in dogfish, the earliest TH-ir groups were those of the posterior tubercle and suprachiasmatic area followed by that of the ventral thalamus/dorsal hypothalamus (*teleosts:* Ekström et al., 1992; *amphibians:* González et al., 1994a, 1995; Manso et al., 1993; *birds:* Puelles and Medina, 1994; *cyclostomes:* Pierre-Simons et al., 2002). In dogfish, these CA populations develop independently but near simultaneously to form interconnected dorsolateral and ventrolateral CA groups in late developmental stages, thus supporting the suggestion that in cartilaginous fish they probably form a complex homologous to the A12-A14 groups of mammals (Stuesse et al., 1994).

The next CA populations to appear in dogfish were those of the rhombencephalon where two main groups were recognized: the rostral, formed by the locus coeruleus/subcoeruleus complex group (S30) and the caudal, formed by the reticular and viscerosensory column (VSC) TH-ir cell populations. These two groups have been observed in most vertebrates although showing some differences in location and number of cells between species (see Smeets and González, 2000). In most vertebrates, as in dogfish, the rostral population develops concurrently with those of the caudal rhombencephalon, with the exception of teleosts, chick and rat in which the development of CA cells of the locus coeruleus precedes that of the caudal rhombencephalic CA groups (see Table II). In particular, teleosts represent a marked difference with the rest of vertebrates since the CA cells of the locus coeruleus are one of the earliest groups to differentiate, concurrently with that of the posterior tubercle.

In contrast with the common presence of diencephalic and rhombencephalic CA populations, those of the synencephalon/mesencephalon and telencephalon do not

develop in all vertebrates. In dogfish, TH-ir cells were observed in the synencephalic/mesencephalic tegmentum (ventral tegmental area and substantia nigra CA groups) from embryos at S31, after the development of the diencephalic and rhombencephalic CA populations. These synencephalic/mesencephalic CA groups lack in teleosts (Ekström et al., 1992; Manso et al., 1993) and cyclostomes (Pierre-Simons et al., 2002; Abalo et al., 2005) and show marked differences in the timing of development among the rest of vertebrates: they are the earliest to develop in reptiles and mammals, whereas in chick differentiate after the diencephalic but earlier than the rhombencephalic CA groups. A pretectal CA population is absent in either developing or adult dogfish (present study) and in other cartilaginous fish, although it is present in other vertebrates groups excepting mammals, being late appearing in teleosts (Ekström et al., 1992; Manso et al., 1993), amphibians (González et al,. 1994a, 1995), reptiles (Medina et al., 1994a,b) and birds (Puelles and Medina, 1994). More variations can be noted in the development of CA telencephalic groups along evolution. The CA population of the olfactory bulb differentiates in all vertebrate groups being one of the later to appear in dogfish (S32) and in most vertebrates (Ekström et al., 1992; Manso et al., 1993; Foster, 1994; Medina et al., 1994a,b; Puelles and Medina, 1994; Pierre-Simons et al., 2002; Abalo et al., 2005), though in amphibians they appear earlier, concurrently with those of the suprachiasmatic and posterior tubercle (González et al,. 1994a, 1995). In the subpallium, CA cells appear to be absent in amphibians, reptiles and rat (Foster, 1994; Medina et al., 1994a,b; González et al,. 1995) but they develop late in teleosts (Manso et al., 1993; Ekström et al., 1992; McLean and Fetcho, 2004a) and very late in dogfish (present results), cyclostomes (Abalo et al., 2005) and chick (Puelles and Medina, 1994). The presence of CA cells in the pallium appears to be exclusive of elasmobranchs. Interestingly, in this work we show that pallial CA cells develops concurrently with that of the synencephalon/mesencephalon and earlier than the subpallial ones.

The temporal differences in the relative time of appearance of CA populations observed among vertebrates may be related with the functional maturation of the different brain regions during development. It has been hypothesized that the shared

presence and early appearance of a CA population during development is revealing an ancient origin, whereas that the CA populations showing large differences in the developmental timing of appearance among vertebrate groups, might be revealing either a recent origin, or convergent evolution from nuclei with different origin (Smeets and González, 2000). According to this, the earliest and most consistent CA populations of nonmammalian vertebrates are those of the posterior tubercle, thalamus/hypothalamus and rhombencephalon which can be considered the most ancient CA groups. However, the mesencephalic, telencephalic and pretectal populations appear heterogeneous as regards its development, suggesting they appeared more recently in evolution.

The CA cell groups in the developing CNS in dogfish

Prosencephalic TH-ir populations

Olfactory bulb (OB)

In the dogfish OB, the first TH-ir neurons were observed within the primordial granule cell layer from the beginning of the second half of the embryonic period (S32) and surrounding the glomeruli (periglomerular cells) from S33. This late appearance of dogfish OB TH-ir cells, concurrently with the beginning of the prehatching stage, could be related with the functional organization of the olfactory structures. When the first TH-ir neurons develop at the S32 OB, the rostrum has accomplished the anatomical characteristics of the prehatching stage. Then, the morphological changes that happened during the S31 could be related with key developmental events in the organization of the olfactory system previous to hatching. In dogfish, catecholamines could be playing a role in olfactory functioning, perhaps exerting an inhibitory control on olfactory input and in the olfactory memory formation as it has been showed in other vertebrates (Keverne et al., 1993; Wilson and Sullivan, 1995; Gurski and Hamilton, 1996).

In contrast with the widespread occurrence of granule TH-ir cells in the developing and adult OB of vertebrates, the existence of CA periglomerular cells in fish is a matter of controversy. These cells have not been reported in developing or adult cyclostomes and neither in developing bony fish, although periglomerular or externally located OB

TH-ir cells have been described in adults of a cladistian (Reiner and Northcutt, 1992), a chondrostean (Adrio et al., 2002) and a teleost (Hornby and Piekut, 1990). In cartilaginous fish, CA juxtaglomerular/periglomerular cells have been observed in adults (Meredith and Smeets, 1987; Stuesse et al., 1994; Sueiro, 2003) and embryos (present results), thus supporting the hypothesis suggested by Adrio and colleagues (2002) that periglomerular or externally located OB TH-ir cells may have been acquired secondarily in several vertebrate lines, being in some bony fish a derived character shared by amniotes, as it has also been suggested by Smeets and González (2000). In adittion, our observation of TH-ir cells externally to the glomerular cell layer showing thick prolongations radially oriented could be indicating that they are migrating from the granular layer, perhaps representing displaced granule cells as it was suggested in chondrosteans (Adrio et al., 2002).

Telencephalic hemispheres

From late embryonic stages (late S32), when the main TH-ir cell groups present in adult dogfish were already recognized, we observed abundant scattered TH-ir cells throughout the dorsal telencephalon (pallium), being more abundant at caudal levels. This distribution pattern of TH-ir neurons observed in the pallium of late embryonic stages of dogfish is maintained in juveniles and adult, and is similar to that reported in adults of other elasmobranchs (*Squalus acanthias*: Northcutt et al., 1988; *Raja radiata*: Molist, 1990; *Platyrhinoidis triseriata*: Stuesse et al., 1990; *Heterodontus francisci*: Stuesse et al., 1991) and in holosteans (*Hydrolagus collei*: Stuesse and Cruce, 1991). Most if not all of these TH-ir cells must be dopaminergic since a similar immunoreactive distribution was observed with an antibody against dopamine in *Raja radiata* (Meredith and Smeets, 1987). Thus the high density of CA cells at pallial regions may be considered a shared character of chondrichthyes.

In the subpallium of dogfish, no TH-ir cells were observed at embryonic stages but some weak stained neurons appeared at the caudal part of the basal superficial area and ventral septum of juveniles and adults. These scattered subpallial TH-ir cells clearly

formed a separate group from the preoptic TH-ir population located more caudally (see below). TH-ir and DA-ir neurons have been reported in the subpallium of adult elasmobranchs (Meredith and Smeets, 1987; Northcutt et al., 1988; Molist, 1990; Stuesse et al., 1990, 1994; Sueiro, 2003) and other fish groups (*cyclostomes:* Yañez, 1992; Pierre et al., 1997; Pombal et al., 1997a, b; *chondrosteans*: Adrio et al., 2002; *teleosts*: Ekström et al., 1990; Sas et al., 1990; Manso et al., 1993; Batten et al., 1993; Meek and Joosten, 1993; Beltramo et al., 1994; Briñón et al., 1998; Rodríguez-Gómez et al., 2000; Rink and Wullimann, 2001; Kaslin and Panula, 2001; Anadón et al., 2002; Vetillard et al., 2002).

Whether the presence of CA cells in the telencephalic hemispheres should be considered a characteristic of vertebrates is controversial. Some authors hypothesized that CA cell bodies in the telencephalon proper are a general feature of vertebrates (Smeets and González, 2000). However, CA cells have been observed in the subpallium/basal telencephalon of mammals and all fish groups (see above) but they are absent in amphibians, reptiles and birds. Moreover, whereas CA cells are very abundant in the cortical/pallial areas of mammals and chondrichthyans, they are lacking in the rest of fish groups, in amphibians and in birds. In reptiles, although CA cell bodies were noted in the dorsal telencephalon of several species, their location varied considerably between species (Smeets and González, 2000). Taking together these observations, we suggest that the pallial CA groups observed in some vertebrates could not be homologous and probably appeared independently in fish and mammals.

In comparison with the early development and the shared presence of diencephalic and rhombencephalic CA groups (suggestive of an ancient origin, see above), those of the telencephalon, when are present, develop very late, just before or at the time of hatching in teleosts (Ekström et al., 1992; Manso et al., 1993; McLean and Fetcho, 2004a) or just after hatching like in elasmobranchs (present results), thus suggesting a more recent origin.

Preoptic area

Periventricular TH-ir cells were observed in the ventrolateral walls of the dogfish preoptic recess from S32 embryos onwards, some of these cells being of CSF-c type (in prehatching embryos). On the basis of its location, this CA cell group could be related with the A15 group of mammals following the nomenclature of Hökfelt and collegues (1984).Our observation of some CSF-c TH-ir in prehatching embryos is exceptional since this cell type was not reported previously in any elasmobranch, neither among the preoptic population of DA-ir cells of *Raja radiata* (Meredith and Smeets, 1987). However, CSF-c TH-ir cells were abundant in the preoptic area of chondrosteans (Adrio et al., 2002) but occasional in teleosts (Sas et al., 1990; Meek and Joosten, 1993; Batten et al., 1993) and absent in amphibians (González and Smeets, 1994b; González et al., 1995).

Diencephalon

Contrasting with the scarcity and late appearance (S32) of the preoptic TH-ir cells, those of the suprachiasmatic nucleus formed a conspicuous postoptic group from early developmental stages (S26). Although the continuity between these groups was observed from late development, both groups could be clearly destinguished by the cell size, orientation of processes and staining density. In teleosts, CA neurons also appeared earlier in the suprachiasmatic nucleus than in the preoptic area (Ekström et al., 1992; Manso et al., 1993; Guo et al., 1999), while in cyclostomes both CA populations appeared precociously during the same developmental period (Pierre-Simons et al., 2002; Abalo et al., 2005). Our results also suport the hypothesis suggested by Ekström and colleagues (1992) in a teleost, that the neurons in the suprachiasmatic nucleus could be homologous to the rostral periventricular cell group (A14) of mammals.

Concurrently with the appearance of TH-ir neurons in the suprachiasmatic nucleus (S26), we report the first TH-ir neurons in the posterior tubercle of dogfish, forming the primordial of the posterior tubercle nucleus. We also report the increasing complexity during development. This caudal diencephalic nucleus partly resembles the A11 CA

group (periventricular grey matter cell group of hypothalamus) in tetrapods (Smeets and González, 2000), although this posterior tubercular TH-ir cell group was also related with caudal diencephalon DA-ir cell groups (A9-A11). The presence of CA cells in the posterior tubercle was observed in all anamniotes (Smeets and González, 2000). In amphibians, this CA population of the posterior tubercle has been related to the mesolimbicstriatal system of tetrapods (González et al., 1994b; Smeets and González, 2000), because of their characteristic connectivity (i.e. strong peptidergic innervations from the striatum; Reiner et al., 1984; Reiner and Anderson, 1990; Smeets et al., 2000). Catecholaminergic projections from the posterior tubercular cells to the striatum have been reported in cyclostomes (Pombal et al., 1997a,b) and teleosts (Rink and Wullimann, 2001, 2004), reinforcing the hypothesis that the CA group of the posterior tubercle in anamniotes may be equivalent to the ventral tegmental/subtantia nigra group of amniotes (see below). Anyway, our results favour the hypothesis of a continuous CA cell band from the hypothalamus to the midbrain based on the time of appearance, the rostrocaudal distribution of TH-ir cells and the possible migration processes, similarly to that noted in amphibians (González et al., 1994a).

At the same time as the appearance of TH-ir cells in the posterior tubercle (S26), the first TH-ir neurons were detected in the marginal walls of the posterior recess, forming the primordium of the posterior recess organ (Pro). Later, at S28, a few TH-ir cells of the Pro showed a ventricular process (CSF-contacting cells), while others were located superficially extending their processes parallel to the outer surface between the CSF-c TH-ir cells and the PTN TH-ir cells, this continuity being specially noted at S30 (see Fig. 2J). The late appearance of CSF-c TH-ir cells in relation with the marginal TH-ir cells and the extension of the marginal cell processes suggest a possible tangential migration of marginal cells from the PTN to the Pro walls. From S32 the number of TH-ir cells in the PTN increased notably with respect to previous stages, but not that of the posterior recess TH-ir cells. After hatching, the scarce TH-ir cells that were observed in the posterior recess and related organ, the paraventricular organ, were CSF-c cells (Rodriguez-Moldes and Anadón, 1987; by using formaldehyde-induced fluorescence;

Molist, 1990; present results) as also reported in other elasmobranchs (Meredith and Smeets, 1987; Stuesse et al., 1990, 1991; Stuesse and Cruce, 1991; Molist et al., 1993). Interestingly, in the equivalent circunventricular organs of *Raja radiata* abundant CSF-c dopamine-immunoreactive cells were observed (Meredith and Smeets, 1987). CSF-c cells immunonegative to TH but immunopositive to dopamine have been noted in the circunventricular organs of the caudal hypothalamus of non mammalian vertebrates that has been interpreted as CA CSF-c cells that could uptake dopamine from the CSF and accumulate it (Smeets and González, 2000). These authors have also suggested that the presence of CA-acumulating perikarya in the circunventricular organs of non mammalian vertebrates is a primitive trait of CA systems in vertebrates that has been lost in mammals and some reptiles. The appeareance of TH-ir neurons in the PTN (slightly earlier) and Pro at the same temporal period (S26) on the dogfish development (Carrera et al., 2005), is in contrast with a different temporal appearance of these nuclei in other fish embryos where the PTN TH-ir cells develop earlier that those of the Pro (*cyclostomes:* Pierre-Simons et al., 2002; Abalo et al., 2005; *teleosts:* Ekström et al., 1992; Manso et al., 1993; Guo et al., 1999), suggesting a temporal divergence of these CA nuclei expression between elasmobranchs and other fish groups during development.

In embryos at S28, when all the diencephalic CA groups (SCN, PTN and Pro) were well recognized, a conspicuous group of large TH-ir neurons extended periventricularly from postchiasmatic regions to the posterior tubercle, dorsally to the paraventricular organ. We have considered that these cells belong to the ventral part of the ventral thalamus, a possible equivalent group of the A11 CA group in mammals (Smeets and González, 2000). During development and in adults, these cells form a continuous band with those of the preoptic area, suprachiasmatic nucleus and posterior tubercle, as mentioned before. In some vertebrates, TH-ir cell groups have been observed in the ventral thalamus during the mid-early development (*cyclostomes*: Pierre-Simons et al., 2002; Abalo et al., 2005; *teleosts*: Ekström et al., 1992; Manso et al., 1993; *amphibians*: González et al., 1994a, 1995). Apart from the A11 CA group of mammals, TH-ir

neurons have been reported in the adult ventral thalamus of non tetrapods, like cyclostomes (Pierre et al., 1997; Pombal et al., 1997b; Abalo et al., 2005), elasmobranchs (Stuesse and Cruce, 1992; Stuesse et al., 1991, 1994), cladistians (Reiner and Northcutt, 1992) and teleosts (Meek, 1994; Ekström et al., 1995; Briñón et al., 1998; Rink and Wulliman, 2001; Kaslin and Panula, 2001; Vetillard et al., 2002; Ma, 2003; Castro et al., 2006). Therefore, it has been considered that the presence of CA cells in the ventral thalamus is a shared feature in vertebrates.

In most vertebrate studied (Smeets and González, 2000), as also observed in elasmobranchs (Stuesse et al., 1991, 1994; Stuesse and Cruce, 1992), TH-ir cell bodies constitute two rostrocaudally oriented columns on each side of the brain, clustered in interconnected groups (preoptic area, suprachiasmatic nucleus, ventral thalamus/dorsal hypothalamus, posterior tubercle). This pattern of interconnected ventral CA cell groups within the diencephalon was also observed in anamniotes (González and Smeets, 1994a,b; Meek, 1994; Pierre et al., 1997; Pombal et al., 1997b; Beltramo et al., 1994; Smeets and González, 2000; Vetillard et al., 2002; Anadón et al., 2002), reptiles (Smeets and Steinbusch, 1990), birds (Bailhache and Balthazart, 1993; Reiner et al., 1994; Moons et al., 1995) and mammals (Leshin et al., 1995, 1996; Tillet, 1994; Marín et al., 2005), suggesting that this feature may be a primitive characteristic of the cetecholaminergic distribution pattern in vertebrates.

Synencephalon and Mesencephalon

In the pretectal region of dogfish, no TH-ir neurons were seen during development (present results) or in adults (Molist et al., 1993). Similar results were reported in adults of other cartilaginous fish (Meredith and Smeets, 1987; Stuesse et al., 1990, 1991; Stuesse and Cruce, 1991, 1992). However, in other fish groups, TH-ir neurons were described in the dorsoposterior thalamic/pretectal region during development (*teleosts:* Ekström et al., 1992; Manso et al., 1993) and adulthood (*cyclostomes*: Pierre et al., 1997; *teleosts*: Sas et al., 1990; Meek, 1994; among others).

Pretectal TH-ir cells have been reported in amphibians (González and Smeets, 1994a; González et al., 1995), reptiles (Smeets, 1994) and birds (Reiner et al., 1994), but not in mammals (Tillet et al, 1994; Marín et al., 2005) and *Polypterus* (Reiner and Northcutt, 1992) which has been considered a derived feature (Smeets and González, 2000).

In the basal tegmentum of the synencephalon and mesencephalon of juveniles and adult dogfish, we have characterized three related TH-ir populations: two clearly separated TH-ir cell groups in the synencephalon (substantia nigra and rostral ventral tegmental area; SN/rVTA) and one in the mesencephalon (caudal ventral tegmental area; cVTA). These three TH-ir groups were profusely interconnected by long processes extended between the SN and the rVTA TH-ir cells (lateromedially) and between both VTA TH-ir cell groups (rostrocaudally). These synencephalic/mesencephalic TH-ir cell groups could be considered homologous of the mammalian substantia nigra and the ventral tegmental area of mammals (A9-A10 cell groups; Smeets and Reiner, 1994; Smeets and González, 2000), on the basis of their size, shape and relative position. Moreover, when taking a segmental approach, the CA cells of the VTA and SN of amniotes present a multisegmental location along the floor plate of three different segments (p1, p2 and mesencephalic) which is roughly comparable to that observed in dogfish (see below).

SN/VTA TH-ir cell groups have been described in most cartilaginous fish (Meredith and Smeets, 1987; Northcutt et al., 1988; Stuesse et al., 1990, 1991; Stuesse and Cruce, 1992), with the exception of the holocephali (Stuesse and Cruce, 1991; Stuesse et al., 1994), generally considered more primitive than elasmobranchs. In other vertebrates, these CA nuclei were observed in holosteans (Parent and Northcutt, 1982), cladistians (Reiner and Northcutt, 1987), amphibians (González and Smeets, 1994a, b), reptiles (Smeets, 1994), birds (Bailhache and Balthazart, 1993) and mammals (Smeets and Reiner, 1994; McRitchie et al., 1996; Verney et al., 2001). However, in cyclostomes, chondrosteans and actinopterygians, TH/DA-ir neurons were absent in the synencephalon/mesencephalo but present in the posterior tubercle (Meek, 1994; Anadón et al., 2002; Pombal et al., 1997b). Some authors (Baumgarten, 1972; Reiner and

Northcutt, 1992; González et al., 1994a, 1995; Pierre et al., 1997) have hypothesized that the posterior tubercle nucleus of fish might represent the primordium of the SN and VTA in tetrapod as a consequence of a TH-ir cell migration to the base of the mesencephalon. Although CA groups of the posterior tubercle and ventral tegmental area/substantia nigra presented different locations (diencephalic and mesencephalic, respectively), when taking a segmental approach of the development of this systems, the embryological studies in tetrapods (González et al., 1994a, 1995; Medina et al., 1994a,b; Puelles and Medina, 1994; Pombal and Puelles, 1999; Smeets and González, 2000) have suggested a similar embryonic origin, supporting the idea of their homology. Our present results also support this view. During development, these TH-ir groups were observed from S31 onwards, representing another middle-late appearing TH-ir cell groups in dogfish development, similar to that reported in tetrapod embryos (*amphibians*: González et al., 1995). This relative late appearance of these TH-ir groups may favour the idea of a migration process from TH-ir nuclei that firstly mature during development. In fact, our present results support the possibility that these synencephalic/mesencephalic groups were migrated populations from the posterior tubercle nucleus where CA cells develop earlier (S30). These migrated cells could have become TH-ir at a relative late moment of their cytodifferentiation and once they have already reached their target areas, as suggested in the CA development of reptiles (Smeets and González, 2000), which may explain that they were not observed until having finished their migration from the posterior tubercle to the SN/VTA and initiate maturation. Our results also support the suggestion that absence of midbrain CA cells in actinopterygians and chondrosteans may represent a derived feature among fish.

Brainstem TH-ir populations

Rhombencephalon

The TH-ir cells of the rhombencephalon were restricted to the rostral (locus coeruleus/subcoeruleus and TH-ir raphe cells of the central grey region) and caudal (viscerosensory column and TH-ir reticular cells) rhombencephalon. From these

middle-late appearing TH-ir cell groups, observed at S30-S31 (except the TH-ir cells of the central grey observed only in adults), the locus coeruleus/subcoeruleus (LC/Sc) was the most prominent cell group of the rostral rhombencephalon. CA cells have been consistently reported in the locus coeruleus and subcoeruleus of all vertebrate studied so far (see Smeets and Reiner, 1994; Smeets and González, 2000). A similar distribution of these nuclei were reported in other elasmobranch species as *Heterodontus* (Stuesse et al., 1991) and *Squalus* (Stuesse and Cruce, 1992) that have been homologated to the A6 NA cell group of mammals (Smeets and Reiner, 1994; Smeets and González, 2000). As in dogfish (present results), the LC/Sc groups in amniotes were also reported from middle development (*reptiles:* Medina et al., 1994a,b; *birds:* Puelles and Medina, 1994; *mammals:* Foster, 1994; Aroca et al., 2006). However, in anamniotes (*teleosts:* Guo et al., 1999; McLean and Fetcho, 2004a; *amphibians:* González et al., 1994a, 1995) the LC develops earlier in relation with the relative developmental sequence of the CA groups (see Table II), being absent only in cyclostomes (Pierre et al., 1997; Abalo et al., 2005). Although the cronological appearance of CA LC/Sc cells differs among vertebrates, its consistent presence should be considered a conserved trait in the evolution of the CA system in vertebrates.

At rostral levels of the trigeminal nerve root, we have observed in adult dogfish a few small TH-ir cells in the medial subependymal layer of the central grey, slightly caudally to the level of LC/Sc TH-ir cell groups. This TH-ir cell group was not seen during embryonic development. These rostral rhombencephalic groups (LC/Sc, central grey cell group) cannot be subdivided in teleost and amphibians due to their low density of cells, although in mammals they were clearly differentiated, being the TH-ir cells of the central grey homologated to the A4 NA cell group (Smeets and González, 2000). Based on the relative position and immunohistochemical localizations, we suggest that the TH-ir cells of the central grey might be closely related with those of the LC, although as in mammals (Smeets and Reiner, 1994), in dogfish they did not form a continuous group. Therefore, our results support the hypothesis that these closely related CA groups (with their heterogenic connections) may form part of the LC

complex, perharps representing the caudal extension of the LC (Smeets and González, 2000). TH-ir cells of the central grey, were present in all the cartilaginous fish studied (*Heterodontus:* Stuesse et al., 1991; *Squalus:* Stuesse and Cruce, 1992; *Platyrhinoidis:* Stuesse et al., 1990) except *Hydrolagus* (Stuesse and Cruce, 1991). Unlike the LC/Sc, this rhombencephalic subventricular TH-ir group was not identifying in other vertebrate groups apart from mammals, suggesting that it is a characteristic feature shared by elasmobranchs and mammals.

In the adult caudal rhombencephalon, the distribution of the dorsomedial TH-ir cells of the viscerosensory column was observed from the caudal levels of the acusticofacial nerve nucleus (VII-VIII) to the obex, similar to that described in other cartilaginous fish (Stuesse et al., 1994). This TH-ir cells may be related with the CA dorsomedial group of the viscerosensory column described in other fish groups (*chondrosteans:* Adrio et al., 2002; *teleosts:* Ekström et al., 1992; Manso et al., 1993) and probably also in cyclostomes (Pombal et al., 1997b; Pierre-Simons et al., 2002; Abalo et al., 2005), although the presence of TH-ir cells in a paraventricular position in cyclostomes make such comparison difficult. These dorsomedial TH-ir group seems to be homologous of the CA group (A2) reported in all tetrapods (Smeets and Reiner, 1994; Smeets and González, 2000). These dorsal TH-ir cells (alar plate) were first seen at S31 in the viscerosensory and visceromotor columns. Unlike the rest of TH-ir rhombencephalic nuclei of dogfish, in these nuclei the number of immunoreactive cells increased considerably during development, although we did not observe important changes in their relative positions. These middle-late appearing (S31) TH-ir cell group in dogfish, has shown large temporal differences in their appearance in other vertebrates, being observed early in teleosts (Manso et al., 1993; Ekström et al., 1994), birds (Guglielmone and Panzica, 1984; Puelles and Medina., 1994) and mammals (Spetch et al., 1981a,b; Smeets and Reiner, 1994) and late in amphibians (González et al., 1994a) reptiles (Medina et al., 1994a,b). As regards the developmental sequence in vertebrates and the heterogeneity observed in this TH-ir populations related with the

viscerosensory column, their consistent presence among all vertebrates suggest they may be considered a conserved feature of the CA system.

In dogfish juveniles and adults, we observed TH-ir cells in the caudal rhombencephalon, from the level of the entry of cranial nerve VIII to the caudal obex level, forming the caudal reticular formation TH-ir cell group. A similar TH-ir cell distribution within the caudal brainstem of dogfish was also reported in other elasmobranchs (Stuesse et al., 1991; Stuesse and Cruce, 1992). This ventrolateral TH-ir group may be homologous of the CA group (A1) located in the ventrolateral tegmentum of mammals (Smeets and Reiner, 1994; Smeets and González, 2000), and also described in the caudal brainstem of all vertebrate groups studied (see Smeets and González, 2000). In the present work, we have observed these TH-ir cell groups from middle development (S30). TH-ir cells formed initially a single group at caudal rhombencephalic levels, showing long apical processes characteristic of migration cells. In later stages, these caudal TH-ir cells were segregated in two different cluster populations, one located immediately lateral to the viscerosensory lobe (dorsolateral orientation processes) and a second group situated slightly caudal and ventrally to the first one (lateroventral orientation processes). These results may suggest a migration pattern of these TH-ir cells to form two conspicuous CA groups, which was also reported in the A1 CA cell group of rat during development (Smeets and González, 2000). These authors have suggested that differences in location of CA cells at caudal rhombencephalon may reflect differences in the degree of migration within the radial column. In dogfish, the close appearance of the viscerosensory column and reticular TH-ir cell groups during development (S30-S31) and their migrating cell morphology suggest a common origin of these populations, although the use of tracing techniques are needed to confirm this hypothesis in dogfish.

Spinal TH-ir populations

Spinal cord

In the adult dogfish spinal cord TH-ir CSF-c cells were located ventrally to the central canal (Sueiro et al., 2003). A similar distribution of CA CSF-c cells was reported in the spinal cord of other cartilaginous fish species (*Raja:* Roberts and Meredith, 1987; *Platyrhinoidis:* Stuesse et al., 1990; *Heterodontus:* Stuesse et al., 1991; *Hydrolagus:* Stuesse and Cruce, 1991; *Squalus:* Stuesse and Cruce, 1992). TH-ir CSF-c cells were also present in all vertebrate groups excepting mammals (Smeets and González, 2000), which suggests that this CA cell type has been well conserved and appears to be a shared feature by all non-mammalian species. During dogfish development, these TH-ir CSF-c cells were first seen at S26, increasing their number considerably during development and forming a continuous column lying ventral to the central canal. A similar early appearance of CA CSF-c cells have been noted in the spinal cord of other vertebrate embryos, such as cyclostomes (*lamprey*: Pierre-Simons et al., 2002; Abalo et al., 2005), some teleosts (*eel* and *trout*: Roberts et al., 1989, 1995), amphibians (*frog*: Heathcote and Chen, 1994; González et al., 1994b), reptiles (*lizard*: Medina et al., 1994a,b) and birds (*chicken*: Smeets and Reiner, 1994). However, TH-ir CSF-c cells were not reported in most of teleosts studied (Smeets and González, 2000; McLean and Fetcho, 2004b) and mammals (Specht et al., 1981a,b; Smeets and Reiner, 1994). In dogfish, TH-ir CSF-c cells of spinal cord showed an identical distribution to those DA-ir CSF-c cells reported in *Raja radiata* (Roberts and Meredith, 1987), although the dogfish TH-ir cells were far more numerous than in this ray, suggesting that they were dopaminergic and can synthesize catecholamines throughout life. Moreover, the presence of CSF-c dopaminergic synthesizing cells in the spinal cord contrasts with the absence or scarcity of these cells in the CA populations of the hypothalamus, being roughly similar to that observed in *Xenopus* (Heathcote and Chen, 1994).

CSF-c TH-ir cells were not the only CA population observed in the dogfish spinal cord. Non-CSF-contacting TH-ir cells were observed lateral and ventral to central canal. These non-CSF-c CA cells have not been described in other chondrycthyans (*Raja:*

Roberts y Meredith, 1987; *Platyrhinoidis:* Stuesse et al., 1990; *Heterodontus:* Stuesse et al., 1991; *Hydrolagus:* Stuesse and Cruce, 1991; *Squalus:* Stuesse and Cruce, 1992) and they were only reported in the ventral and lateral horn of lampreys (Schotland et al., 1996; Pierre et al., 1997; Pierre-Simons et al., 2002; Abalo et al., 2005) and eels (Roberts et al., 1995). During dogfish development, non-CSF-c TH-ir cells were observed from S33 onwards in the ventral horn of the rostral spinal cord, but not in caudal levels, suggesting differences in the maturation time of the caudal cord as regards more rostral regions, but we cannot rule out that this difference was genuine. Interstingly, some CSF-c TH-ir cells were seen becoming multipolar cells during chick ontogeny after losing the CSF-contacting process (Wallace et al., 1987, 1996; Okado et al., 1991), which has not been observed in dogfish. The functional significance of the CSF/non-CSF-c CA cells in the spinal cord of vertebrates is not fully understood, but on the basis of localization of fibers and receptor distribution, it is generally accepted that they play a role in nociception, autonomic functions and motor control (Smeets and González, 2000).

Segmental organization of the brain TH-ir populations

The use of a segmental approach in comparative neuroanatomy has proven to be a useful framework to explain possible topographical relationships (Puelles, 1995; Smeets and González, 2000). The distribution of CA populations in relation to the brain segmentation has been described for reptiles, birds and mammals (Medina et al., 1994a,b; Puelles and Verney, 1998; Vitalis et al., 2000; Marín et al., 2005) and in a lesser extension for amphibians (Smeets and González, 2000) and bony fish (Wullimann and Rink, 2001, 2002; Piñuela and Northcutt, 2007). Considering that a similar segmental pattern for all vertebrates exists (Pombal and Puelles, 1999; Smeets and González, 2000; Puelles and Rubenstein, 2003), we have comparatively analized the mature organization and development of the CA cell groups in the dogfish brain with respect to the segmental plan. We have followed the segmental organization proposed by Puelles and Rubenstein (2003) in the vertebrate forebrain and by Gilland

and Baker (1993) and Kuratani and Horigome (2000) in the cat shark rhombencephalon. In brief, the segmental framework of the vertebrate brain in early stages of development consists of eight rhombomeres in the hindbrain (r1-r8), one neuromere in the mesencephalon, while the diencephalon has been proposed to consist of three prosomeres (p1-p3).

The CA cell groups observed in the dogfish olfactory bulb, telencephalon, preoptic area, suprachiasmatic nucleus, paraventricular organ and posterior recess organ could not be ascribed to any precise location within the neuromeric model proposed. These groups may correspond to the classical A16-A11 CA cell groups described in the basal forebrain of mammals, which are also assigned at regions out of the three (p1-p3) prosomeric segments (Smeets and González, 2000).

In dogfish, the posterior tubercle group occupies the basal domain of p3 from S30 and seems to be continuous caudally with the VTA/SN cell groups from S31. The rostral VTA and SN are also basally located at medial and lateral regions, respectively, of the caudal part of p2 and the entire p1, while the caudal VTA is medially located at the basal mesencephalic segment. This observation supports the suggestion made in tetrapods that mesencephalic CA groups may have migrated from the posterior tubercle to form a CA cell column through several segments in tetrapods (Smeets and González, 2000). In teleosts, were CA cells are absent from synencepalic and mesencephalic territories, Rink and Wullimann (2001, 2002) have proposed that the posterior tubercle nucleus (p2) could be comparable, in a segmental approach, with the amniote SN and VTA (A9-A10). In fact, from a segmental approach the CA cells of the A10 complex of mammals, which have been generally ascribed to the mesencephalon, extend across several segments including the diencephalic p1-p3 (Smeets and Gonzalez, 2003). Moreover, the ventral part of the thalamus in dogfish is located at p3 and may correspond to the zona incerta (A11) in mammals that is formed by TH-ir cells in the zona incerta (the border between the hypothalamus and thalamus; Ekström et al., 1992). A similar observation has been made in teleosts (Sas et al., 1990; Ekström et al., 1994), and reptiles show a possible homologue of the A11 formed by the caudal continuation

of the "rostrodorsal periventricular hypothalamic" cell group (Smeets and Steinbusch, 1990; Medina et al., 1994a,b).

Based on the relative position of rhomomeres described in the cat shark by Kuratani and Horigome (2000), we have considered that the conspicuous CA groups of the dogfish locus coeruleus and subcoeruleus were located at r1 and r2, respectively. These alar CA cell groups, which could correspond to the classical A6 and A5, have been described in other vertebrates and also ascribed to the rhombomeres r1 and r2 (König et al., 1988; Puelles and Medina, 1994; Smeets and González, 2000). The TH-ir cell group of the central grey area observed in the adult dogfish is located at the rostral part of r3 and may correspond to the classical A4 group, also located at r3.

Finally, the viscerosensory column (A2) was found from the caudal levels of the acusticofacial nerve nucleus (VII-VIII) to the obex, extending from r5 to r8, while the ventrolateral reticular TH-ir cells (A1) were seen from the caudal levels of the abducens motor nucleus to the obex, extending therefore, throughout r7 and r8. Interestingly, from the middle-late embryonic stages of dogfish it is clearly observed a segmental organization in the TH-ir cells of the viscerosensory column, ass it has been reported in adults of other species of cartilaginous fish (Stuesse et al., 1992; Smeets and Reiner, 1994). Stuesse and cols. (1992) have hypothesized that the number of visceral sensory lobes or external bulges in cartilaginous fish would be equal to the number of gill arches, assuming a direct relationship between the repetitive TH-ir cell units and the branchial arches in cartilaginous fish. However, trace labeling techniques are needed to confirm this hypothesis. These CA rhombencephalic groups of the dogfish could correspond to the classical A1 and A2 groups, although they have been assigned to r7 and r8. Thus, in dogfish these caudal rhombencephalic CA groups seemed to extend throughout more rhombomeres than those reported in mammals.

In conclusion, our results support the observations made in other vertebrates that most neuromeres seem to contribute to the formation, development and maturation of the CA systems, and that the variation of CA groups observed among vertebrates is probably due to the loss of expression of TH/DA-ir or differentiation/migration within a segment (Smeets and González, 2000).

Development of the CA innervation in the dogfish CNS

CA fibers were found in the CNS of *Scyliorhinus canicula* from the telencephalon to the spinal cord. The present study provides evidence of two distinct phases in the formation of CA axonal pathways in the dogfish CNS, with some temporal overlap. The first phase reflect the axon elongation process, which is the period of primary pathway development, that in dogfish was observed from S30 and continues until juveniles when TH-ir longitudinal fibers extend from the prosencephalon to the spinal cord (descending tracts) and to the telencephalon (ascending tracts). The second phase, which happens between S32 and late juveniles, corresponds to the development of selective TH-ir axonal pathways to reach the structures that have to receive the CA innervation or to develop CA axon terminal fields. These two axonal developmental phases observed in dogfish seem to roughly fit with the extensive description of the brain TH-ir innervations made previously in mammals by Smeets and Reiner (1994).

The first phase starts at S30 with the development of the main CA longitudinal pathways. In these embryos, descending axons formed a longitudinal TH-ir fiber tract that coursed through the basal mesencephalon, not reaching the isthmus until S31. The origin of these TH-ir axons seems to be the TH-ir PTN cells although, considering that these TH-ir cells were forming a continuous population with that of the ventral thalamus, the possibility that these cells also contribute to the main descending pathway remains. This conspicuous descending longitudinal pathway continued caudally at later stages, coursing basal and medially throughout the rostral rhombencephalic tegmentum at S32, and blending later with the TH-ir ascending fibers of the spinal cord at the caudal rhombencephalon (S33-34). This descending pathway appears to coincide with the diencephalospinal pathways described in adult dogfish using tracers (Smeets and Timerick, 1981; Timerick et al., 1992). In other vertebrates, a rhombencephalic CA projection was also observed during development (*teleosts*: Ekström et al., 1992; McLean and Fetcho, 2004a,b; *amphibians*: Sánchez-Camacho et al., 2002a,b; González et al., 1995; *mammals*: Guo et al., 1999) and in adults (*cyclostomes*: Pombal et al.,

1997b; *chondrosteans*: Adrio et al., 2002; *teleosts*: Becker et al., 1997; Ma, 1997, 2003; McLean and Fetcho, 2004a,b; *mammals*: Peyron et al., 1995), and being mainly originated by CA cells of the preoptic (*teleosts*: Becker et al., 1997) and posterior tubercle groups (*teleosts*: McLean and Fetcho, 2004a,b; *amphibians*: Sanchez-Camacho et al., 2002a,b). At the beginning of S32, a different descending TH-ir fibers tract was observed coursing at the ventrolateral alar plate, from the caudal diencephalic TH-ir cell groups. The origin of these descending alar TH-ir fibers seems to be the TH-ir cells of the posterior tubercle and the ventral thalamus/dorsal hypothalamus. Later (S33-34), both alar and basal CA descending longitudinal tracts coursed through the rhombencephalic tegmentum blending with the spinal cord TH-ir ascending fibers. These descending TH-ir longitudinal fiber tracts were well discerned by their straight course without branching and the presence of abundant axon-ending bulbous dilatations (growth cones) that revealed a clear migrating pattern, characteristic of the first phase in the formation of CA pathways.

In adult of both *Scyliorhinus* and *Raja*, CA descending fibers, probably originated from CA cells of the suprachiasmatic nucleus and preoptic area, were described along the hypothalamic floor forming part of the hypothalamo-hypophyseal tract that innervated the neurointermediate lobe of the hypophysis (Meredith and Smeets, 1987; Molist et al., 1993). Our present results revealed the development of this tract, since that from S30 TH-ir fibers were observed coursed caudally, first from the TH-ir cells of the suprachiasmatic nucleus (S30) and later also from that of the preoptic area (S33), to increase progresively in density throughout development to form a leading thick bundle that could be followed through the infundibular floor along the median eminence to reach the neurointermediate lobe of the hypophysis (S32). The development of the CA fibers of the hypothalamo-hypophyseal tract in dogfish was earlier than in other fishes, where the CA fibers reaches the hypophysis at postembryonic phases (larval stages) as reported in cyclostomes (Abalo et al., 2005) and teleosts (Ekström et al., 1992; McLean and Fetcho, 2004a,b). Interestingly, in dogfish a few TH-ir fibers were observed at the epithelium of the saccus vasculosus from late embryonic stages (S32) to adult. Considering that in dogfish, as in other elasmobranchs, the saccus vasculosus walls are

continuous with the neurointermediate lobe, it is possible that some TH-ir fibers of the hypothalamo-hypophyseal tract abandoned the route to the neurointermediate lobe and invaded the saccus vasculosus. In postembryonic stages (juveniles and adults), part of the TH-ir innervation of the saccus vasculosus can be originated from some TH-ir cells. The possibility that these CA neurons originate a saccofugal component cannot be ruled out, although TH-ir fibers were not observed coursing in the saccus vasculosus tract. Since the saccus vasculosus CA structures had a late development in dogfish and were not reported in the saccus vasculosus of bony fishes, the present results lead us to suggest that these saccular CA structures were acquired secondarily in elasmobranchs, i.e. after divergence from primitive bony fishes.

The main ascending TH-ir fiber pathways in dogfish were constituted by longitudinal fiber tracts that coursed from the spinal cord to the rhombencephalon form S31, and from the rostral hypothalamic TH-ir cell groups to the basal telencephalon form S30. At S31, the TH-ir CSF-c cells of the ventral spinal cord gives rise to the ascending longitudinal fibers that coursed throughout the ventrolateral region of the ventral horn and the lateral marginal nucleus, corresponding to the ventromedial and lateral funiculi, and reaching the caudal level of the abducens motor nucleus, in the rhombencephalic tegmentum. These lateral TH-ir ascending longitudinal fibers coursed mainly through the ventral alar plate of the rhombencephalic tegmentum, while the ventromedial ascending fibers coursed through the ventral region of the basal plate, and both of them were observed blending at S33-34 with the TH-ir descending fiber pathways described above. Also in some tetrapods, developmental studies have reported ascending fibers form TH/DA-ir CSF-c cells of the spinal cord (González et al., 1994a; Medina et al., 1994a,b).

From S30 some large multipolar TH-ir neurons of the posterior tubercle nucleus extended some projections towards the rostral hypothalamus (suprachiasmatic group), forming a TH-ir fiber longitudinal tract that course in the diencephalon, probably in relation with the medial forebrain bundle. Later in development (from S32), ascending longitudinal fibers reach the preoptic area and some of them also extended rostrally to the preoptic area, just reaching the caudal telencephalon. TH-ir cells of the preoptic area

and suprachiasmatic nucleus/posterior tubercle groups appeared to contribute to these ascending TH-ir longitudinal fibers. The straight pathway of these TH-ir fibers, the presence of some endings dilatations similar to grothw cones and the absence of TH-ir fibers in the subpallium at this stage (S32), support the ascending direction of this CA fibers tract, in spite of the presence of TH-ir cells in the telencephalon (pallium and olfactory bulb), which must be responsible of the intrinsic telencephalic CA innervation. In juveniles, these TH-ir fibers appeared to contribute to the innervation of the subpallium, mainly the basal superficial area and the periventricular ventrolateral area. The existence of this ascending CA tract has been suggested in adults of other elasmobranchs species (Meredith and Smeets, 1987; Northcutt et al., 1988) and in developing and adults of teleosts and cyclostomes (Ekström et al., 1992; Briñon et al., 1998; Rink and Wullimann, 2001; Pierre-Simons et al., 2002; Anadón et al., 2002; Ma, 2003; Abalo et al., 2005). Moreover, the preoptic and posterior tubercle groups are thought to mainly contribute to the CA innervation of the telencephalon in teleosts (Ma, 1994; Rink and Wullimann, 2001; Ma, 2003; McLean and Fetcho, 2004a).

The mesostriatal projection in mammals have been extensively studied (Lindvall et al., 1984; Jimenez-Castellanos and Graybiel, 1987; Lynd-Balta and Haber, 1994a,b; Smeets and Reiner, 1994; Tan et al., 1995) because of their involvement in neurological diseases (Parkinson´s disease). Hodological studies have shown that in tetrapods this ascending projection from the substantia nigra is topological organized (see Smeets and González, 2000). In some elasmobranchs, CA fibers were described leaving the synencephalic/mesencephalic region toward the telencephalon (Meredith and Smeets, 1984; Stuesse et al., 1991; Stuesse and Cruce, 1992; Stuesse et al., 1994), suggesting the existence of a telencephalic projection from these regions. In spite that hodological studies are neccessary to demonstrate this projection, our observation of some TH-ir axons with growth cone endings extending rostrally from the VTA cells of late embryos towards the posterior tubercle, supports its existence. According to some authors (Rink and Wullimann, 2001), the ascending CA fiber tracts reported in the mesencephalic and diencephalic regions of zebrafish could be homologous to the mesostriatal/pallial system recognized in amniotes. In elasmobranchs, the telencephalic region

homologuous to the striatum has not been unequivocally identified, althoug different locations have been proposed: the periventricular ventrolateral area (Northcutt et al., 1988), the lateral subpalial region (Smeets et al., 1983) or both (Sueiro, 2003), and on the basis of its densest dopaminergic innervation, the internal zone of the basal superficial area has also been considered (Meredith and Smeets, 1987). Although some TH-ir density was reported at the ventrolateral subpallium in the adult dogfish (Smeets et al., 2000), our present results revealed that the periventricular ventrolateral area and the basal superficial area are the subpallial regions with the densest TH-ir innervation by TH-ir fibers, supporting the possibilitiy that these regions, probable recipients of the ascending CA innervations, could be related with the homologous region of the striatum of amniotes. Dense subpallial TH-ir innervation has been observed in lampreys (Pombal et al., 1997b) and teleosts (Reiner et al., 1998).

The second phase, which was related to the development of the mature TH-ir axonal branching pattern and axon terminal fields, began at S32 of dogfish development. During this phase, the TH-ir fibers were observed leaving the main longitudinal tracts, branching profusely, innervating most brain and spinal cord regions. The development of the axonal arborization and terminal fields at prehatching stages (S32-S34) was especially notable at the hypothalamic nuclei, ventral tegmental areas and the viscerosensory column. The diencephalon (especially the basal regions), the dorsal rhombencephalic tegmentum and spinal cord have acquired moderate to dense innervation by the branching of the main ascending and descending TH-ir fiber tracts, generating the mature CA axonal circuitry seen in adults.

BIBLIOGRAPHY

Abalo, X.M.; Villar-Cheda, B.; Anadón, R.; Rodicio, M.C. (2005) Development of the dopamine-immunoreactive system in the central nervous system of the sea lamprey. Brain Res Bull. 66:560-564.

Adrio, F.; Anadón, R.; Rodriguez-Moldes, I. (2002) Distribution of tyrosine hydroxylase (TH) and dopamine beta-hydroxylase (DBH) immunoreactivity in the central nervous system of two chondrostean fishes (*Acipenser baeri* and *Huso huso*). J Comp Neurol. 448:280-297.

Anadón, R.; Rodríguez-Moldes, I.; González, A. (2002) Tyrosine hydroxylase immunoreactive neurons in the forebrain of the trout: organization, cellular features and innervation. Brain Res Bull. 57:389-392.

Aroca, P.; Lorente-Cánovas, B.; Mateos, F.R.; Puelles, L. (2006) Locus coeruleus neurons originate in alar rhombomere 1 and migrate into the basal plate: Studies in chick and mouse embryos. J Comp Neurol. 496:802-818.

Aston-Jones, G.; Bloom, F.E. (1981) Activity of norepinephrine-containing locus coeruleus neurons in behaving rats anticipates fluctuations in the sleep-waking cycle. J Neurosci. 1:876-886.

Bailhache, T.; Balthazart, J. (1993) The catecholaminergic system of the quail brain: immunocytochemical studies of dopamine beta-hydroxylase and tyrosine hydroxylase. J Comp Neurol. 329:230-256.

Bajic, D.; Proudfit, H.K. (1999) Projections of neurons in the periaqueductal gray to pontine and medullary catecholamine cell groups involved in the modulation of nociception. J Comp Neurol. 405:359-379.

Ballard, W.W.; Mellinger, J.; Lechenault, H. (1993) A series on normal stages for development of *Scyliorhinus canicula*, the lesser-spotted dogfish (Chondrichthyes: Scyliorhinidae). J Exp Zool. 267:318-336.

Batten, T.F.; Berry, P.A.; Maqbool, A.; Moons, L.; Vandesande, F. (1993) Immunolocalization of catecholamine enzymes, serotonin, dopamine and L-dopa in the brain of *Dicentrarchus labrax* (Teleostei). Brain Res Bull. 31:233-252.

Baumgarten, H.G. (1972) Biogenic monoamines in the cyclostome and lower vertebrate brain. Prog Histochem Cytochem. 4:1-90.

Becker, T.; Wullimann, M.F.; Becker, C.G.; Bernhardt, R.R.; Schachner, M. (1997) Axonal regrowth after spinal cord transection in adult zebrafish. J Comp Neurol. 377:577-595.

Beltramo, M.; Calas, A.; Chernigovskaya, E.; Borisova, N.; Polenova, O.; Tillet, Y.; Thibault, J.; Ugrumov, M. (1994) Postnatal development of the suprachiasmatic nucleus in the rat. Morpho-functional characteristics and time course of tyrosine hydroxylase immunopositive fibers. Neurosci. 63:603-610.

Bolliet, V.; Ali, MA. (1992) Immunohistochemical study of the development of serotoninergic neurons in the brain of the brook trout, *Salvelinus fontinalis*. Brain Behav Evol. 40: 234-249.

Briñón, J.G.; Arévalo, R.; Weruaga, E.; Crespo, C.; Alonso, J.R.; Aijón, J. (1998) Tyrosine hydroxylase-like immunoreactivity in the brain of the teleost fish *Tinca tinca*. Arch Ital Biol. 136:17-44.

Carrera, I.; Sueiro, C.; Molist, P.; Ferreiro, S.; Adrio, F.; Rodríguez, M.A.; Anadón, R.; Rodríguez-Moldes, I. (2005) Temporal and spatial organization of tyrosine hydroxylase-immunoreactive cell groups

in the embryonic brain of an elasmobranch, the lesser-spotted dogfish *Scyliorhinus canicula.* Brain Res Bull. 66:541-545.

Castro, A.; Becerra, M.; Manso, MJ.; Anadón, R. (2006) Calretinin immunoreactivity in the brain of the zebrafish, *Danio rerio*: distribution and comparison with some neuropeptides and neurotransmitter-synthesizing enzymes. I. Olfactory organ and forebrain. J Comp Neurol. 494:435-459.

Di Porzio, U.; Zuddas, A.; Cosenza-Murphy, D.B.; Barker, J.L. (1990) Early appearance of tyrosine hydroxylase immunoreactive cells in the mesencephalon of mouse embryos. Int J Dev Neurosci. 8:523-532.

Ekström, P.; Honkanen, T.; Steinbusch, H.W. (1990) Distribution of dopamine-immunoreactive neuronal perikarya and fibers in the brain of a teleost, *Gasterosteus aculeatus L*. comparison with tyrosine hydroxylase- and dopamine-beta-hydroxylase-immunoreactive neurons. J Chem Neuroanat. 3:233-260.

Ekström, P.; Honkanen, T.; Borg, B. (1992) Development of tyrosine hydroxylase-, dopamine- and dopamine beta-hydroxylase-immunoreactive neurons in a teleost, the three-spined stickleback. J Chem Neuroanat. 5:481-501.

Ekström, P.; Honkanen, T.; Borg, B. (1994) Development of central catecholamine neurons in teleosts, in: W.J.A.J. Smeets, A. Reiner (Eds.), Phylogeny and development of catecholamine systems in the CNS of vertebrates, pp: 325-341; The Cambridge University Press, Cambridge.

Ekström, P.; Holmqvist, B.I.; Panula, P. (1995) Histamine-immunoreactive neurons in the brain of the teleost *Gasterosteus aculeatus L*. Correlation with hypothalamic tyrosine hydroxylase- and serotonin-immunoreactive neurons. J Chem Neuroanat. 8:75-85.

Foster, G.A. (1994) Ontogeny of catecholaminergic neurons in the central nervous system of mammalian species: general aspects, in: W.J.A.J. Smeets, A. Reiner (Eds.), Phylogeny and development of catecholamine systems in the CNS of vertebrates, pp: 405-434; The Cambridge University Press, Cambridge.

Gilland, E.; Baker, R. (1993) Conservation of neuroepithelial and mesodermal segments in the embryonic vertebrate head. Acta Anat (Basel). 148:110-123.

González, A.; Smeets, W.J. (1991) Comparative analysis of dopamine and tyrosine hydroxylase immunoreactivities in the brain of two amphibians, the anuran *Rana ridibunda* and the urodele *Pleurodeles waltlii*. J Comp Neurol. 303:457-477.

González, A.; Smeets, W.J. (1994a) Catecholamine systems in the CNS of amphibians, in: W.J.A.J. Smeets, A. Reiner (Eds.), Phylogeny and development of catecholamine systems in the CNS of vertebrates, pp: 77-101; The Cambridge University Press, Cambridge.

González, A.; Smeets, W.J. (1994b) Distribution of tyrosine hydroxylase immunoreactivity in the brain of *Typhlonectes compressicauda* (Amphibia, Gymnophiona): further assessment of primitive and derived traits of amphibian catecholamine systems. J Chem Neuroanat. 8:19-32.

González, A.; Tuinhof, R.; Smeets, W.J. (1993) Distribution of tyrosine hydroxylase and dopamine immunoreactivities in the brain of the South African clawed frog *Xenopus laevis*. Anat Embryol. 187:193-201.

González, A.; Marín, O.; Tuinhof, R.; Smeets, W.J. (1994a) Ontogeny of catecholamine systems in the central nervous system of anuran amphibians: an immunohistochemical study with antibodies against tyrosine hydroxylase and dopamine. J Comp Neurol. 346:63-79.

González, A.; Muñoz, M.; Muñoz, A.; Marín, O.; Smeets, W.J. (1994b) On the basal ganglia of amphibians: dopaminergic mesostriatal projections. Eur J Morphol. 32:271-274.

González, A.; Marín, O.; Smeets, W.J. (1995) Development of catecholamine systems in the central nervous system of the newt *Pleurodeles waltlii* as revealed by tyrosine hydroxylase immunohistochemistry. J Comp Neurol. 360:33-48.

Guglielmone, R.; Panzica, G.C. (1984) Typology, distribution and development of the catecholamine-containing neurons in the chicken brain. Cell Tissue Res. 237:67-79.

Guo. S.; Wilson, S.W.; Cooke, S.; Chitnis, A.B.; Driever, W.; Rosenthal, A. (1999) Mutations in the zebrafish unmask shared regulatory pathways controlling the development of catecholaminergic neurons. Dev Biol. 208:473-487.

Gurski, M.R.; Hamilton, K.A. (1996) Effects of dopamine and fluphenazine on field potential amplitude in the salamander olfactory bulb. Exp Brain Res. 108:236-246.

Heathcote, R.D.; Chen, A. (1994) Morphogenesis of catecholaminergic interneurons in the frog spinal cord. J Comp Neurol. 342:57-68.

Hökfelt, T.; Everitt, B.J.; Theodorsson-Norheim, E.; Goldstein, M. (1984) Occurrence of neurotensinlike immunoreactivity in subpopulations of hypothalamic, mesencephalic, and medullary catecholamine neurons. J Comp Neurol. 222:543-559.

Hornby, P.J.; Piekut, D.T. (1990) Distribution of catecholamine-synthesizing enzymes in goldfish brains: presumptive dopamine and norepinephrine neuronal organization. Brain Behav Evol. 35:49-64.

Jimenez-Castellanos, J.; Graybiel, A.M. (1987) Subdivisions of the dopamine-containing A8-A9-A10 complex identified by their differential mesostriatal innervation of striosomes and extrastriosomal matrix. Neurosci. 23:223-242.

Karle, E.J.; Anderson, K.D.; Medina, L.; Reiner, A. (1996) Light and electron microscopic immunohistochemical study of dopaminergic terminals in the striatal portion of the pigeon basal ganglia using antisera against tyrosine hydroxylase and dopamine. J Comp Neurol. 369:109-124.

Kaslin, J.; Panula, P. (2001) Comparative anatomy of the histaminergic and other aminergic systems in zebrafish (*Danio rerio*). J Comp Neurol. 440:342-377.

Keverne, E.B.; Levy, F.; Guevara-Guzmán, R.; Kendrick, K.M. (1993) Influence of birth and maternal experience on olfactory bulb neurotransmitter release. Neurosci. 56:557-565.

Kuratani, S.; Horigome, N. (2000) Developmental morphology of branchiomeric nerves in a cat shark, *Scyliorhinus canicula*, with special reference to rhombomeres, cephalic mesoderm, and distribution patterns of cephalic crest cells. Zool Sci. 7:893-909.

Leshin, L.S.; Kraeling, R.R.; Kiser, T.E. (1995) Immunocytochemical localization of the catecholamine-synthesizing enzymes, tyrosine hydroxylase and dopamine-beta-hydroxylase, in the hypothalamus of cattle. J Chem Neuroanat. 9:175-194.

Leshin, L.S.; Kraeling, R.R.; Kineman, R.D.; Barb, C.R.; Rampacek, G.B. (1996) Immunocytochemical distribution of catecholamine-synthesizing neurons in the hypothalamus and pituitary gland of pigs: tyrosine hydroxylase and dopamine-beta-hydroxylase. J Comp Neurol. 364:151-168.

Lindvall, O.; Björklund, A.; Skagerberg, G. (1984) Selective histochemical demonstration of dopamine terminal systems in rat di- and telencephalon: new evidence for dopaminergic innervation of hypothalamic neurosecretory nuclei. Brain Res. 306:19-30.

Lynd-Balta, E.; Haber, S.N. (1994a) Primate striatonigral projections: a comparison of the sensorimotor-related striatum and the ventral striatum. J Comp Neurol. 345:562-578.

Lynd-Balta, E.; Haber, S.N. (1994b) The organization of midbrain projections to the ventral striatum in the primate. Neurosci. 59:609-623.

Ma, P.M. (1994) Catecholaminergic systems in the zebrafish. II. Projection pathways and pattern of termination of the locus coeruleus. J Comp Neurol. 344:256-269.

Ma, P.M. (1997) Catecholaminergic systems in the zebrafish. III. Organization and projection pattern of medullary dopaminergic and noradrenergic neurons. J Comp Neurol. 381:411-427.

Ma, P.M. (2003) Catecholaminergic systems in the zebrafish. IV. Organization and projection pattern of dopaminergic neurons in the diencephalon. J Comp Neurol. 460:13-37.

Maeda, Y.; Yamada, K.; Hasegawa, T.; Iyo, M.; Fukui, S.; Nabeshima, T. (1994) Inhibitory effects of salmon calcitonin on the tail-biting and scratching behavior induced by substance P and three excitatory amino acids. J Neural Transm Gen Sect. 96:125-133.

Manso, M.J.; Becerra, M.; Molist, P.; Rodriguez-Moldes, I.; Anadón, R. (1993) Distribution and development of catecholaminergic neurons in the brain of the brown trout. A tyrosine hydroxylase immunohistochemical study. J Hirnforsch. 34:239-260.

Marchand, R.; Poirier, L.J. (1983) Isthmic origin of neurons of the rat substantia nigra. Neurosci. 9:373-381.

Marín, O.; González, A.; Smeets, W.J. (1997) Basal ganglia organization in amphibians: afferent connections to the striatum and the nucleus accumbens. J Comp Neurol. 378:16-49.

Marín, O.; González, A.; Smeets, W.J. (1998a) Amphibian basal ganglia control of tectal function: a complex matter. Trends Neurosci. 21:336-337.

Marín, O.; González, A.; Smeets, W.J. (1998b) Basal ganglia organization in amphibians: evidence for a common pattern in tetrapods. Prog Neurobiol. 55:363-397.

Marín, F.; Herrero, M.T.; Vyas, S.; Puelles, L. (2005) Ontogeny of tyrosine hydroxylase mRNA expression in mid- and forebrain: neuromeric pattern and novel positive regions. Dev Dyn. 234:709-717.

McLean, D.L.; Fetcho, J.R. (2004a) Ontogeny and innervation patterns of dopaminergic, noradrenergic, and serotonergic neurons in larval zebrafish. J Comp Neurol. 480:38-56.

McLean, D.L.; Fetcho, J.R. (2004b) Relationship of tyrosine hydroxylase and serotonin immunoreactivity to sensorimotor circuitry in larval zebrafish. J Comp Neurol. 480:57-71.

McRitchie, D.A.; Hardman, C.D.; Halliday, G.M. (1996) Cytoarchitectural distribution of calcium binding proteins in midbrain dopaminergic regions of rats and humans. J Comp Neurol. 364:121-150.

Medina, L.; Puelles, L.; Smeets, W.J. (1994a) Ontogenesis of catecholamines systems in the brain of the lizard *Gallotia galloti*, in: W.J.A.J. Smeets, A. Reiner (Eds.), Phylogeny and development of catecholamine systems in the CNS of vertebrates, pp: 361-377; The Cambridge University Press, Cambridge.

Medina, L.; Puelles, L.; Smeets, W.J. (1994b) Development of catecholamine systems in the brain of the lizard *Gallotia galloti*. J Comp Neurol. 350:41-62.

Meek, J. (1994) Catecholamines in the brains of Osteichthyes (bony fishes), in: W.J.A.J. Smeets, A. Reiner (Eds.), Phylogeny and development of catecholamine systems in the CNS of vertebrates, pp: 49-74; The Cambridge University Press, Cambridge.

Meek, J.; Joosten, H.W. (1993) Tyrosine hydroxylase-immunoreactive cell groups in the brain of the teleost fish *Gnathonemus petersii.* J Chem Neuroanat. 6:431-446.

Meredith, G.E.; Smeets, W.J. (1987) Immunocytochemical analysis of the dopamine system in the forebrain and midbrain of *Raja radiata*: evidence for a substantia nigra and ventral tegmental area in cartilaginous fish. J Comp Neurol. 265:530-548.

Molist, P. (1990) Estudio inmunohistoquímico de algunos sistemas del encéfalo de seláceos. Doctoral Thesis. University Santiago de Compostela. Spain.

Molist, P.; Rodriguez-Moldes, I.; Anadón, R. (1993) Organization of catecholaminergic systems in the hypothalamus of two elasmobranch species, *Raja undulata* and *Scyliorhinus canicula*. A histofluorescence and immunohistochemical study. Brain Behav Evol. 41:290-302.

Moons, L.; D'Hondt, E.; Pijcke, K.; Vandesande, F. (1995) Noradrenergic system in the chicken brain: immunocytochemical study with antibodies to noradrenaline and dopamine-beta-hydroxylase. J Comp Neurol. 360:331-348.

Murase, S.; Takayama, M.; Nosaka, S. (1993) Chemical stimulation of the nucleus locus coeruleus: cardiovascular responses and baroreflex modification. Neurosci Lett. 153:1-4.

Northcutt, R.G.; Reiner, A.; Karten, H.J. (1988) Immunohistochemical study of the telencephalon of the spiny dogfish, *Squalus acanthias*. J Comp Neurol. 277:250-267.

Okado, N.; Ishihara, R.; Ito, R.; Homma, S.; Kohno, K. (1991) Immunohistochemical study of tyrosine-hydroxylase-positive cells and fibers in the chicken spinal cord. Neurosci Res. 11:108-118.

Parent, A.; Northcutt, R.G. (1982) The monoamine-containing neurons in the brain of the garfish, *Lepisosteus osseus*. Brain Res Bull. 9:189-204.

Parent, A.; Mackey, A.; Smith, Y.; Boucher, R. (1983) The output organization of the substantia nigra in primate as revealed by a retrograde double labeling method. Brain Res Bull. 10:529-537.

Peyron, C.; Luppi, P.H.; Kitahama, K.; Fort, P.; Hermann, D.M.; Jouvet, M. (1995) Origin of the dopaminergic innervation of the rat dorsal raphe nucleus. Neuroreport. 6:2527-2531.

Pierre, J.; Mahouche, M.; Suderevskaya, E.I.; Reperant, J.; Ward, R.; (1997) Immunocytochemical localization of dopamine and its synthetic enzymes in the central nervous system of the lamprey *Lampetra fluviatilis*. J Comp Neurol. 380:119-135.

Pierre-Simons, J.; Reperant, J.; Mahouche, M.; Ward, R. (2002) Development of tyrosine hydroxylase-immunoreactive systems in the brain of the larval lamprey *Lampetra fluviatilis*. J Comp Neurol. 447:163-176.

Piñuela, C.; Northcutt, R.G. (2007) Immunohistochemical organization of the forebrain in the white sturgeon, *Acipenser transmontanus*. Brain Behav Evol. 69:229-253.

Pombal, M.A.; Puelles, L. (1999) Prosomeric map of the lamprey forebrain based on calretinin immunocytochemistry, Nissl stain, and ancillary markers. J Comp Neurol. 414:391-422.

Pombal, M.A.; El Manira, A.; Grillner, S. (1997a) Organization of the lamprey striatum - transmitters and projections. Brain Res. 766:249-254.

Pombal, M.A.; El Manira, A.; Grillner, S. (1997b) Afferents of the lamprey striatum with special reference to the dopaminergic system: a combined tracing and immunohistochemical study. J Comp Neurol. 386:71-91.

Puelles, L. (1995) A segmental morphological paradigm for understanding vertebrate forebrains. Brain Behav Evol. 46:319-337.

Puelles, L.; Medina, L. (1994) Development of neurons expressing tyrosine hydroxilase and dopamine in the chicken brain: a comparative segmental analysis, in: W.J.A.J. Smeets, A. Reiner (Eds.), Phylogeny and development of catecholamine systems in the CNS of vertebrates, pp: 381-404; The Cambridge University Press, Cambridge.

Puelles, L.; Verney, C. (1998) Early neuromeric distribution of tyrosine-hydroxylase-immunoreactive neurons in human embryos. J Comp Neurol. 394:283-308.

Puelles, L.; Rubenstein, J.L. (2003) Forebrain gene expression domains and the evolving prosomeric model. Trends Neurosci. 26:469-476.

Reiner, A.; Anderson, K.D. (1990) The patterns of neurotransmitter and neuropeptide co-occurrence among striatal projection neurons: conclusions based on recent findings. Brain Res Rev. 15:251-265.

Reiner, A.; Northcutt, R.G. (1987) An immunohistochemical study of the telencephalon of the African lungfish, *Protopterus annectens*. J Comp Neurol. 256:463-481.

Reiner, A.; Northcutt, R.G. (1992) An immunohistochemical study of the telencephalon of the Senegal bichir (*Polypterus senegalus*). J Comp Neurol. 319:359-386.

Reiner, A.; Brauth, S.E.; Karten, H.J. (1984) Evolution of the amniote basal ganglia, Trends Neurosci. 7:320-325.

Reiner, A.; Karle, E.J.; Anderson, D.; Medina, L. (1994) Catecholaminergic perikarya and fibers in the avian nervous system, in: W.J.A.J. Smeets, A. Reiner (Eds.), Phylogeny and development of catecholamine systems in the CNS of vertebrates, pp: 135-175; The Cambridge University Press, Cambridge.

Reiner, A.; Medina, L.; Veenman, C.L. (1998) Structural and functional evolution of the basal ganglia in vertebrates. Brain Res Bull. 28:235-285.

Rink, E.; Wullimann, M.F. (2001) The teleostean (zebrafish) dopaminergic system ascending to the subpallium (striatum) is located in the basal diencephalon (posterior tuberculum). Brain Res. 889:316-330.

Rink, E.; Wullimann, M.F. (2002) Development of the catecholaminergic system in the early zebrafish brain: an immunohistochemical study. Brain Res Dev. 137:89-100.

Rink, E.; Wullimann, M.F. (2004) Connections of the ventral telencephalon (subpallium) in the zebrafish (*Danio rerio*). Brain Res. 1011:206-220.

Roberts, B.L.; Meredith, G.E. (1987) Immunohistochemical study of a dopaminergic system in the spinal cord of the ray, *Raja radiate.* Brain Res. 437:171-175.

Roberts, B.L.; Meredith, G.E.; Maslam, S. (1989) Immunocytochemical analysis of the dopamine system in the brain and spinal cord of the European eel, *Anguilla anguilla*. Anat Embryol. 180:401-412.

Roberts, B.L.; Maslam, S.; Scholten, G.; Smit, W. (1995) Dopaminergic and GABAergic cerebrospinal fluid-contacting neurons along the central canal of the spinal cord of the eel and trout. J Comp Neurol. 354:423-437.

Rodríguez-Gómez, F.J.; Rendon-Unceta, M.C.; Sarasquete, C.; Muñoz-Cueto, J.A. (2000) Localization of tyrosine hydroxylase-immunoreactivity in the brain of the Senegalese sole, *Solea senegalensis*. J Chem Neuroanat. 19:17-32.

Rodríguez-Moldes, I.; Anadón, R. (1987) Aminergic neurons in the hypothalamus of the dogfish, *Scyliorhinus canicula L*. (Elasmobranch). A histofluorescence study. J Hirnforsch. 28:685-693.

Rubenstein, J.L.; Martínez, S.; Shimamura, K.; Puelles, L. (1994) The embryonic vertebrate forebrain: the prosomeric model. Science. 266:578-580.

Sánchez-Camacho, C.; Marín, O.; Smeets, W.J.; Ten Donkelaar, H.J.; González, A. (2001) Descending supraspinal pathways in amphibians. II. Distribution and origin of the catecholaminergic innervation of the spinal cord. J Comp Neurol. 434:209-232.

Sánchez-Camacho, C.; Marín, O.; López, J.M.; Moreno, N.; Smeets, W.J.; ten Donkelaar, H.J.; González, A. (2002a) Origin and development of descending catecholaminergic pathways to the spinal cord in amphibians. Brain Res Bull. 57:325-330.

Sánchez-Camacho, C.; Martín, O.; Ten Donkelaar, H.J.; González, A. (2002b) Descending supraspinal pathways in amphibians: III. Development of descending projections to the spinal cord in *Xenopus laevis* with emphasis on the catecholaminergic inputs. J Comp Neurol. 446:11-24.

Sas, E.; Maler, L.; Tinner, B. (1990) Catecholaminergic systems in the brain of a gymnotiform teleost fish: an immunohistochemical study. J Comp Neurol. 292:127-162.

Schotland, J.L.; Shupliakov, O.; Grillner, S.; Brodin, L. (1996) Synaptic and nonsynaptic monoaminergic neuron systems in the lamprey spinal cord. J Comp Neurol. 372:229-244.

Smeets W.J. (1994) Catecholamine systems in the CNS of reptiles: structure and functional correlations, in: W.J.A.J. Smeets, A. Reiner (Eds.), Phylogeny and development of catecholamine systems in the CNS of vertebrates, pp: 103-129; The Cambridge University Press, Cambridge.

Smeets, W.J.; Gonzalez, A. (2000) Catecholamine systems in the brain of vertebrates: new perspectives through a comparative approach. Brain Res Brain Res Rev. 33:308-379.

Smeets W.J.; Reiner, A. (1994) Catecholamines in the CNS of vertebrates: current concepts of evolution and functional significance, in: W.J.A.J. Smeets, A. Reiner (Eds.), Phylogeny and development of catecholamine systems in the CNS of vertebrates, pp: 463-478; The Cambridge University Press, Cambridge.

Smeets, W.J.; Steinbusch, H.W. (1990) New insights into the reptilian catecholaminergic systems as revealed by antibodies against the neurotransmitters and their synthetic enzymes. J Chem Neuroanat. 3:25-43.

Smeets, W.J.; Timerick, S.J. (1981) Cells of origin of pathways descending to the spinal cord in two chondrichthyans, the shark *Scyliorhinus canicula* and the ray *Raja clavata*. J Comp Neurol. 202:473-491.

Smeets, W.J.; Nieuwenhuys, R.; Roberts, BL. (1983) The central nervous system of cartilaginous fishes: structure and functional correlations. Springer-Verlag, Berlin.

Smeets, W.J.; Marín, O.; Gonzalez, A. (2000) Evolution of the basal ganglia: new perspectives through a comparative approach. J Anat. 196:501-517.

Specht, L.A.; Pickel, V.M.; Joh, T.H.; Reis, D.J. (1981a) Light-microscopic immunocytochemical localization of tyrosine hydroxylase in prenatal rat brain. I. Early ontogeny. J Comp Neurol. 199:233-253.

Specht, L.A.; Pickel, V.M.; Joh, T.H.; Reis, D.J. (1981b) Light-microscopic immunocytochemical localization of tyrosine hydroxylase in prenatal rat brain. II. Late ontogeny. J Comp Neurol. 199:255-276.

Stuesse, S.L.; Cruce, W.L.; Northcutt, R.G. (1990) Distribution of tyrosine hydroxylase- and serotonin-immunoreactive cells in the central nervous system of the thornback guitarfish, *Platyrhinoidis triseriata.* J Chem Neuroanat. 3:45-58.

Stuesse, S.L.; Cruce, W.L. (1991) Immunohistochemical localization of serotoninergic, enkephalinergic, and catecholaminergic cells in the brainstem and diencephalon of a cartilaginous fish, *Hydrolagus colliei*. J Comp Neurol. 309:535-548.

Stuesse, S.L.; Cruce, W.L.; Northcutt, R.G. (1991) Localization of serotonin, tyrosine hydroxylase, and leu-enkephalin immunoreactive cells in the brainstem of the horn shark, *Heterodontus francisci*. J Comp Neurol. 308:277-292.

Stuesse, S.L., Cruce, W.L. (1992) Distribution of tyrosine hydroxylase, serotonin, and leu-enkephalin immunoreactive cells in the brainstem of a shark, *Squalus acanthias*. Brain Behav Evol. 39:77-92.

Stuesse, S.L.; Cruce, W.L.; Northcutt, R.G. (1994) Localization of catecholamines in the brains of Chondrichthyes (cartilaginous fishes), in: W.J.A.J. Smeets, A. Reiner (Eds.), Philogeny and development of catecholamine systems in the CNS of vertebrates, pp: 21-47; The Cambridge University Press, Cambridge.

Sueiro, C. (2003) Estudio inmunohistoquímico de los sistemas gabaérgicos del sistema nervioso central de peces elasmobranquios y su relación con sistemas catecolaminérgicos y peptidérgicos. Doctoral Thesis. University Santiago de Compostela. Spain.

Tan, Y.; Brog, J.S.; Williams, E.S.; Zahm, D.S. (1995) Morphometric analysis of ventral mesencephalic neurons retrogradely labeled with Fluoro-Gold following injections in the shell, core and rostral pole of the rat nucleus accumbens. Brain Res. 689:151-156.

Tillet, Y. (1994) Catecholaminergic neuronal systems in the diencephalon of mammals, in: W.J.A.J. Smeets, A. Reiner (Eds.), Phylogeny and development of catecholamine systems in the CNS of vertebrates, pp: 207-236; The Cambridge University Press, Cambridge.

Tillet, Y.; Thibault, J.; Krieger, M. (1994) Aromatic L-amino acid decarboxylase immunohistochemistry in the suprachiasmatic nucleus of the sheep. Comparison with tyrosine hydroxylase immunohistochemistry. Brain Res. 648:319-323.

Timerick, S.J.; Roberts, B.L.; Paul, D.H. (1992) Brainstem neurons projecting to different levels of the spinal cord of the dogfish *Scyliorhinus canicula*. Brain Behav Evol. 39:93-100.

Verney, C.; Zecevic, N.; Ezan, P. (2001) Expression of calbindin D28K in the dopaminergic mesotelencephalic system in embryonic and fetal human brain. J Comp Neurol.429:45-58.

Vetillard, A.; Benanni, S.; Saligaut, C.; Jego, P.; Bailhache, T. (2002) Localization of tyrosine hydroxylase and its messenger RNA in the brain of rainbow trout by immunocytochemistry and in situ hybridization. J Comp Neurol. 449:374-389.

Vitalis, T.; Cases, O.; Engelkamp, D.; Verney, C.; Price, D.J. (2000) Defect of tyrosine hydroxylase-immunoreactive neurons in the brains of mice lacking the transcription factor Pax6. J Neurosci. 20:6501-6516.

Wallace, J.A.; Mondragon, R.M.; Allgood, P.C.; Hoffman, T.J.; Maez, R.R. (1987) Two populations of tyrosine hydroxylase-positive cells occur in the spinal cord of the chick embryo and hatchling. Neurosci Lett. 83:253-258.

Wallace, J.A.; Romero, A.A.; Gabaldon, A.M.; Roe, V.A.; Saavedra, S.L.; Lobner, J. (1996) Tyrosine hydroxylase-containing neurons in the spinal cord of the chicken. I. Development and analysis of catecholamine synthesis capabilities. Cell Mol Neurobiol. 16:625-648.

Wicht, H.; Himstedt, W. (1988) Topologic and connectional analysis of the dorsal thalamus of *Triturus alpestris* (amphibia, urodela, salamandridae). J Comp Neurol. 267:545-561.

Wilson, D.A.; Sullivan, R.M. (1995) The D2 antagonist spiperone mimics the effects of olfactory deprivation on mitral/tufted cell odor response patterns. J Neurosci. 15:5574-5581.

Wullimann, M.F.; Rink, E. (2001) Detailed immunohistology of Pax6 protein and tyrosine hydroxylase in the early zebrafish brain suggests role of Pax6 gene in development of dopaminergic diencephalic neurons. Brain Res Dev Brain Res. 131:173-191.

Wullimann, M.F.; Rink, E. (2002) The teleostean forebrain: a comparative and developmental view based on early proliferation, Pax6 activity and catecholaminergic organization. Brain Res Bull. 57:363-370.

Yáñez, J. (1992). Estudio histoquímico e inmunohistoquímico sobre la organización larvaria de algunos sistemas monoaminérgicos y peptidérgicos del encéfalo de la lamprea de mar (*Petromyzon marinus L.*). Doctoral Thesis. University of Santiago de Compostela. Spain.

ABBREVIATIONS

AC	cerebellar auricula
ACS	central superficial area
APV	ventrolateral periventricular area
ASB	basal superficial area
Cb	cerebellum
cc	central canal
Cg	central grey
CN	cerebellar nucleus
CSF-c	cerebrospinal fluid contacting
Di	diencephalon
DH	dorsal horn
fl	fasciculus retroflexus
Gl	glomerular layer of the olfactory bulb
Gr	granular layer of the olfactory bulb
GR	granular eminences of the cerebellum
Ha	habenula
H	hypophysis
Hpd	dorsal hypothalamus
IHL	inferior hypothalamic lobe
i	infundibulum
IP	interpeduncular nucleus
IS	isthmus
LC	locus coeruleus
ME	median eminence
Mes	mesencephalon
MLF	medial longitudinal fascicle
MOL	molecular layer of the cerebellum
OB	olfactory bulb
Ofl	olfactory fiber layer
On	optic nerve
OT	optic tectum
P	pallium
Pc	posterior commissure
Pi	pineal organ
Pl	lateral pallium
Po	preoptic area
Pr	posterior recess
Pro	posterior recess organ
PTN	posterior tubercle nucleus
PVO	paraventricular organ
R	Rathke's pouch
r1-r8	rhombomeres
Ret	tegmental reticular groups
Rh	rhombencephalon
Rpo	preoptic recess
Sc	locus subcoeruleus
SCN	suprachiasmatic nucleus
Si	infundibuli saccus
SN	substantia nigra
Sp	subpallium
Spc	spinal cord
SV	saccus vasculosus
Syn	synencephalon
Td	dorsal thalamus
Tv	ventral thalamus
VH	ventral horn
VMC	visceromotor column
VSC	viscerosensorial column
VTA	ventral tegmental area
cVTA	ventral tegmental area pars caudalis
rVTA	ventral tegmental area pars rostralis
III	oculomotor nucleus
IIIr	oculomotor nerve root
IV	trochlear nucleus
V/m	trigeminal nucleus
Vr	trigeminal nerve root
VI/m	abducens nucleus
VIIIm	magnocellular octaval nucleus

		EMBRYO STAGES										
		25	26	27	28	29	30	31	32	33	34	Juv Adult
Tel	OB								■	■	■	■
	P							■	■	■	■	■
	Sp											■
Di	Po								■	■	■	■
	SCN		■	■	■	■	■	■	■	■	■	■
	Tv				■	■	■	■	■	■	■	■
	PTN		■	■	■	■	■	■	■	■	■	■
	Pro		■	■	■	■	■	■	■	■	■	■
	PVO									■	■	■
	SV											■
Syn	SN/rVTA							■	■	■	■	■
Mes	cVTA							■	■	■	■	■
Rh	LC						■	■	■	■	■	■
	Sc							■	■	■	■	■
	Cg											■
	VSC							■	■	■	■	■
	Ret						■	■	■	■	■	■
Spc	CSF-c		■	■	■	■	■	■	■	■	■	■
	Non-CSF-c									■	■	■

Table I. Timetable of the appearance of TH-ir cell groups in the dogfish CNS.

	Telencephalon			Diencephalon				Di/Mes	Rhombencephalon	
	OB	**P**	**Sp**	**Po**	**SCN**	**T v**	**Hyp**	**SN/ VTA**	**LC/ Sc/ Cg**	**VSC/ VMC**
S. canicula (present study)	5th	4th	6th	5th	1st	2nd	1st	4th	3rd	3rd
Lampetra fluviatilis (Pierre-Simons et al., 2002)	3rd	-	-	1st	2nd	4th	1st	-	4th	4th
Danio rerio (McLean and Fetcho, 2004)	2nd	-	2nd	2nd	-	3rd	1st	-	1st	2nd
Gasterosteus aculeatus (Ekström et al., 1992)	-	-	3rd	3rd	2nd	4th	1st	-	1st	2nd
Salmo trutta fario (Manso et al., 1993)	3rd	-	2nd	1st	1st	2nd	1st	-	1st	1st
Pleurodeles waltii (González et al., 1995)	2nd	-	-	4th	2nd	-	1st	3rd	2nd	2nd
Gallotia galloti (Medina et al., 1994)	4th	-	-	5th	3rd	3rd	2nd	1st	4th	4th
Chick (Puelles and Medina, 1994)	6th	-	6th	3rd	2nd	1st	1st	3rd	4th	5th
rat (Foster, 1994)	6th	-	-	2nd	2nd	5th	3rd	1st	4th	5th

Table II. Comparison of the order of appearance of brain TH-ir cell groups among vertebrates.

Figure 1. Schematic representations of sagittal sections of brains of dogfish embryos at S26 (**A**), S28 (**B**), S30 (**C**), S31 (**D**) and S33 (**E**) showing the distribution of TH-ir cells (circles) and fibers (thin lines). The diencephalic-mesencephalic and mesencephalic-rhombencephalic boundaries are represented by broken lines. The location of the exit of some cranial nerves (IIIr,Vr), and the tentative location of rhombomeres (r1-r8) are also shown. Scale bars: 100 µm (A-D); 250 µm (E).

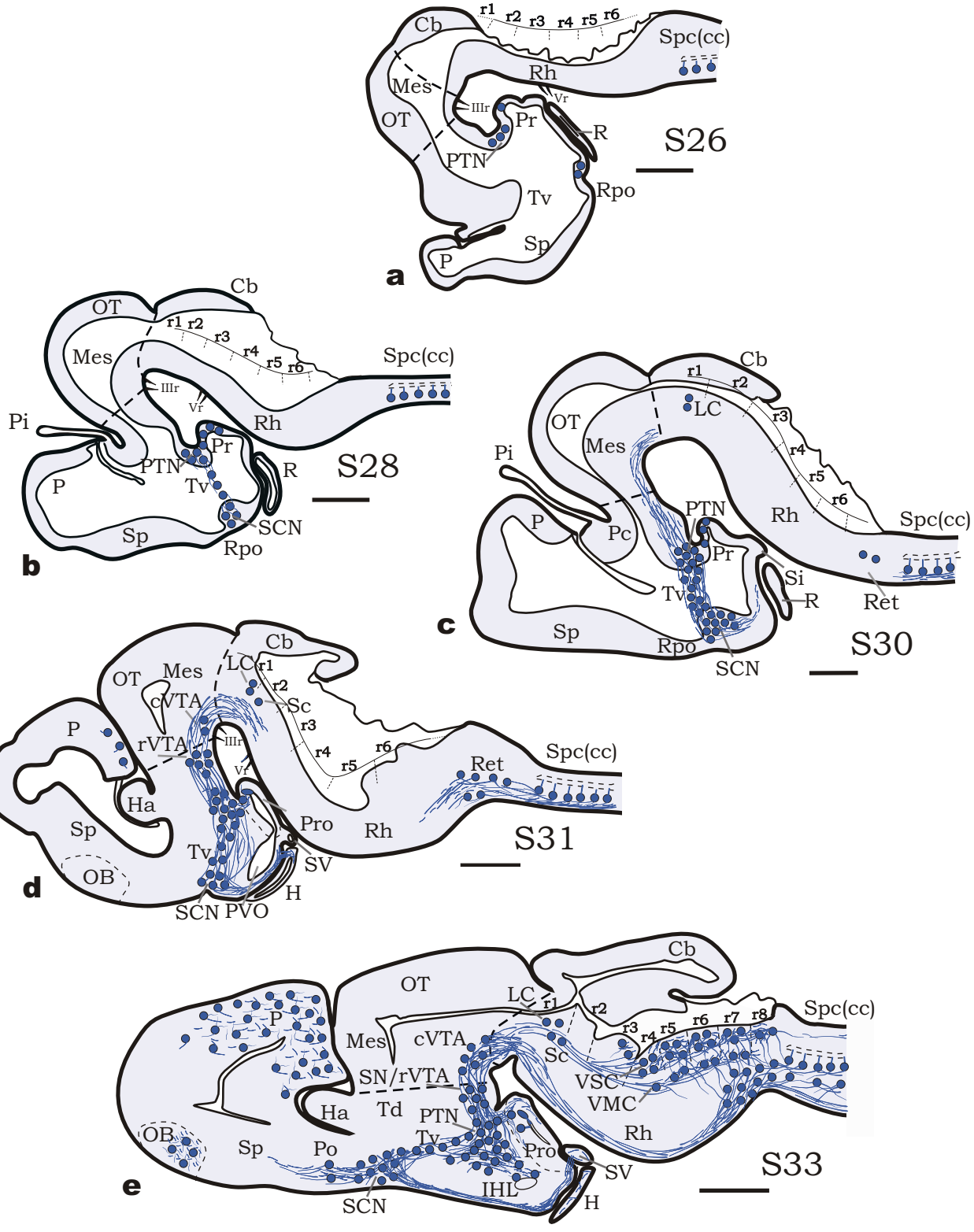
a
Cb
r1 r2 r3 r4 r5 r6
Spc(cc)
Mes
Rh
Vr
IIIr
OT
Pr
R
S26
PTN
Tv
Rpo
Sp
P
b
Cb
OT
r1 r2
r3
r4
r5 r6
Mes
Spc(cc)
IIIr
Vr
Pi
Rh
Pr
PTN
R
S28
P
Tv
SCN
Sp
Rpo
c
Cb
r1
r2
LC
OT
r3
Mes
r4
Pi
r5
r6
PTN
Rh
Spc(cc)
P
Pc
Pr
Si
Tv
R
Ret
Sp
Rpo
SCN
S30
d
Cb
LC
r1
OT
Mes
r2
cVTA
Sc
P
r3
rVTA
IIIr
r4
r6
Spc(cc)
r5
Ret
Vr
Ha
Pro
Sp
Rh
Tv
S31
OB
SV
H
SCN
PVO
e
Cb
OT
LC
r1
r2
P
r3
r4
r5
r6
r7
r8
Spc(cc)
Mes
cVTA
Sc
SN/rVTA
VSC
VMC
Ha
Td
PTN
Rh
OB
Sp
Po
Tv
Pro
SV
S33
IHL
H
SCN

Fig. 1

Figure 2. Sagittal (**A-M**) and transverse (**N**) sections throughout the dogfish brain (**A,C-E,G-M**) and spinal cord (**B,F,N**) of embryos at S26 (**A,B**), S28 (**C-F**) and 30 (**G-N**) showing TH-ir cells and fibers. **A.** Detail of the caudal diencephalon at S26 showing a few TH-ir cells in the PTN (arrows) and in the external walls of the Pro (arrowhead). **B.** Rostral spinal cord at S26 showing CSF-c TH-ir cells ventrally to the central canal (dotted lines). Note the thick apical process contacting to the ventricle (arrows). **C.** Detail of the caudal diencephalon at S28 showing two types of TH-ir cells at the Pro walls: CSF-c cell in the primordial Pro (arrow) and a TH-ir non-CSF-c cell at the marginal layer (arrowhead). Note also the increased density of the TH-ir cells at the PTN (compare with Figure A). **D.** Sagittal section of the diencephalon to show TH-ir cells in the SCN and PTN and between them, corresponding to the primordial ventral thalamus TH-ir cell group. **E.** Detail of the squared area in figure D, to show a few TH-ir cells and their processes (arrowheads). **F.** TH-ir CSF-c cells at the rostral spinal cord at S28. **G.** Sagittal section of the hypothalamus at S30 showing abundant TH-ir cells in the SCN and faintly TH-ir fibers that coursed throughout the hypothalamic floor forming the primordial hypothalamic-hypophyseal tract (arrowheads). Rostral is at the left. **H.** Sagittal section of the diencephalon of S30 showing a band of TH-ir cells from the PTN to the SCN. **I.** Detail of the squared area in H, showing some apparently migrating processes of TH-ir cells with their growth cones towards the SCN (arrows). **J.** Posterior recess walls at S30 showing TH-ir CSF-c cells (arrow) and non-CSF-c cells (arrowhead). Note a few TH-ir fibers coursing in the external layer between the PTN and the Pro. **K.** Sagittal section of the basal diencephalon showing TH-ir descendent fibers (arrowheads) coursing throughout the synencephalon, from the TH-ir cells of the PTN. **L.** Detail of the squared area in K, showing the descendent TH-ir fibers. **M.** Caudal rhombencephalon at S30 showing TH-ir reticular cells (arrows) and their vertical processes. **N.** Transverse section at a rostral spinal cord level showing TH-ir CSF-c cells (arrow) ventral to the central canal (star), and TH-ir fibers coursing ventrolaterally to them (arrowheads). For abbreviations, see list. Scale bars: 100µm (A,I-K); 50µm (B,E-G,L); 25µm (C,M); 250µm (D,H).

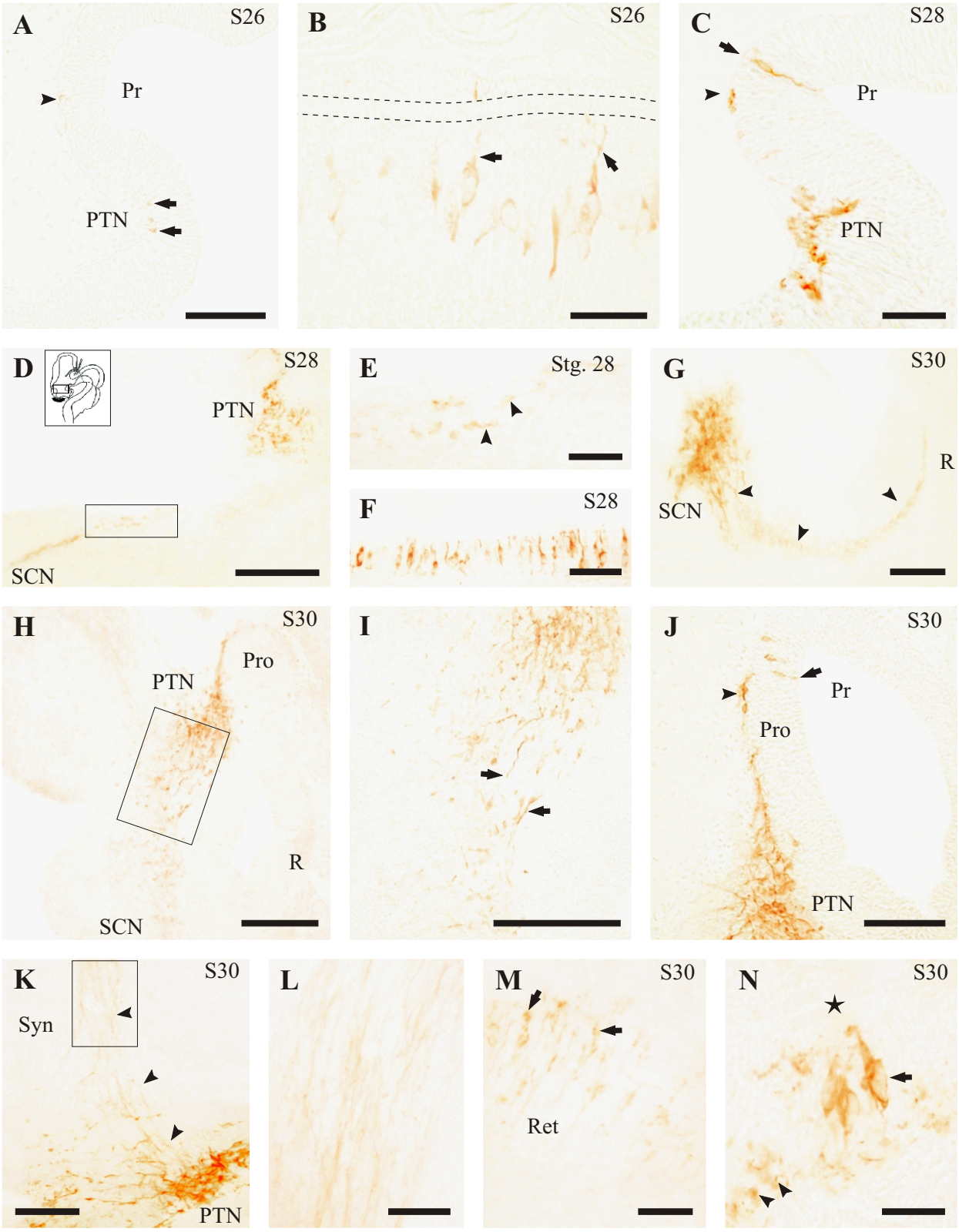
A
S26
Pr
PTN
B
S26
C
S28
Pr
PTN
D
S28
PTN
SCN
E
Stg. 28
F
S28
G
S30
R
SCN
H
S30
Pro
PTN
R
SCN
I
J
S30
Pr
Pro
PTN
K
S30
Syn
PTN
L
M
S30
Ret
N
S30

Fig. 2

Figure 3. Sagittal sections throughout the brain of S31 embryos showing TH-ir cells and fibers. **A.** Some faintly TH-ir cells at the caudal pallium (arrows). **B.** TH-ir cells and fibers are abundant in the PTN but scarce in the VTA (arrow). Note also TH-ir fibers in the external walls of the posterior recess (arrowhead). **C.** Panoramic view of a section medial to the level of the figure B showing descendent TH-ir fibers (arrowheads) coursing from the PTN to the rostral rhombencephalon throughout the basal tegmentum. **D.** Detail of the squared area in C, showing some TH-ir migrating processes (arrowheads). **E.** Faintly TH-ir cells at the LC (arrowhead). **F.** Caudal rhombencephalon showing some faintly TH-ir reticular cells (arrowhead). **G.** Caudal rhombencephalon and rostral spinal cord showing ascendent TH-ir fibers (arrows) probably coursing from the TH-ir cells of the spinal cord (arrowhead). **H.** Detail of the area squared in G showing ascendent TH-ir leading processes with growth cones (arrow). For abbreviations, see list. Scale bars: 50µm (A,F,H); 100µm (B,D,E,G); 250µm (C).

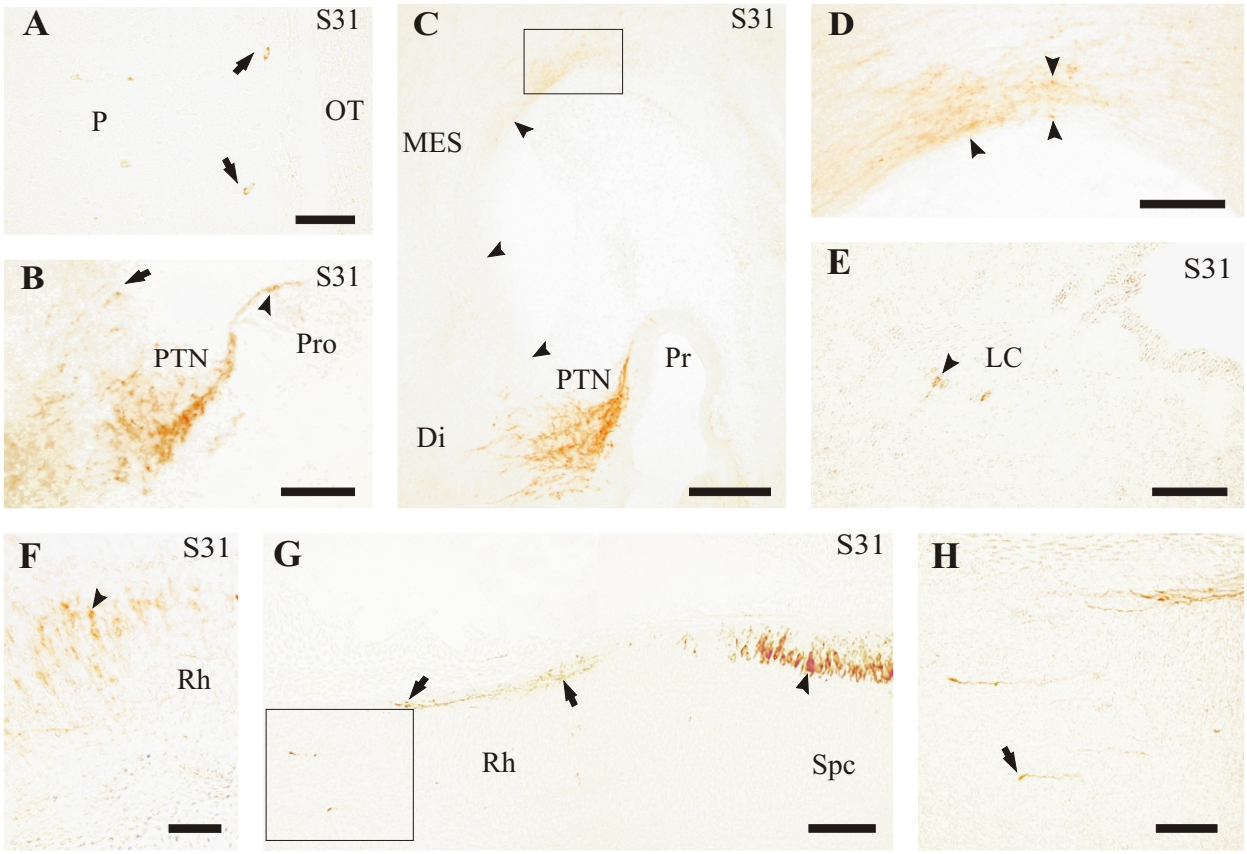
A
S31
P
OT
B
S31
PTN
Pro
C
S31
MES
PTN
Pr
Di
D
E
S31
LC
F
S31
Rh
G
S31
Rh
Spc
H

Fig. 3

Figure 4. Drawing of a parasagittal section of the dogfish brain that schematically represents the main ascending and descending TH-ir fiber pathways at S31 (dark color arrows) and S32-33 (light color arrows). Scale bar: 100 μm.

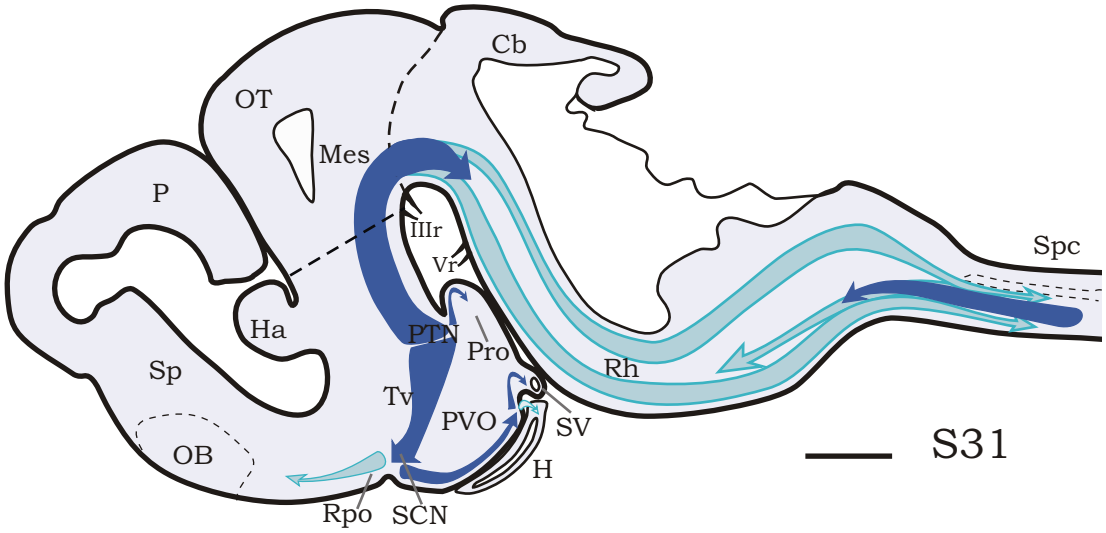

Fig. 4

Figure 5. Transverse (**A-C,F-H,K,N**) and sagittal (**D,E,I,J,L,M,O,P**) sections throughout the brain (**A-K,M-P**) and spinal cord (**L**) of S32 embryos showing TH-ir cells and fibers. **A**. Some TH-ir cells (arrow) and fibers (arrowhead) are observed at the granular cell layer of the olfactory bulb. Note the absence of TH-ir innervation at the glomerular and olfactory fiber layer. **B**. TH-ir cells (arrows) at the caudal pallium. **C**. TH-ir cells (arrow) and fibers at the preoptic area. Asterisk marks the ventricle. **D**. Panoramic view showing TH-ir diencephalic cell populations and both descending (arrowheads) and ascending (thick arrow) TH-ir fibers. Note also TH-ir fibers in the hypothalamic-hypophyseal tract (long arrow) and some cells in the VSC. **E**. Detail of a sagittal section at the diencephalon showing the continuity between TH-ir cell groups of the PTN, Tv, SCN and the VTA/SN (arrows). Note the descendent TH-ir fiber tract (arrowheads). **F**. Transverse section showing TH-ir cells at the caudal SCN and at the Tv (arrows) with their processes laterally oriented. Note the high density of TH-ir cells in the SCN. Asterisk marks the ventricle. **G**. Transverse section showing intense TH-ir cells in the Tv and in the VTA/SN group. Some descendent TH-ir fibers (arrowheads) coursed to the synencephalon. **H.** Detail of a transverse section showing both TH-ir LC (arrowhead) and SC (arrow) cell groups. Midline is to the right. **I.** Sagittal section at the caudal rhombencephalic level to show the reticular TH-ir cells (arrowheads) and the TH-ir cells of the VSC and VMC separated by the sulcus limitans (arrow). Note the segmentary TH-ir cell organization at these levels. Rostral is to the left. **J.** Detail of a sagittal section showing the numerous TH-ir cells (arrowheads) of the VSC and the dense TH-ir innervation. **K.** Transverse section at the obex level to show TH-ir cells of the dorsolateral (arrowhead) and ventrolateral (arrow) reticular groups. Note also TH-ir CSF-c cells ventral to the central canal (white arrowhead). **L.** Sagittal section of the rostral spinal cord showing the numerous TH-ir CSF-c cells. Dotted lines mark the central canal. **M.** Detail of the left squared area in D to show the dense TH-ir innervation of the hypothalamic-hypophyseal tract (arrowheads). **N.** Detail of a transverse section of the caudal hypothalamus showing TH-ir fibers (arrowheads) coursing between the external walls of the hypothalamus and the saccus vasculosus. Note the high density of TH-ir fibers in the floor of the hypothalamus. **O.** Detail of the midle area squared in D to show a descendent TH-ir fiber with a growth cone (arrowhead). **P.** Detail of the right area squared in D to show some ascendent TH-ir fiber with growth cones (arrowheads). For abreviations see list. Scale bars: 100µm (A-C,E,H,J,M,N); 250µm (D,F,G,I,K,); 50µm (L,O,P).

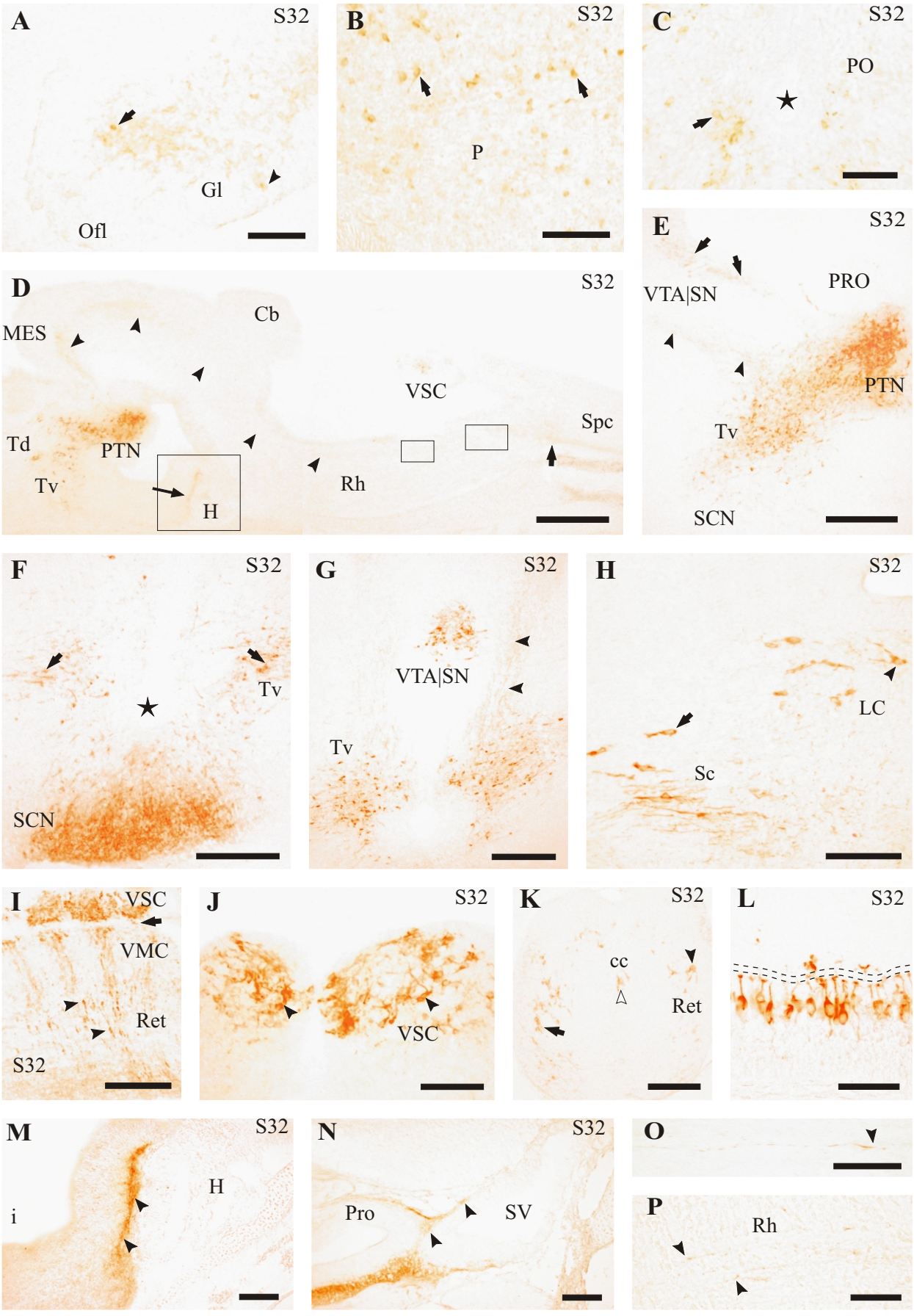
A
S32
Gl
Ofl
B
S32
P
C
S32
PO
D
S32
MES
Cb
VSC
Spc
Td
PTN
Tv
H
Rh
E
S32
VTA|SN
PRO
PTN
Tv
SCN
F
S32
Tv
SCN
G
S32
VTA|SN
Tv
H
S32
LC
Sc
I
VSC
VMC
Ret
S32
J
S32
VSC
K
S32
cc
Ret
L
S32
M
S32
H
i
N
S32
Pro
SV
O
P
Rh

Fig. 5

Figure 6. Transverse (**A-C,F,G,I,J**) and sagittal (**D,E,H**) sections throughout the brain (**A-H,J**) and spinal cord (**I**) of embryos at S33 (**A-G**) and S34 (**H-J**) showing TH-ir cells and fibers. **A.** Transverse section of the olfactory bulb showing TH-ir cells at the granular layer. Note periglomerular TH-ir cells (arrowheads) and the dense network of TH-ir fibers. **B.** Detail of the olfactory bulb to show some periglomerular ventrally oriented TH-ir cells (arrowheads) at the glomerular layer. **C.** Detail of a transverse section through the dorsal pallium to show high density of TH-ir cells. **D.** Sagittal section showing both rVTA (black arrow) and cVTA (white arrow) TH-ir cell groups separated by the fasciculus retroflexus (arrowhead). The dotted line marks the plane of the section of the figure F. **E.** Sagittal section of S33 showing a profuse descendent TH-ir fiber tract (arrows) coursing from the PTN. TH-ir fibers (arrowhead) were also seen in the external walls of the Pro. The dotted line marks the plane of the section of the figure G. **F.** Detail of a transverse section at the level marked in figure D showing synencephalic TH-ir cell groups laterally (SN; white arrow) and medially (rVTA; black arrow) located. Some TH-ir cells of the cVTA (black arrowhead) were also seen at the mesencephalic region. **G.** Detail of a transverse section at the level marked in figure E to show some TH-ir CSF-c cells in the PVO walls (arrowhead). **H.** Abundant TH-ir cells and intrinsic fibers in the VSC of a prehatching embryo. **I.** Transverse section at rostral level of the spinal cord to show TH-ir CSF-c cells (black arrow) ventrally to the central canal (star) and a TH-ir non-CSF-c cells (black arrowhead) at the ventral region of the spinal cord. Note also TH-ir fibers at the ventral funiculus (white arrow). **J.** Transverse section of the SV to show some thick TH-ir fibers (arrowheads) coursing through the external part of the neuroepithelium. For abreviations see list. Scale bars: 250µm (A,D-G); 100µm (B,C,H); 50µm (I,J).

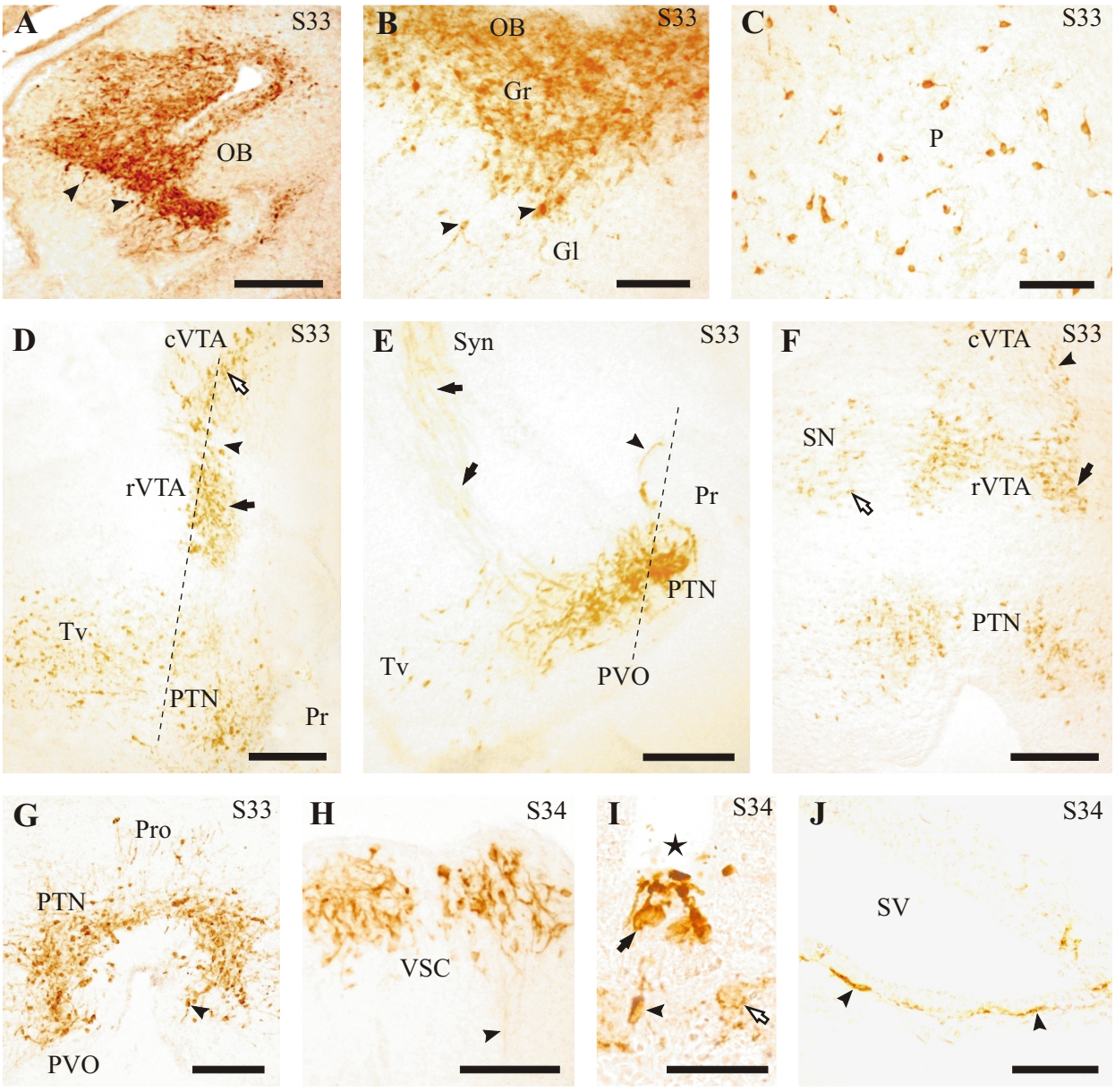
A
S33
OB
B
OB
S33
Gr
Gl
C
S33
P
D
cVTA
S33
rVTA
Tv
PTN
Pr
E
Syn
S33
Pr
PTN
Tv
PVO
F
cVTA
S33
SN
rVTA
PTN
G
S33
Pro
PTN
PVO
H
S34
VSC
I
S34
J
S34
SV

Fig. 6

Figure 7. Schematic drawings of transverse sections through the brain and rostral spinal cord of a juvenile dogfish, showing at the right the distribution of TH-ir perikarya and fibers and at the left the anatomical landmarks. Upper drawing represents a sagittal section of the brain showing the level of transverse sections. See abbreviation list. Scale bars: 2 mm.

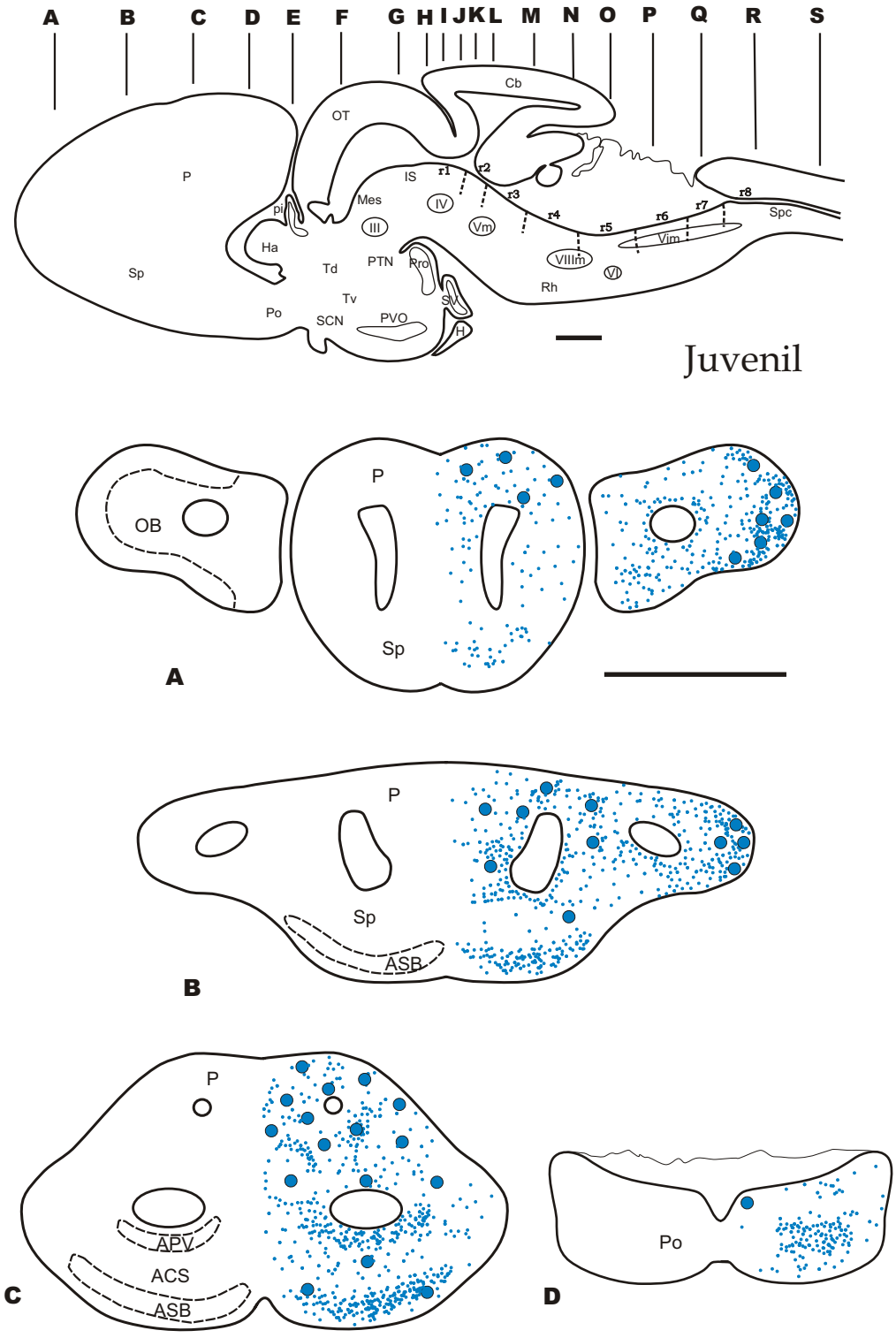
A B C D E F G H I J K L M N O P Q R S
Cb
OT
P
IS
r1
r2
r3
r4
r5
r6
r7
r8
Spc
Mes
IV
III
Vm
Vim
pi
Ha
Sp
Td
PTN
Rrd
VIIIm
VI
Rh
Tv
Po
SCN
PVO
SV
H
Juvenil
OB
P
Sp
A
P
Sp
ASB
B
P
APV
ACS
ASB
C
Po
D

Fig. 7

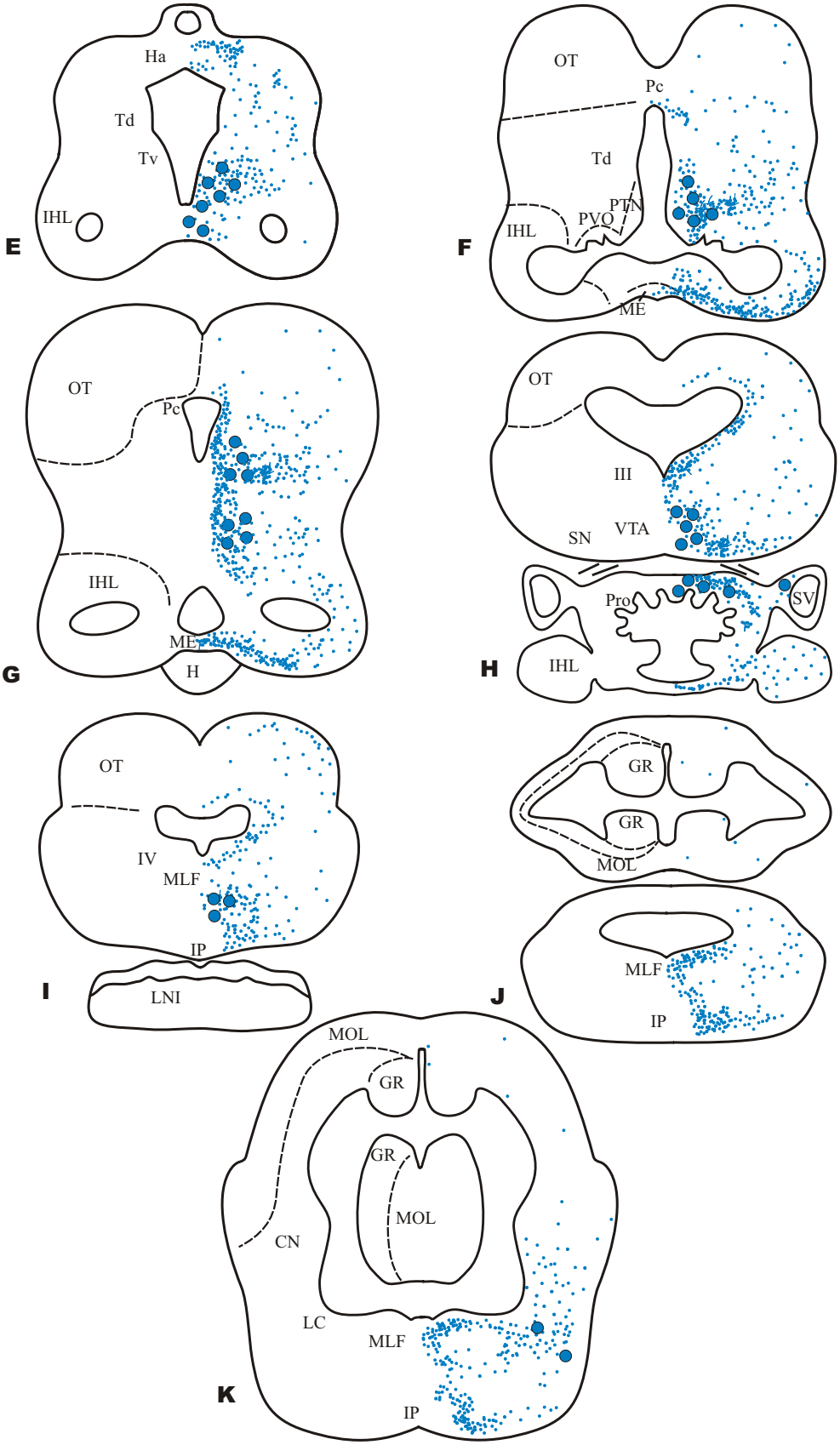
E
Ha
Td
Tv
IHL
F
OT
Pc
Td
PTN
PVO
IHL
ME
G
OT
Pc
IHL
ME
H
H
OT
III
SN
VTA
Pro
SV
IHL
I
OT
IV
MLF
IP
LNI
J
GR
GR
MOL
MLF
IP
K
MOL
GR
GR
MOL
CN
LC
MLF
IP

Fig. 7 (cont. I)

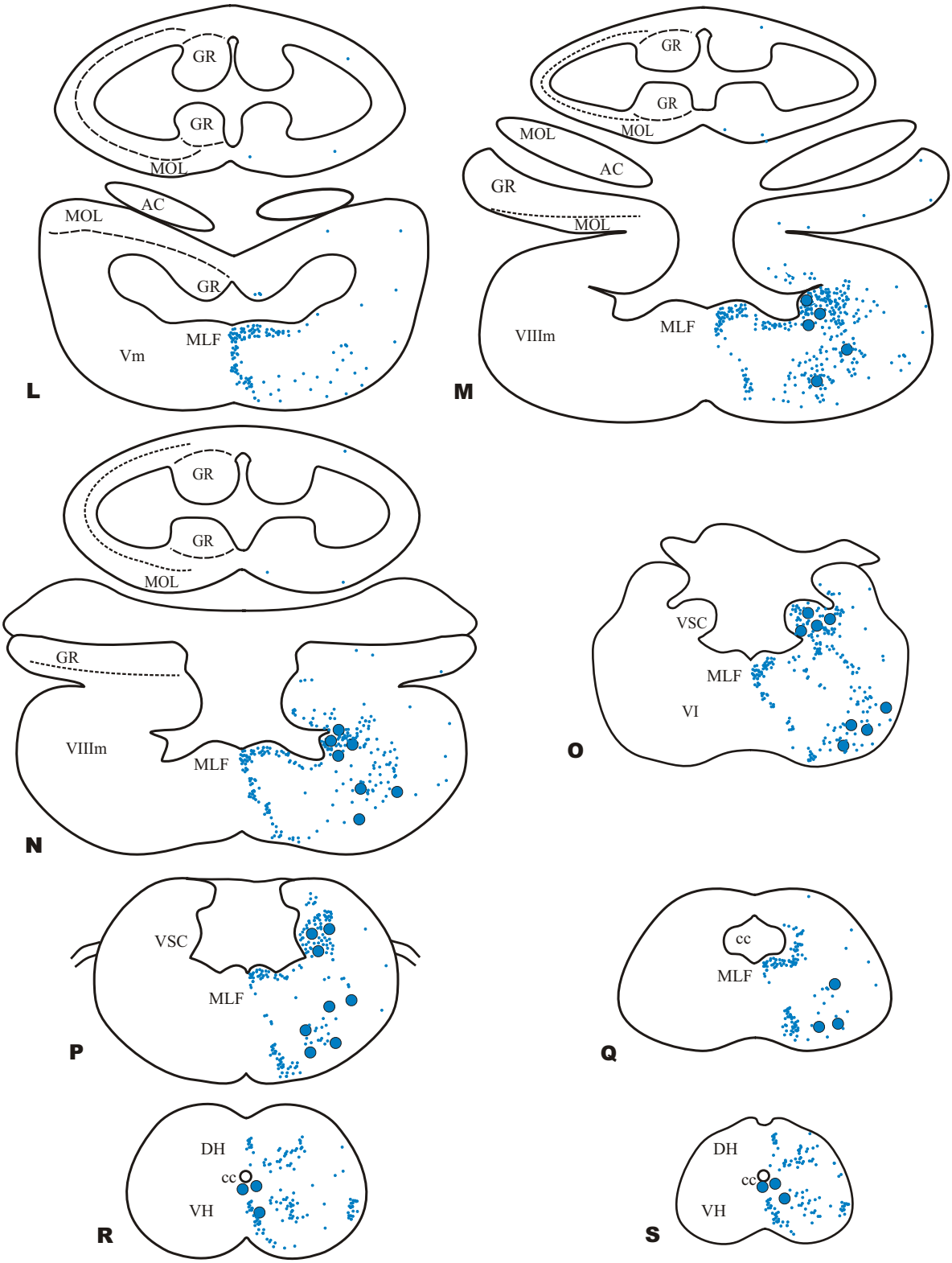
GR
GR
MOL
AC
MOL
GR
MLF
Vm
L
GR
GR
MOL
MOL
AC
GR
MOL
VIIIm
MLF
M
GR
GR
MOL
GR
VIIIm
MLF
N
VSC
MLF
VI
O
VSC
MLF
P
cc
MLF
Q
DH
cc
VH
R
DH
cc
VH
S

Fig. 7 (cont. II)

Figure 8. Transverse (**A-E,J-M**) and sagittal (**F-I,N**) sections throughout the brain of dogfish showing TH-ir cells and fibers in juveniles (**A-F,H,J,M**) and adults (**G,I,K,L,N**). **A.** Transverse section of the olfactory bulb to show numerous TH-ir cells (arrowheads) in the granular and glomerular cell layers. Note the intense TH-ir innervation at the all layers except in the olfactory fiber layer. **B.** Detail of the olfactory bulb to show numerous glomerular (arrow) and some periglomerular (arrowhead) TH-ir cells. **C.** Detail of the dorsal pallium showing numerous TH-ir neurons. **D.** Numerous TH-ir cells (arrowheads) at the lateral pallium of the juvenile telencephalon. **E.** A few TH-ir cells (arrowheads) in the juvenile subpallium. **F.** Sagittal section of the rostral diencephalon to show some probably ascending TH-ir fiber tract (arrowheads) coursing between the TH-ir diencephalic cell groups (SCN, Tv and PTN) and the telencephalon, below the TH-ir cells of the preoptic area (arrow). **G.** Sagittal section showing TH-ir longitudinal fibers (arrowheads) coursing between the diencephalic TH-ir cell groups and the subpallium. **H.** Sagittal section showing both rVTA (black arrow) and cVTA (white arrow) TH-ir cell groups in juveniles. Note the fasciculus retroflexus between them. **I.** Sagittal section of the diencephalon showing the close aggregation of the main diencephalic TH-ir cell groups. Note the dense TH immunoreactivity at the PTN. **J.** TH-ir longitudinal fibers (arrowheads) coursing between the PTN and the synencephalon. **K.** Transverse section of the synencephalon to show the medial (rVTA) and the lateral (SN) TH-ir cell groups. Note the lateral TH-ir processes that extend between both groups. **L.** Transverse section to show TH-ir cells of both rVTA and cVTA cell groups. Note TH-ir thick prolongations (arrowhead) coursing radially and vertically through the midline. **M.** Transverse section to show the TH-ir cells (arrowhead) of the LC cell group. Abundant TH-ir fibers (arrow) were seen in the periventricular area of the rostral rhombencephalic tegmentum. **N.** Detail of a sagittal section of the adult rostral rhombencephalon to show the TH-ir cells at the LC and Sc. For abreviations see list. Scale bars: 250µm (A,C,E-H,K-M); 50µm (B); 100µm (D,J,N); 500µm (I).

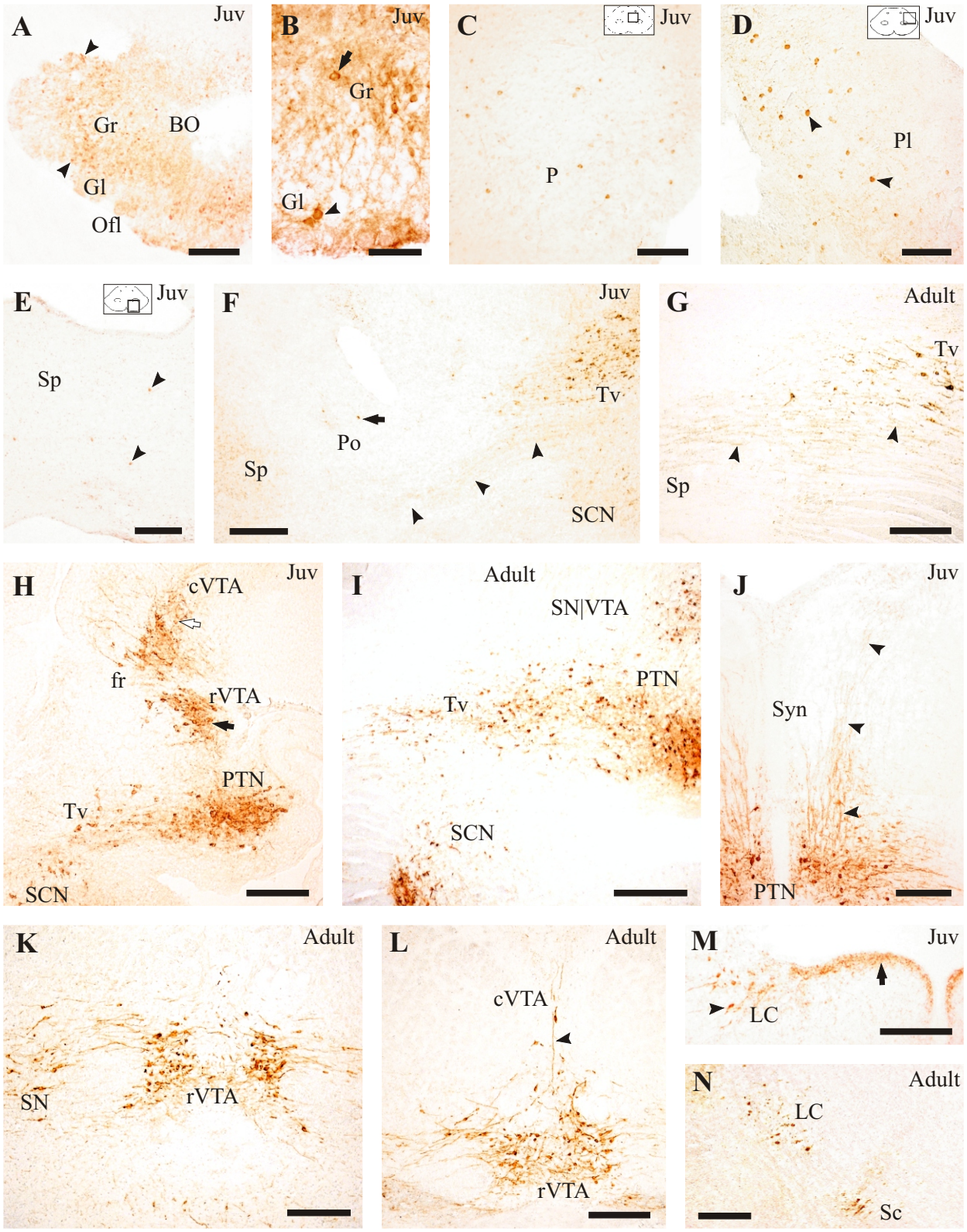
A
Juv
Gr
BO
Gl
Ofl
B
Juv
Gr
Gl
C
Juv
P
D
Juv
Pl
E
Juv
Sp
F
Juv
Tv
Po
Sp
SCN
G
Adult
Tv
Sp
H
Juv
cVTA
fr
rVTA
PTN
Tv
SCN
I
Adult
SN|VTA
PTN
Tv
SCN
J
Juv
Syn
PTN
K
Adult
SN
rVTA
L
Adult
cVTA
rVTA
M
Juv
LC
N
Adult
LC
Sc

Fig. 8

Figure 9. Transverse (**A-C,E,G-J**) and sagittal (**D,F**) sections throughout the brain (**A-I**) and spinal cord (**J**) of juveniles (**A,D-F,H,J**) and adults (**B,C,G,I**) showing TH-ir cells and fibers. **A.** Transverse section of the rostral rhombencephalon to show TH-ir cells (arrowheads) located dorsally and ventrally to the LC region. Note the absence of TH-ir innervation in the rostral cerebellum. **B.** Transverse section of the adult rhombencephalic showing a few TH-ir cells at the central grey area. Midline is to the right. **C.** Transverse section of the viscerosensory lobe to show the mature distribution of TH-ir cells (arrow) and intrinsic fibers (arrowheads). Note that the fiber density is higher than those cells. **D.** Sagittal section of the caudal rhombencephalon to show TH-ir cells (arrowheads) vertically oriented. **E.** Transverse section of the habenula showing a mass of TH-ir fibers (arrowheads) on the habenular dorsolateral nucleus and dorsolateral area. **F.** Sagittal section of the hypophysis to show the dense TH-ir hypothalamic-hypophyseal fiber tract (arrowhead) coursing between the hypothalamic floor and the hypophysis. Note the profuse TH-ir innervation of the hypophysis. **G.** Detail of the caudal hypothalamus to show TH-ir fibers coursing through the rostral walls of the saccus vasculosus. **H.** Transverse section of the juvenile optic tectum to show some TH-ir innervation at the periventricular layers (arrows). **I.** Transverse section at the rostral rhombencephalic tegmentum to show TH-ir fiber dorsal and medially to the medial longitudinal bundle (arrowheads). **J.** Transverse section of the rostral spinal cord showing numerous TH-ir CSF-c cells ventrally to the central canal (star) of juveniles. Note the absence of TH-ir fibers near the ventricle. For abreviations see list. Scale bars: 500µm (A); 100µm (B,C,F,G,H); 250µm (D,E,J,I).

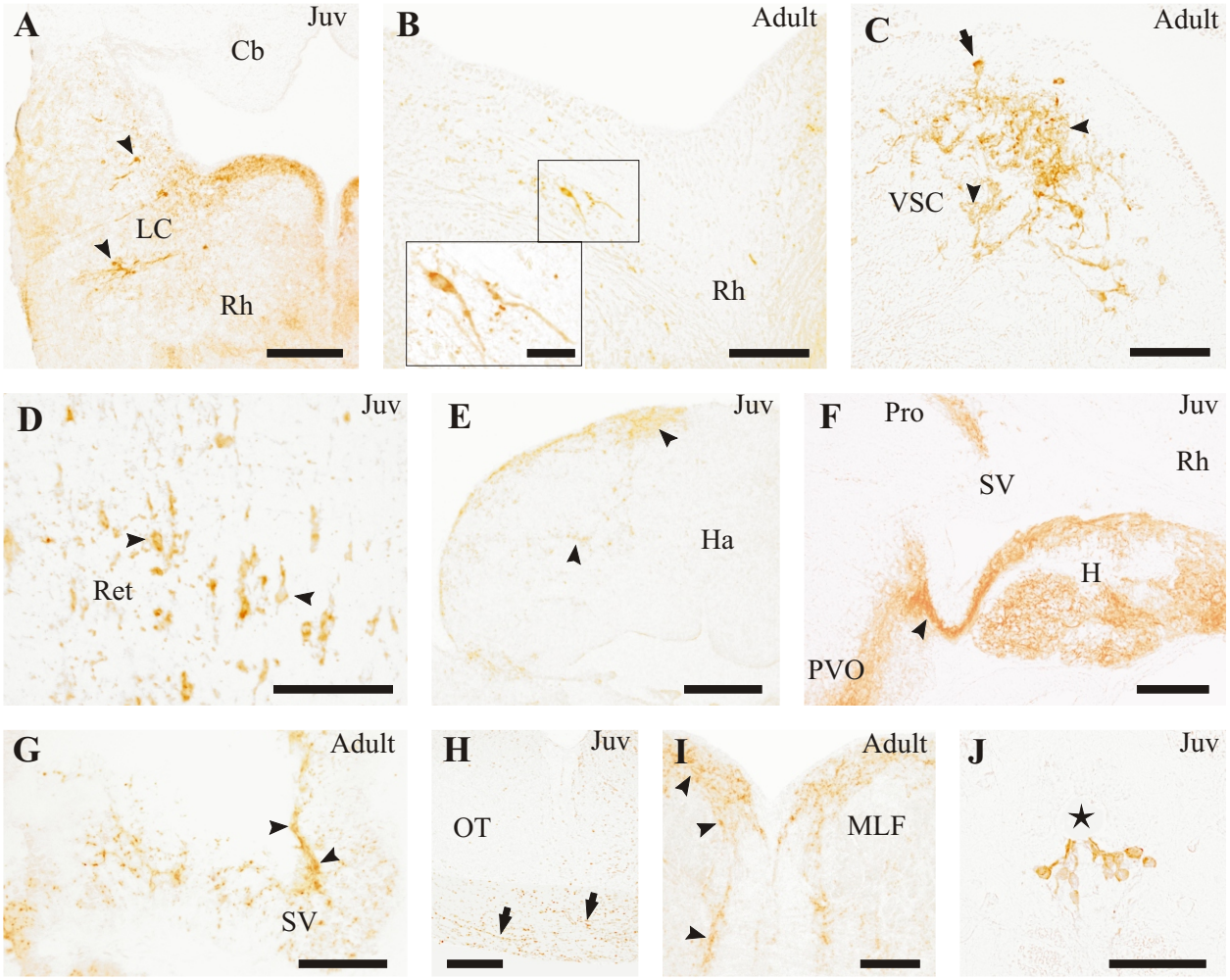
A
Juv
Cb
LC
Rh
B
Adult
Rh
C
Adult
VSC
D
Juv
Ret
E
Juv
Ha
F
Pro
Juv
Rh
SV
H
PVO
G
Adult
SV
H
Juv
OT
I
Adult
MLF
J
Juv

Fig. 9

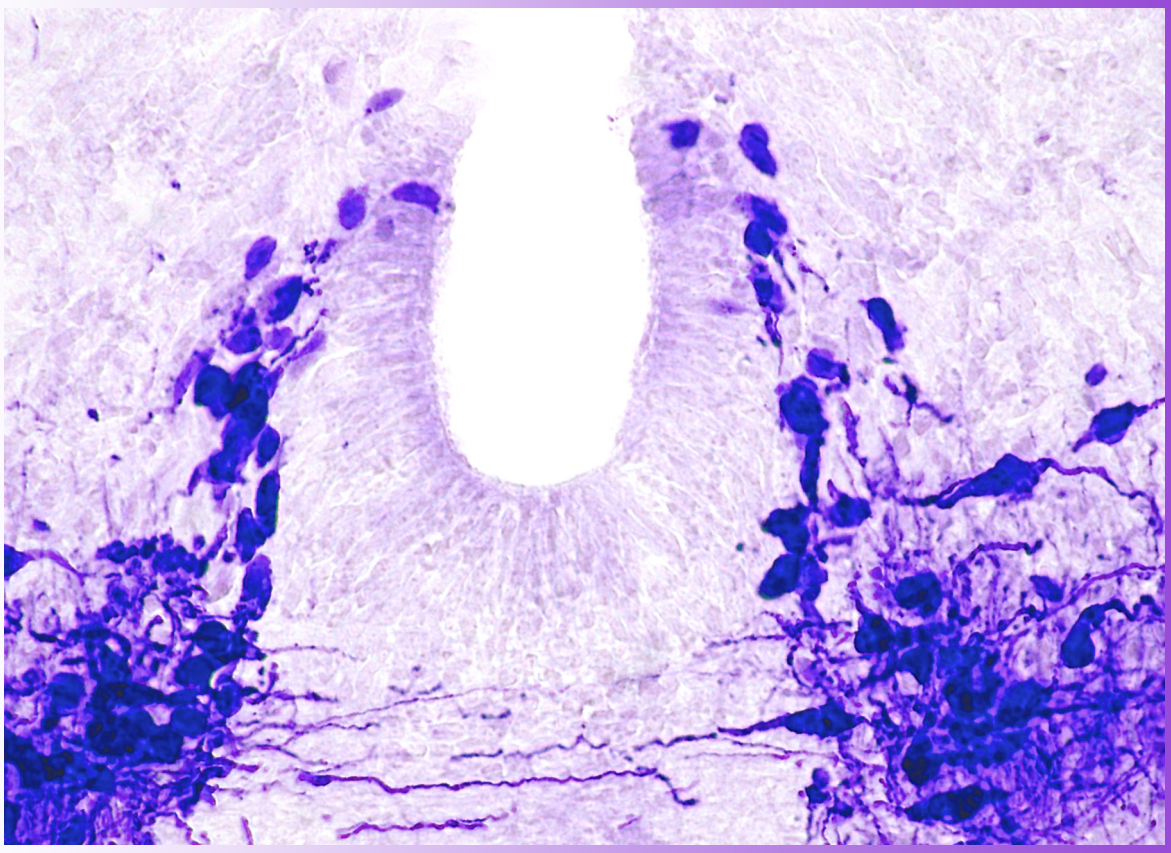

CAPÍTULO 3

Development of the Serotoninergic System in the Central Nervous System of the lesser-spotted dogfish (*Scyliorhinus canicula)*. An Immunohistochemical Study

CAPÍTULO 3

Development of the Serotoninergic System in the Central Nervous System of the lesser-spotted dogfish (*Scyliorhinus canicula)*. An Immunohistochemical Study

INTRODUCTION

Serotonin (5-hydroxytryptamine) is a ubiquitous neurotransmitter in the vertebrate central nervous system (CNS). It is synthesized from the amino acid tryptophan in two steps and released to the intercellular space by serotoninergic fibers, which probably act by "volume transmission". Serotonin (5-HT) affects many aspects of brain function including sensory processing, motor program execution, cognition, sleep and learning (for review, see van Kesteren and Spencer, 2003). The results of early morphological studies with formaldehyde-induced fluorescence (FIF) methods suggested that the distribution of serotoninergic groups in the brain is remarkably constant throughout vertebrate phylogeny (Parent et al., 1984). Sensitive immunohistochemical techniques for detecting 5-HT were introduced in the early 1980s and provided great detail about the serotoninergic structures of a number of vertebrate groups (*mammals*: Steinbusch, 1984; Hornung and Fritschy, 1988; *birds*: Sano et al., 1983; Sako et al., 1986; *reptiles*: Ueda et al., 1983; Smeets and Steinbusch, 1988; *amphibians*: Yoshida et al., 1982; Ueda et al., 1984; Fasolo et al., 1986; Corio et al., 1992; Clairambault et al., 1994; *chondrosteans*: Adrio et al., 1999; *teleosts*: Kah and Chambolle, 1983; Yoshida et al., 1983; Ekström and van Veen, 1984; Ekström and Ebbesson; 1989; Corio et al., 1991; Chiba and Oka, 1999; Rodríguez-Gómez et al., 2000; *chondrichthyes*: Ritchie et al., 1983; Yamanaka et al., 1990; Stuesse et al., 1990, 1991a,b, 1995; Stuesse and Cruce, 1991, 1992; *cyclostomes*: Steinbusch et al., 1981; Kadota, 1991; Pierre et al., 1992; Abalo et al., 2007). As a result, the adult serotoninergic system is one of

the best known neuronal systems from a comparative point of view. Studies in the CNS of adult Chondrichthyes (or cartilaginous fishes) have revealed that the serotoninergic populations of this group of fishes are roughly similar to those of teleosts, although differences in the distribution of serotoninergic neurons have been noted (Ritchie et al., 1983; Stuesse and Cruce, 1991, 1992; Stuesse et al., 1991a, b, 1995).

Developmental immunohistochemical studies have revealed that 5-HT is one of the earliest appearing neurotransmitters in the brain, as reported in birds and mammals (Lidov and Molliver, 1982a,b; Wallace and Lauder, 1983; Wallace, 1985; Sako et al., 1986; Lauder, 1990; Okado et al., 1992). The early appearance of 5-HT coincides with many differentiation and growth events. This has led to the proposal of roles for 5-HT as a signal molecule for neuronal development (Lauder, 1990), inducing and regulating neurogenesis and neuronal differentiation and affecting functions as diverse as cell division, migration, axonal growth, and synaptogenesis (Lauder, 1993; Whitaker-Azmitia et al., 1996; Petrova and Otellin, 2007). Moreover, during CNS development 5-HT is involved in the maturation of neuronal networks (Gaspar et al., 2003) and in the control of the ontogeny of other neurotransmitter systems (Allain et al., 2005). The development of serotoninergic systems has also been studied in amphibians (van Mier et al., 1986; Clairambault et al., 1994; Woolston et al., 1994), some teleosts (Ekström et al., 1985; Bolliet and Ali, 1992; Bolliet et al., 1994; Ekström, 1994; McLean and Fetcho, 2004a) and cyclostomes (Yáñez, 1992; Antri et al., 2006; Abalo et al., 2007). However, as far as we are aware there are no studies of the ontogeny of the serotoninergic system in cartilaginous fishes.

Chondrichthyes are currently considered the sister group of the Teleostomi, i.e. the group of jawed vertebrates with a bony skeleton that gave rise to land vertebrates, including mammals. Although this is a key group for understanding the early evolutionary history of vertebrates, developmental studies are still scarce. Knowledge of the development of neurotransmitter systems in Chondrichthyes is limited to a few studies of catecholaminergic and GABAergic systems in the lesser-spotted dogfish *Scyliorhinus canicula* (Sueiro et al., 2003, 2004; 2007; Carrera et al., 2005, 2006, 2008; Ferreiro-Galve et al., 2008). This dogfish species has also been used in studies of gene expression during very early brain development (Sauka-Spengler et al., 2001, 2003; Derobert et al., 2002a, b).

The aim of the present study was to investigate the temporo-spatial developmental pattern of the 5-HT-immunoreactive (ir) neurons and axonal pathways in the CNS of the lesser-spotted dogfish. A further aim was to compare the development of the 5-HT system in elasmobranchs with that of other vertebrate groups, to achieve a better understanding of the developmental evolution of this system. This study provides the first description of the development of the serotoninergic system in the CNS of an elasmobranch, revealing the appearance, migration and segmental organization of the serotoninergic cell groups, the growth of main ascending and descending 5-HT-ir tracts, and the establishment of the adult innervation pattern.

MATERIAL AND METHODS

Experimental animals

Embryos and juveniles of the lesser-spotted dogfish (*Scyliorhinus canicula*) were kindly provided by the "Aquário Vasco da Gama" and the "Oceanário" of Lisbon (Portugal) and the *Aquarium Finisterrae* (A Coruña, Spain). The embryonic stages were identified on the basis of their external features according to Ballard et al. (1993). The following stages of dogfish embryos were analyzed: stage 25 (S25, four pairs of open pharyngeal clefts; three embryos), stage 26 (S26, five pairs of open pharyngeal clefts, simple gill bars; three embryos), stage 27 (S27, diamond- shaped mouth and primordial gill filaments; three embryos), stage 28 (S28, transverse oval mouth, gills with external filaments; four embryos), stage 29 (S29, three embryos), stages 30 (S30 and S31, with a detectable rostrum and long branchial filaments in stage 31; four embryos of each stage), stage 32 (S32, regression of branchial filaments and initial eye pigmentation; five embryos), stages 33 and 34 (S33 and S34, prehatching; three embryos of each stage). Four small juvenile (between 9 and 12 cm in length) and five adult dogfish (40-60 cm total length; provided by a local fisherman) were also used. All procedures conformed to the guidelines established by the Spanish Royal Decree 223/1998 for animal experimentation and were approved by the ethics committee of the University of Santiago.

Tissue preparation

Embryos were anesthetized with 0.05% tricaine methane sulfonate (MS-222; Sigma, St. Louis, MO) in seawater, separated from the yolk and fixed by immersion in 4% paraformaldehyde in 0.1 M elasmobranch phosphate buffer at pH 7.4 (EPB: 0.1M phosphate buffer containing 670mM urea, pH 7.4). Adult and juvenile dogfish were deeply anesthetized with 0.05% MS-222 in seawater, then perfused intracardially with elasmobranch Ringer's solution (1.7 % NaCl, 0.024% KCl, 0.031% $CaCl_2$, 0.044% $MgCl_2$, 0.113% Na_2SO_4, 0.049% $NaCO_3H$, and 2.7% urea) followed by perfusion with the same fixative used for embryos (20 min). The brains and the cervical-pectoral spinal cord regions were then dissected out and immersed in the same fixative for 4 hours.

Embryos and brains and spinal cords of juvenile and adults were cryoprotected with 30% sucrose in phosphate buffer (PB), embedded in OTC compound (Tissue Tek, Torrance, CA) and frozen with liquid-nitrogen-cooled isopentane. Parallel series of sagittal and transverse (coronal) sections (14-18 μm thick) were cut on a cryostat and mounted on Superfrost Plus (Menzel-Glasser®) slides.

Immunocytochemistry

The sections were pretreated with H_2O_2 to eliminate endogenous peroxidase, rinsed twice in 0.05M Trizma-buffered saline containing 0.1% Tween-20 at pH 7.4 (TBS-T) (10-min each) and then incubated overnight with a rabbit polyclonal antibody against 5-HT coupled to bovine serum albumin with paraformaldehyde (DiaSorin, Stillwater, USA; code 20080, batch 051007; dilution 1:5,000). The sections were then successively rinsed in TBS-T (two 10-min rinses), incubated in goat IgG anti-rabbit (Dako, Glostrup, Denmark; 1:100) for 1 hour, rinsed in TBS-T (two 10-min rinses), and incubated in rabbit PAP complex (Dako, 1:100) for 1 hour. The immunoreaction was developed with 0.005% diaminobenzidine (DAB; Sigma St Louis, MO) and 0.003% H_2O_2. All dilutions were with TBS-T, and sections were always incubated in a humid chamber at room temperature. Finally, the sections were dehydrated and coverslipped.

The commercial 5-HT antiserum used was generated in rabbit with 5-HT coupled to bovine serum albumin with paraformaldehyde. The antiserum has previously been tested in several non-mammalian species, including fishes, and shows no cross reaction with other monoamines (Stuesse and Cruce, 1992; Marín et al., 1998; Adrio et al., 1999; Antri et al., 2006; Abalo et al., 2007). Moreover, the serotonin antiserum diluted 1/20,000 does not react with 5µM, 10µM and 25µM amounts of any of the following substances in the BSA/HRP labeling method: 5-hydroxytryptophan, 5-hydroxyindole-3-acetic acid or dopamine (technical information supplied by the manufacturer). As negative controls, the primary, secondary or tertiary antibodies were omitted. No immunostaining was observed in these control sections.

In order to compare the distribution of 5-HT-ir populations with that of tyrosine hydroxylase (TH)-ir neurons previously described in chapter 2. Series of sections of embryos and juveniles were processed for TH immunohistochemistry in parallel to the series used for 5-HT, following a procedure similar to previously indicated.

To compare the location of serotoninergic brainstem structures with that of cholinergic motor nuclei, some series of adult and juvenile brains were processed for double immunofluorescence with a cocktail of the anti-5-HT serum (dilution: 1:2,500) and a purified goat anti-ChAT serum (anti-human placental ChAT, code AB144P; batch 0510012059, Chemicon, Temecula, CA; dilution: 1:50). As secondary antibodies, a cocktail of rhodamine-labeled donkey anti-goat serum (DAG, code A-11058, Alexa, The Netherlands; dilution 1:20) and a fluorescein-labeled swine anti-rabbit serum (SAR, code F0205; batch 108, Dako, Glostrup, Denmark; dilution 1:30) was used. The sections were mounted with Vectashield (Vector, Burlingame, CA) and observed either with an Olympus fluorescence microscope or with a spectral confocal laser scanning microscope (Leica TCS-SP2). The anti-ChAT antiserum has been previously characterized in western blots of dogfish brain extracts, where it labeled protein bands similar to those labeled in rat brain protein extracts run in parallel (Anadón et al., 2000). For further details about the distribution of ChAT-ir neurons in the adult dogfish brain see Anadón et al. (2000).

Imaging

The sections were photographed with an Olympus microscope equipped with a color digital camera. The photographs were adjusted for brightness and contrast with Corel Photo Paint (Corel, Ottawa, Canada), and photos were composed with Corel Draw.

RESULTS

The chronological development of serotoninergic neuronal groups in the dogfish CNS is summarized in Table I. The first serotonin-immunoreactive (5-HT-ir) cells appeared in the rostral rhombencephalon at S26. At S28, 5-HT-ir cells occupied the anterior half of the brainstem (superior reticular formation) and first appeared in the spinal cord. From early S29, 5-HT-ir cells extended throughout the posterior half of the brainstem (inferior reticular formation). In the diencephalon, hypothalamic 5-HT-ir cell groups were first observed at S31 whereas in the preoptic area the first 5-HT-ir cells differentiated at a later stage (S33). Transient serotonin expression was observed in the pretectum (S32 to juvenile), pineal organ (S31) and habenula (S34). All the serotoninergic cell groups observed in post-embryonic stages (juveniles and adults) were already recognized in S33. This "mature"-type organization was characterized by the presence of few 5-HT-ir neurons in the preoptic area and abundant labeled cells in the hypothalamus [paraventricular and posterior recess organs, following the nomenclature of Meurling and Rodríguez (1990)] and in the reticular formation, where two main 5-HT-ir raphe (medial) cell groups (superior and inferior raphe groups), and two main 5-HT-ir reticular (lateral) cell groups (superior and inferior reticular groups, each with several subgroups) were distinguished. Moreover, 5-HT-ir neurons were present in the ventral and lateroventral walls of the spinal cord. 5-HT-ir neurons of cerebrospinal fluid-contacting (CSF-c) type were observed in the preoptic area, hypothalamus and rostral rhombencephalon. The first 5-HT-ir fibers were observed at S26, and the main ascending and descending serotoninergic pathways were established at S31. By

S32, a large number of branched fibers and terminals appeared in most brain regions, which represents the beginning of an active phase of maturation of the serotoninergic system. The distribution of 5-HT-ir fibers in S33 was similar to that observed in juveniles and adults and represents the "mature"-type innervation pattern characterized by highly dense 5-HT-ir fibers in the hypothalamus and rhombencephalic tegmentum, moderately dense fibers in the telencephalic hemispheres and preoptic area, and a low density of the fibers in the olfactory bulbs, optic tectum and cerebellum.

Distribution of 5-HT-ir cells and fibers during embryonic development

The distribution of 5-HT-ir cells and fibers in the CNS of the developing dogfish is schematically represented in Fig. 1. The 5-HT-ir cell groups of the reticular formation were tentatively related to the segmental (rhombomeric) organization of the rhombencephalon described by Kuratani and Horigome (2000) in a closely related species (*Scyliorhinus torazame*), using cranial nerves as recognizable landmarks.

Stages 26-28 (S26-S28)

No 5-HT-ir structures were observed in the CNS of embryos at stages earlier than S26. At this stage, a few 5-HT-ir neurons appeared in the ventral midline of the rostral rhombencephalic tegmentum (isthmic level) and extended to the rostral level of the trigeminal nerve root (V), probably corresponding to the extension of rhombomeres 1 and 2. These 5-HT-ir cells were located on either side of the floor plate to form two longitudinally elongated groups (Figs. 1A, 2A-C) and were weakly stained and loosely packed. A few thin 5-HT-ir fibers were observed close to these 5-HT-ir cells in the ventrolateral region of the rostral rhombencephalon. The distal end of fibers (growth cones) showed a small dilatation where thin spike-like processes were sometimes appreciable. These ascending 5-HT-ir fibers did not extend beyond the isthmus. Some descending 5-HT-ir fibers coursed to the caudal rhombencephalon (obex level) running laterally to the floor plate (Fig. 2D). As in ascending fibers, a typical growth cone was often observed in the leading process.

At S27, no 5-HT-ir cells were observed caudal to the level of the trigeminal nerve root (Figs. 2E,F). However, at S28 the density of 5-HT-ir neurons was notably higher than in previous stages (Fig. 1B, 2G), and 5-HT-ir cells were observed beyond the exit of the trigeminal nerve (Fig. 2H). No 5-HT-ir cells were observed in the caudal rhombencephalon, where descending 5-HT-ir fibers with growth cones were clearly visible (Fig. 2I). In addition, weak 5-HT-ir cells were first observed in the ventral walls of the rostral spinal cord (Fig. 1B).

Stages 29-30 (S29-S30)

From early S29, 5-HT-ir cells extended along the rhombencephalon, from the isthmus to the obex region (Figs. 2J-O). Although 5-HT-ir cells formed a continuous longitudinal column, there was a marked decrease in the density of the medial (rapheal) 5-HT-ir cells at the level of the acusticofacial (VII-VIII) nerve entry (Fig. 2M). The diminishing density of 5-HT-ir cells observed at this level enabled identification of the possible boundary between the superior and inferior 5-HT-ir rhombencephalic groups. At this stage, four superior and three inferior raphe nuclei, and two superior and one inferior reticular groups were distinguishable. The nomenclature used here to describe 5-HT-ir reticular groups follows that employed by Stuesse and colleagues in adults of several elasmobranch species (Stuesse et al. 1991b, 1995; Stuesse and Cruce, 1992). For correspondence with other nomenclatures used in adult elasmobranchs, see Table II.

The most rostral rhombencephalic 5-HT-ir neurons were located at both sides of the midline forming the primordial raphe *linearis* (Fig. 2J). Their large round somata were strongly stained, and their processes were directed dorsoventrally and rostrocaudally, and some of them crossed the midline. These rapheal cells seemed to have migrated from the ventricular zone just lateral to the floor plate. Dorsally to this population, small 5-HT-ir cells with their somata located in the ependyma or subependimarily displayed a characteristic dendritic process contacting the CSF. We have called this serotoninergic CSF-c cell group as the primordial raphe *dorsalis anterioris* (Fig. 2J). From this origin, 5-HT-ir cells appeared to migrate ventrally to form the rapheal cell groups located at both sides of the floor plate. Some of these apparently migrated 5-HT-ir cells extended a long lateral process parallel to

the ventral surface, with a growth cone-like ending, being probably the origin of the lateral reticular 5-HT-ir cell group observed latter at this level (primordium of the B9 group). This 5-HT-ir reticular group was located laterally to the raphe *linearis* at the same rostral level, representing the rostralmost superior reticular group (Fig. 2J). More caudally, the rostral rhombencephalon contained abundant large 5-HT-ir cells that occupied the midline and probably correspond to the primordium of the caudalmost superior raphe group, the r. *centralis superioris*. Dorsally to it, a few faintly stained 5-HT-ir cells located at the subependymal zone were seen extending long processes ventrally, coursing from the ventricular zone to the ventral rapheal group following a conspicuous migration route, and being the probable origin of the reticular formation groups at this level. From the medial 5-HT-ir cell groups, some large 5-HT-ir cells that extended long lateral guiding processes might represent the primordia of the 5-HT-ir reticular *pontis oralis* nuclei (Figs. 2K-L). These primordial reticular 5-HT-ir cells had intensely stained fusiform perikarya and long thick processes, and appeared to be migrating laterally from the raphe through two different pathways, intermediate and ventral. At this level, some large round 5-HT-ir cells were seen invading the floor plate, which probably represents a contralateral cell migration process noted initially by the growth of processes towards the contralateral side (Fig. 2J), followed by the perikarya that finally appeared to cross the midline (Fig. 2K). At levels rostral to the trigeminal nerve exit, small 5-HT-ir oval cells were located medially just ventral to the ventricle and probably correspond to the primordium of the raphe *dorsalis* (Fig. 2L).

The primordia of the inferior raphe 5-HT-ir cell groups were observed in the caudal rhombencephalon from the level of the acusticofacial nerve entry (characterized by a huge decrease in density of 5-HT-ir cells by comparison with the rostral groups, Fig. 2M) to the obex. Large round 5-HT-ir cells were located ventrally, which probably correspond to the primordium of the raphe *magnus* (Fig. 2N), whereas scattered small 5-HT-ir oval-shaped perikarya were observed ventrally and dorsally on both sides of the midline of the caudal rhombencephalon, which may correspond to the primordia of the raphe *pallidus* (ventrally) and raphe *obscurus* (dorsally), respectively (Fig. 2O). Some 5-HT-ir oval neurons with lateral processes located laterally and ventrolaterally along the midcaudal rhombencephalon probably represent the primordium of the reticular *magnocellularis* nuclei (Fig. 2N). At this

embryonic stage, there were far less reticular (lateral) serotoninergic cells than raphe cells. From S29, intensely labeled 5-HT-ir neurons were observed in the ventral margin of the rostral spinal cord (Figs. 2P,Q). Some of these 5 HT-ir neurons extended a process toward the ependyma (Fig. 2Q).

From the rhombencephalon, ascending 5-HT-ir fibers coursed ventrally along the ventrolateral margin of the mesencephalic tegmentum and synencephalon (Fig. 2G) to diencephalic levels, where a few 5-HT-ir fibers reached the posterior tubercle. Descending longitudinal 5-HT-ir tracts could be followed along the ventrolateral regions of the rhombencephalon to the spinal cord. Here, most of the descending 5-HT-ir fibers of rhombencephalic origin formed a small tract just lateral to the dorsal horn primordium that extended progressively to more caudal spinal levels (Fig. 2P).

Stage 31 (S31)

The S31 was characterized by the notable lateral extension of brainstem serotoninergic cell groups (reticular), the appearance of 5-HT-ir cells in the hypothalamus and pineal organ, and the rostral progression of the main ascending 5-HT-ir fiber tracts to the telencephalon (Figs. 1C, 3A-H, 4). The number of 5-HT-ir cells increased notably in the rhombencephalon (Figs. 1C, 3A), which was coincidental with an increasing proportion of lateral (reticular) *vs.* medial (raphe) 5-HT-ir cells. 5-HT-ir cells of the most lateral reticular cell groups, the subcoeruleus and the gigantocellularis, were first recognizable at this stage.

In the hypothalamus, a few 5-HT-ir cells with moderately stained ventricular dendrites were observed in the posterior recess walls and in the dorsal infundibular walls (primordia of the posterior recess and paraventricular organs, respectively) (Fig. 3D). The 5-HT-ir cells of the posterior recess organ primordium were more abundant and more strongly immunoreactive than those of the paraventricular organ primordium. A few faintly stained 5-HT-ir cells were observed in the pineal organ, mainly in its distal part (Fig. 3G). The distribution of 5-HT-ir neurons in the spinal cord was similar to that observed in the previous stage, and the neurons were located along the ventral midline (Fig. 3I).

The number of ascending fibers increased considerably at this stage, and they formed a loose but conspicuous longitudinal pathway that coursed along the mesencephalon and

diencephalic levels (synencephalon and posterior tubercle) to finally reach the telencephalon (Figs. 3A-H, 4). From the caudal diencephalon, this longitudinal tract gave rise to a few collateral branches running transversely to the brain longitudinal axis. One ventral branch coursed in the posterior tubercle and crossed the midline between the primordia of the inferior and posterior hypothalamic lobes (Fig. 4). Other transverse fibers ascended either diffusely through the pretectal region towards the posterior commissure or followed the fasciculus retroflexus toward the habenula forming a clearly defined thin tract (Figs. 3B,C, 4). Some 5-HT-ir fibers crossed the posterior commissure and abundant 5-HT-ir fibers coursed longitudinally throughout the lateral thalamic walls (Figs. 3B,C,H). Along the postoptic region, the main longitudinal 5-HT-ir pathway gave rise to fibers that course toward the ventral region of the tuber (Figs. 3D, 4). Finally, in the postoptic region it gave rise to a conspicuous "transverse" tract with numerous 5-HT-ir fibers (Fig. 3E, 4) that entered the caudal telencephalon ventrally (telencephalic peduncle) to innervate the subpallium. From this basal telencephalic region, some 5-HT-ir fibers grew rostrodorsally surrounding the anterior aspect of the telencephalon and ascended to the pallium primordium through the thin marginal region (Fig. 4). They innervated progressively more dorsal and dorsocaudal pallial regions. A few 5-HT-ir fibers diverged laterally from the telencephalic peduncle, and coursed through the border between the pallium and subpallium, which was distinguishable by a subtle external groove (the lateral palliosubpallial sulcus; Fig. 3F). All of these ascending pathways were conspicuous before pathways from prosencephalic 5-HT-ir populations had developed, which indicated that they arose from rhombencephalic 5-HT-ir populations. The straight course of these 5-HT-ir fibers, the absence of fiber branching outside the tract branching regions, and the presence of terminal bulbous dilatations (growth cones) in many fibers reveal that this phase of tract formation precedes the establishment of the innervation pattern characteristic of specific brain centers. Descending longitudinal 5-HT-ir tracts were also observed from the brainstem to caudal regions of the spinal cord (Fig. 4), gathered in small tracts that occupied the marginal layer of the lateral lower two-thirds (Figs. 3I,J). This longitudinal tract was denser than in previous stages. Clear distinction between fibers of spinal and rhombencephalic origins was not possible, although those arising from spinal cells probably coursed through ventral regions.

Stage 32 (S32)

The serotoninergic system of this stage was characterized by the differentiation of the first 5-HT-ir cells in the pretectum, the progressively increasing density of 5-HT-ir cells in the reticular formation, the arrival of first 5-HT-ir fibers to the olfactory bulbs and the differential distribution of immunoreactive fibers in the pallium and subpallium (Figs. 5A-E), which represents the beginning of the maturation of the serotoninergic innervation in the prosencephalon. In the olfactory bulbs, the few 5-HT fibers observed were mainly distributed in the glomerular layer (Fig. 5A). In the telencephalic hemispheres a moderate amount of 5-HT-ir fibers coursed between the lateral pallium and the dorsal pallium pars superficialis, whereas 5-HT-ir fibers moderately innervated the medial pallium (Fig. 5B). At caudal pallial levels the density of 5-HT-ir decreased considerably. In the subpallium, a high density of 5-HT-ir fibers was observed in the marginal zone of the basal superficial area and the septal region (Fig. 5C), whereas the moderate 5-HT-ir innervation of the area periventricularis ventrolateralis and area centralis superficialis was in contrast with the very scarce innervation of most of the basal superficial area (Fig. 5C).

In the pretectal region, faintly stained 5-HT-ir cells were observed medially surrounding the fasciculus retroflexus in its proximal part and also more laterally (Fig. 5D). The 5-HT-ir CSF-c cells were considerably denser in the posterior recess organ and the dorsal walls of the paraventricular organ than in previous stages. These hypothalamic regions showed very rich serotoninergic innervation. From this stage onwards a few thin beaded serotoninergic fibers were observed in the saccus vasculosus walls (Sueiro et al., 2007). Interestingly, some 5-HT-ir fibers were observed in the optic chiasm and throughout the optic nerve (Fig. 5E). Varicose 5-HT-ir fibers sparsely innervated the lateral nucleus of the left habenula whereas moderate innervation was observed in the subcommissural organ. In this stage, 5-HT-ir cells were not observed in the pineal organ, but 5-HT-ir fibers were observed throughout its stalk, especially in the proximal region.

Stages 33- 34 (S33-S34 prehatching)

The distribution of 5-HT-ir cells and fibers in these late embryos (Fig. 1D) was similar to that observed in post-embryonic stages (see description of juveniles and adults),

although the density of 5-HT-ir fibers increased with development (Figs. 5F-K). From S33, 5-HT-ir cells were observed in the ventricular walls of the preoptic area and most were CSF-contacting cells (Fig. 5I). No 5-HT-ir cells were observed in the pineal organ, but its 5-HT-ir innervation was moderate (Fig. 5J), as in the habenula, the subcommissural organ and the posterior commissure. In the brainstem, double immunofluorescence (ChAT/5-HT) was used to compare the location of several cranial nerve nuclei with the reticular formation groups of S33 and juveniles. Results of these experiments confirmed the segmental distribution of the several reticular formation nuclei observed in the previous developmental stages by their relative locations with respect to the cranial motor nuclei (results not shown).

In S34 embryos, a few round or oval-shaped 5-HT-ir neurons were observed in both habenulae showing moderate to weak immunoreactivity (Fig. 5K). The density and intensity of staining of the 5-HT-ir pretectal cells were less than in the previous stage. The number of migrated lateral (reticular) 5-HT-ir cells was considerably higher than in previous stages especially at isthmic levels, where the 5-HT-ir reticular neurons of the B9 group occupied a ventromedial position. From S33, 5-HT-ir neurons in the spinal cord were located in the ventral and ventromedial margins throughout its entire length.

5-HT-ir fibers and terminals were widely distributed in all layers of the olfactory bulbs, but were scarce in the glomerular layer (Fig. 5F). In the supballium, the most highly 5-HT-ir innervated regions were the marginal zone of the basal superficial area, the septum, the area centralis superficialis, the area periventricularis ventrolateralis and the lateral region at the palliosubpallial border (Fig. 5G). In the pallium, dense fields of 5-HT-ir fibers and terminals were observed at the medial pallium and dorsal pallium pars superficialis (Fig. 5H). In prehatching embryos, 5-HT-ir fibers first innervated the optic tectum, particularly the medial inner layers and the cerebellum, where some 5-HT-ir fibers were observed crossing the midline in the intracerebellar commissure and innervating the granular layer and the inner region of the cerebellar peduncle. 5-HT-ir fibers were observed throughout the entire length of the mesencephalic tegmentum and basal rhombencephalon, although the most densely innervated region was the dorsal part of the viscerosensory lobe. From the level of the obex to the half length of the spinal cord, longitudinal 5-HT-ir fibers were also located dorsally to

the central canal, although their density decreased caudally. These 5-HT-ir fibers coursed along the ventrolateral, lateral and commissural areas.

Distribution of 5-HT-ir cells and fibers in juveniles and adults

Telencephalon

5-HT-ir cells. No immunoreactive cells were observed in the telencephalon of juveniles and adults.

5-HT-ir fibers. Wide regions of the telencephalon of juveniles and adults contained a network of thin beaded 5-HT-ir fibers, but in the olfactory bulb only a moderate amount of 5-HT-ir fibers was observed in the granule cell layer whereas these fibers were very scarce in the glomerular layer and lacked from in the olfactory fiber layer (Figs. 6A, 7A). In the telencephalic hemispheres the density of 5-HT-ir fibers was higher in the subpallium than in the pallium (Figs. 6A-C, 7B-D). In the pallium, the serotoninergic innervation was moderate to dense in the dorsal pallium pars superficialis (Fig. 7B) and medial pallium, and scarce to moderate in the lateral pallium. 5-HT-ir fibers and boutons were particularly dense at the pallial/subpallial border (the region ventral to the lateral pallium and dorsolateral to the basal superficial area; Figs. 6B,C, 7C). Moderate to dense serotoninergic innervation was observed in some subpallial areas such as the septal region, the area periventricularis ventrolateralis and the basal superficial area (Figs. 6B,C, 7C,D). The striatum and the area centralis superficialis showed a low to moderate density of 5-HT-ir fibers, which was in sharp contrast with the high density observed in embryos. Although the organization of serotoninergic fibers was basically similar in juveniles and adults, the density of 5-HT-ir fibers in the marginal region of the basal superficial area and area periventricularis ventrolateralis of juveniles was higher than in adults.

Preoptic area

5-HT-ir cells. From a level just caudal to the anterior commissure some 5-HT-ir CSF-c cell bodies were observed in the ventrolateral walls of the preoptic area (Figs. 6D,

7E). They were in ependymal or subependymal location and their basal processes emerged either perpendicular or parallel to the ventricle (Fig. 7E).

5-HT-ir fibers. Abundant 5-HT-ir fibers coursed in the medial forebrain bundle, while the remaining regions of the preoptic area showed a moderate density of 5-HT-ir fibers (Fig. 6D).

Hypothalamus and posterior tubercle

5-HT-ir cells. In the hypothalamus, the highest density of 5-HT-ir neurons was observed in a continuum of circumventricular organs that extended caudally from the dorsolateral infundibular walls to the walls of the posterior recess (Figs. 6E-H, 7F). Most of the 5-HT-ir neurons in these organs were CSF-c cells, densely grouped with their somata located at ependymal and subependymal levels. A few non-CSF-c 5-HT-ir cells were also observed in periependymal location. Fewer 5-HT-ir CSF-c neurons were observed in the smooth dorsal walls of the lateral recess organ (Figs. 6F,G, 7G).

5-HT fibers. The highest density of 5-HT-ir fibers was observed in the dorsal region of the paraventricular organ and in the outer neuropil of the posterior recess organ (Fig. 7F). The 5-HT-ir innervation was moderate to dense in the external region of the inferior hypothalamic lobes, and moderate to weak in the internal region (diffuse nucleus) of these lobes (Figs. 6F-H, 7F) and in the posterior tubercle. Serotoninergic fibers ran along the hypothalamic floor (Figs. 6E-H, 7F) and were moderately abundant in the median eminence (Figs. 6F,G, 7H). A few 5-HT-ir fibers were observed in the caudal part of the neurointermediate lobe (Figs. 6I, 7I).

Epithalamus

5-HT-ir cells. No 5-HT-ir cells were observed in the epithalamus of juveniles and adults.

5-HT-ir fibers. Dense 5-HT-ir innervation was observed in the habenula, and these fibers were mainly located at the laterodorsal region (Figs. 6E, 7J). Abundant 5-HT-ir fibers coursed in the habenular commissure and in the pineal organ of juveniles (Figs. 6E, 7J,K), but they were scarce in adults. A few 5-HT-ir fibers coursed in the posterior commissure

(Figs. 6F, 7L). In juveniles, some thin 5-HT-ir fibers were observed among the epithelial cells of the subcommissural organ and even reached the ventricle (Figs. 7L,M), although these fibers were not observed in adults.

Thalamus and pretectum

5-HT-ir cells. In juveniles, occasional 5-HT-ir cells were observed surrounding the fasciculus retroflexus ventrally in its proximal part (Fig. 7L), though not in adults.

5-HT-ir fibers. The 5-HT-ir innervation was scarce in the dorsal thalamus and moderate in the ventrolateral thalamus (Figs. 6E,F).

Mesencephalon and rhombencephalon

5-HT-ir cells. No 5-HT-ir cells were observed in the mesencephalic tegmentum, although numerous 5-HT-ir cell groups were observed in the reticular formation of the rhombencephalon (Figs. 6H-Q, 8A-G). In the isthmus and almost the entire basal rhombencephalon, 5-HT-ir neurons were observed in medial (raphe) and lateral (reticular) populations (Figs. 6H-Q, 9, 10). 5-HT-ir cells were observed throughout the entire extension of the rhombencephalic tegmentum, except between the caudal level of the trigeminal motor nucleus and a level rostral to the facial motor nucleus (Fig. 6N, see also 8D). This represents an anatomical separation between the superior and inferior raphe and reticular nuclei. Four superior and three inferior raphe nuclei, and four superior and two inferior reticular groups were identified in dogfish juveniles and adults, as previously described in embryos. The position of serotoninergic nuclei of the brainstem was assessed in relation to that of ChAT-immunoreactive motor nuclei described in *S. canicula* by Anadón et al. (2000). The serotoninergic reticular nuclei of the dogfish showed an apparent segmental pattern and the relation with the cholinergic motor nuclei and rhombomeres is shown in Figs. 9 and 10.

<u>*Superior raphe nuclei*.</u> Two raphe serotoninergic groups were distinguished in the isthmus, caudal to the oculomotor nucleus and dorsal to the interpeduncular nucleus. The dorsalmost is the raphe *dorsalis anterioris* (RaDa) that was formed by 5-HT-ir cells scattered in medial subependymal layers, some of them sending a thin process directed to the ventricle (Figs. 6H,I, 8A). Ventrally to it is the raphe *linearis* (RaL), which was located

on both sides of the midline forming a longitudinal band that extends more caudally than the RaDa: (Figs. 6H,I). It consists of strongly stained 5-HT-ir cells with round or oval somata with a major process that extended dorsoventrally (Fig. 8B). From the caudal level of the interpeduncular nucleus to the level of the trigeminal motor nucleus, 5-HT-ir cells were sparsely distributed close to the midline representing the raphe *centralis superioris* (RaC; Figs. 6J-M). Most of them were bipolar cells with the most prominent process coursing ventrolaterally (Fig. 8C). The raphe *dorsalis* (RaD) was found in the central gray coextensive with the midcaudal extension of the trigeminal motor nucleus (Fig. 6L), and contained weakly 5-HT-ir oval cells located dorsolaterally to the medial longitudinal fascicle.

Superior reticular nuclei. Scattered reticular 5-HT-ir cells were observed in the rostral rhombencephalic tegmentum lateral to the interpeduncular nucleus and to the rostral extension of the raphe *linearis* (Figs. 6H,I, 8B). This reticular group corresponds with the B9 group described in other elasmobranchs (Table II). Other three 5-HT-ir cell groups that correspond with the reticular *subcoeruleus* (RSc), reticular *pontis oralis lateralis* (ROL), and reticular *pontis oralis medialis* (ROM) were recognized between the caudal level of the trochlear nucleus and the level of the exit of the trigeminal nerve (Figs. 6J-L, 8C). The correspondence of these groups with those reported in other cartilaginous fishes is indicated in Table II. The RSc was located ventrally to the TH-immunoreactive cells of the *locus coeruleus* (Carrera et al., 2005), and consists of scattered round cells (Figs. 6K, 8C). Ventral to the RSc, the 5-HT-ir fusiform cells of the ROL exhibiting obliquely oriented processes were observed (Figs. 6J-L, 8C). Lateral to the interpeduncular nucleus, a different 5-HT-ir reticular group, the ROM, was identified by their round and moderately stained somata with horizontally oriented processes (Figs. 6J-L, 8C).

Inferior raphe nuclei. From postrigeminal levels to the obex, 5-HT-ir raphe populations displayed triangular, multipolar and fusiform somata and vertically oriented processes, and formed a longitudinal band on both sides of the midline. Three inferior raphe nuclei were recognized on the basis of differences in position and size. The rostralmost was the raphe *magnus* (RaM; Fig. 6O), which extended to the rostral level of the viscerosensory column (Fig. 8E). Their somata were located close to the midline and were larger than those of the

other inferior raphe groups. Caudal to this group, two clusters of moderately stained 5-HT-ir cell bodies formed the raphe *obscurus* (RaO, dorsally) and raphe *pallidus* (RaP, ventrally; Figs. 6P,Q, 8F,G). At caudal rhombencephalic levels these two raphe groups merged and only one group was apparent (Figs. 6Q, 8G).

Inferior reticular nuclei. The inferior reticular groups displayed moderate 5-HT-ir fusiform cells with processes that extended transversely through the caudal rhombencephalon parallel to its ventral margin. Some of them occupied a lateral position and formed the reticular *magnocellularis* (RM; Figs. 6O-Q, 8G), whereas the other group was located ventrolaterally and showed more intense 5-HT immunoreactivity, corresponding to the reticular *gigantocellularis* (RG; Figs. 6O-Q, 8G). No ventral reticular group was observed at the obex level corresponding with the reticular *magnocellularis ventralis* reported in some elasmobranchs (Stuesse et al., 1990, 1991a, b; Stuesse and Cruce, 1991, 1992).

5-HT-ir fibers. In the optic tectum, weak to moderate 5-HT-ir varicose fibers were observed in all layers, although the most densely innervated were the *stratum medullare externum* and the *strata cellulare* and *medullare internum* (Figs. 6F-I, 8H).

Most regions of the mesencephalic tegmentum of juveniles displayed moderate to dense 5-HT-ir innervation, whereas few 5-HT-ir fibers were observed in the oculomotor nucleus, region of the medial longitudinal fascicle and the lateral tegmental nucleus.

In the cerebellum, moderate 5-HT-ir innervation was observed in the auricular lobes and fewer 5-HT-ir varicose fibers and terminals were observed in the granular cell layer of the corpus cerebelli, some of which crossed the midline (Figs. 6J-N, 8I). A few 5-HT-ir fibers were also observed in the lateral areas of the molecular layers and in the cerebellar peduncle (Fig. 6K). In the cerebellar nucleus, most 5-HT-ir fibers coursed along the inner and outer superficial regions, and only a few 5-HT-ir fibers innervated the central region.

In the rostral basal rhombencephalon of juveniles and adults, moderate to dense 5-HT-ir innervation was observed in the central grey and raphe, as well as an intrinsic innervation surrounding the different reticular nuclei (Figs. 6H-Q, 8A-G). The nucleus G of Smeets (recognizable by the ChAT-immunoreactivity of its cells; Anadón et al., 2000) and the region located between the *locus coeruleus* and the medial longitudinal fascicle exhibited

moderate 5-HT-ir innervation (Figs. 6K, 8C). There was also moderate 5-HT-ir innervation around the interpeduncular nucleus, especially ventrally and ventrolaterally to it, although serotoninergic innervation was very scarce in its neuropil (Figs. 6I-K, 8C). 5-HT-ir innervation was scarce in the remaining regions of the isthmic tegmentum.

At more caudal rhombencephalic levels, abundant 5-HT-ir fibers innervated the central gray, whereas moderate to dense 5-HT-ir innervation was observed in the dorsal part of the viscerosensory column, including the Cajal's commissural nucleus (Figs. 6O-Q, 8J). At caudalmost rhombencephalic levels, moderately dense 5-HT-ir varicose fibers were observed in the inferior olivary nucleus (Figs. 6P,Q, 8G). Sparsely 5-HT-ir varicose fibers were observed in the remaining rhombencephalic areas.

Spinal cord

5-HT-ir cells. The spinal cord contained 5-HT-ir neurons throughout its entire length in juveniles and adults. The neurons were located ventrally or ventrolaterally to the central canal, and laterally to the medial longitudinal fascicle (Figs. 6R,S, 8K,L). In the spinal cord these 5-HT-ir neurons were most dense at rostral levels.

5-HT-ir fibers. 5-HT-ir fibers were also observed throughout the entire extension of the spinal cord, and although they occupied both white and gray matter, they were preferentially located in the marginal nucleus (see Anadón et al., 2000) of the spinal cord (Fig. 8M) and in the dorsal margin area of the dorsal horn (Fig. 8N).

DISCUSSION

The development of serotonin-immunoreactive cells and fibers was investigated in the CNS of the lesser-spotted dogfish, which represents the first study of the development of the serotoninergic system in elasmobranchs. One major finding was the notable precedence of rhombencephalic 5-HT-ir populations over those of the diencephalon, which in some stages allowed study of the growth of hindbrain ascending serotoninergic pathways without

interference from those originating from the hypothalamus. This revealed a striking similarity with mammals in terms of the development and basic branching of ascending tracts. Moreover, in the embryonic rhombencephalon and spinal cord, the serotoninergic populations were found to arise from cells adjacent to the floor plate, and they give rise early on to both laterally migrating and midline cell populations. Another interesting finding was that the three hindbrain regions originating laterally migrating serotoninergic cells exhibit a clear segmental pattern. The establishment of the mature pattern of serotoninergic innervation and its relation to the morphological differentiation of the corresponding centers was also followed in detail throughout the dogfish brain.

Chronology of the development of the serotoninergic populations in dogfish: comparison with other vertebrates

The time course of embryonic development differs considerably among vertebrate groups, even among species pertaining to the same group, making it difficult to compare the absolute chronology of appearance of neuronal populations in the different groups. Moreover, in contrast with other fish groups, elasmobranch eggs produce slow-developing large embryos that at hatching exhibit an adult appearance. We compared the relative order of appearance of the various serotoninergic groups in the dogfish CNS with those reported in other vertebrates, as shown in table III. This comparison, especially with other fish groups, has shown some interesting differences and many similarities.

The main differences noted were in the timing of development of the 5-HT-ir groups in relation to the length of the embryonic period. Whereas in *Scyliorhinus canicula* the 5-HT-ir cells were seen for the first time at S26, which occurs at about the first quarter or third of the total embryonic period, in teleosts such as *Scomber scombrus* (Bolliet et al., 1994), *Gasterosteus aculeatus* (Ekström et al., 1985), *Salvelinus fontinalis* (Bolliet and Ali, 1992) and *Danio rerio* (McLean and Fetcho, 2004a), the first appearance of a central serotoninergic population occurs after a half to two thirds of the total embryonic period. It has been suggest that the timing of the developmental sequence of 5-HT-ir neuron

populations reflects the embryonic development duration period (Bolliet and Ali, 1992), which is supported by the present results.

The order of appearance of the rhombencephalic and spinal serotoninergic populations in dogfish is generally similar to that reported in teleosts (Ekström et al., 1985; Bolliet and Ali, 1992; Bolliet et al., 1994). In both groups, the first population was located in the rostral rhombencephalon, followed later on by 5-HT-ir cells of the inferior reticular formation and then by spinal 5-HT-ir cells. The order of appearance of rostral and caudal brainstem populations is also similar in mammals and birds (Wallace and Lauder, 1983; Wallace, 1985). There are greater differences in the order of appearance of hypothalamic serotoninergic populations than in rhombencephalic populations. In dogfish, serotoninergic populations of the paraventricular organ and posterior recess organs appear in rather late embryos, and both groups appear at similar times after differentiation of most rhombencephalic populations. Studies in sea lamprey (Abalo et al., 2007) and chick embryos (Wallace, 1985) also revealed that isthmic populations appear before those of the hypothalamus. However, in teleosts, the hypothalamic groups appear relatively early; in some species the serotoninergic cells of the paraventricular organ appear earlier than the isthmic groups (see Table III), which suggests that the faster development is a derived feature of teleosts and that the genetic mechanisms of specification of prosencephalic and rhombencephalic serotoninergic populations differ. The finding that the rhombencephalic, pineal and hypothalamic serotoninergic cells express each one of three different genes for tryptophan hydroxylase (the first enzyme involved in biosynthesis of serotonin) in the zebrafish (Bellipanni et al., 2002; Teraoka et al., 2004) also suggests that the regulation of the embryonic development of these populations is independent, probably as a result of gene duplication processes that have occurred in early vertebrates (Wang et al., 2006). This would explain both the large variations observed among vertebrates in the order of appearance of the different serotoninergic brain populations, and the drastic reduction or complete loss of prosencephalic serotoninergic populations in amniotes without any accompanying effect on brainstem populations.

The serotoninergic cell groups in the developing CNS in dogfish

Prosencephalic 5-HT-ir populations

In the brain of the lesser-spotted dogfish, the most rostral 5-HT-ir neurons were located in the preoptic area. These late-appearing cells were first observed in S33 and most of them were of CSF-c type. This serotoninergic population was not reported in *Scyliorhinus torazame* (Yamanaka et al., 1990), although 5-HT-ir cells have been described in the preoptic area of *Dasyatis sabina* (Ritchie et al., 1983) and *Platyrhinoidis triseriata* (Stuesse et al., 1990). Likewise, the 5-HT-ir cells described in nucleus Q of *Squalus* by Northcutt et al. (1988) may correspond to the preoptic group of dogfish. 5-HT-ir cells have also been described in the preoptic area of some bony fishes (Grant et al., 1989; Johnston et al., 1990; Ebbesson et al., 1992; Adrio et al., 1999; Piñuela and Northcutt, 2007).

The dogfish hypothalamus contains a very large population of 5-HT-ir cells, most of which are of CSF-c type that extend throughout the infundibulum the dorsal and lateral regions of the lateral recess and the posterior recess, corresponding to the paraventricular and posterior recess circumventricular organs. The organization of these circumventricular organs is similar to that reported in other adult elasmobranchs (Ritchie et al., 1983; Yamanaka et al., 1990; Meurling and Rodríguez, 1990; Stuesse et al., 1990; Stuesse and Cruce, 1991, 1992). In the present study, we observed that development of serotonin expression in circumventricular organs appears “explosive”. Only a few pale serotoninergic cells appeared in the primordia of these organs between S30-S31, but at S32 the circumventricular organs exhibited a very large number of intensely 5-HT-ir CSF-c cells forming a continuous populations. In lampreys, the first CSF-c serotoninergic cells appeared in the tuberal region and then in the mammillary recess (posterior hypothalamus), but the two serotoninergic populations became continuous gradually during development (Abalo et al., 2007). In zebrafish, the first 5-HT-ir cells appear in the posterior recess nucleus (McLean and Fetcho, 2004a), unlike in lamprey and dogfish. Continuity between the 5-HT-ir paraventricular and posterior recess organs primordia is also established during development in teleosts (Ekström et al., 1985; Bolliet and Ali, 1992; Bolliet et al., 1994; McLean and Fetcho, 2004a), which represents a common development pattern of the hypothalamic

serotoninergic populations. In other dogfish diencephalic nuclei (habenula, pretectum), serotonin expression in cells appears to be transient. In the habenula, we observed only a few 5-HT-ir cells in S34 (prehatching), whereas no serotoninergic cells have been reported in the habenula of adult elasmobranchs (Ritchie et al., 1983; Yamanaka et al., 1990; Stuesse and Cruce, 1991; present results). The habenula of a salmon species also exhibits a transient serotoninergic population (Ekström and Ebbesson, 1988, 1989). Timing of 5-HT-ir expression in these salmon cells coincides with changes associated with smolt transformation (Ekström et al., 1992). In mammals, transient expression of serotonin in some brain areas has been related to the role(s) of serotonin as a modulator in the maturation of certain neuronal systems (Lebrand et al., 1996), which may also occur in dogfish.

A transient 5-HT-ir population was observed in the dogfish pretectum from late embryos (S32) to juveniles. The number of 5-HT-ir cells and the intensity of immunoreaction diminished after hatching, suggesting that serotonin expression in these cells is related to maturation of visual centers. The 5-HT-ir cells described in the dorsal thalamus and pretectal areas of some adult elasmobranchs (*Platyrhinoidis*: Stuesse et al., 1990; *Hydrolagus*: Stuesse and Cruce, 1991; *Squalus*: Stuesse and Cruce, 1992) probably correspond to this dogfish population. Dorsal thalamic/pretectal serotoninergic groups have also been described in adult lampreys (Pierre et al., 1992; Antri et al., 2006; Abalo et al., 2007), chondrosteans (Adrio et al., 1999) and teleosts (Kah and Chambolle, 1983; Yoshida et al., 1983; Ekström and van Veen, 1984; Frankenhuis-van den Heuvel and Nieuwenhuys, 1984; Grant et al., 1989; Meek and Joosten, 1989; Johnston et al., 1990; Bolliet and Ali, 1992; Khan and Thomas, 1993; Batten et al., 1993). As observed in the dogfish, the serotoninergic pretectal/dorsal thalamic populations appear rather late in development in lampreys (Abalo et al., 2007) and teleosts (Ekström et al., 1985; Ekström and Ebbesson, 1989; Bolliet et al., 1994; McLean and Fetcho, 2004a). It appears likely that the different 5-HT-ir populations described in the thalamic-pretectal regions of fishes are evolutionarily related. No serotoninergic cells have been described in the pretectal areas of amniotes.

No 5-HT-ir cells were observed in the pineal of adult elasmobranchs (Ritchie et al., 1983; Yamanaka et al., 1990; Stuesse et al., 1990; 1991a, b; Stuesse and Cruce, 1991, 1992; present results), which is in contrast with observations in lampreys (Tamotsu et al., 1990,

1997; Di Prisco et al., 1994; Pombal et al., 1999; Yáñez et al., 1999) and some teleosts (van Veen et al., 1980, 1984; Ekström and van Veen, 1984; Falcon et al., 1984; Margolis-Kazan et al., 1985; Ekström and Ebbesson, 1988, 1989; Ekström and Meissl, 1990). We only observed faint 5-HT-ir cells in the pineal organ of S31, which suggests that serotonin expression is transient. The weakness of immunostaining in these dogfish embryos is in contrast with the intense 5-HT immunoreactivity observed in cells and fibers of other brain regions, possibly indicating that these cells contain very low levels of 5-HT. Photoneuroendocrine cells of the pineal organ synthesize melatonin (pineal hormone involved in the regulation of circadian rhythms) from 5 HT (van Veen et al., 1984; Guerlotte et al., 1986; Tamotsu et al., 1990). Dogfish pineal cells probably only accumulate detectable levels of serotonin before melatonin synthesis begins, which is in contrast with observations made in other fishes. If this hypothesis is correct, detection of serotonin would approximately indicate the start of melatonin synthesis in the developing pineal organ.

Brainstem 5-HT-ir populations

The distribution of the serotoninergic brainstem nuclei in the juvenile and adult lesser-spotted dogfish is roughly similar to that observed in other elasmobranchs (Ritchie et al., 1983; Yamanaka et al., 1990; Stuesse et al., 1991a, b; Stuesse and Cruce, 1991, 1992), and they are organized into midline (raphe) and lateral (reticular) populations. Analysis of development of these populations indicate that they originate caudal to the mid/hindbrain boundary, i.e. they are rhombencephalic, although most authors have described in adult elasmobranchs both mesencephalic and rhombencephalic serotoninergic populations. Discrepancy between the present and previous results appears to arise from misinterpretation of the mid/hindbrain limit in “transverse” sections caused by the deep curvature of the elasmobranch midbrain around the cephalic flexure (probably caused by the great growth differences between tectal and tegmental regions). Thus, isthmic basal regions below the optic tectum are very often interpreted as mesencephalic. However, present results in dogfish indicate that the presence of serotoninergic cells in the caudal midbrain is uncommon. This result is coincident with that of recent developmental studies in zebrafish

(Teraoka et al., 2004) and lampreys (Abalo et al., 2007), which show the restriction of brainstem serotoninergic populations to the rhombencephalon.

We identified four 5-HT-ir superior raphe nuclei (two in the rostralmost rhombencephalic levels and two more caudal nuclei within the rostral rhombencephalon) and three 5-HT-ir inferior raphe nuclei. Most of these raphe nuclei, except the raphe *dorsalis anterioris* nucleus, have been described in other elasmobranchs (Ritchie et al., 1983; Stuesse et al., 1991a, 1995; Stuesse and Cruce, 1992; see Table II). The raphe *dorsalis anterioris* nucleus was the only dogfish brainstem population formed by 5-HT-ir CSF-c cells and located in medial subependymal layers of the isthmic recess. A similar CSF-c serotoninergic population has been described in chondrosteans (Adrio et al., 1999). In dogfish, serotoninergic cells lateral to the raphe form four superior and two inferior reticular nuclei, an organization that is similar to that described in most elasmobranchs (Stuesse and Cruce, 1992; Stuesse et al., 1990, 1991a, 1995). The distribution of serotoninergic reticular nuclei throughout the brainstem in adult elasmobranchs is markedly discontinuous, with widely separated anterior (isthmic, superior) and posterior (inferior) groups (Ritchie et al., 1983; Yamanaka et al., 1990; Stuesse et al., 1990, 1991a,b, 1995; Stuesse and Cruce, 1991, 1992; present study).

We observed two separate 5-HT-ir groups -superior and inferior- in early stages of the dogfish rhombencephalon. Similar rhombencephalic superior and inferior 5-HT-ir groups have been reported in other vertebrates during early development (lampreys: Abalo et al., 2007; teleosts: Ekström et al., 1985; Bolliet and Ali, 1992; Bolliet et al., 1994; Ekström, 1994; birds: Wallace, 1985; mammals: Wallace and Lauder, 1983; Botchkina and Morin, 1993). This pattern is conserved in adult cyclostomes (Kadota, 1991; Pierre et al., 1992; Abalo et al., 2007; Antri et al., 2006), which suggests that the primitive vertebrate pattern is the presence of a discontinuous column of 5-HT-ir rhombencephalic cell groups. This pattern evolved in the brainstem of jawed fishes giving rise to more complex adult 5-HT-ir populations such as those found in chondrosteans (Adrio et al., 1999) as well as in adult teleosts, in which serotoninergic populations form a continuous column along the rhombencephalon (Ekström and van Veen, 1984; Ekström and Ebbesson, 1989; Chiba and

Oka, 1999). Segregation of these major serotoninergic rhombencephalic groups into distinct subpopulations has occurred in most vertebrate lines.

The first 5-HT-ir neurons in the brain appeared in the rostral rhombencephalic tegmentum at S26 close to the ventral midline, i.e. the floor plate. In further stages, these weakly stained ventricular 5-HT-ir cells seemed to be the origin of a ventral migration route that forms the primordia of raphe, from which primordial reticular groups become first distinguishable by the horizontal orientation of perikarya and their long processes that ended in a growth cone. This vertical migration route has been already reported in zebrafish (Teraoka et al., 2004), who evidenced the hedgehog signaling from the floor plate as a key induction factor for the migration process of serotoninergic rapheal cells. All 5-HT-ir raphe groups observed in adults become recognizable at S29 while the set of 5-HT-ir reticular groups cannot be clearly identified before S31, which suggests that the 5-HT-ir raphe groups become specified earlier than the reticular groups. Moreover, some of the 5-HT-ir cells following the vertical route appeared to extend laterally a thick and long guiding process, which is the first evidence of the lateral migration from midline groups that originates the 5-HT-ir reticular cell groups. The lateral (tangential) migration of 5-HT-ir cells seemed to take two main routes, an intermediate route that was followed by the dorsalmost 5-HT-ir reticular populations, and a ventrolateral route that was followed by the ventral and lateral reticular cell groups. Interestingly, the lateral migration of 5-HT-ir in dogfish embryos was restricted to three transverse rhombencephalic regions, which indicates a segmental pattern (see below). In these regions, too, the presence of some 5-HT-ir cells in the midline and/or extending processes contralaterally suggests that some perikarya may cross the midline in their migration towards the contralateral side. These regions also exhibit prominent serotoninergic commissures. This behavior was not observed at other levels of the rhombencephalon, where 5-HT-ir cells are only found on the side where they first differentiate. Similar migration towards the midline has been reported in the B4-B9 complex (metencephalon) of developing hamster (Botchkina and Morin, 1993), which suggests that serotoninergic cells of elasmobranchs and mammals respond similarly to midline molecular clues.

It has been hypothesized that in fishes and amphibians, 5-HT-ir brainstem cells are primarily restricted to the raphe region but that in birds and mammals they spread laterally (Parent et al., 1984). Results from studies of adult and developing elasmobranchs indicate that the laterally migrated 5-HT-ir reticular nuclei appear early on in this line of jawed fishes. Moreover, during dogfish development, lateralization of serotoninergic reticular cells begins at about the same time as the appearance of raphe nuclei, which indicates that birth of these reticular cells is an early event. This suggests that either the appearance of complex patterns of migrated serotoninergic nuclei has occurred several times during vertebrate phylogeny, or that the less complex patterns observed in some extant groups of bony fishes and amphibians are a result of secondary simplification or loss of reticular populations. In lampreys, too, serotoninergic hindbrain populations exhibit a clearly different pattern of migration (Abalo et al., 2007).

Segmental organization of the brainstem 5-HT-ir populations. During vertebrate development, prominent ventricular bulges and sulci divide the rhombencephalon into transverse segmental units, the rhombomeres, which are separated by cytoarchitectonic boundaries and/or glia specializations. The facial motor nucleus exhibits a conspicuous segmental distribution in vertebrate embryos, including elasmobranchs (Gilland and Baker, 1993; Kuratani and Horigome, 2000). The entry of branchiomeric nerves (trigeminal, facial, glossopharyngeal and vagal nerves) is also correlated with some inter-rhombomeric boundaries in birds (Lumsden and Keynes, 1989). In adults, rhombomeres are no longer visible but the segmental disposition of motor nuclei remains, as revealed in birds (Medina and Reiner, 1994), reptiles (Medina et al., 1993), amphibians (Marín et al., 1997b) and dogfish (Anadón et al., 2000) by use of antibodies against choline acetyltransferase (ChAT). Taking advantage of the ability of these antibodies to reveal these nuclei, we used double immunolabeling ChAT/5-HT to assess the segmental disposition of the serotoninergic nuclei in the brainstem of late (S33) and juveniles. After comparing the results obtained with the rhombomeric organization described by Kuratani and Horigome (2000) in early embryos of a closely related species, we characterized three rhombomeric boundaries in *S. canicula*:

- The isthmic boundary between mesencephalon and rhombencephalon -which in juveniles has been placed at a level just caudal to the oculomotor nerve root (Kuratani and

Horigome, 2000)- coincided approximately with the rostral level of three reticular 5-HT-ir nuclei (raphe *linearis*, raphe *dorsalis anterioris* and reticular B9).

- The rostral level of the trigeminal motor nucleus defined the boundary between rhombomere 2 (r2) and 3 (r3) in dogfish (Kuratani and Horigome, 2000), which in juveniles has been placed tentatively at a level caudal to the locus coeruleus and G nucleus, which also represents a rhombomeric boundary reference in most vertebrates (Gilland and Baker, 1993; Marín et al., 1997b; Anadón et al., 2000). This r2/r3 boundary coincides approximately with the caudal level of three reticular 5-HT-ir nuclei (*subcoeruleus*, *pontis oralis medialis* and *lateralis*) and the rostral level of the raphe *dorsalis*.

- The absence of 5-HT-ir cell bodies in confined regions between the caudal level of the trigeminal motor nucleus and the rostral level of the VII motor nucleus may represent a boundary between rhombomeres 3 (r3) and 4 (r4). In zebrafish, combination of expression analyses of some transcription factor-encoding genes with rhombomere identity markers, has demonstrated that the rhombomere 3 represents a hindbrain boundary between the superior and inferior serotoninergic hindbrain populations (Lillesaar et al., 2007), which is strikingly similar to that observed in dogfish.

Two of these segmental boundaries already observed at S33 may be especially important in the development of the reticular formation nuclei. These two boundaries are: (1) the midbrain/hindbrain boundary, which may be the rostral organizer center of the superior raphe/reticular formation during development. This midbrain/hindbrain boundary was also reported in zebrafish as an organizer center for r1-r2 serotoninergic raphe populations (Lillesaar et al., 2007); (2) The boundary between the third and fourth rhombomeres, which marks the separation between the superior and inferior raphe/reticular formation groups, was also reported in zebrafish (Lillesaar et al., 2007). This boundary is reflected in the organization of the reticular formation of juveniles and adult dogfish. Moreover, we tentatively indicate the possible relation of raphe/reticular groups with the six rhombomeres reported in *Scyliorhinus torazame* by Kuratani and Horigome (2000), and also with a seventh rhombomere that almost coincides with the rostrocaudal extension of the reticular *magnocellularis* and *gigantocellularis* cell groups. Studies with rhombomeric gene

markers combined by double labeling studies are needed to confirm these rhombencephalic segmental distributions.

Spinal populations

In the rostral spinal cord of juvenile dogfish, we recognized two 5-HT-ir cell groups, located near the meninges ventrolaterally and near the midline ventral to the central canal, respectively. This distribution is much wider than that reported in adult *Scyliorhinus torazame* (Yamanaka et al., 1990), but similar to that observed in some other elasmobranchs (Ritchie and Leonard, 1982; Ritchie et al., 1983; Stuesse et al., 1991; Stuesse and Cruce, 1992). Spinal 5-HT-ir cells were also described in adult cyclostomes (Kadota, 1991; Zhang et al., 1996; Abalo et al., 2007), chondrosteans, holosteans and teleosts (Bollliet and Ali, 1992; Adrio et al., 1999; Chiba, 2007; Wai et al., 2007).

During early development (S28-S31), the spinal 5-HT-ir cells were located ventromedially close to the ventral region of the slit-shaped central canal. From S33 to adults, some 5-HT-ir cells migrate to the superficial region of the ventral and ventrolateral funicules and progressively acquire the adult pattern. As reported for rhombencephalic populations, these cells arise from the ventricular zone adjacent to the floor plate. Similarly, the first spinal 5-HT-ir cells in zebrafish originate close to the floor plate (McLean and Fetcho, 2004a).

Spatial and temporal patterns of 5-HT-ir innervation in the dogfish CNS

The present study provides evidence for two distinct phases in the development of the serotoninergic innervation in the dogfish brain, which partially overlap. The first phase is characterized by the growth and navigation of axons towards their target regions, which in dogfish begins at S26 (with the appearance of first 5-HT-ir neurons) and continues until axons in the medial forebrain bundle enter the telencephalon (S31). The second phase is characterized by the branching of 5-HT-ir fibers and appearance of dense fields of terminals in different brain structures, which mainly occurs between S32 and juveniles. Similar phases of axonal development have been described in the serotoninergic system of mammals (Lidov and Molliver, 1982a,b; Botchkina and Morin, 1993).

In the initial phase, the anterior rhombencephalic 5-HT-ir neurons gave rise to axons that project caudally and rostrally and exhibit a characteristic growth cone at their ends. The early 5-HT-ir fiber pathways, especially the descending bundles, show intense serotonin immunoreactivity in growth cones, which indicates the presence of high levels of this transmitter, as also described in other vertebrates (Lidov and Molliver, 1982a,b; Wallace and Lauder, 1983; McLean and Fetcho, 2004a). These early 5-HT-ir fibers follow longitudinal trajectories along the brain or the spinal cord, some after crossing the midline floor plate. Progressively more and more axons are added to these pathways. The descending 5-HT-ir fiber bundles ran caudally through the rhombencephalon and the spinal cord without giving rise to any conspicuous transverse branches. However, early ascending pathways formed collateral bundles in a few forebrain regions. By the end of this phase the ascending 5-HT-ir longitudinal bundles that extended to the postchiasmatic region have originated transverse tracts coursing either dorsally (toward the posterior commissure, habenula and basal telencephalon) or ventrally (towards the posterior tubercle, postoptic region) to the flexured brain axis. The pattern of these early serotoninergic collateral pathways in the dogfish is strikingly similar to that reported in hamster (Botchkina and Morin, 1993). The most conspicuous path is that entering the basal telencephalon, which represents a right angle collateral tract arising from the main longitudinal tract, which is directed to the postoptic commissural plate. In the prosomeric model (Puelles and Rubenstein, 1993, 2003) the whole telencephalon is regarded as a dorsal evagination of the rostral neural tube, which is consistent with the striking right angle trajectory followed in dogfish embryos by the serotoninergic fibers entering the telencephalon as regards the trajectory of the main developing rhombencephalo-prosencephalic pathways, which identify them as tract collaterals.

During the second phase of the development of serotoninergic innervation, 5-HT-ir fibers branch extensively and innervate profusely most brain and spinal cord regions. In most brain regions this phase began at S32, and is coincidental with the start of important cytoarchitectural changes in the walls of the neural tube. The development of the axonal arborization was especially notable at telencephalic levels. During this phase, the pallial and subpallial regions acquire dense innervation by the branching of ascending 5 HT-ir fibers of

the medial forebrain bundle, which coursed through the marginal zone of the basal superficial area and septal region (subpallium) before entering the pallium by its most rostral aspect. Other 5-HT-ir fibers deviate from the medial bundle to course along the pallial/subpallial boundary toward the lateral pallium and the olfactory bulbs, which in dogfish embryos are located lateral to the telencephalic lobes. Progressively, these axonal pathways reach every telencephalic region and form extremely dense 5-HT-ir terminal fields in some subpallial areas. Medial and lateral pathways of pioneer serotoninergic axons ascending throughout the telencephalon have also been described in mammals (Lidov and Molliver, 1982a; Wallace and Lauder, 1983; Botchkina and Morin, 1993).

In the spinal cord, the 5-HT-ir fibers have two different origins: A descending axonal innervation that extends from the reticular formation to the caudal regions of the spinal cord via the lateral funiculus, and an intrinsic spinal cord innervation arising from the 5-HT-ir spinal cell bodies, which is similar to that described in cyclostomes (Brodin et al., 1986) and teleosts (McLean and Fetcho, 2004a, b). Experimental studies in adult dogfish have revealed large neurons of the reticular formation and cells of the inferior raphe nucleus that project to the spinal cord (Smeets and Timerick, 1981; Timerick et al., 1992). The presence of 5-HT-ir cells in the superior and inferior reticular nuclei and inferior raphe nuclei suggests that some of them may give rise to the descending serotoninergic fibers observed during development. However, to know which rhombencephalic 5-HT-ir groups actually give rise to descending spinal projections need to be approached experimentally.

The pattern of distribution of 5-HT-ir fiber pathways during development observed in this study is consistent with the descriptions of Lidov and Molliver (1982a) and Wallace and Lauder (1983) in the rat, despite the slightly different temporal sequences of appearance of 5-HT-ir cell groups in elasmobranchs and mammals. Accordingly, the development of the main 5-HT-ir axonal pathways of the dogfish may be representative of the basic pattern common to vertebrates.

Innervation of the main dogfish brain centers

Olfactory bulb

The dogfish olfactory bulb (OB) is innervated by 5-HT-ir fibers extending from the lateral hindbrain-telencephalic bundles as early as the S31, which indicates that these fibers probably originate from hindbrain serotoninergic populations. Developmental studies in mammals have also revealed that early 5-HT-ir fibers that innervate the OB arise from raphe cells (McLean and Shipley, 1987; Botchkina and Morin, 1993; Philpot et al., 1994; Luque et al., 1998; Zhou et al., 2000). In mammals, OB innervation by serotoninergic fibers was first observed at the beginning of the second half of the embryonic brain development, similarly to that observed in the dogfish. Since the differentiation of dogfish hypothalamic 5-HT-ir cells start at S32, our results cannot rule out the presence of serotoninergic fibers of other origins in the OB of later embryos and adults.

The present results suggest that the appearance of the first serotoninergic afferents in the dogfish OB is related to some crucial events in the olfactory organs. During S31, the embryo enters in direct contact with sea water because hatching gland secretions digest the egg jelly and the cement that seals the slits at the four corners of the eggshell (Ballard et al., 1993). When the first 5-HT-ir axons reach the OB in embryos at S32, the olfactory nerve has entered the bulb and glomeruli are visible, suggesting that the olfactory system becomes functional prior to hatching. In dogfish, serotonin may play a role in modulation of olfactory transmission and olfactory learning, as reported in mammals (McLean et al., 1993; Kang et al., 2001; Hardy et al., 2005).

Telencephalic hemispheres

In adult *Scyliorhinus canicula,* serotoninergic fibers are widely distributed throughout the telencephalic hemispheres, as reported in other elasmobranch species (*Dasyatis*: Ritchie et al., 1983; *Squalus*: Northcutt et al., 1988; *Scyliorhinus torazame*: Yamanaka et al., 1990). The common pattern in elasmobranchs is characterized by a lower density of 5-HT-ir fibers in the pallium than in the subpallium, with the medial pallium and the basal superficial area being the most densely innervated areas. In non-teleost actinopterygians (*Acipenser*: Adrio et al., 1999; Piñuela and Northcutt, 2007; *Lepisosteus*:

Parent and Northcutt, 1982; Chiba and Oka, 1999) and amphibians (Ueda et al., 1984; Dicke et al., 1997), the ventral telencephalon contains a higher density of serotoninergic fibers than the dorsal telencephalon, which is in contrast with the observation in teleosts and in amniotes that the 5-HT-ir innervation is denser in dorsal (specially in medial and lateral pallium) than in ventral telencephalic regions.

As reported in other elasmobranchs (Ritchie et al., 1983; Northcutt et al., 1988; Yamanaka et al., 1990), in adult dogfish the basal superficial area is richly innervated by serotoninergic fibers, unlike in adjacent areas. During the embryonic period the cell-rich band of the basal superficial area is poorly innervated by 5-HT-ir fibers, in contrast with its adjacent dorsal (inner) region, the central superficial area, a region with loosely arranged cells densely coated with substance P-ir boutons (Rodríguez-Moldes et al., 1993), and particularly the external/marginal region, which showed very rich serotoninergic innervation. In *Squalus*, Northcutt et al. (1988) have suggested that the basal superficial area may be homologous to both the *globus pallidus* and the olfactory tubercle of mammals. The two regions distinguished in the basal superficial area of late embryos on the basis of the serotoninergic innervation -a poorly innervated central band with densely-packed neurons and a cell-poor external (marginal) part that contains rich serotonin innervation- may correspond respectively to the mammalian ventral pallidum (which shows scarce serotoninergic innervation) and olfactory tubercle (with richer innervation).

From embryos to adults, the highest density of 5-HT-ir fibers in this marginal subpallial zone is observed in the dorsolateral region, just ventral to the lateral pallium. This region may correspond to the lateral palliosubpallial border described in *Squalus* (Northcutt et al., 1988). Interestingly, the pioneer 5-HT-ir fibers that reach the telencephalon coursed along this border, which in some embryonic stages can be identified by a shallow external sulcus. Since the first telencephalic 5-HT-ir fibers appear at S31, after the differentiation of isthmic 5-HT-ir cells (S26) but simultaneous to the appearance of first hypothalamic 5-HT-ir cells, we consider that the early serotoninergic fibers in the telencephalon probably arise from the raphe/reticular formation. Serotoninergic cells of the raphe nuclei projecting to the telencephalon have been observed in teleosts during development (Ekström et al., 1985; McLean and Fetcho, 2004a), and tract-tracing studies in adults showed cells from the raphe

nuclei projecting onto the telencephalon (Echteler and Saidel, 1981; Holmes and Northcutt, 2003; Folgueira et al., 2004a, b; Rink and Wullimann, 2004). This raphe-telencephalic connection has also been described in tetrapods (Northcutt and Ronan, 1992; Siemen and Kunzle, 1994; Medina and Reiner, 1995; Wild and Farabaugh, 1996; Dubbeldam et al., 1997; Marín et al., 1997a; Font et al., 1997, 1998; Lanuza et al., 1998; Smeets et al., 2000; Roden et al., 2005). Immunohistochemical analysis of the development of serotoninergic pathways supports the rapheal origin of the first serotoninergic telencephalic fibers, although hodological experiments must be performed to demonstrate this origin in dogfish.

Hypothalamus

The distribution of 5-HT-ir fibers in the median eminence and neurointermediate lobe of the hypophysis of the dogfish was similar to that observed in other adult elasmobranchs (Ritchie et al., 1983; Yamanaka et al., 1990; Stuesse and Cruce, 1991). Our developmental observations reveal that first serotoninergic fibers course along the hypothalamic floor at about the time of appearance of hypothalamic serotoninergic cells, suggesting that cells of the paraventricular organ give rise to the serotoninergic innervation of the median eminence and neurointermediate lobe. This origin has been described in teleosts after application of tracer techniques (Rao et al., 1993; Holmqvist and Ekström, 1995). The late appearance of these fibers during dogfish ontogeny is probably related to late maturation of the hypophysis, as reported in teleosts (Ekström et al., 1985; McLean and Fetcho, 2004a).

Pineal organ

Fairly abundant 5-HT-ir fibers were observed in the dogfish pineal organ from S32 onwards, when no 5-HT-ir pineal cells are evident. Although we cannot rule out the possibility that these 5-HT-ir fibers may originate from pineal cells with low levels of serotonin, undetectable by immunohistochemistry, it appears likely that they were pinealopetal fibers. This interpretation is supported by the observation of labeled cells in the pretectal region after application of the tract tracer DiI to the dogfish pineal organ (Mandado et al., 2001), a region where 5-HT-ir cells were observed (present results). The decreasing

density of serotoninergic fibers in the pineal from juveniles to adulthood may be related to the observed decrease in 5-HT immunoreactivity of these cells from prehatching embryos to juveniles. Together with the presence of a rich GABAergic innervation in the pineal neuroepithelium (Carrera et al., 2006), these results suggest a more complex modulation of dogfish pineal function by neurotransmitters. Our immunocytochemical results are consistent with the results of electron microscopical studies, which indicate that the dogfish pineal organ has a rich basoepithelial neuropil with various types of synaptic boutons (Rüdeberg, 1969).

Mesencephalon and rhombencephalon

In the present study, we report a widespread distribution of 5-HT-ir fibers in the brainstem basal plate during the second half of the embryonic developmental period, which rapidly reaches the organization observed in adults, which is similar to that reported in other cartilaginous fishes (Ritchie et al., 1983; Yamanaka et al., 1990; Stuesse et al., 1992). The serotoninergic innervation is especially dense in medial, ventral and lateroventral tegmental areas and in the vagal lobes, regions that also have a rich serotoninergic innervation in other vertebrate groups, particularly the lateral and basal mesencephalic tegmental regions.

In the optic tectum, from S34, serotoninergic fibers were observed at middle layers of the optic tectum (stratum fibrosum et griseum centrale). The origin of these 5-HT-ir fibers may be the reticular formation groups and/or the pretectal 5-HT-ir cells observed at S32, similarly to that described in zebrafish (McLean and Fetcho, 2004b) and frog (Zhao and Debski, 2005). The late innervation of the optic tectum by 5-HT-ir fibers observed during dogfish development is similar to that reported in teleosts (McLean and Fetcho, 2004a,b), amphibians (Zhao and Debski, 2005) and mammals (Lidov and Molliver, 1982a; Wallace and Lauder, 1983; Botchkina and Morin., 1993; Luque et al., 1998). Experimental studies have demonstrated that the optic tectum is the main retinorecipient center in the adult dogfish brain (Smeets, 1981). In the dogfish retina, neuronal differentiation begins at stage 29, whereas first photoreceptors appeared at the stage 31 (personal observations). The innervation of the dogfish optic tectum by 5-HT-ir fibers begins after these stages, indicating

that serotonin is not involved in early stages of maturation of the tectum, though it might be important for functional aspects of the mature tectum.

Within the cerebellum, the 5-HT-ir fibers were first observed crossing the cerebellar commissure and in the granular layer at S34. A few 5-HT-ir fibers were also observed in the bordering areas of the molecular layers and in the cerebellar peduncle. The late appearance of serotoninergic innervation of the cerebellum during development has also been described in teleosts (McLean and Fetcho, 2004a, b) and mammals (Lidov and Molliver, 1982a,b; Wallace and Lauder, 1983; Botchkina and Morin., 1993; Luque et al., 1998). The corpus cerebellum of the adult dogfish presents slight serotoninergic innervation; most of which was distributed in the granular cell layer, although some scattered 5-HT-ir fibers were also observed in the molecular layer and in the cerebellar peduncle at rostral levels. This serotoninergic distribution of 5-HT-ir fibers was similar to that described in *Scyliorhinus torazame* (Yamanaka et al., 1990) and *Dasyatis sabina* (Ritchie et al., 1983), although no 5-HT-ir staining was observed in the molecular layers in the stingray. In general, scarce or very scarce 5-HT-ir innervation in the granular cell layer of the cerebellum has been described in most vertebrate groups, which suggests a shared pattern.

Spinal cord

The first 5-HT-ir fibers of the spinal cord were observed at S26, running laterally to the floor plate at the obex level. In later stages, the density of this 5-HT-ir innervation increase gradually, reaching the mature distribution at S33, where 5-HT-ir fibers coursed along the ventrolateral, lateral, dorsolateral and commissural areas of the anterior half of the spinal cord. The density of 5-HT-ir innervation decrease caudally (posterior half of the spinal cord), and is mainly located in the ventrolateral and lateral regions of the spinal cord. This pattern of development is comparable to that observed in other vertebrate groups such as teleosts (McLean and Fetcho, 2004a, b), amphibians (Ten Eyck et al., 2005) and mammals (Wallace and Lauder, 1983; Luque et al., 1998).

BIBLIOGRAPHY

Abalo, X.M.; Villar-Cheda, B.; Meléndez-Ferro, M.; Pérez-Costas, E.; Anadón, R.; Rodicio, MC. (2007) Development of the serotonergic system in the central nervous system of the sea lamprey. J Chem Neuroanat. 34:29-46.

Adrio, F.; Anadón, R.; Rodríguez-Moldes, I. (1999) Distribution of serotonin (5HT)-immunoreactive structures in the central nervous system of two chondrostean species (*Acipenser baeri* and *Huso huso*). J Comp Neurol. 407:333-348.

Allain, A.E.; Meyrand, P.; Branchereau, P. (2005) Ontogenic changes of the spinal GABAergic cell population are controlled by the serotonin (5-HT) system: Implication of 5-HT1 receptor family. J Neurosci. 25:8714-8724.

Anadón, R.; Molist, P.; Rodríguez-Moldes, I.; López, J.M.; Quintela, I.; Cerviño, M.C.; Barja, P.; González, A. (2000) Distribution of choline acetyltransferase immunoreactivity in the brain of an elasmobranch, the lesser spotted dogfish (*Scyliorhinus canicula*). J Comp Neurol. 420:139-170.

Antri, M.; Cyr, A.; Auclair, F.; Dubuc, R. (2006) Ontogeny of 5-HT neurons in the brainstem of the lamprey, *Petromyzon marinus*. J Comp Neurol. 495:788-800.

Ballard, W.; Mellinger, J.; Lechenault, H. (1993) A series of normal stages for development of *Scyliorhinus canicula*, the lesser spotted dogfish (Chondrichthyes *Scyliorhinidae*). J Exp Zool. 267:318-336.

Batten, T.F.; Berry, P.A.; Maqbool, A.; Moons, L.; Vandesande, F. (1993) Immunolocalization of catecholamine enzymes, serotonin, dopamine and L-dopa in the brain of *Dicentrarchus labrax* (Teleostei). Brain Res Bull. 31:233-252.

Bellipanni, G.; Rink, E.; Bally-Cuif, L. (2002) Cloning of two tryptophan hydroxylase genes expressed in the diencephalon of the developing zebrafish brain. Mech Dev. 119:S215-220.

Bolliet, V.; Ali, M.A. (1992) Immunohistochemical study of the development of serotoninergic neurons in the brain of the brook trout *Salvelinus fontinalis*. Brain Behav Evol. 40:234-249.

Bolliet, V.; Perreault, S.; Ali, M.A. (1994) Development of serotoninergic neurons in the brain of the mackerel, *Scomber scombrus*. An immunohistochemical study. J Fish Biol. 44:241-253.

Botchkina, G.I.; Morin, L.P. (1993) Development of the hamster serotoninergic system: cell groups and diencephalic projections. J Comp Neurol. 338:405-431.

Brodin, L.; Buchanan, J.T.; Hökfelt, T.; Grillner, S.; Verhofstad, A.A. (1986) A spinal projection of 5-hydroxytryptamine neurons in the lamprey brainstem; observed from combined retrograde tracing and immunohistochemistry. Neurosci Lett. 67:53-57.

Carrera, I.; Sueiro, C.; Molist, P.; Ferreiro, S.; Adrio, F.; Rodríguez, M.A.; Anadón, R.; Rodríguez-Moldes, I. (2005) Temporal and spatial organization of tyrosine hydroxylase-immunoreactive cell groups in the embryonic brain of an elasmobranch, the lesser-spotted dogfish. Brain Res Bull. 66:541-545.

Carrera, I.; Sueiro, C.; Molist, P.; Holstein, G.R.; Martinelli, G.P.; Rodríguez-Moldes, I.; Anadón, R. (2006) GABAergic system of the pineal organ of an elasmobranch (*Scyliorhinus canicula*): a developmental immunocytochemical study. Cell Tissue Res. 13:1-9.

Carrera, I.; Ferreiro-Galve, S.; Sueiro, C.; Anadón, R.; Rodríguez-Moldes, I. (2008) Tangentially migrating GABAergic cells of subpallial origin invade massively the pallium in developing sharks. Brain Res Bull. 75:405-409.

Chiba, A. (2007) Serotonergic neuron system in the spinal cord of the gar *Lepisosteus oculatus* (Lepisosteiformes, Osteichthyes) with special regard to the juxtameningeal serotonergic plexus as a paracrine site. Neurosci Lett. 413:6-10.

Chiba, A.; Oka, S. (1999) Serotonin-immunoreactive structures in the central nervous system of the garfish *Lepisosteus productus* (Semionotiformes, Osteichthyes). Neurosci Lett. 261:73-76.

C**lairambault, P**.; Christophe, N.; Pairault, C.; Herbin, M.; Ward, R.; Repérant, J. (1994) Organization of the serotoninergic system in the brain of two amphibian species, *Ambystoma mexicanum* (Urodela) and *Typhlonectes compressicauda* (Gymnophiona). Anat Embryol. 190:87-99.

Corio, M.; Peute, J.; Steinbusch, H.W. (1991) Distribution of serotonin- and dopamine-immunoreactivity in the brain of the teleost *Clarias gariepinus*. J Chem Neuroanat. 4:79-95.

Corio, M.; Thibault, J.; Peute, J. (1992) Distribution of catecholaminergic and serotoninergic systems in forebrain and midbrain of the newt, *Triturus alpestris* (Urodela). Cell Tissue Res. 268:377-387.

Derobert, Y.; Plouhinec, J.L.; Sauka-Spengler, T.; Le Mentec, C.; Baratte, B.; Jaillard, D.; Mazan, S. (2002a) Structure and expression of three Emx genes in the dogfish *Scyliorhinus canicula*: functional and evolutionary implications. Dev Biol. 247:390-404.

Derobert, Y.; Baratte, B.; Lepage, M.; Mazan, S. (2002b) Pax6 expression patterns in *Lampetra fluviatilis* and *Scyliorhinus canicula* embryos suggest highly conserved roles in the early regionalization of the vertebrate brain. Brain Res Bull. 57:277-280.

Di Prisco, G.V.; Dubuc, R.; Grillner, S. (1994) 5-HT innervation of reticulospinal neurons and other brainstem structures in lamprey. J Comp Neurol. 342:23-34.

Dicke, U.; Wallstein, M.; Roth, G. (1997) 5-HT-like immunoreactivity in the brains of plethodontid and salamandrid salamanders (*Hydromantes italicus*, *Hydromantes genei*, *Plethodon jordani*, *Desmognathus ochrophaeus*, *Pleurodeles waltl*): an immunohistochemical and biocytin double-labelling study. Cell Tissue Res. 287:513-523.

Dubbeldam, J.L.; den Boer-Visser, A.M.; Bout, R.G. (1997) Organization and efferent connections of the archistriatum of the mallard, *Anas platyrhynchos* L.: an anterograde and retrograde tracing study. J Comp Neurol. 388:632-657.

Ebbesson, L.O.; Holmqvist, H.; Östholm, T.; Ekström, P. (1992) Transient serotonin-immunoreactive neurons coincide with a critical period of neural development in coho salmon (*Oncorhynchus kisutch*). Cell Tissue Res. 268:389-392.

Echteler, S.M.; Saidel, W.M. (1981) Forebrain connections in the goldfish support telencephalic homologies with land vertebrates. Science. 212:683-685.

Ekström, P. (1994) Developmental changes in the brain-stem serotonergic nuclei of teleost fish and neural plasticity. Cell Mol Neurobiol. 14:381-393.

Ekström, P.; Van Veen, T.; (1984) Distribution of 5-hydroxytryptamine (serotonin) in the brain of the teleost *Gasterosteus aculeatus* L. J Comp Neurol. 226:307-320.

Ekström, P.; Ebbesson, S.O. (1988) The left habenular nucleus contains a discrete serotonin-immunoreactive subnucleus in the coho salmon (*Oncorhynchus kisutch*). Neurosci Lett. 91:121-125.

Ekström, P.; Ebbesson, S.O. (1989) Distribution of serotonin-immunoreactive neurons in the brain of sockeye salmon fry. J Chem Neuroanat. 2:201-213.

Ekström, P.; Meissl, H. (1990) Electron microscopic analysis of S-antigen- and serotonin-immunoreactive neural and sensory elements in the photosensory pineal organ of the salmon. J Comp Neurol. 292:73-82.

Ekström, P.; Nyberg, L.; van Veen, T. (1985) Ontogenetic development of serotoninergic neurons in the brain of teleost, the three-spined stickleback. An immunohistochemical analysis. Brain Res. 349:209-224.

Ekström, P.; Ostholm, T.; Ebbesson, S.O. (1992) A morphometric study of age-related changes in serotonin-immunoreactive cell groups in the brain of the coho salmon, *Oncorhynchus kisutch Walbaum*. Exp Neurol. 116:204-209.

Falcon, J.; Geffard, M.; Juillard, M.T.; Steinbusch, H.W.; Seguela, P.; Collin, J.P. (1984) Immunocytochemical localization and circadian variations of serotonin and N-acetylserotonin in photoreceptor cells. Light and electron microscopic study in the teleost pineal organ. J Histochem Cytochem. 32:486-492.

Fasolo, A.; Franzoni, M.F.; Gaudino, G.; Steinbusch, H.W. (1986) The organization of serotonin-immunoreactive neuronal systems in the brain of the crested newt, *Triturus cristatus carnifex Laur*. Cell Tissue Res. 243:239-247.

Ferreiro-Galve, S.; Carrera, I.; Candal, E.; Villar-Cheda, B.; Anadón, R.; Mazan, S.; Rodríguez-Moldes, I. (2008) The segmental organization of the developing shark brain based on neurochemical markers, with special attention to the prosencephalon. Brain Res Bull. 75:236-240.

Folgueira, M.; Anadón, R.; Yáñez, J. (2004a) An experimental study of the connections of the telencephalon in the rainbow trout (*Oncorhynchus mykiss*). I: Olfactory bulb and ventral area. J Comp Neurol. 480:180-203.

Folgueira, M.; Anadón, R.; Yáñez, J. (2004b) Experimental study of the connections of the telencephalon in the rainbow trout (*Oncorhynchus mykiss*). II: Dorsal area and preoptic region. J Comp Neurol. 480:204-233.

Font, C.; Lanuza, E.; Martínez-Marcos, A.; Hoogland, P.V.; Martínez-García, F. (1997) Septal complex of the telencephalon of the lizard *Podarcis hispanica*. II. Afferent connections. J Comp Neurol. 383:489-511.

Font, C.; Martínez-Marcos, A.; Lanuza, E.; Hoogland, P.V.; Martínez-García, S. (1998) Septal complex of the telencephalon of lizards: III. Efferent connections and general discussion. J Comp Neurol. 401:525-548.

Frankenhuis-van den Heuvel, T.H.; Nieuwenhuys, R. (1984) Distribution of serotonin-immunoreactivity in the diencephalon and mesencephalon of the trout, *Salmo gairdneri*. Cell bodies, fibers and terminals. Anat Embryol. 169:193-204.

Gaspar, P.; Cases, O.; Maroteaux, L. (2003) The developmental role of serotonin: news from mouse molecular genetics. Nat Rev Neurosci. 4:1002-1012.

Gilland, E.; Baker, R. (1993) Conservation of neuroepithelial and mesodermal segments in the embryonic vertebrate head. Acta Anat. 148:110-123.

Grant, K.; Clausse, S.; Libouban, S.; Szabo, T. (1989) Serotoninergic neurons in the mormyrid brain and their projection to the preelectromotor and primary electrosensory centers: immunohistochemical study. J Comp Neurol. 281:114-128.

Guerlotte, J.; Falcon, J.; Voisin, P.; Collin, J.P. (1986) Indoles in the photoreceptor cells of the lamprey pineal complex. Ann Endocrinol. 47:62-64.

Hardy, A.; Palouzier-Paulignan, B.; Duchamp, A.; Royet, J.P.; Duchamp-Viret, P. (2005) 5-Hydroxytryptamine action in the rat olfactory bulb: in vitro electrophysiological patch-clamp recordings of juxtaglomerular and mitral cells. Neuroscience. 131:717-731.

Holmes, P.H.; Northcutt, R.G. (2003) Connections of the pallial telencephalon in the Senegal bichir, *Polypterus*. Brain Behav Evol. 61:113-147.

Holmqvist, B.I.; Ekström, P. (1995) Hypophysiotrophic systems in the brain of the Atlantic salmon. Neuronal innervation of the pituitary and the origin of pituitary dopamine and nonapeptides identified by means of combined carbocyanine tract tracing and immunocytochemistry. J Chem Neuroanat. 8:125-145.

Hornung, J.P.; Fritschy, J.M. (1988) Serotoninergic system in the brainstem of the marmoset: a combined immunocytochemical and three-dimensional reconstruction study. J Comp Neurol. 270:471-487.

Johnston, S.A.; Maler, L.; Tinner, B. (1990) The distribution of serotonin in the brain of *Apteronotus leptorhynchus*: An immunohistochemical study. J Chem Neuroanat. 3:429-465.

Kadota, T. (1991) Distribution of 5-HT (serotonin) immunoreactivity in the central nervous system of the inshore hagfish, *Eptatretus burgeri*. Cell Tissue Res. 266:107-116.

Kah, O.; Chambolle, P. (1983) Serotonin in the brain of the goldfish, *Carassius auratus*. An immunocytochemical study. Cell Tissue Res. 234:319-333.

Kang, T.C.; Lee, J.C.; Choi, K.Y.; Park, S.K.; Jeong, Y.G.; Won, M.H. (2001) Distribution of serotonin immunoreactivity in the olfactory bulb of Mongolian gerbil. Anat Histol Embryol. 30:117-120.

Khan, I.A.; Thomas, P. (1993) Immunocytochemical localization of serotonin and gonadotropin-releasing hormone in the brain and pituitary gland of the Atlantic croaker *Micropogonias undulatus*. Gen Comp Endocrinol. 91:167-180.

Kuratani, S.; Horigome, N. (2000) Developmental morphology of branchiomeric nerves in a cat shark, *Scyliorhinus torazame*, with special reference to rhombomeres, cephalic mesoderm, and distribution patterns of cephalic crest cells. Zool Sci. 17:893-909.

Lanuza, E.; Belekhova, M.; Martínez-Marcos, A.; Font, C.; Martínez-García, F. (1998) Identification of the reptilian basolateral amygdala: an anatomical investigation of the afferents to the posterior dorsal ventricular ridge of the lizard *Podarcis hispanica*. Eur J Neurosci. 10:3517-3534.

Lauder, J.M. (1990) Ontogeny of the serotonergic system in the rat: serotonin as a developmental signal. Ann NY Acad Sci. 600:297-313.

Lauder, J.M. (1993) Neurotransmitters as growth regulatory signals: role of receptors and second messengers. Trends Neurosci. 16:233-239.

Lebrand, C.; Cases, O.; Adelbrecht, C.; Doye, A.; Alvarez, C.H.; Mestikawy, S.E.; Seif, I.; Gaspar, P. (1996) Transient uptake and storage of serotonin in developing thalamic neurons. Neuron. 17:991-1003.

Lidov, H.G.; Molliver, M.E. (1982a) An immunohistochemical study of serotonin neuron development in the rat: ascending pathways and terminal fields. Brain Res Bull. 8:389-430.

Lidov, H.G.; Molliver, M.E. (1982b) Immunohistochemical study of the development of serotonergic neurons in the rat CNS. Brain Res Bull. 9:559-604.

Lillesaar, C.; Tannhäuser, B.; Stigloher, C.; Kremmer, E.; Bally-Cuif, L. (2007) The serotonergic phenotype is acquired by converging genetic mechanisms within the zebrafish central nervous system. Dev Dyn. 236:1072-1084.

Lumsden, A.; Keynes, R. (1989) Segmental patterns of neuronal development in the chick hindbrain. Nature. 337:424-8.

Luque, J.M.; Biou, V.; Nicholls, J.G. (1998) Three-dimensional visualization of the distribution, growth, and regeneration of monoaminergic neurons in whole mounts of immature mammalian CNS. J Comp Neurol. 390:427-438.

Mandado, M.; Molist, P.; Anadón, R.; Yáñez, J. (2001) A DiI-tracing study of the neural connections of the pineal organ in two elasmobranchs (*Scyliorhinus canicula* and *Raja montagui*) suggests a pineal projection to the midbrain GnRH-immunoreactive nucleus. Cell Tissue Res. 303:391-401.

Margolis-Kazan, H.; Halpern-Sebold, L.R.; Schreibman, M.P. (1985) Immunocyto-chemical localization of serotonin in the brain and pituitary gland of the platyfish, *Xiphophorus maculatus*. Cell Tissue Res. 240:311-314.

Marín, O.; González, A.; Smeets, W.J. (1997a) Basal ganglia organization in amphibians: efferent connections of the striatum and the nucleus accumbens. J Comp Neurol. 380:23-50.

Marín, O.; Smeets, W.J.; González, A. (1997b) Distribution of choline acetyltransferase immunoreactivity in the brain of anuran (*Rana perezi*, *Xenopus laevis*) and urodele (*Pleurodeles waltl*) amphibians. J Comp Neurol. 382:499-534.

Marín, O.; Smeets, W.J.; González, A. (1998) Basal ganglia organization in amphibians: chemoarchitecture. J Comp Neurol. 392:285-312.

McLean, D.L.; Fetcho, J.R. (2004a) Ontogeny and innervation patterns of dopaminergic, noradrenergic, and serotonergic neurons in larval zebrafish. J Comp Neurol. 480:38-56.

McLean, D.L.; Fetcho, J.R. (2004b) Relationship of tyrosine hydroxylase and serotonin immunoreactivity to sensorimotor circuitry in larval zebrafish. J Comp Neurol. 480:57-71.

McLean, J.H.; Shipley, M.T. (1987) Serotonergic afferents to the rat olfactory bulb: II. Changes in fibre distribution during development. J Neurosci. 7:3029-3039.

McLean, J.H.; Darby-King, A.; Sullivan, R.M.; King, S.R. (1993) Serotonergic influence on olfactory learning in the neonate rat. Behav Neural Biol. 60:152-162.

Medina, L.; Reiner, A. (1994) Distribution of choline acetyltransferase immunoreactivity in the pigeon brain. J Comp Neurol. 342:497-537.

Medina, L.; Reiner, A. (1995) Neurotransmitter organization and connectivity of the basal ganglia in vertebrates: implications for the evolution of basal ganglia. Brain Behav Evol. 46:235-258.

Medina, L.; Smeets, W.J.; Hoogland, P.V.; Puelles, L. (1993) Distribution of choline acetyltransferase immunoreactivity in the brain of the lizard *Gallotia galloti*. J Comp Neurol. 331:261-285.

Meek, J.; Joosten, H.W. (1989) Distribution of serotonin in the brain of the mormyrid teleost *Gnathonemus petersii*. J Comp Neurol. 281:206-224.

Meurling, P.; Rodríguez, E.M. (1990) The paraventricular and posterior recess organs of elasmobranchs: a system of cerebrospinal fluid-contacting neurons containing immunoreactive serotonin and somatostatin. Cell Tissue Res. 259:463-473.

Northcutt, R.G.; Ronan, M. (1992) Afferent and efferent connections of the bullfrog medial pallium. Brain Behav Evol. 40:1-16.

Northcutt, R.G.; Reiner, A.; Karten, H.J. (1988) Immunohistochemical study of the telencephalon of the spiny dogfish, *Squalus acanthias*. J Comp Neurol. 277:250-267.

Okado, N.; Sako, H.; Homma, S.; Ishikawa, K. (1992) Development of serotoninergic system in the brain and spinal cord of the chick. Prog Neurobiol. 38:93-123.

Parent, A.; Northcutt, R.G. (1982) The monoamine-containing neurons in the brain of the garfish, *Lepisosteus osseus*. Brain Res Bull. 9:189-204.

Parent, A.; Poitras, D.; Dubé, L. (1984) Comparative anatomy of central monoaminergic system. In: Björklund A, Hökfelt T, editors. Handbook of chemical neuroanatomy, Vol 2: Classical transmitters in the CNS, Part I. Amsterdam: Elsevier. p 409-439.

Petrova, E.S.; Otellin, V.A. (2007) Serotonin is involved in the regulation of histogenetic processes in rat embryonic neocortex. Bull Exp Biol Med. 143:372-375.

Philpot, B.D.; Jazaeri, A.A.; Brunjes, P.C. (1994) The development of serotonergic projections to the olfactory bulb of *Monodelphis domestica* (the grey, short-tailed opossum). Dev Brain Res. 77:265-270.

Pierre, J.; Repérant, J.; Ward, R.; Vesselkin, N.P.; Rio, J.P.; Miceli, D.; Kratskin, I. (1992) The serotoninergic system of the brain of the lamprey, *Lampetra fluviatilis*: an evolutionary perspective. J Chem Neuroanat. 5:195-219.

Piñuela, C.; Northcutt, R.G. (2007) Immunohistochemical organization of the forebrain in the white sturgeon, *Acipenser transmontanus*. Brain Behav Evol. 69:229-253.

Pombal, M.A.; Yáñez, J.; Marín, O.; González, A.; Anadón, R. (1999) Cholinergic and GABAergic neuronal elements in the pineal organ of lampreys, and tract-tracing observations of differential connections of pinealofugal neurons. Cell Tissue Res. 295:215-223.

Puelles, L.; Rubenstein, J.L.R. (1993) Expression patterns of homeobox and other putative regulatory genes in the embryonic mouse forebrain suggest a neuromeric organization. Trends Neurosci. 16:472-479.

Puelles, L.; Rubenstein, J.L. (2003) Forebrain gene expression domains and the evolving prosomeric model. Trends Neurosci. 26:469-476.

Rao, P.D.; Job, T.C.; Schreibman, M.P. (1993) Hypophysiotropic neurons in the hypothalamus of the catfish *Clarias batrachus*: a cobaltous lysine and HRP study. Brain Behav Evol. 42:24-38.

Rink, E.; Wullimann, M.F. (2004) Connections of the ventral telencephalon (subpallium) in the zebrafish (*Danio rerio*). Brain Res. 1011:206-220.

Ritchie, T.C.; Leonard, R.B. (1982) Immunocytochemical demonstration of serotonergic cells, terminals and axons in the spinal cord of the stingray, *Dasyatis sabina*. Brain Res. 240:334-337.

Ritchie, T.C.; Livingston, C.A.; Hughes, M.G.; McAdoo, D.J.; Leonard, R.B. (1983) The distribution of serotonin in the CNS of an elasmobranch fish: immunocytochemical and biochemical studies in the Atlantic stingray, *Dasyatis sabina*. J Comp Neurol. 221:429-443.

Roden, K.; Endepols, H.; Walkowiak, W. (2005) Hodological characterization of the septum in anuran amphibians: I. Afferent connections. J Comp Neurol. 483:415-436.

Rodríguez-Gómez, F.J.; Rendón-Unceta, M.C.; Sarasquete, C.; Muñoz-Cueto, J.A. (2000) Distribution of serotonin in the brain of the Senegalese sole, *Solea senegalensis*: an immunohistochemical study. J Chem Neuroanat. 18:103-115.

Rodríguez-Moldes, I.; Manso, M.J.; Becerra, M.; Molist, P.; Anadón, R. **(**1993) Distribution of substance P-like immunoreactivity in the brain of the elasmobranch *Scyliorhinus canicula*. J Comp Neurol. 335:228-244.

Rüdeberg, C. (1969) Light and electron microscopic studies on the pineal organ of the dogfish, *Scyliorhinus canicula* L. Z Zellforsch. 96:548-581.

Sako, H.; Kojima, T.; Okado, N. (1986) Immunohistochemical study on the development of serotoninergic neurons in the chick: I. Distribution of cell bodies and fibers in the brain. J Comp Neurol. 253:61-78.

Sano, Y.; Ueda, S.; Yamada, H.; Takeuchi, Y.; Goto, M.; Kawata, M. (1983) Immunohistochemical demonstration of serotonin-containing CSF-contacting neurons in the submammalian paraventricular organ. Histochem. 77:423-430.

Sauka-Spengler, T.; Baratte, B.; Shi, L.; Mazan, S. (2001) Structure and expression of an Otx5-related gene in the dogfish *Scyliorhinus canicula*: observed for a conserved role of Otx5 and Crx genes in the specification of photoreceptors. Dev Genes Evol. 211:533-544.

Sauka-Spengler, T.; Baratte, B.; Lepage, M.; Mazan, S. (2003) Characterization of brachyury genes in the dogfish *S. canicula* and the lamprey *L. fluviatilis*. Insights into gastrulation in a chondrichthyan. Dev Biol. 263:296-307.

Siemen, M.; Kunzle, H. (1994) Connections of the basal telencephalic areas c and d in the turtle brain. Anat Embryol. 189:339-359.

Smeets, W.J. (1981) Efferent tectal pathways in two chondrichthyans, the shark *Scyliorhinus canicula* and the ray *Raja clavata*. J Comp Neurol. 195:13-23.

Smeets, W.J.; Steinbusch, H.W. (1988) Distribution of serotonin immunoreactivity in the forebrain and midbrain of the lizard *Gekko gecko*. J Comp Neurol. 271:419-434.

Smeets, W.J.; Timerick, S.J.B. (1981) Cells origin of pathways descending to the spinal cord in two chondrichthyans, the shark *Scyliorhinus canicula* and the ray *Raja clavata*. J Comp Neurol. 202:473-491.

Smeets, W.J.; Marín, O.; González, A. (2000) Evolution of the basal ganglia: new perspectives through a comparative approach. J Anat. 196:501-517.

Steinbusch, H.W. (1984) Serotonin-immunoreactive neurons and their projections in the CNS. In: Björklund A, Kuhar MJ, Hökfelt T, editors. Handbook of chemical neuroanatomy, Vol 3: classical transmitters and transmitter receptors in the CNS, Part II. Amsterdam: Elsevier. pp. 68-125.

Steinbusch, H.W.; Verhofstad, A.A.; Penke, B.; Varga, J.; Joosten, H.W. (1981) Immunohistochemical characterization of monoamine-containing neurons in the central nervous system by antibodies to serotonin and noradrenalin. A study in the rat and the lamprey (*Lampetra fluviatilis*). Acta Histochem Suppl. 24:107-122.

Stuesse, S.L.; Cruce, W.L. (1991) Immunohistochemical localization of serotoninergic, enkephalinergic, and catecholaminergic cells in the brainstem and diencephalon of a cartilaginous fish, *Hydrolagus colliei*. J Comp Neurol. 309:535-548.

Stuesse, S.L.; Cruce, W.L. (1992) Distribution of tyrosine hydroxylase, serotonin, and leu-enkephalin immunoreactive cells in the brainstem of a shark, *Squalus acanthias*. Brain Behav Evol. 39:77-92.

Stuesse, S.L.; Cruce, W.L.; Northcutt, R.G. (1990) Distribution of tyrosine hydroxylase- and serotonin-immunoreactive cells in the central nervous system of the thornback guitarfish, *Platyrhinoidis triseriata*. J Chem Neuroanat. 3:45-58.

Stuesse, S.L.; Cruce, W.L.; Northcutt, R.G. (1991a) Localization of serotonin, tyrosine hydroxylase, and leu-enkephalin immunoreactive cells in the brainstem of the horn shark, *Heterodontus francisci*. J Comp Neurol. 308:277-292.

Stuesse, S.L.; Cruce, W.L.; Northcutt, R.G. (1991b) Serotoninergic and enkephalinergic cell groups in the reticular formation of the bat ray and two skates. Brain Behav Evol. 38:39-52.

Stuesse, S.L.; Stuesse, D.C.; Cruce, W.L. (1995) Raphe nuclei in three cartilaginous fishes, *Hydrolagus colliei*, *Heterodontus francisci*, and *Squalus acanthias*. J Comp Neurol. 358:414-427.

Sueiro, C.; Carrera, I.; Rodríguez-Moldes, I.; Molist, P.; Anadón, R. (2003) Development of catecholaminergic systems in the spinal cord of the dogfish *Scyliorhinus canicula* (Elasmobranchs). Dev. Brain Res. 142:141-150.

Sueiro, C.; Carrera, I.; Molist, P.; Rodríguez-Moldes, I.; Anadón, R. (2004) Development and distribution of glutamic acid decarboxylase (GAD)-immunoreactive systems in the spinal cord of the dogfish *Scyliorhinus canicula* (Elasmobranchs). J. Comp Neurol. 478:189-206.

Sueiro, C.; Carrera, I.; Ferreiro, S.; Molist, P.; Adrio, F.; Anadón, R.; Rodríguez-Moldes, I. (2007) New insights on saccus vasculosus evolution: A developmental and immunohistochemical study in elasmobranchs. Brain Behav Evol. 70:187-204.

Tamotsu, S.; Korf, H.W.; Morita, Y.; Oksche, A. (1990) Immunocytochemical localization of serotonin and photoreceptor-specific proteins (rod-opsin, S-antigen) in the pineal complex of the river lamprey, *Lampetra japonica*, with special reference to photoneuroendocrine cells. Cell Tissue Res. 262:205-216.

Tamotsu, S.; Samejima, M.; Suzuki, N.; Morin, Y. (1997) Three-dimensional reconstruction of serotonin-immunoreactive photoreceptors in the pineal organ of the river lamprey, *Lampetra japonica*. Biol Signals. 6:184-190.

Ten Eyck, G.R.; Jermakowicz, W.J.; Chinn, A.F.; Summers, C.H. (2005) Ontogeny of central serotonergic neurons in the directly developing frog, *Eleutherodactylus coqui*. Anat Embryol. 210:221-233.

Teraoka, H.; Russell, C.; Regan, J.; Chandrasekhar, A.; Concha, M.L.; Yokoyama, R.; Higashi, K.; Take-Uchi, M.; Dong, W.; Hiraga, T.; Holder, N.; Wilson, S.W. (2004) Hedgehog and Fgf signaling pathways regulate the development of tphR-expressing serotonergic raphe neurons in zebrafish embryos. J Neurobiol. 60:275-288.

Timerick, S.J.; Roberts, B.L.; Paul, D.H. (1992) Brainstem neurons projecting to different levels of the spinal cord of the dogfish *Scyliorhinus canicula*. Brain Behav Evol. 39:93-100.

Ueda, S.; Takeuchi, Y.; Sano, Y. (1983) Immunohistochemical demonstration of serotonin neurons in the central nervous system of the turtle (*Clemmys japonica*). Anat Embryol. 168:1-19.

Ueda, S.; Nojyo, Y.; Sano, Y. (1984) Immunohistochemical demonstration of the serotonin neuron system in the central nervous system of the bullfrog, *Rana catesbeiana*. Anat Embryol. 169:219-229.

van Kesteren, R.E.; Spencer, G.E. (2003) The role of neurotransmitters in neurite outgrowth and synapse formation. Rev Neurosci. 14:217-231.

van Mier, P.; Joosten, H.W.; van Rheden, R.; ten Donkelaar, H.J. (1986) The development of serotonergic raphespinal projections in *Xenopus laevis*. Int J Dev Neurosci. 4:465-475.

van Veen, T.; Ekström, P.; Borg, B.; Moller, M. (1980) The pineal complex of the three-spined stickleback, *Gasterosteus aculeatus* L.: a light-, electron microscopic and fluorescence histochemical investigation. Cell Tissue Res. 209:11-28.

van Veen, T.; Ekström, P.; Nyberg, L.; Borg, B.; Vigh-Teichmann, I.; Vigh, B. (1984) Serotonin and opsin immunoreactivities in the developing pineal organ of the three-spined stickleback, *Gasterosteus aculeatus* L. Cell Tissue Res.. 237:559-564.

Wai, M.S.; Lorke, D.E.; Zhang, A.; Kung, H.F.; Yew, D.T. (2007) Study of the spinal cords of the sturgeon Acipenser schrenckii, gar Lepisosteus oculatus, and goldfish *Carassius auratus* by morphological, immunohistochemical, and biochemical approaches. Microsc Res Tech. 70:1079-1090.

Wallace, J.A.; (1985) An immunocytochemical study of the development of central serotoninergic neurons in the chick embryo. J Comp Neurol. 236:443-453.

Wallace, J.A.; Lauder, J.M. (1983) Development of the serotonergic system in the rat embryo: an immunocytochemical study. Brain Res Bull. 10:459-479.

Wang, Y.; Takai, R.; Yoshioka, H.; Shirabe, K. (2006) Characterization and expression of serotonin transporter genes in zebrafish. Tohoku J Exp Med. 208:267-274.

Whitaker-Azmitia, P.M.; Druse, M.; Walker, P.; Lauder, J.M. (1996) Serotonin as a developmental signal. Behav Brain Res. 73:19–29.

Wild, J.M.; Farabaugh, S.M. (1996) Organization of afferent and efferent projections of the nucleus basalis prosencephali in a passerine, *Taeniopygia guttata*. J Comp Neurol. 365:306-328.

Woolston, A.M.; Wedderburn, J.F.; Sillar, K.T. (1994) Descending serotonergic spinal projections and modulation of locomotor rhythmicity in *Rana temporaria* embryos. Proc R Soc Lond. 255:73-79.

Yamanaka, S.; Honma, Y.; Ueda, S.; Sano, Y. (1990) Immunohistochemical demonstration of serotonin neuron system in the central nervous system of the Japanese dogfish, *Scyliorhinus torazame* (Chondrichthyes). J Hirnforsch. 31:385-397.

Yáñez, J. (1992) Estudio histoquímico e inmunohistoquímico sobre la organización larvaria de algunos sistemas monoaminérgicos y peptidérgicos del encéfalo de la lamprea de mar (*Petromyzon marinus* L.). PhD Thesis. University of Santiago de Compostela, Santiago de Compostela.

Yáñez, J.; Pombal, M.A.; Anadón, R. (1999) Afferent and efferent connections of the parapineal organ in lampreys: a tract tracing and immunocytochemical study. J Comp Neurol. 403:171-189.

Yoshida, M.; Nagatsu, I.; Kondo, Y.; Karasawa, N.; Ohno, T.; Spatz, M. Nagatsu, T. (1982) Two cell types in monoamine-containing "liquor contacting" neuron system of frog brain. Experient. 38:1097-1099.

Yoshida, M.; Nagatsu, I.; Kawakami-Kondo, Y.; Karasawa, N.; Spatz, M.; Nagatsu, T. (1983) Monoaminergic neurons in the brain of goldfish as observed by immunohistochemical techniques. Experientia. 39:1171-1174.

Zhang, W.; Pombal, M.A.; el Manira, A.; Grillner, S. (1996) Rostrocaudal distribution of 5-HT innervation in the lamprey spinal cord and differential effects of 5-HT on fictive locomotion. J Comp Neurol. 374:278-290.

Zhao, B.; Debski, E.A. (2005) Serotonergic reticular formation cells in *Rana pipiens*: categorization, development, and tectal projections. J Comp Neurol. 487:441-456.

Zhou, F.C.; Sari, Y.; Zhang, J.K. (2000) Expression of serotonin transporter protein in developing rat brain. Dev Brain Res. 119:33-45.

ABBREVIATIONS

AC cerebellar auricula
ACS central superficial area
APV ventrolateral periventricular area
ASB basal superficial area
B9 nucleus reticularis B9
Cb cerebellum
cc central canal
CN cerebellar nucleus
DH dorsal horn
Di diencephalon
FP floor plate
Fr fascilus retroflexus
GR cerebellar granular layer
H hypophysis
Ha habenula
i infundibulum
IHL inferior hypothalamic lobe
III oculomotor nucleus
IIIr oculomotor nerve root
IP interpeduncular nucleus
IS isthmus
IV trochlear nucleus
IX glossopharyngei nucleus
LC locus coeruleus
LNI neurointermediate lobe
ME median eminence
Mes mesencephalon
mlf medial longitudinal fascicle
MOL cerebellar molecular layer
n notochord
OB olfactory bulb
On optic nerve
OT optic tectum
P pallium
Pc posterior commissure
pi pineal organ
PO preoptic area
Pr posterior recess
Pret pretectum
Pro posterior recess organ
PTN posterior tubercle nucleus
PVO paraventricular organ
R Rathke's pouch
r1-r8 rhombomeres
RaC raphe centralis superior nucleus
RaD raphe dorsalis nucleus
RaDa raphe dorsalis anterioris nucleus
RaL raphe linearis nucleus
RaM raphe magnus nucleus
RaO raphe obscurus nucleus
RaP raphe pallidus nucleus
RG gigantocellular reticular nucleus
Rh rhombencephalon
RM magnocellular reticular nucleus
RO nucleus reticularis pontis oralis
ROL nucleus reticularis pontis oralis, lateral part
ROM nucleus reticularis pontis oralis, medial part
Rpo preoptic recess
RSc subcoeruleus reticular nucleus
SCN suprachiasmatic nucleus
Sp subpallium
Spc spinal cord
SV saccus vasculosus
Syn synencephalon
Td dorsal thalamus
Tel telencephalon
Tv ventral thalamus
VH ventral horn
VI abducens nucleus
VII facial nucleus
VII+VIIIr acusticofacial nerve root
VIIIm magnocellular octaval nucleus
VIM visceromotor column
VIS viscerosensory column
Vm trigeminal motor nucleus
Vr trigeminal nerve root
VTA/SN ventral tegmental area/substantia nigra
X vagus nucleus

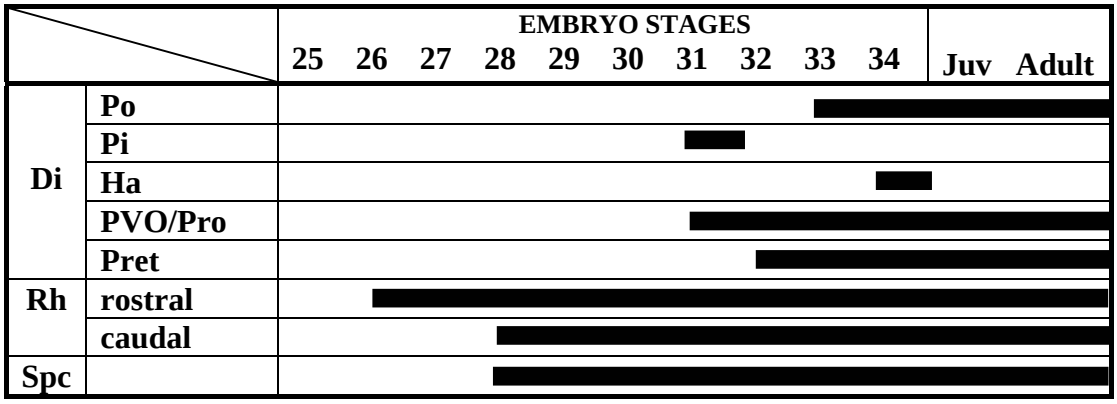

Table I. Timetable of the appearance of 5-HT-ir cell groups in the dogfish brain during development.

	(Ritchie et al., 1983) *Dasyatis sabina*	(Yamanaka et al., 1990) *Scyliorhinus torazame*	(Stuesse et al.,1991a) *H. francisci* (Stuesse and Cruce, 1992) *Squalus acanthias* (present study) *S. canicula*	
Spinal cord	group I	group S1	spinal cord cells	INFERIOR RAPHE AND RETICULAR GROUPS
Rhombencephalon	group II	group S2	raphe pallidus	
	—	group S3	raphe obscurus	
	—	—	raphe magnus	
	—	—	retic. gigantocellularis	
	—	—	retic. magnocellularis	
	scattered cells	group S4	raphe dorsalis	SUPERIOR RAPHE AND RETICULAR GROUPS
	group IV	group S5	raphe centralis superior	
	scattered cells	—	subcoeruleus	
	group IV	group S6	retic. pontis oralis medialis/ lateralis	
	group V	group S7	raphe linearis	
	group VI	group S7	B9	
	—	—	raphe dorsalis anterioris	

Table II. Comparison of the nomenclatures used for brainstem serotoninergic cell groups in different cartilaginous fish. The 5-HT-ir raphe cell groups are shown in gray boxes.

	Po	PVO/ tuber	Pro / mamillary region	Pret	Isthmus/sup. raphe n.	Caudal Rh/ Inf. raphe n.	Spinal cord
S. canicula (present study)	5th	4th	4th	6th*	1st	2nd	3rd
Petromyzon marinus (Abalo et al., 2007)	7th	3rd	5th	6th	1st	4th	2nd
Gasterosteus aculeatus (Ekström et al., 1985)	-	1st	3rd	2nd	1st	1st	?
Salvelinus fontinalis (Bolliet and Ali, 1992)	-	2nd	6th	4th	1st	3rd	5th
Scomber scombrus (Bolliet et al., 1994)	-	1st	5th	4th	2nd	3rd	?
Danio rerio (McLean and Fetcho, 2004)	-	4th	1st	4th	3rd	4th	2nd
Chick (Wallace, 1985)	-	4th	-	-	1st	2nd	3rd
Rat (Wallace and Lauder. 1983)	-	-	-	-	1st	2nd	3rd

(*), transient 5-HT-ir cells. For abbreviations, see list.

Table III. Comparison of the order of appearance of CNS serotoninergic cell groups among vertebrates.

Figure 1. Schematic representations of sagittal sections of brains of dogfish embryos at S26 (**a**), S28 (**b**), S31 (**c**) and S33 (**d**) showing the distribution of 5-HT-ir cells (circles) and fibers (thin lines). The diencephalic-mesencephalic and mesencephalic-rhombencephalic boundaries are represented by broken lines. The location of the exit of some cranial nerves (III,V,VII,VIII), and the tentative location of rhombomeres (r1-r8) are also shown. Scale bars: 100 μm (A-C); 250 μm (D).

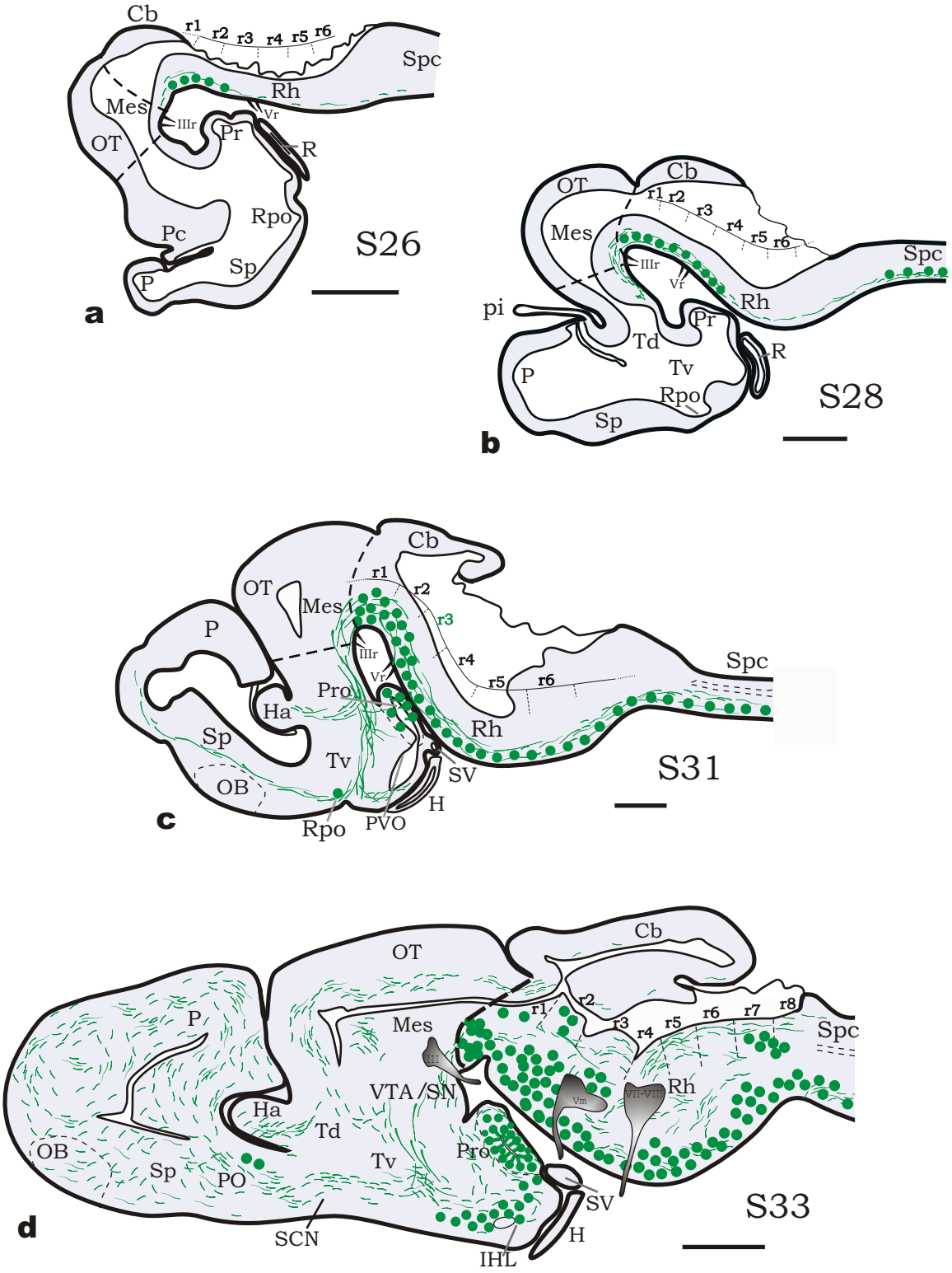
Cb
r1 r2 r3 r4 r5 r6
Spc
Rh
Mes
IIIr
Vr
Pr
R
OT
Rpo
Pc
Sp
P
S26
a
OT
Cb
r1 r2 r3 r4 r5 r6
Mes
IIIr
Vr
Spc
pi
Rh
Pr
Td
R
P
Tv
Rpo
Sp
S28
b
Cb
OT
r1
r2
Mes
r3
P
IIIr
Vr
r4
r5
r6
Spc
Pro
Ha
Rh
Sp
Tv
SV
S31
OB
H
c
Rpo
PVO
Cb
OT
P
r1
r2
Mes
r3
r4
r5
r6
r7
r8
Spc
VTA/SN
Rh
Ha
Td
OB
Pro
Sp
Tv
PO
SV
S33
d
SCN
H
IHL

Fig. 1

Figure 2. Photomicrographs of sagittal (**A,B,G-I**) and transverse (**C-F,J-Q**) sections through the brain (**A–C,E-O**) and spinal cord (**D,P,Q**) of embryos of *Scyliorhinus canicula*, showing the distribution of 5-HT-ir cells and fibers at S26 (**A-D**), S27 (**E,F**), S28 (**G-I**) and S29 (**H-Q**). **A,** Rostral brainstem of S26 showing 5-HT-ir cells of the superior reticular formation group (arrowheads). The broken line marks the mesencephalic rhombencephalic boundary. Rostral is to the left. **B,** Detail of the squared area in **A**, showing some faint 5-HT-ir perikarya in the superior reticular formation group (arrowheads). **C,** Section at the isthmus level of S26 showing some faint 5-HT-ir perikarya at ventral levels (arrowheads). Star marks the ventricle. **D,** Rostral spinal cord of S26, showing 5-HT-ir fibers (arrow) at both sides of the floor plate. **E,** Transverse section of S27 at the rostral level of the trigeminal nerve exit showing the absence of 5-HT-ir cells. Note the longitudinal 5-HT-ir fibers (arrows) in the basal plate. **F,** Detail of the squared area in E, showing some longitudinal 5-HT-ir fibers (arrows). **G,** Sagittal section at S28 showing 5-HT-ir cells at a rostral rhombencephalic level (arrowheads). Note some ascending 5-HT-ir fibers along the mesencephalic and synencephalic tegmenti, rostral to the isthmus (arrows). The broken line marks the mesencephalic-rhombencephalic boundary. **H,** Parasagittal section of the rhombencephalon at S28 showing 5-HT-ir cells (arrowheads) caudal to the trigeminal nerve exit. **I,** 5-HT-ir leading process with growing cones (arrow) emerged from rhombencephalic cells (arrowhead) at late S28. Caudal is to the right. **J,** Section at a rostral rhombencephalic level in S29 showing 5-HT-ir cells in the primordia of the *raphe dorsalis anterioris* (arrowhead), *raphe linearis* (white arrowhead) and *B9* reticular group (white arrows). Note the 5-HT-ir cell processes that cross the basal plate (arrow). **K,** Section at a more caudal level showing 5-HT-ir cells in the primordia of the raphe *centralis superioris* (arrows) and reticular *pontis oralis* (arrowheads). Note abundant 5-HT-ir cells and fibers in the basal plate (thin arrow). **L,** Section rostral to the acusticofacial nerve level showing the primordial 5-HT-ir cells of raphe *dorsalis* (arrow), raphe *centralis superioris* (white arrow) and reticular *pontis oralis* (arrowhead) nuclei at S29. **M,** Section at the acusticofacial nerve level showing low density of 5-HT-ir cells (arrow). **N,** Section at a level caudal to the former figure showing 5 HT-ir cells in the raphe *magnus* (arrowhead) and reticular *magnocellularis* (arrow). **O,** Section at the caudal rhombencephalon showing 5-HT-ir cells in the raphe *obscurus* (arrowhead) and raphe *pallidus* (arrow) at S29. **P,** Section of the rostral spinal cord showing some ventral 5-HT-ir cells (arrow) and 5-HT-ir fibers in the ventral (black arrowhead), lateroventral (white arrow) and lateral (white arrowhead) margin. **Q,** Detail of the ventral part of the rostral spinal cord showing a 5-HT-ir cell process (arrow) extended towards the ventricle (cc) in S29. Scale bars: 250 μm (A,G); 50 μm (B-D,F,I-L,N,O); 100 μm (E,H,M,P); 25 μm (Q).

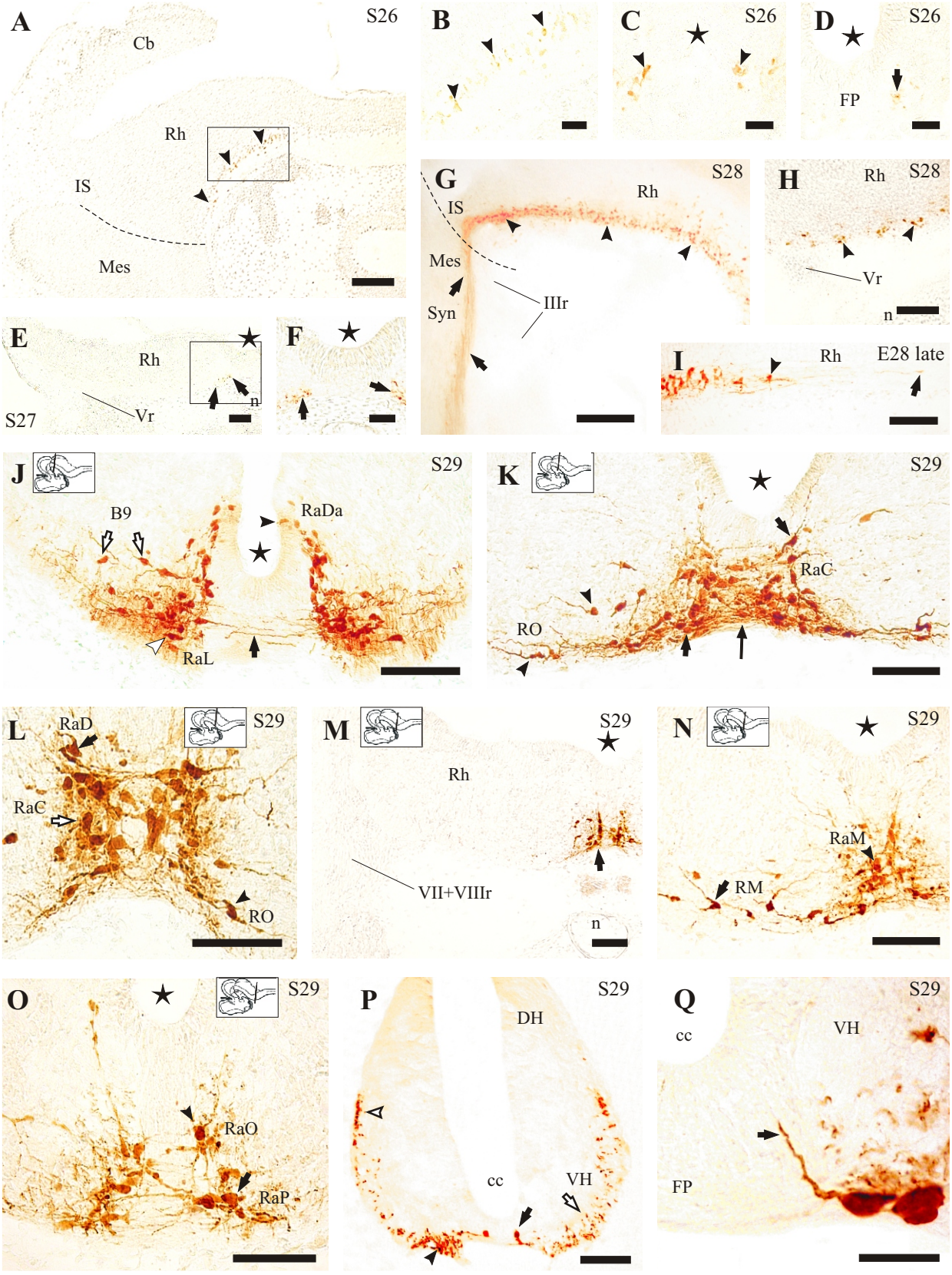
A
S26
Cb
Rh
IS
Mes
B
C
S26
D
S26
FP
G
S28
Rh
IS
Mes
Syn
IIIr
H
Rh
S28
Vr
n
E
Rh
n
S27
Vr
F
I
Rh
E28 late
J
S29
B9
RaDa
RaL
K
S29
RaC
RO
L
RaD
S29
RaC
RO
M
S29
Rh
VII+VIIIr
n
N
S29
RaM
RM
O
S29
RaO
RaP
P
S29
DH
cc
VH
Q
S29
cc
VH
FP

Fig. 2

Figure 3. Photomicrographs of sagittal (**A-E**) and transverse (**F-J**) sections through the brain (**A-H**) and spinal cord (**I,J**) of S31 (**A-J**) of *Scyliorhinus canicula* showing the distribution of 5 HT-ir cells and fibers. **A,** Sagittal section showing 5-HT-ir cells in the basal rhombencephalon (arrowhead), which is the source of 5-HT-ir fibers that course throughout the mesencephalon and diencephalons regions (arrows). **B,** Detail of a parasagittal section parallel to the former figure showing the ascending 5-HT-ir fibers in the mesencephalon and diencephalon. Note the 5-HT-ir fibers that course parallel to the fasciculus retroflexus (arrow). **C,** Detail of the squared area in B, showing a thin fascicle of 5-HT-ir fibers (arrow) that reach the habenula. Note some 5-HT-ir fibers in the posterior commissure. **D,** Faint 5-HT-ir cells are observed in the posterior recess (arrows) and paraventricular (white arrow) nuclei at S31. Note also the 5-HT-ir fibers that innervate the margin of the posterior (white arrowhead) and anterior (black arrowhead) hypothalamic walls. **E,** Section more lateral to that of figure A showing 5-HT-ir fibers innervating the rostral diencephalon, and the first 5-HT-ir fibers innervating the telencephalon (arrows). **F,** Transverse section of the telencephalon showing a few 5-HT-ir fibers coursing rostrally through the palliosubpallial border (arrowhead). **G,** Transverse section of the pineal organ of S31, showing some faint 5-HT-ir cells (arrowheads). **H,** 5-HT-ir fibers coursing longitudinally through the lateral diencephalic tegmentum (arrowhead) while some 5-HT-ir fibers cross the posterior commissure (arrow). **I,** Rostral spinal cord of S31 showing 5-HT-ir cells in the ventral margin (arrow) and longitudinal fibers in the laterodorsal margin (arrowhead). **J,** Mid-rostrocaudal level of the spinal cord showing 5-HT-ir fibers coursing longitudinally along the lateral margin (arrowhead). Note the absence of 5-HT immunoreactivity in ventral regions. Scale bars: 500 μm (A,B); 100 μm (C,H-J); 250 μm (D,E); 50 μm (F,G).

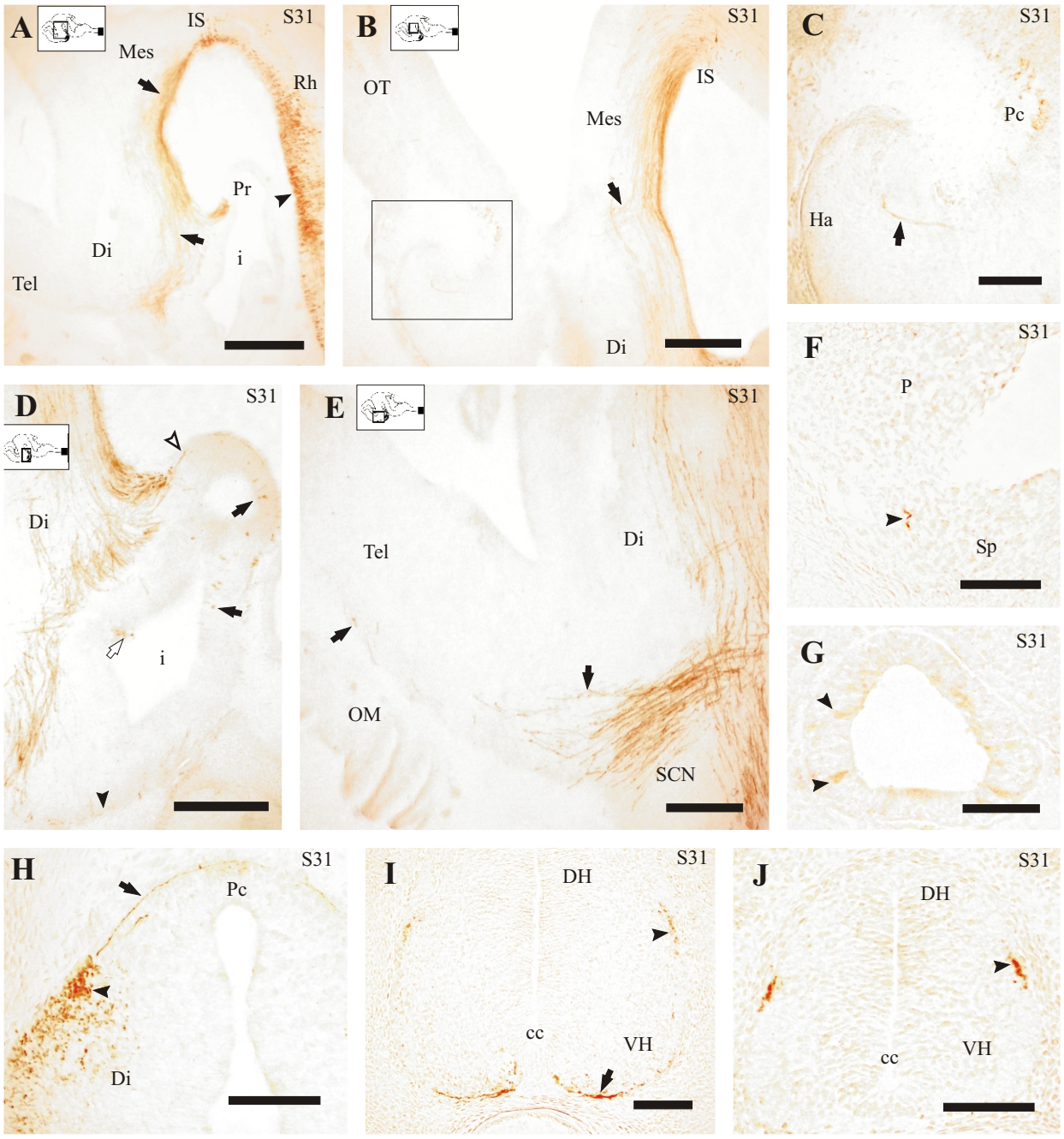
A
IS
S31
Mes
Rh
Pr
Di
i
Tel
B
S31
OT
IS
Mes
Di
C
S31
Pc
Ha
F
S31
P
Sp
D
S31
Di
i
E
S31
Tel
Di
OM
SCN
G
S31
H
S31
Pc
Di
I
S31
DH
cc
VH
J
S31
DH
cc
VH

Fig. 3

Figure 4. Drawing of a parasagittal section of the dogfish brain that schematically represents the main ascending and descending serotoninergic fiber pathways at S31. Scale bar: 100 µm.

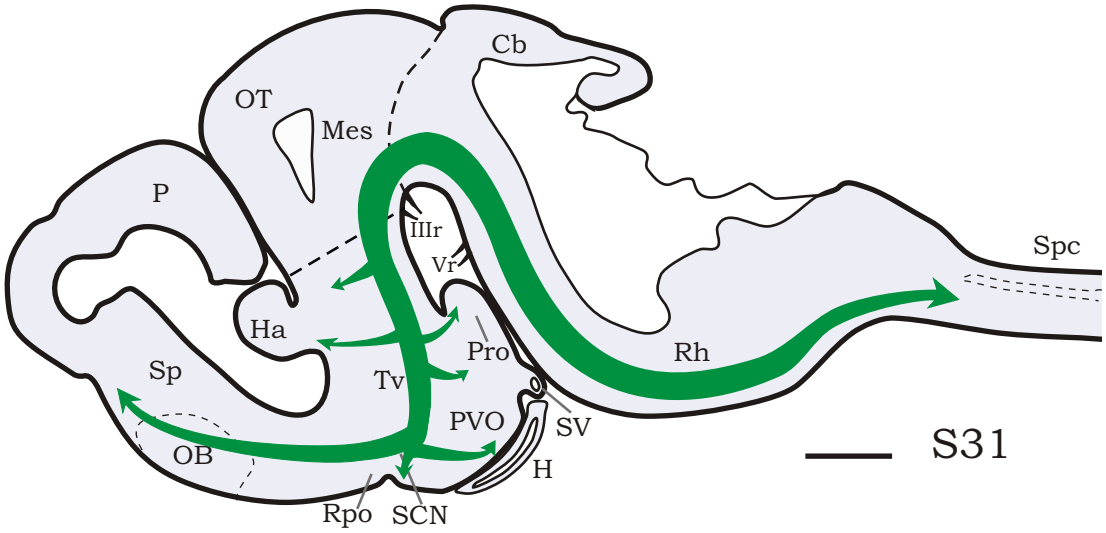

Fig. 4

Figure 5. Photomicrographs of transverse sections through the brain of S32 (**A-E**) and S33-S34 (**F-K**) showing the distribution of 5-HT-ir cells and fibers. **A,** 5-HT-ir fibers are observed in the margin of the olfactory bulb (arrowhead) in S32. **B,** 5-HT-ir fibers course throughout the lateral pallium (arrow) to the medial pallium (arrowhead). **C,** 5-HT-ir innervation is abundant in the marginal region of the subpallium (arrow) of S32, whereas it is scarce in the cell-rich band of the basal superficial area (arrowhead). Note the abundant 5-HT-ir innervation in the septum region (white arrowhead). **D,** 5-HT-ir cells (arrowheads) in the pretectum. Medial is to the left. **E,** Section at the level of the optic chiasm showing some 5-HT-ir fibers in the optic nerve (arrow) of S32. Medial is to the right. **F,** 5-HT-ir fibers innervate the olfactory bulb granule cell layer of a late S33. **G,** Subpallium of S33 containing few 5-HT-ir fibers in the basal superficial area (arrowhead) and abundant fibers in the dorsal and ventral areas. Note also the density of 5-HT-ir fibers in the palliosubpallial border (arrow). **H,** Detail of the dorsal telencephalon showing the 5-HT-ir innervation in the dorsal pallium at S33. **I,** Preoptic area of S33 showing 5-HT-ir cells, some of them CSF-c (arrowheads) cells. **J,** Pineal organ of S33 showing some 5-HT-ir fibers (arrowheads) in the pineal stalk. **K,** Some 5-HT-ir cells are observed in the habenula of a prehatching embryo (arrowheads). Note also the moderate density of 5-HT-ir fibers in the laterodorsal region (arrow). Insets: Details of the faint 5-HT-ir habenular cells. Scale bars: 50 μm (A,D,I,J); 250 μm (B,C,G); 100 μm (E,F,H,K); 25 μm (K details).

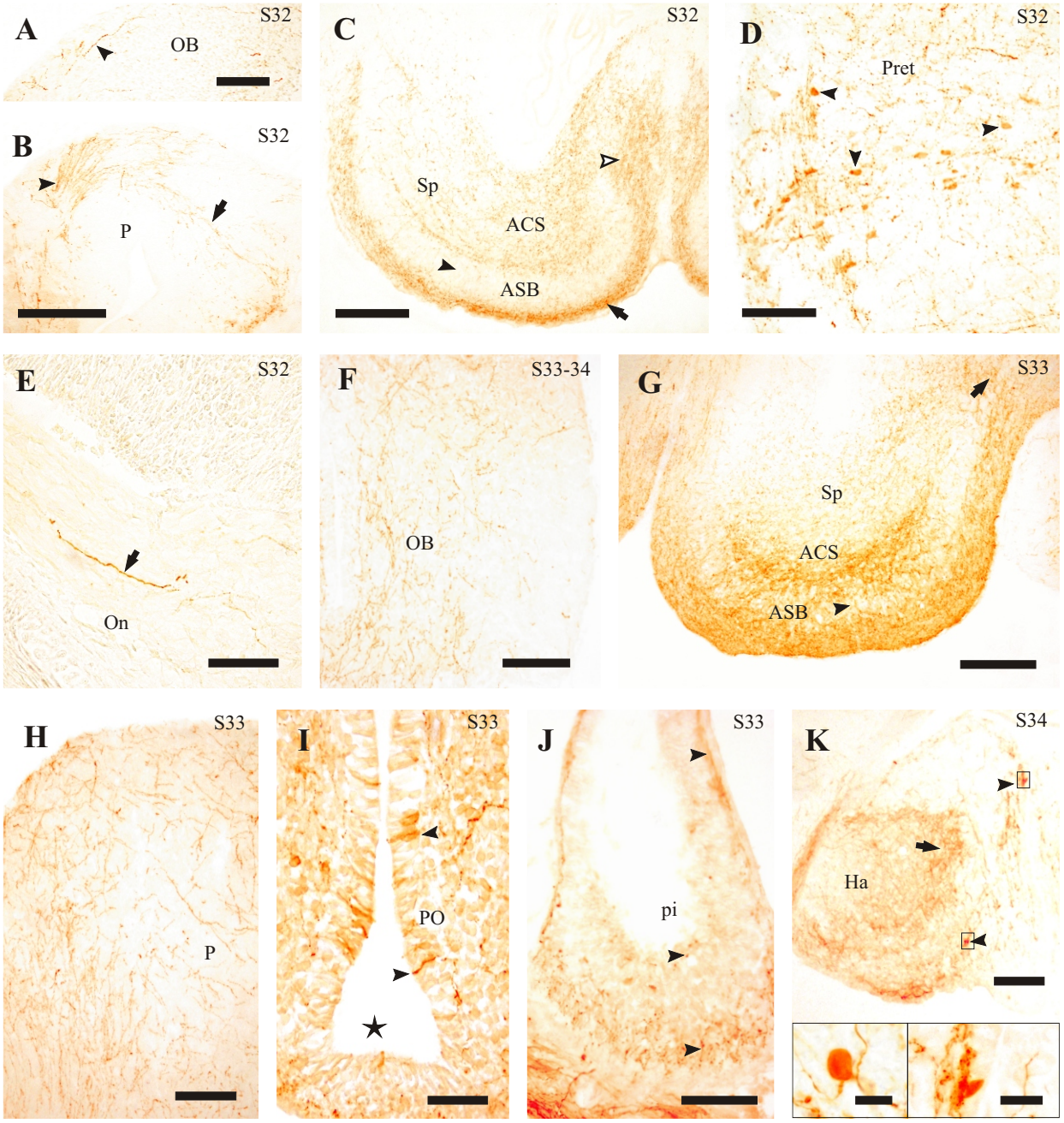
A
S32
OB
B
S32
P
C
S32
Sp
ACS
ASB
D
S32
Pret
E
S32
On
F
S33-34
OB
G
S33
Sp
ACS
ASB
H
S33
P
I
S33
PO
J
S33
pi
K
S34
Ha

Fig. 5

Figure 6. (A-S). Schematic drawings of transverse sections through the brain and rostral spinal cord of a juvenile dogfish, showing at the right the distribution of 5-HT-ir perikarya and fibers and at the left the anatomical landmarks. Upper drawing represents a sagittal section of the brain showing the level of transverse sections. For abbreviations, see list. Scale bars: 2 mm.

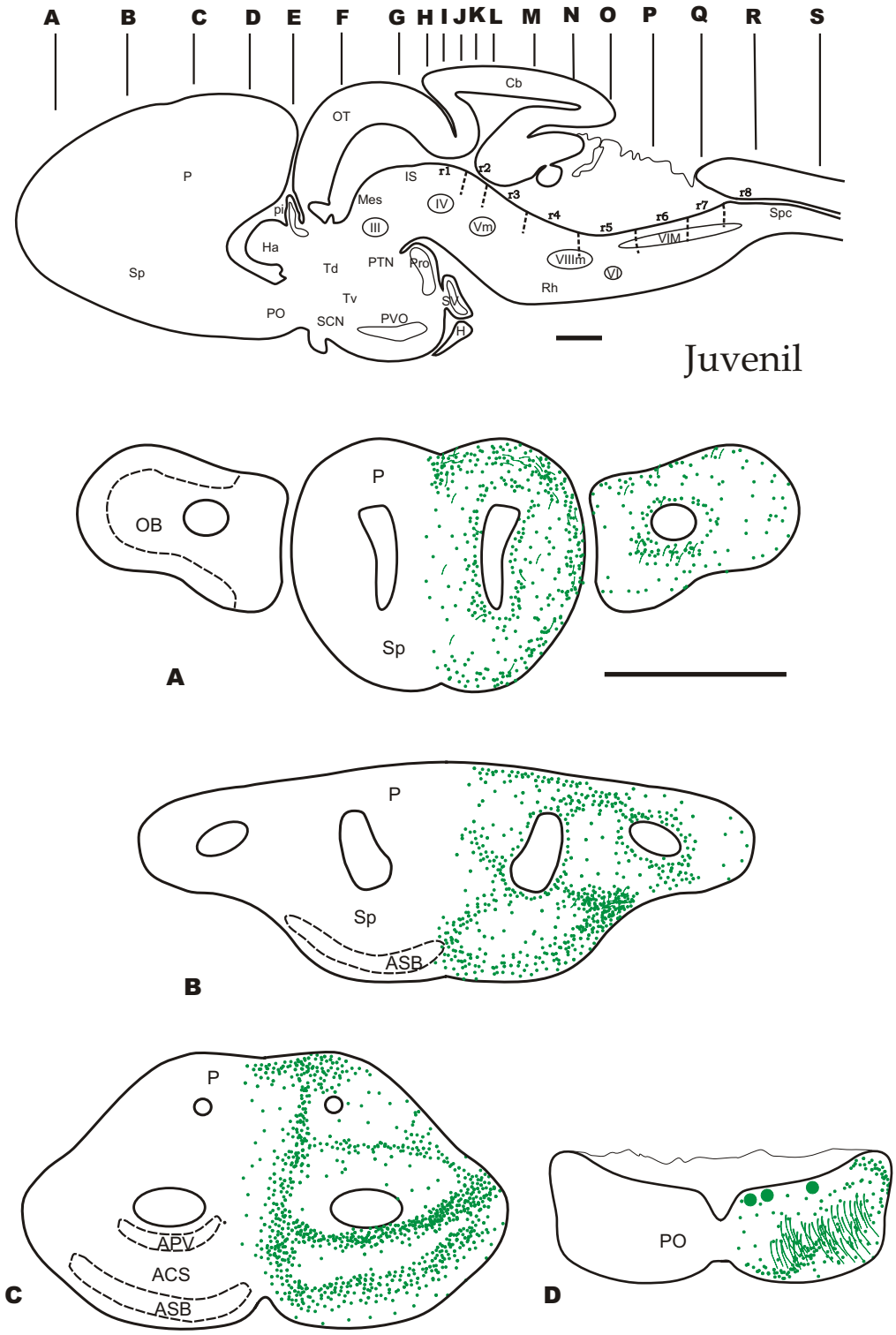
A B C D E F G H I J K L M N O P Q R S
Cb
OT
P
IS
r1
r2
r3
r4
r5
r6
r7
r8
Mes
IV
Vm
III
pi
Ha
Sp
Td
PTN
Rro
Tv
PO
SCN
PVO
H
VIIIm
VI
VIM
Spc
Rh
Juvenil
OB
P
Sp
A
P
Sp
ASB
B
P
APV
ACS
ASB
C
PO
D

Fig. 6

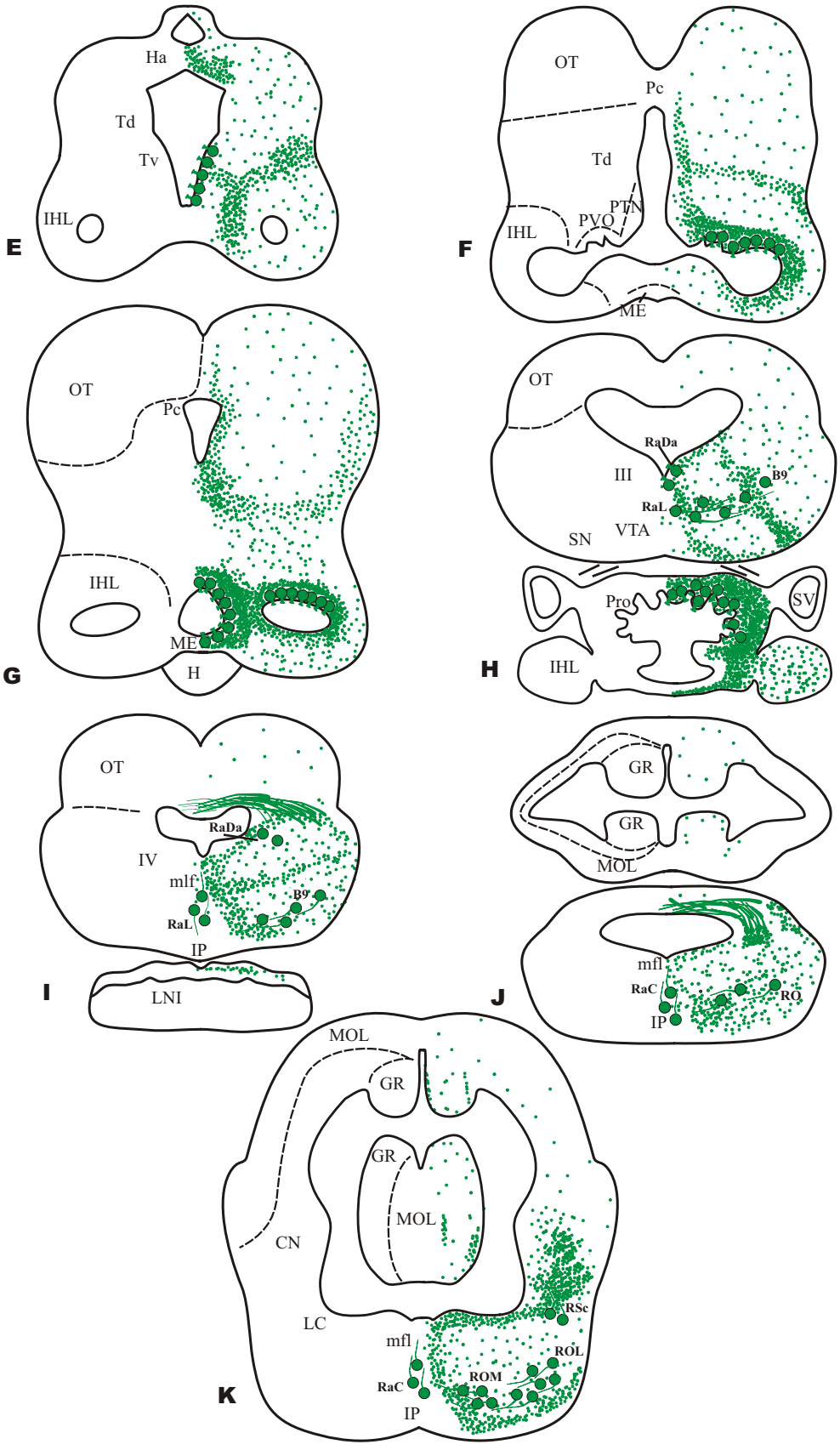
E
Ha
Td
Tv
IHL
F
OT
Pc
Td
PTN
PVO
IHL
ME
G
OT
Pc
IHL
ME
H
H
OT
RaDa
III
B9
RaL
VTA
SN
Pro
SV
IHL
I
OT
RaDa
IV
mlf
B9
RaL
IP
LNI
J
GR
GR
MOL
mfl
RaC
RO
IP
K
MOL
GR
GR
MOL
CN
LC
RSc
mfl
ROL
RaC
ROM
IP

Fig. 6 (cont. I)

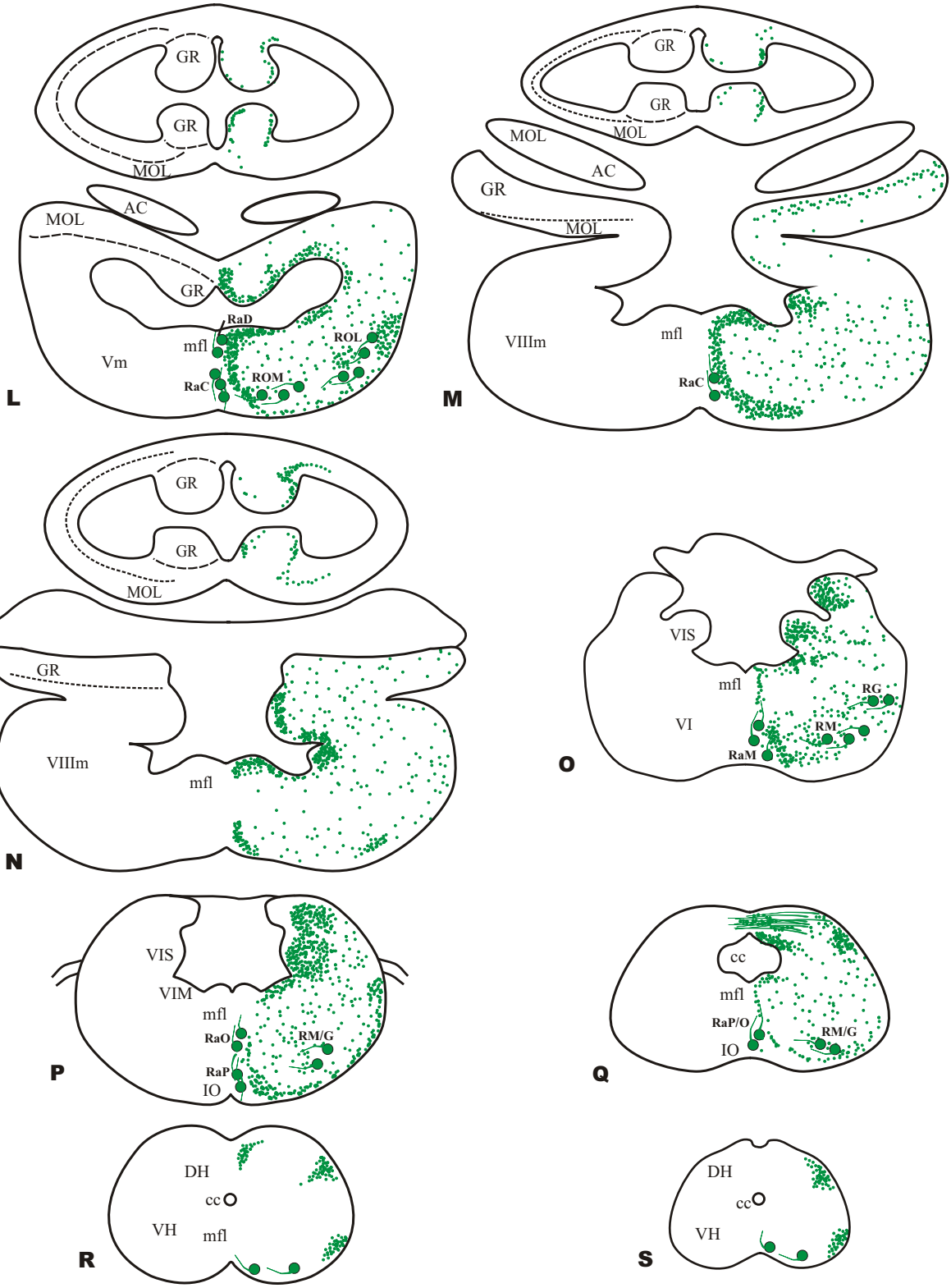
GR
GR
MOL
AC
MOL
GR
RaD
mfl
ROL
Vm
RaC
ROM
L
GR
GR
MOL
MOL
AC
GR
MOL
VIIIm
mfl
RaC
M
GR
GR
MOL
GR
VIIIm
mfl
N
VIS
mfl
RG
VI
RM
RaM
O
VIS
VIM
mfl
RaO
RM/G
RaP
IO
P
cc
mfl
RaP/O
RM/G
IO
Q
DH
cc
VH
mfl
R
DH
cc
VH
S

Fig. 6 (cont. II)

Figure 7. Photomicrographs of transverse (**A-J,L,M**) and sagittal (**K**) sections of the telencephalon (**A-D**), preoptic area (**E**) and diencephalon (**F-M**) of adults (**A,G-I**) and juveniles (**B-F,J-M**) of *Scyliorhinus canicula* showing the distribution of 5-HT-ir cells and fibers. **A,** 5-HT-ir fibers in the olfactory bulb are moderately abundant in the granule cell layer and scarce in the glomerular cell layer (arrow). Note the lack of 5-HT-ir fibers in the olfactory fiber layer (arrowhead). **B,** 5-HT-ir fibers in dorsal pallium (white arrows). **C**, 5-HT-ir fibers in caudal subpallium of a juvenile. Note that 5-HT-ir fibers are more abundant in the ventral and marginal regions of the basal superficial area (ASB, arrow) and in the palliosubpallial border (white arrow). **D,** Section of the caudal subpallium showing abundant 5-HT-ir fibers in the septal region (white arrow). **E,** 5-HT-ir cells and fibers in preoptic area of a juvenile. **F,** Transverse section of the caudal hypothalamus of a juvenile showing 5-HT-ir cells and fibers in the posterior recess organ (arrow) and the paraventricular organ (arrowhead). Note the scarce 5-HT-ir innervation in the inferior hypothalamic lobe, and the moderate innervation in the hypothalamic floor. **G,** Some 5-HT-ir CSF-c cells in the dorsal walls of the inferior hypothalamic lobe (arrows). **H,** Transverse section showing 5-HT-ir fibers in the median eminence (arrows). Note the absence of immunoreactivity in the adenohypophysis (A). **I,** Section showing some 5-HT-ir fibers (arrow) in the caudal part of the neurointermediate lobe of an adult. **J,** Abundant 5-HT-ir fibers were observed in the habenular laterodorsal region (arrow) while a conspicuous tract was observed in the habenular commissure (arrowhead). Note also 5-HT-ir fibers in other habenular regions. **K,** Sagittal section of a juvenile pineal organ, showing 5-HT-ir fibers in the pineal stalk (arrowheads). **L,** Transverse section at the level of the pretectum showing a 5-HT-ir cell (arrowhead) lateral to the fasciculus retroflexus of a juvenile. **M,** A single 5-HT-ir fiber reaching the ventricle in the subcommissural organ (arrow) of a juvenile. For abbreviations see list. Scale bars: 100 µm (A,I,K,L); 250 µm (B-D,F,H,J); 50 µm (E,G,M).

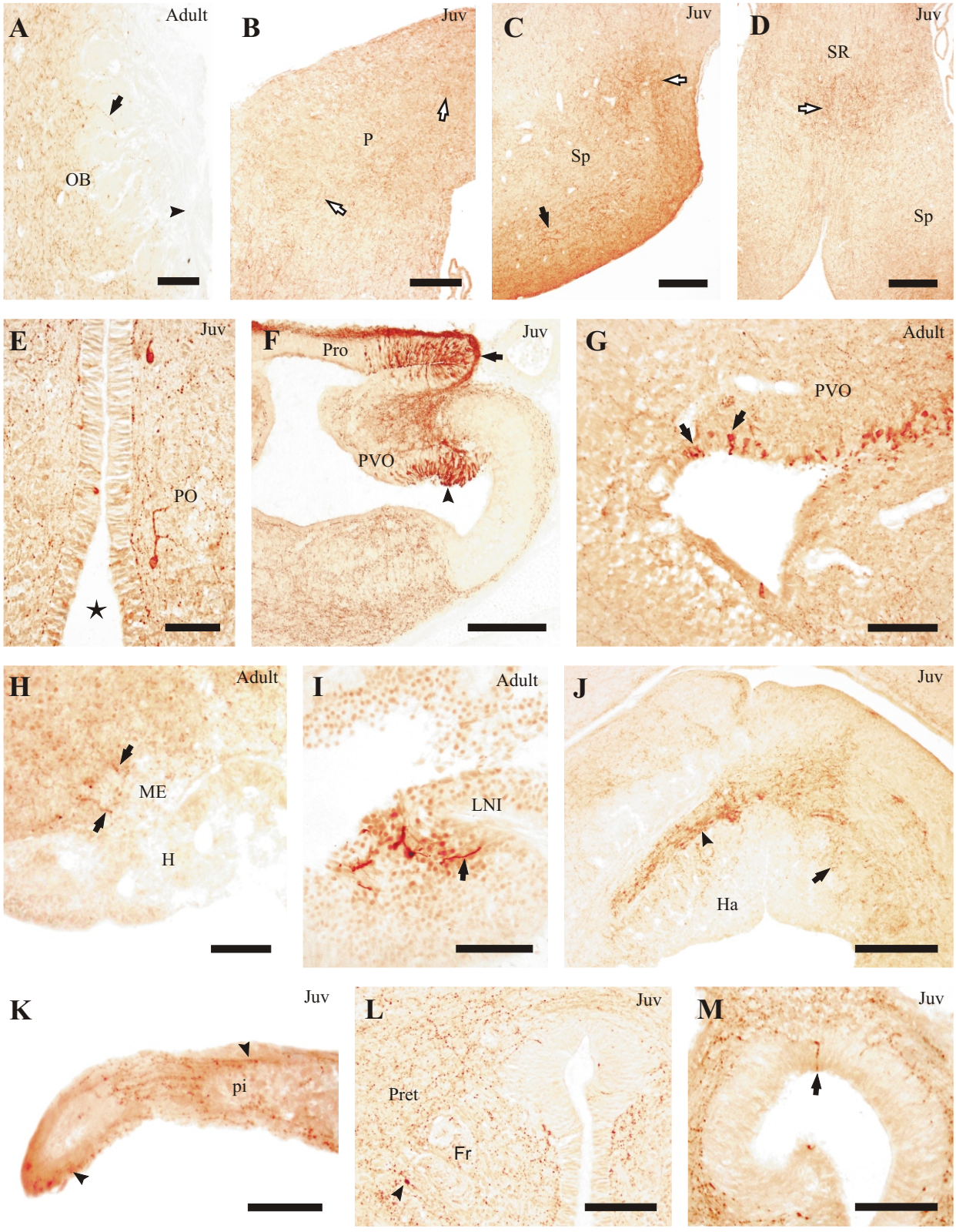
A
Adult
OB
B
Juv
P
C
Juv
Sp
D
Juv
SR
Sp
E
Juv
PO
F
Juv
Pro
PVO
G
Adult
PVO
H
Adult
ME
H
I
Adult
LNI
J
Juv
Ha
K
Juv
pi
L
Juv
Pret
Fr
M
Juv

Fig. 7

Figure 8. Photomicrographs of transverse sections through the mesencephalon (A,B), rhombencephalon (C-J) and spinal cord (K-N) of adult (A-C,H-J,M,N) and juvenile (D-G,K,L) dogfish showing the distribution of 5-HT-ir cells and fibers. **A,** Section at the level of the oculomotor nucleus showing 5-HT-ir CSF-c cells (arrowheads) in the raphe *dorsalis anterioris*. **B,** Section at the level of the trochlear nucleus showing 5-HT-ir cells in the raphe *linearis* nucleus (arrow) and reticular B9 nucleus (arrowhead). **C,** Section at rostral level of the trigeminal motor nucleus showing 5-HT-ir cells in the raphe *centralis superioris* nucleus (arrow), medial (arrowhead) and lateral (white arrowhead) reticular *pontis oralis* nuclei and reticular *subcoeruleus* nucleus (white arrow). **D,** Transversal level caudal to trigeminal motor nucleus showing the absence of 5-HT-ir cells at this level of the rhombencephalic tegmentum. **E,** Section at the caudal level of VIII motor nucleus showing-5-HT-ir cells in the raphe *magnus* nucleus. **F,** Section at mid-level of the abducens nucleus showing 5-HT-ir cells in the raphe *obscurus* (white arrowhead) and in the raphe *pallidus* (white arrow). (Medial is to left). **G,** Section at the caudal level of the abducens nucleus showing 5-HT-ir cells in the raphe *obscurus*/*pallidus* (white arrowhead) and reticular *magnocellularis* (white arrow) and *gigantocellularis* (black arrow). Medial is to the right. **H,** 5-HT-ir fibers in the optic tectum. Note a 5-HT-ir fiber coursing in the dorsoventral plane (arrow). **I,** Some 5-HT-ir fibers in the granular eminence (arrowheads) of the cerebellum. Note some 5-HT-ir fibers crossing the intracerebellar commissure (arrow). **J,** Section showing 5-HT-ir fibers in the dorsal part of the viscerosensory column (arrow). **K-L,** Sections showing 5-HT-ir somata (white arrowheads) and process (arrowhead) in the ventral margin of the rostral spinal cord. Medial is to the right. **M-N,** Sections of the spinal cord showing the density of 5-HT-ir fibers in the marginal nucleus (arrow in M), and in the dorsal marginal area of the dorsal horn (arrowheads in N). Scale bars: 50 μm (A,K,L); 250 μm (B,C,H-J,M,N); 100 μm (D-G).

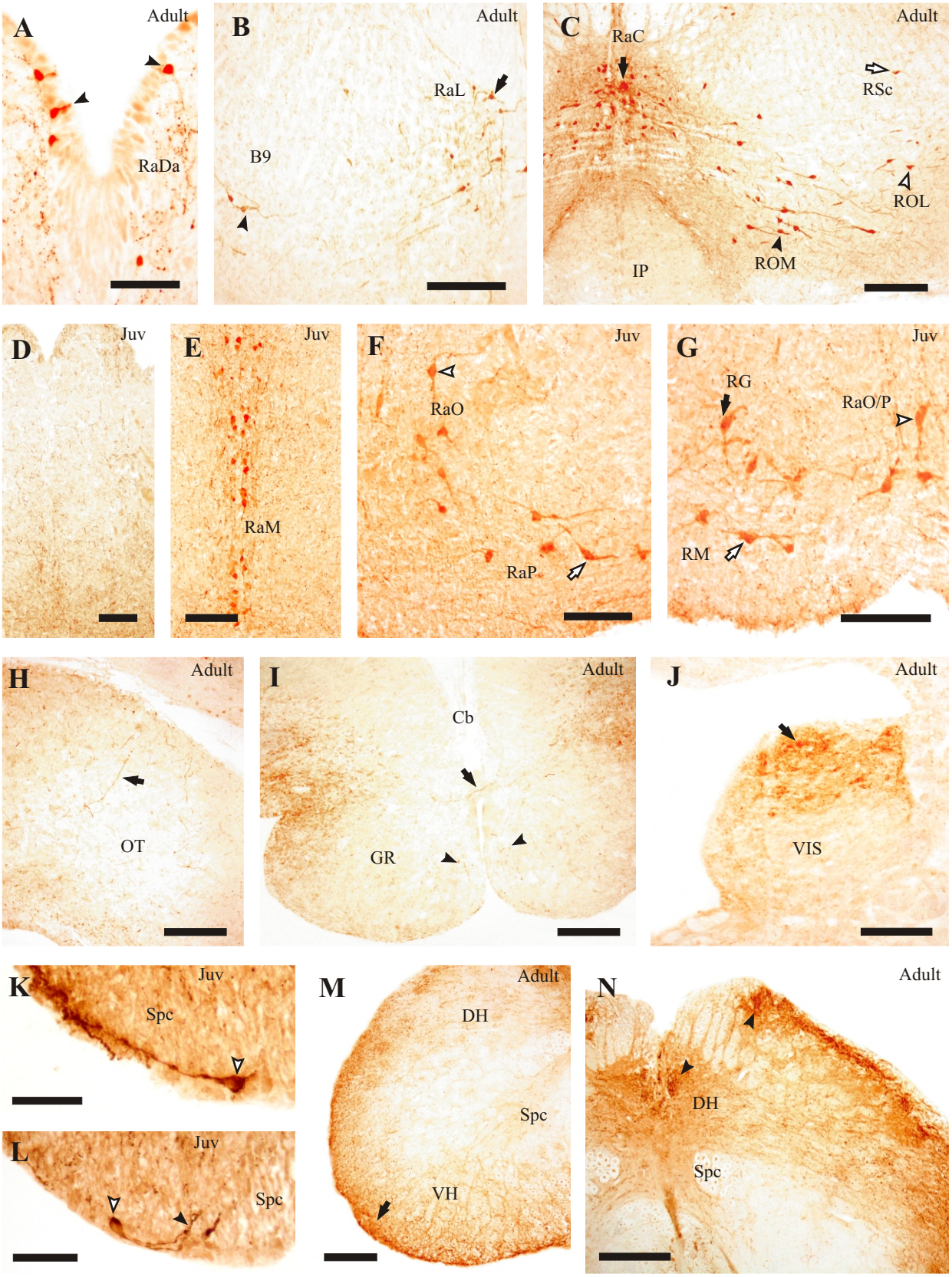
A
Adult
RaDa
B
Adult
RaL
B9
C
Adult
RaC
RSc
ROL
ROM
IP
D
Juv
E
Juv
RaM
F
Juv
RaO
RaP
G
Juv
RG
RaO/P
RM
H
Adult
OT
I
Adult
Cb
GR
J
Adult
VIS
K
Juv
Spc
L
Juv
Spc
M
Adult
DH
Spc
VH
N
Adult
DH
Spc

Fig. 8

Figure 9. Midsagittal schematic representation of the possible segmental subdivisions of the dogfish brainstem at S33 (A) and juvenile (B) and present results on distribution of 5-HT-ir cell clusters. The broken lines mark the putative rhombomeric boundaries, whereas the color dots/bars represent the brainstem 5-HT-ir cell groups. Scale bars: 250 μm (A); 2.5 mm (B).

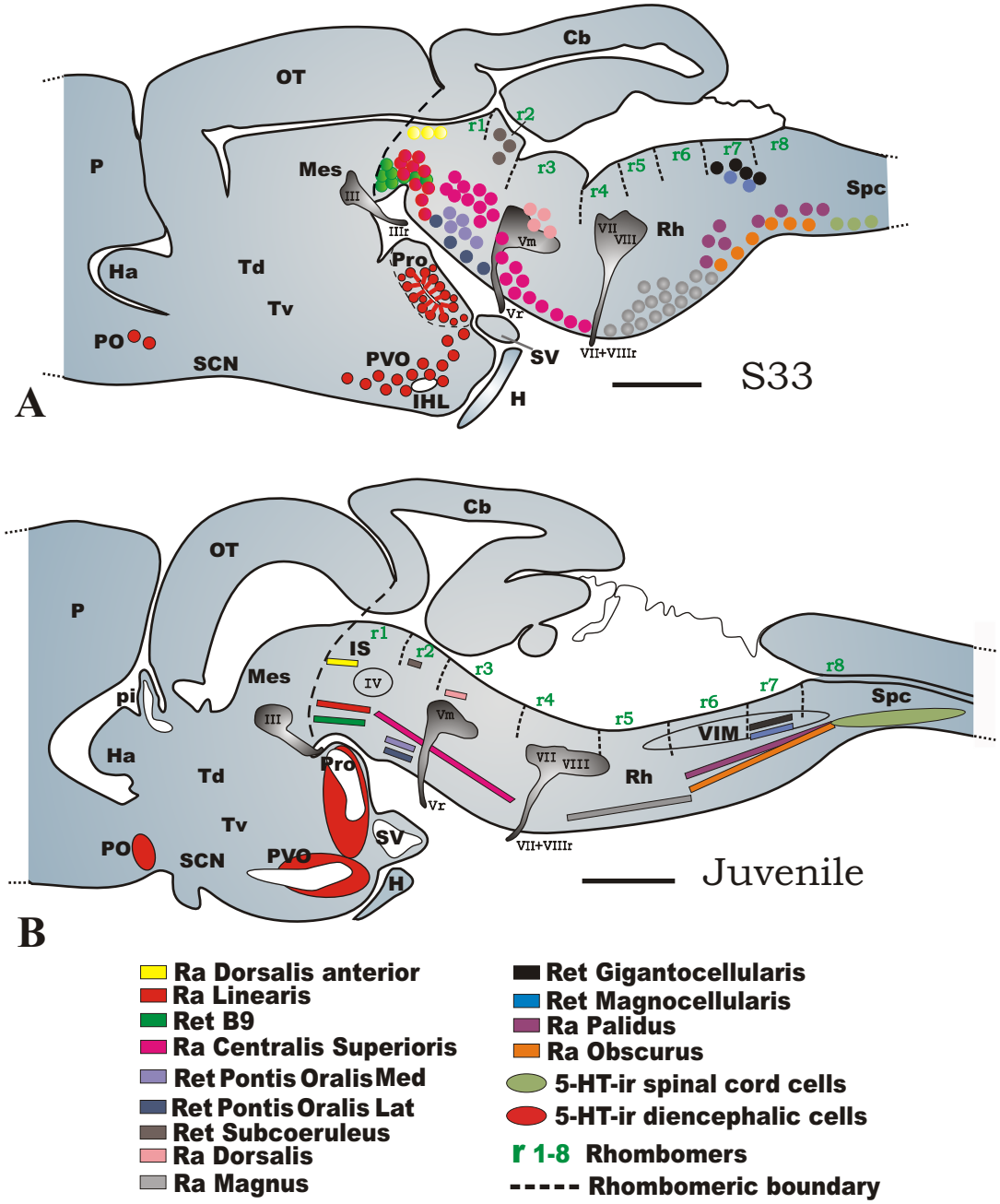
A
Cb
OT
P
Mes
r1
r2
r3
r4
r5
r6
r7
r8
Spc
III
IIIr
Vm
VII
VIII
Rh
Ha
Td
Pro
Tv
Vr
PO
SCN
PVO
SV
VII+VIIIr
IHL
H
S33
B
Cb
OT
P
r1
IS
r2
r3
r8
Mes
IV
pi
r4
r7
Spc
r5
r6
III
Vm
VIM
Ha
Td
Pro
VII
VIII
Rh
Vr
Tv
SV
PO
SCN
PVO
VII+VIIIr
H
Juvenile
Ra Dorsalis anterior
Ra Linearis
Ret B9
Ra Centralis Superioris
Ret Pontis Oralis Med
Ret Pontis Oralis Lat
Ret Subcoeruleus
Ra Dorsalis
Ra Magnus
Ret Gigantocellularis
Ret Magnocellularis
Ra Palidus
Ra Obscurus
5-HT-ir spinal cord cells
5-HT-ir diencephalic cells
r 1-8 Rhombomers
Rhombomeric boundary

Fig. 9

Figure 10. Schematic representation of a dorsal view of the brainstem of the juvenile dogfish showing segmental subdivisions based on the topographic location of cranial nerve motor nuclei (III-X), their entrance roots and present results on differential distribution of 5-HT-ir cell clusters. The broken line marks the putative rhombomeric boundaries, whereas the color bars represent the brainstem 5-HT-ir cell groups. For correspondence of 5-HT-ir cell groups, see list in Figure 9. Scale bar: 2.9 mm.

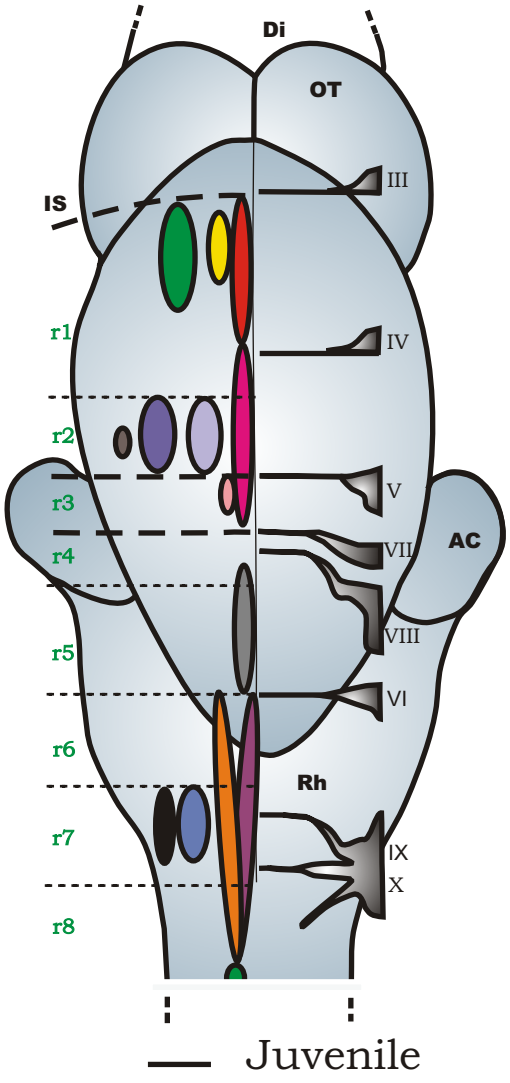
Di
OT
III
IS
r1
IV
r2
V
r3
AC
VII
r4
VIII
r5
VI
r6
Rh
r7
IX
X
r8
Juvenile

Fig. 10

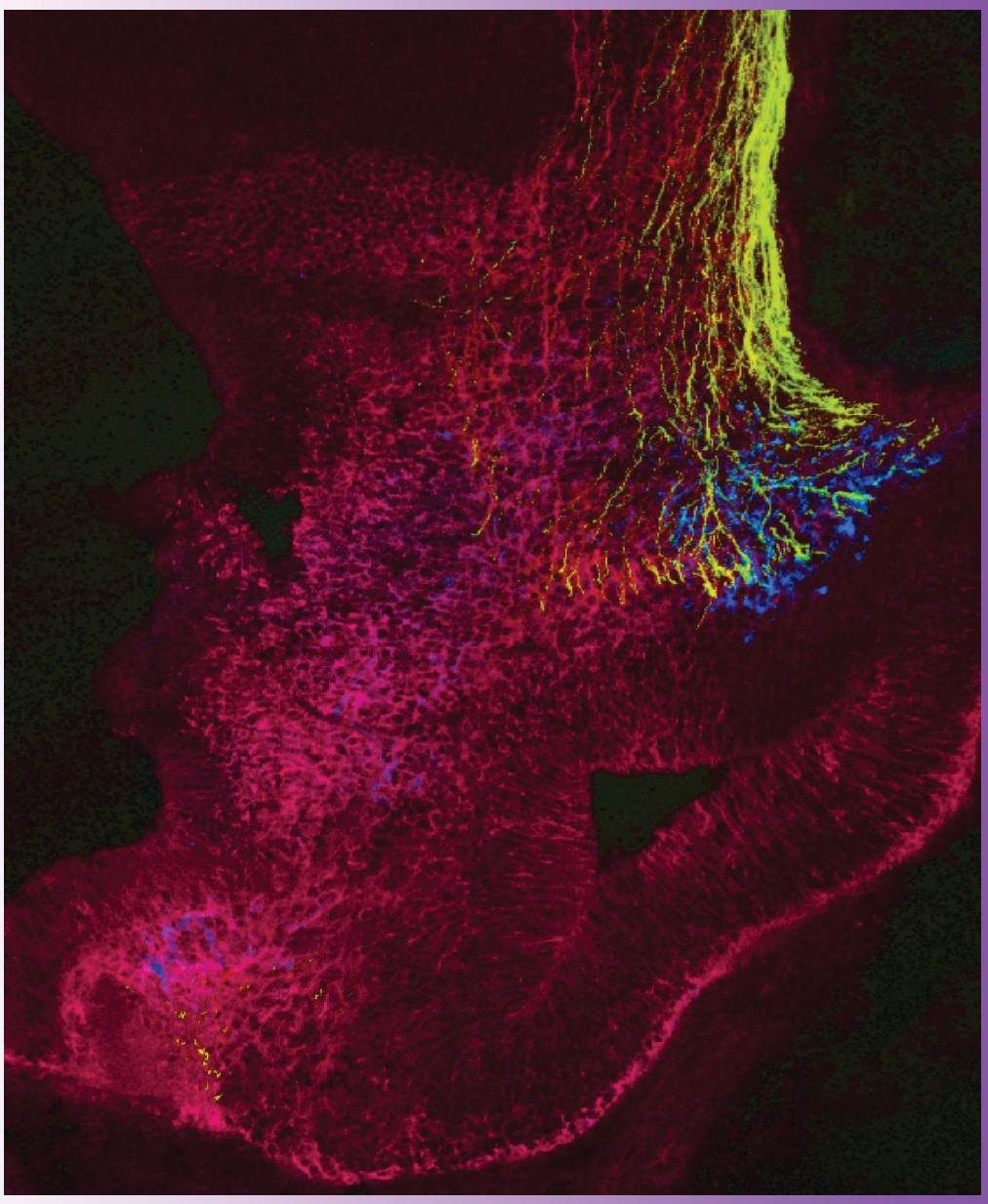

CAPÍTULO 4

Relationships of GABAergic, Catecholaminergic and Serotoninergic Systems in Developing and Mature dogfish Central Nervous System

CAPÍTULO 4

Relationships of GABAergic, Catecholaminergic and Serotoninergic Systems in Developing and Mature dogfish Central Nervous System.
An Immunofluorescence Study

INTRODUCTION

Over the recent decades, numerous data have been accumulated on the important functional significance of the neurotransmitters in neuronal communication of the adult central nervous system (CNS). However, during early neuronal development, some classic neurotransmitters (i.e. GABA, dopamine, serotonin) were reported to function as a neurotrophic and/or morphogenetic factors in vertebrates and invertebrates, while at later stages might paying functions in target selection and synapse formation (van Kersten and Spencer, 2003). Moreover, depletion of transmitters during embryonic development results in developmental deficits of the vertebrate brain (Lauder et al., 1981; Yan et al., 1997; Dorig and Hornung, 2000; Sivam et al., 2001), suggesting that transmitters have crucial roles as morphogens and/or neurotrophic factors.

In this manner, GABA was reported to modulate the neuroplastic capacity of neurons (Wolff et al., 1993), to regulate the GABAergic synapse formation (Madtes and Redburn, 1983) and to exert excitatory actions leading to a number of changes in neuronal structure and function during development (Liu et al., 1997; Obrietan et al., 2002; Fiszman and Schousboe, 2004). Moreover, GABA was also thought to exert a trophic effect, mediated by $GABA_A$ receptors, in embryonic brain development of the monoamine neurons (Liu et al., 1997; Lauder et al., 1998), focused in neurite outgrowth, target selection and synapse formation.

Serotonin was reported to be involved in neuronal proliferation and differentiation (Zhou et al., 2000; Buznikov et al., 2001; Branchereau et al., 2002; Pflieger et al., 2002; Petrova and Otellin, 2007), acting as a growth factor during embryogenesis (Sodhi and Sanders-Bush, 2004; De Lucchini et al., 2005; Vitalis et al., 2007). In tetrapods, the serotonergic system was seen to interact with brain-derived neurotrophic factor (BDNF), S100beta, and other chemical messengers, in addition to cross talk with the GABAergic, glutamatergic, and dopaminergic systems to contribute in the refining connectivity and cytoarchitecture during development of the CNS (Sodhi and Sanders-Bush, 2004). The crucial role of serotonin is supported by several studies, such as the early expression of 5HT receptors even before neural development in rodents (Menegola et al., 2004), the retinal histogenesis and eye morphogenesis by supporting cell proliferation and survival reported in *Xenopus* (De Lucchini et al., 2005), and the loss of neuronal morphogenesis and differentiation by deprivation (Menegola et al., 2004) or depletion of serotonin and their receptors (Vitalis et al., 2007).

During ontogenesis, also catecholamines play a relevant role in the development of vertebrate embryos, regulating the morphogenesis of the CNS (Smeets and Reiner, 1994) mainly of the hypothalamus, neuroendocrine system and midbrain (Di Porzio et al., 1990; Engele, 1998), and exerting a facilitator effect on the regeneration of other structures containing neurotransmitters as serotoninergic axons (Liu et al., 2003). Moreover, dopamine produced during early development induces both growth cone attraction and collapse of target and non-target cell growth cones, affecting growth cone motility, target cell selection and specific synaptogenesis in invertebrates (Spencer et al., 2003) and may also have neurotrophic and/or morphogenetic roles in rodents (Di Porzio et al., 1990; Engele, 1998), similar functions to that reported for GABA and serotonin.

Therefore, there is a vast amount of literature that seems to support the hypothesis that the release of some neurotransmitter such as GABA, dopamine and serotonin in the developing CNS is crucial for proper brain development. For example, growth cones of developing neurons are known to release neurotransmitters (Young and Poo, 1983; Haydon and Zoran, 1989; Gao and van den Pol, 2000; Spencer et al., 2000; Yao et al.,

2000;) and respond to neurotransmitters released from other neurons (Haydon et al., 1984; Lankford et al., 1988; Mattson, 1988; McCobb and Kater, 1988, Owen and Bird, 1997). It is generally assumed that neurotransmitters found in the same nuclei/area may well interact, probably modulating or controlling reciprocally their functions. To know the common distribution pattern of different neurochemical substances in the CNS is a powerful tool for determining homologous structures among vertebrate classes (Bissoli and Niso, 1990).

The present report is the first attempt to characterize the main regions of the dogfish CNS that express different classical neurotransmitters as GABA, catecholamines and serotonin TH and 5-HT by using double and triple labelling of immunomarkers against GABA, glutamic acid decarboxylase (GAD, the GABA synthesis enzyme), tyrosine hydroxylase (TH, the rate-limiting enzyme of the catecholamine synthesis) and serotonin (5-HT) in mid-late developmental stages (S30, S31) and in mature stages (juveniles). Although TH-, GABA/GAD-, and 5-HT-immunoreactive cells and fibers were extended in most parts of the CNS, in some areas the accumulation of two or even three of these neurochemical immunomarkers was especially dense. In that follows, we will point out cell groups and areas in which these neurotransmitters co-distribute.

MATERIAL AND METHODS

Experimental animals

Embryos and juveniles of the lesser-spotted dogfish (*Scyliorhinus canicula*) were kindly provided by the "Aquário Vasco da Gama" and the "Oceanário" of Lisbon (Portugal) and the *Aquarium Finisterrae* (A Coruña, Spain). The embryonic stages were identified on the basis of their external features according to Ballard and colleagues (1993). Two dogfish embryos at stage 31 (S31) were used for double immunofluorescence to GAD and 5-HT, to TH and GAD, and to TH and 5-HT. Two small juveniles (between 9 and 12 cm in length) were also used in the double immunofluorescence to TH and 5-HT. For the triple immunofluorescence, two embryos at stage 30 were used. All procedures conformed to the guidelines established by the

Spanish Royal Decree 223/1998 for animal experimentation and were approved by the ethics committee of the University of Santiago.

Tissue preparation

Embryos were anesthetized with 0.05% tricaine methane sulfonate (MS-222) in seawater, separated from the yolk and fixed by immersion in 4% paraformaldehyde in 0.1 M elasmobranch phosphate buffer at pH 7,4. Juvenile dogfish were deeply anesthetized with 0.05% MS-222 in seawater, then perfused intracardially with elasmobranch Ringer's solution followed by perfusion with the same fixative used for embryos (20 min). The brains and the cervical-pectoral spinal cord regions were then dissected out and immersed in the same fixative for 4 hours.

Brains and spinal cords of embryos and juveniles were cryoprotected with 30% sucrose in phosphate buffer (PB), embedded in OTC compound and frozen with liquid-nitrogen-cooled isopentane. Parallel series of sagittal and transverse (coronal) sections (14-18 μm thick) were cut on a cryostat and mounted on Superfrost Plus slides.

Immunofluorescence processing and confocal laser scanning microscopy

Double immunofluorescence

Selected sagittal sections of S31 embryos were processed for double immunofluorescence against TH and 5-HT, GAD and 5-HT, or GAD and TH, while juvenile sagittal and transverse sections were processed for doble immunofluorescence against TH and 5-HT. The following antibodies were used: mouse monoclonal anti-TH antiserum (Chemicon; Temecula, CA. batch: 0509010596), rabbit polyclonal antibody anti-5-HT (DiaSorin, Stillwater, USA; code 20080, batch 051007) and sheep polyclonal anti-$GAD_{65/67}$ (dilution: 1:2,500; kindly provided by Dr. E. Mugnaini). Sections were pretreated with H_2O_2 to eliminate endogenous peroxidases, and then sequentially incubated with 15% normal donkey (Chemicon), swine (Dako) or goat (Dako) preimmune sera overnight at room temperature with a mixture of 1) mouse TH (dilution 1:500) and rabbit 5-HT (dilution 1:2,500) antisera, or 2) sheep anti-$GAD_{65/67}$ (dilution:

1:2,500) and rabbit anti-5-HT (dilution 1:2,500), or 3) sheep anti-$GAD_{65/67}$ (dilution 1:2,500) and mouse anti-TH (dilution 1:500). Sections were then rinsed (3×10 min) in 0.05M TRIS-buffered saline pH 7.4, containing 0.1% Tween 20 (TBS-T), incubated in 1) rhodamine-conjugated goat antimouse immunoglobulin (Alexa Fluor; Batch: A 11005; dilution 1:200) and fluorescein-conjugated swine antirabbit immunoglobulin (Dako; Batch: F0205; dilution 1:30) for TH/5-HT, or 2) rhodamine-conjugated goat antirabbit immunoglobulin (FluoProbes; dilution 1:50) and fluorescein-conjugated donkey antisheep immunoglobulin (FluoProbes; Batch: E11L71; dilution 1:200) for GAD/5-HT, or 3) fluorescein-conjugated donkey antisheep immunoglobulin (FluoProbes; dilution 1:200) and rhodamine-conjugated goat antimouse immunoglobulin (Alexa Fluor; dilution 1:200) for GAD/TH. All antibodies were diluted in Tris-buffered saline containing 0.2% Triton X-100. Control sections were processed as described in the preceding chapters.

Triple immunofluorescence

To compare the late distribution of the GABAergic, catecholaminergic and serotoninergic pattern systems in the CNS of dogfish, some sagittal sections of embryos at S30 were processed for triple immunofluorescence with a cocktail of the anti-GAD/TH/5-HT serum. The selected sections followed the same immunofluorescence processing method described above. Briefly, tor the antibodies mixture we have used the same primary antibodies indicated in the previous section. The secondary antibody mixture was formed by rhodamine-conjugated goat antirabbit immunoglobulin (FluoProbes; dilution 1:50), Cy3-conjugated donkey antimouse immunoglobulin (FluoProbes; dilution 1:100) and fluorescein-conjugated donkey antisheep immunoglobulin (FluoProbes; dilution 1:200). Sections were processed and photographed.

Imaging

Sections were observed and photographed with a spectral confocal microscope (Leica TCS-SP2). For presentation of some figures, single channel stack projections were adjusted for brightness and contrast in Corel Photo Paint (Corel, Ottawa, Canada), and photos were composed with Corel Draw.

RESULTS

Double and triple immunofluorescence experiments were carried out in the dogfish CNS to investigate the potential co-distribution of the three neurochemical substances observed when we comparatively analyze the results obtained in the three previous chapters, as it is represented in Fig. 1. Triple immunofluorescence was performed in embryos at S30 because it is a key stage to easily characterize the several neurochemical markers distribution patterns before becoming extremely complex and difficult to compare them clearly. Double immunofluorescence was also used in embryos at S31 and juveniles to complete the characterization of the main regions that showed co-distribution in triple labelling experiments at S30.

Comparison of the distribution of three different neurochemical markers

Stages 30 and 31 (S30-31)

The dogfish telencephalon at this stages shows numerous GABAergic cells mainly located in the subpallial region, observed from the externalmost part of the intermediate zone to the ventricular epithelium, while longitudinally GABAergic fibers occupied the marginal zone. From S30, ascending 5-HT-ir longitudinal fibers entered the basal telencephalon along the subpallial GABAergic cells (Figs. 2A; 3A,B). These "pioneer" serotoninergic fibers coursed along the same pathway as the GABAergic fibers, which formed a conspicuous bundle that arched dorsally to the preoptic recess (Figs. 2A; 3B). Ascending serotoninergic fibers, probably originated by the

rhombencephalic 5-HT-ir cell groups, formed a conspicuous longitudinal tract that coursed along the mesencephalon and diencephalon (Figs. 2B-F; 3B-G) in parallel with GAD- and TH-ir fibers (Figs. 2B-F; 3B,C,F,G).

In the preoptic area and suprachiasmatic nucleus, the distribution of TH-ir and GABAergic cells was similar at these stages. Double immunofluorescence revealed that neurons containing these neurochemical substances were co-distributed in these areas, probably co-localizing, although the cell density of both neuronal groups was higher at the suprachiasmatic nucleus (Figs. 2A,B). Moreover, double labeling also revealed that TH-ir cells of the suprachiasmatic nucleus received a dense serotoninergic innervation (Figs. 2B,E; 3D,E).

At S30, TH and GAD were together contained in some fibers that coursed through the ventral hypothalamic walls along the hypothalamo-hypophyseal tract (Fig. 2A). Some longitudinal 5-HT-ir fibers were also observed at S30 (Fig. 2A) and S31 (Figs. 3H), intermingled with the TH-ir fibers of this tract, but co-localization of both substances was not observed (Fig. 3H).

GABAergic cells (mostly CSF-c cells) were observed in the walls of the paraventricular organ at S30 (Figs. 2A-F) but not the TH-ir and 5-HT-ir cells, which differentiate later. At S31, numerous 5-HT-ir cells (most of them CSF-c cells) were also observed in the walls of the paraventricular organ (Figs. 3F,G), sharing the same distribution as GAD-ir cells, although no co-localization was observed in any somata. Numerous immunoreactive fibers to GAD and 5-HT were observed at the dorsal walls of the paraventricular organ, (Figs. 2B,E; 3C). TH-ir fibers were scarce in this region and mainly occupied the caudal region (Fig. 2E; 3G). At the dorsal area of the paraventricular organ (S30), some GABAergic fibers seemed to co-distribute with TH- and 5-HT-ir fibers (Figs. 2B,E).

In the posterior recess organ of embryos at S30, numerous GABAergic cells (most of them CSF-c cells) were observed mainly at the caudal walls. A few GABAergic cells located at the proximal walls (adjacent to the posterior tubercle) also expressed TH (Figs. 2C,D), although these two immunoreactive products showed different cytoplasmic distribution (Fig. 2D). However, the majority of immunoreactive cells of

the posterior recess walls did not show co-localization between GAD and TH (Figs. 2A,C,D,F).

At S30, GABAergic and TH-ir cells co-distributed in the rostral region of the ventral thalamus (Fig. 2A). This population was also innervated by numerous ascending TH-ir fibers (Figs. 2A,E), which probably coursed from the rostral rhombencephalic populations (Fig. 2G) throughout the caudal prosencephalon (Figs. 2A,E,F) and innervating the ventral thalamus, suprachiasmatic nucleus (Figs. 2A,B,E) and the paraventricular organ (Figs. 2B,E).

Although GAD, TH and 5-HT immunoreactivities were observed in cells of the posterior tubercle, co-localization was not observed and these markers were contained in different neurons thus forming different subgroups (Figs. 2A-F). GABAergic cells were restricted to the caudal area of the posterior tubercle (adjacent to the rVTA), TH-ir cells occupied the rostral portion (close to the dorsal walls of the PVO) and the 5-HT-ir cells were observed at the caudal area, adjacent to this two other populations (Figs. 2A-D). At S30, ascendent 5-HT-ir fibers reached these tubercle subgroups (Figs. 2B,E). Later, a dense serotoninergic innervation was observed surrounding the numerous TH-ir cells of the posterior tubercle (Figs. 3F,G).

At the stages studied, GAD- and TH- ir cells were observed in the ventral tegmental area. Moreover, double immunofluorescence revealed that TH-ir cells of the ventral tegmental area and the substantia nigra were surrounded by numerous 5-HT-ir fiber (Figs. 3G,I).

Within the rhombencephalon, double and triple immunofluorescence have revealed that GAD, TH and 5-HT are contained in different cells and no co-localization was observed in any immunoreactive rhombencephalic cell (Figs. 2A,C,D,F-H; 3F,I-N). However, different immunoreactive cells were observed co-distributing at the same region. TH and 5-HT-ir cells were observed in the subcoeruleus at both embryonic stages (S30-S31), although with different location (Fig. 3J). Triple immunofluorescence revealed that the marginal zone of the rhombencephalic tegmentum contained the majority of the serotoninergic cells (reticular formation) and the longitudinal GABAergic fibers of the basal pathway (Figs. 2A,C,D,F-H; 3K,L), while the

GABAergic cells were mainly located at different levels of the intermediate zone, together with some longitudinal TH- and 5-HT-ir fibers (Figs. 2C,F,G,H; 3K,L). In both triple and double immunofluorescence sections numerous longitudinal fibers were observed at the ventral rhombencephalic tegmentum that revealed co-localization of 5-HT and GAD (Figs. 2F,H; 3K,L), at both embryonic stages. In the alar plate of the caudal rhombencephalon, GABAergic cells were also observed gathered in repetitive conspicuous groups forming the GABAergic population of the viscerosensory column (Fig. 3L). Also at this location, numerous TH-ir cells were densely innervated by 5-HT-ir fibers and synaptic bouttons that sourrounded their perycaria (Figs. 3M,N).

In the rostral spinal cord of S30 and S31, GAD, TH and 5-HT immunoreactive cell populations codistributed at the ventral cord (Figs. 2H,I; 3O,P). Moreover, co-localization of GAD and TH was observed at some CSF-c cells located ventrally to the central canal (Figs. 2H,I; 3O,P), and also at some longitudinal fibers lateral to the floor plate (Fig. 3P).

Juvenile

Confocal microscopy double labeling immunofluorescence experiments, with TH and 5-HT in sections of the juvenile brain (Figs. 4A-M), have shown that co-distribution pattern of these two neurochemical markers is maintained in the regions already observed at mid-late embryonic stages (S30-S31) but the increased density of TH-ir and 5-HT-ir fibers allowed to better appreciate the relations between TH- and 5-HT-ir structures.

The TH-ir cells at the preoptic and postoptic (suprachiasmatic nucleus) areas were densely innervated by 5-HT-ir fibers, while only few TH-ir fibers were observed in the proximity of the scarce 5-HT-ir cells at the preoptic area (Figs. 4A,B). Abundant 5-HT-ir fibers and scarcer TH-ir ran longitudinally throughout these rostral diencephalic regions to the basal telencephalon (Figs. 4A,B). More caudally, the TH-ir cell groups of the ventral thalamus and the posterior tubercle nucleus were also densely innervated by 5-HT-ir fibers (Figs. 4A-D), being this innervation denser than that observed in embryos (S30-31). The paraventricular and posterior recess organs showed a massive

population of 5-HT-ir cells, most of them CSF-c cells, and a few intermingled TH-ir cells, some of them CSF-c cells, but colocalization between TH and 5-HT could not be observed (Figs. 4A,C-E). Moreover, although TH-ir fibers that run through the external walls of both of these circunventricular organs were intermingled with those 5-HT-ir (Figs. 4A,C-E), colocalization between TH and 5-HT in these fibers was not be observed. The TH-ir cells of the ventral tegmental area and substantia nigra were massively innervated by 5-HT-ir fibers and numerous 5-HT-ir bouttons (probably synaptic contacts) were observed on TH-ir somata of these populations (Figs. 4F,G). The mesencephalic–rhombencephalic boundary can be distinguished ventrally by the sharp separation between the caudalmost tyrosine hydroxylase immunoreactive (TH-ir) cells of the ventral tegmental area and the rostralmost serotonergic (5-HT-ir) cells of the reticular formation (Fig. 4G).

In the rhombencephalon, the innervation pattern observed in the caudal prosencephalon was inverted, and the majority of the 5-HT-ir cell groups (reticular formation) received a dense TH-ir innervation. TH-ir fiber were observed surrounding and apparently contacting the main serotoninergic populations of the reticular formation, from rostral (Figs. 4G-J) to caudal (Figs. 4K,M) tegmental levels. A moderate TH-ir innervation was observed at the 5-HT-ir cells of the subcoeruleus, where TH-ir cells were also co-distributed with those serotoninergic cells (Fig. 4H), being in different locations within the subcoeruleus area. A dense 5-HT-ir and, especially, TH-ir innervation was observed in the central grey periventricular area (Figs. 4I,J) and at the midlateral areas were some rapheal and dorsolateral reticular 5-HT-ir cells were also observed (Figs. 4I,J). These fibers were immunoreactive to both TH and 5-HT (Figs. 4I,J). Co-distribution between TH- and 5-HT-ir cells was observed at caudal levels of the rhombencephalic tegmentum, where reticular TH-ir cells located at lateral regions were observed at the same level as the rapheal and reticular 5-HT-ir cells located at the midline and ventrolaterally (Fig. 4K). The viscerosensory column showed the same pattern for TH and 5-HT as observed in mid-late embryos (S30-31), although the density of the 5-HT-ir innervation surrounding massively the TH-ir cells was much higher in juvenile (Fig. 4L). At the obex level, the pattern of TH- and 5-HT-ir cells was

similar to that observed in more rostral levels: reticular TH-ir cells scarcely innervated by 5-HT-ir fibers were located dorsolaterally to the ventral 5-HT-ir cells moderately surrounded by TH-ir fibers (Fig. 4M).

DISCUSSION

Our present results show that some early appearing neurotransmitters (GABA, TH and 5-HT) are expressed in neurons at the same regions and/or neuronal groups within the CNS of dogfish. From rostral to caudal, the main regions showing co-distribution of neurons and fibers are the preoptic area, suprachiasmatic nucleus, paraventricular/posterior recess organs, posterior tubercle, ventral tegmental area, rhombencephalic tegmentum, viscerosensory column and spinal cord.

Co-distribution of GAD-, TH- and 5-HT-ir cells in the developing CNS of dogfish

Prosencephalic populations

Preoptic area

In adult dogfish, the presence of aminergic cells in the preoptic recess walls was already reported by histofluorescence (Rodriguez-Moldes and Anadón, 1987) although no comparative studies were made with other neurotransmitters (i.e. GABA). In teleosts, the dopaminergic neurons observed in this area are known to project to the pituitary (Kah et al., 1987; Holmqvist and Ekström, 1995), which is believed to be the source of the dopaminergic inhibition of the GTH2 secretion (Kah et al., 1987; Linard et al., 1996). In dogfish, this area also contains numerous GABAergic neurons probably acting as interneurons modulating the activity of central neuroendocrine systems, especially the GnRH system and/or the dopaminergic system as seen in other vertebrates (see Smeets and Reiner, 1994). The dense GABAergic innervation we observe in the ventral wall of the dogfish preoptic recess, suggesting a possible role of GABA on the control of dopaminergic neurons, as demonstrated in teleosts (Trudeau et al., 1993).

Postoptic area (suprachiasmatic nucleus)

This nucleus consists of a group of scattered bipolar cells with a ventral orientation among the decussating optic tract. In dogfish embryos (S30-S31), co-localization of GAD and TH (the violet color in some neurons is due to co-expression of both markers) was observed in many of these suprachiasmatic neurons that were also innervated by numerous 5-HT-ir and some TH-ir fibers. TH-ir cells innervated by 5-HT-ir fibers were also reported in the garfish (Parent and Northcutt, 1982), while TH- and 5-HT-ir fibers were seen densely innervating the suprachiasmatic neurons in other teleost (Corio et al, 1991). In rodents, serotoninergic inputs are observed on dopaminergic neurons involved in the control of pituitary hormone release and it has been hypothesized that the action of serotonin on pituitary hormone is mediated at least by dopamine and serotonin (Tillet, 1994). In rats this functional relationship between these two neuromodulators seems to exist since it was demonstrated that the central administration of serotonin decreases the TH catalytic activity and mRNA levels in the tuberoinfundibular dopaminergic neurons (Mathiasen et al., 1992).

In anamniotes, the suprachiasmatic cells receive retinal input (Pinganaud and Clairambault, 1979; Northcutt and Wullimann, 1988) and send projections to the hypophysis (Anglade et al., 1993; Holmqvist and Ekström, 1995; Jansen et al., 1997), probably modulating its hormonal activity. In the rainbow trout, these hypophysiotrophic neurons are positive to TH/DA (Holmqvist and Ekström, 1995; Linard et al., 1996) and to GABA (Anglade et al., 2000), and were co-located at the hypophysiotropic neurons in amphibians, as seen in dogfish, being probably involved in the control of MSH release (Jansen et al., 1997; Ubink et al., 1998). In dogfish, as in other elasmobranchs, the neurons of this nucleus seem to receive retinal projections (Northcutt, 1991; Smeets, 1981; Repérant et al., 1986) and send projections to the hypophysis (present results). Moreover, in embryos co-localization of GAD and TH was observed in the fibers of the hypothalamo-hypophyseal tract along with also course 5-HT-ir fibers (see below).

Paraventricular and posterior recess organs

The paraventricular organ is formed by numerous cells surrounding the ventricular walls of the infundibulum, most of them being CSF-c cells. In these walls, CSF-c cells showing immunoreactivity to 5-HT and to TH were co-distributing but co-localization of both substances could not be observed. Moreover, most of CSF-c cells expressed 5-HT while only a few of them showed positivity to TH. However, in S30-S31 embryos and in juveniles, double and triple immunofluorescence showed that fiber at the same region also showed co-distribution to GAD/TH/5-HT and TH/5-HT, respectively. In rays, TH- and 5-HT-ir cells were also found at the paraventricular organ (Stuesse et al., 1991a, b), showing the same co-distribution pattern as seen in dogfish. The CSF-c hypothalamic cells that are found in most vertebrate groups except mammals (see Smeets and Reiner, 1994), are thought to play a role in either sensing levels of chemical substances within the cerebrospinal fluid or/and in secreting substances into the ventricle (CSF). Co-distribution of TH- and 5-HT-cells at the periventricular walls of the hypothalamus was also reported in *Lepisosteus* (Parent and Northcutt, 1982), teleosts (Corio et al., 1991; Ekström et al., 1995; Kaslin and Panula, 2001) and mammals (Shim et al., 2001). Moreover, in the paraventricular organ walls of some teleosts (Batten et al., 1993) and amphibians (Corio et al., 1992), a few TH-ir cells were observed although numerous DA- and 5-HT-ir cells were reported presenting a similar distribution and morphology, which indicates an accumulation of dopamine by uptake from the ventricle, rather than by synthesis and release (Ekström et al., 1990; Sas et al., 1990; Batten et al., 1993), although some electron microscopic studies (Meek, 1999) suggested also the release of these monoamines by the paraventricular organ neurons. Adjacent to the caudal paraventricular organ, some GAD- and TH-ir cells were observed co-distributing at the proximal walls of the posterior recess organ at S30. Also at these proximal walls, some TH- and 5-HT-ir fibers were observed coursing through the external layers in both S31 and juvenile, indicating a possible role in the maturation of the posterior recess organ of dogfish.

Thalamus

The co-distribution of GAD and TH in numerous cells of the ventral thalamus/dorsal hipothalamus has been demonstrated by triple immunofluorescence in the dogfish embryo at S30. Some of them were double labeled cells located adjacent to the dorsal walls of the paraventricular organ and were continuous with the double labeled cells of the suprachiasmatic organ. However, cells of the ventral thalamus in teleosts showed immunorreactivity to TH and 5-HT (Corio et al, 1991), which was not observed in dogfish.

Posterior tubercle

From S30, the dogfish posterior tubercle contains cells immunoreactive to the three markers studied, each one being contained in independent cell subgroups, without evidences of co-localization. While GABAergic cells were at caudal levels, TH-ir cells occupied the rostral portion and 5-HT-ir cells the marginal area. Co-distribution of TH and 5-HT in cells of the posterior tubercle was reported in teleosts (Corio et al., 1991; Kaslin and Panula, 2001) and in amphibians (Corio et al., 1992). Although very few is known about the interaction between catecholamines and serotonin and between them and GABA, the fact that they were early expressed in the dogfish posterior tubercle suggest a functional implication of these neurochemical systems in the development of this brain region in elasmobranch, perhaps playing a multifunctional role in the maturation of this region.

Ventral tegmental area

As noted in previous chapters, the midbrain catecholaminergic system shows evolutionary variations between amniotes and anamniotes. In dogfish development, GAD- and TH- ir cells were co-distributed in the ventral tegmental area although they showed different locations within this region. Using double immunofluorescence we observed that numerous 5-HT-ir fibers and bouttons surrounded the TH-ir cells of the ventral tegmental area and the substantia nigra. In mammals and birds the tegmental dopaminergic neurons are known to innervate various telencephalic targets, most

notably the striatal part of the basal ganglia, that may play a key role in movement control (Tillet, 1994). The loss of this catecholaminergic input (as in human Parkinson´s disease) or pharmacological blockade of this input slow movements and impairs its initiation Electrophysiological and immunohistochemical studies in tetrapods have demonstrated the localization of $GABA_B$ receptors in the midbrain monoamine containing neurons (Wirtshafter and Sheppard, 2001) which suggests that GABA has inhibitory effects on dopaminergic cells in the substantia nigra (Grace and Bunney, 1979, 1985; Rieke 1981; Reiner and Anderson, 1990), supporting that the released GABA from the nigral terminals may influence body movements. If this inhibitory process also occurs in elasmobranchs is a hypothesis that remain to be solved.

Brainstem populations

The most conservative catecholaminergic cell group of the CNS in vertebrates is the locus coeruleus, being present in all classes of vertebrates. In mammals and birds the locus coeruleus has widespread projections to the brain and spinal cord and exerts a modulatory influence over diverse regions (see Smeets and Reiner, 1994). Although TH- and 5-HT-ir cells were observed in the locus coeruleus of developing and mature dogfish, no such longitudinal projections were seen running from these aminergic cells, however, the dorsolateral TH-ir fibers observed in the rhombencephalon may be in close relation with this cell population. In other elasmobranchs, 5-HT-ir cells were found at the subcoeruleus as the TH-ir cells (Stuesse et al., 1991a; Stuesse and Cruce, 1992), although they were at different location similar to that observed in dogfish. Co-distribution of TH- and 5-HT-ir cells was also reported in the subcoeruleus of birds (Dubé and Parent, 1981).

The viscerosensory complex is known to be linked to the sympathetic nervous system by the caudal rhombencephalic cell groups. In dogfish embryos and juveniles, the viscerosensory column has a rich plexus of serotoninergic fibers in addition to catecholaminergic and GABAergic cells. Double labeling for TH and 5-HT showed that 5-HT-ir bouttons were surrounding the somata and of TH-ir cells at the dorsomedial

position. That 5-HT-ir fibers were surrounding the TH-ir cells of the viscerosensory column was already observed comparing the distribution of TH-ir and 5-HT-ir structures at this region in some elasmobranch and teleost species (Stuesse et al., 1992; Batten et al., 1993). Our results reinforce the idea that these serotoninergic fibers may modulate the activity of the catecholaminergic cells located in the vicinity as Pickel and colleagues (1984) postulated.

Double and triple labeling have shown that in the rhombencephalic tegmentum of dogfish, GAD- and 5-HT-ir cells were co-distributing although co-expression of both markers in rhombencephalic cells could not be observed. Also co-distribution but not co-localization was observed with some reticular TH-ir cells at the caudal rhombencephalic levels. However in dogfish, the longitudinal fibers that courses throughout the basal tegmentum and in close association to the 5-HT-ir cells showed immunofluorescence to both GAD and 5-HT, which indicates that both markers co-localized in these fibers and visualized as yellow fibers. In mammals and birds the caudal group of reticular formation contained numerous catecholaminergic cells that originated ascending projections to parabranchial and hindbrain regions and descending projections to sympathetic preganglionic spinal cord neurons (influencing the vascular tone; see Smeets and Reiner, 1994). The similar distribution and connectivity of these neurons observed in reptiles and some anamniotes has been also related to sympathetic functions (Smeets and Reiner, 1994). If the longitudinal fibers containing 5-HT and/or GAD that coursed throughout the basal tegmentum are also related with sympathetic function could not be discerned in the present work but our results indicate that these neurochemical markers are essencial for the development and establishment of the mature organization of the brainstem in elasmobranchs.

Spinal populations

GABA is known to play an inhibitory role in development and the adult spinal cord of fish (Veselkin and Batueva, 1999; Pombal et al., 2005), while a possible regulating role in the morphogenesis of the locomotor circuits was also considered

(Meléndez et al., 2003; Higashijima et al., 2004; Ruiz et al., 2004). In dogfish spinal cord the GAD-ir neurons were mainly observed at the ventricular and intermediate zone while a few of them were located ventrally to the central canal like the TH-ir CSF-c cells. Since the distribution of GAD-ir and TH-ir cells around the central canal was markedly different, they appear to represent separate CSF-c populations, except for those ventral to the central canal. The possibility of co-localization of TH and GAD in the same CSF-c cells was investigated in embryonic dogfish with experiments of double labeling immunofluorescence and confocal microscopy. Present results indicate that the ventral GAD-ir and TH-ir CSF-c cells represent the same neuronal population, at least in embryos, indicating for the first time in elasmobranchs the presence of these two synthesizing enzymes in the same spinal cell. A similar distribution of GABA- and TH-ir cells was reported in the ventromedial regions of the spinal cord of sturgeon, garfish and goldfish (Wai et al., 2007), indicating a similar distribution pattern of these neurotransmitters among the spinal cord CSF-c cells of fish.

5-HT-ir cells showing no co-distribution pattern with other immunoreactive substance, were observed in the ventral horn in all elasmobranchs studied (Stuesse et al., 1991; Stuesse and Cruce, 1992), similar to that seen in dogfish and in other fish groups (Wai et al., 2007). Interestingly, 5-HT-ir CSF-c cells were reported in the hagfish *Myxine glutinosa* (Vigh and Vigh-Teichmann, 1992) spinal cord, suggesting that they may take up some chemical information from the central canal as seen in the paraventricular organ of most vertebrates.

In dogfish, the triple labeling has shown that the location of the TH-ir and GABAergic cells ventral to the central canal does not correspond to the location of serotoninergic cells, which were found more ventrally, but without any contact to the ventricle. Moreover, the rostral spinal cord has a rich GABAergic network of fibers that overlaps mostly the TH-ir and 5-HT-ir fibers. The co-distribution of GAD -, TH- and 5-HT-ir cells in the spinal cord seems to be roughly similar among fish, although some variations were observed indicating possible adaptations related to the life-style of these fish.

BIBLIOGRAPHY

Alonso, J.R.; Coveñas, R.; Lara, J.; Arévalo, R.; de León, M.; Aijón, J. (1989) Tyrosine hydroxylase immunoreactivity in a subpopulation of granule cells in the olfactory bulb of teleost fish. Brain Behav Evol. 34:318-324.

Anglade, I.; Mazurais, D.; Douard, V.; Le Jossic-Corcos, C.; Mañanos, E.L.; Michel, D.; Kah, O. (1999) Distribution of glutamic acid decarboxylase mRNA in the forebrain of the rainbow trout as studied by in situ hybridization. J Comp Neurol. 410:277-289.

Ballard, W.; Mellinger, J.; Lechenault, H. (1993) A series of normal stages for development of *Scyliorhinus canicula*, the lesser spotted dogfish (Chondrichthyes: Scyliorhinidae). J Exp Zool. 267:318-336.

Barbeau, A.; Dallaire, L.; Buu, N.T.; Veilleux, F.; Boyer, H.; de Lanney, L.E.; Irwin, I.; Langston, E.B.; Langston, J.W. (1985) New amphibian models for the study of 1-methyl-4-phenyl-1,2,3,6-tetrahydropyridine (MPTP). Life Sci. 36:1125-1134.

Barker, J.L. (1988) The role of GABA: Neurotrophic activity of GABA during development. Science 240:548-549.

Batten, T.F.; Berry, P.A.; Maqbool, A.; Moons, L.; Vandesande, F. (1993) Immunolocalization of catecholamine enzymes, serotonin, dopamine and L-dopa in the brain of *Dicentrarchus labrax* (Teleostei). Brain Res Bull.31:233-252.

Bissoli, R.; Battistini, S.; Guarnieri, T.; Contestabile, A. (1988) Regional levels of neurotransmitter markers in the pigeon telencephalon: a comparison with possibly homologous areas of the rat telencephalon. J Neurochem. 50:1731-1737.

Bissoli, R.; Contestabile, A. (1988) Evolution of neurotransmitter-related markers in the vertebrate telencephalon. Comparative microchemical study in discrete brain regions of a frog and a turtle. Comp Biochem Physiol C. 89:241-248.

Bodznick, D.; Northcutt, R.G. (1984) An electrosensory area in the telencephalon of the little skate, *Raja erinacea*. Brain Res. 298:117-124.

Branchereau, P.; Chapron, J.; Meyrand, P. (2002) Descending 5-hydroxytryptamine raphe inputs repress the expression of serotonergic neurons and slow the maturation of inhibitory systems in mouse embryonic spinal cord. J Neurosci. 22:2598-2606.

Buznikov, G.A.; Lambert, H.W.; Lauder, J.M. (2001) Serotonin and serotonin-like substances as regulators of early embryogenesis and morphogenesis. Cell Tissue Res. 305:177-186.

Chevins, P.F. (1972) Ultrastructure of the pituitary complex in the genus *Raia* (elasmobranchii). I. The pars neurointermedia. Z Zellforsch Mikrosk Anat. 130:193-204.

Corio, M.; Peute, J.; Steinbusch, H.W. (1991) Distribution of serotonin- and dopamine-immunoreactivity in the brain of the teleost *Clarias gariepinus*. J Chem Neuroanat. 4:79-95.

Corio, M.; Thibault, J.; Peute, J. (1992) Distribution of catecholaminergic and serotoninergic systems in forebrain and midbrain of the newt, *Triturus alpestris* (Urodela). Cell Tissue Res. 268:377-387.

De Lucchini, S.; Ori, M.; Cremisi, F.; Nardini, M.; Nardi, I. (2005) 5-HT2B-mediated serotonin signaling is required for eye morphogenesis in *Xenopus*. Mol Cell Neurosci. 29:299-312.

Di Porzio, U.; Zuddas, A.; Cosenza-Murphy, D.B.; Barker, J.L. (1990) Early appearance of tyrosine hydroxylase immunoreactive cells in the mesencephalon of mouse embryos. Int J Dev Neurosci. 8:523-532.

Dubé, L.; Parent, A. (1981) The monoamine-containing neurons in avian brain: I. A study of the brain stem of the chicken (*Gallus domesticus*) by means of fluorescence and acetylcholinesterase histochemistry. J Comp Neurol. 196:695-708.

Durig, J.; Hornung, J.P. (2000) Neonatal serotonin depletion affects developing and mature mouse cortical neurons. Neuroreport 11:833-837.

Ekström, P.; Ebbesson, S.O. (1989) Distribution of serotonin-immunoreactive neurons in the brain of sockeye salmon fry. J Chem Neuroanat. 2:201-213.

Ekström, P.; Honkanen T.; Steinbusch, H.W. (1990) Distribution of dopamine-immunoreactive neurons and fibers in the brain of teleost, *Gasterosteus aculeatus* comparison with tyrosine hydroxylase- and dopamine-beta-hydroxylase-immunoreactive neurons. J Chem Neuroanat. 3:233-260.

Engele, J. (1998) Spatial and temporal growth factor influences on developing midbrain dopaminergic neurons. J Neurosci Res. 53:405-414.

Fiszman, M.L.; Schousboe, A. (2004) Role of calcium and kinases on the neurotrophic effect induced by gamma-aminobutyric acid. J Neurosci Res.76:435-441.

Gao, X.B.; van den Pol, A.N. (2000) GABA release from mouse axonal growth cones. J Physiol. 3:629-637.

Grace, A.A.; Bunney, B.S. (1979) Paradoxical GABA excitation of nigral dopaminergic cells: indirect mediation through reticulata inhibitory neurons. Eur J Pharmacol. 59:211-218.

Grace, A.A.; Bunney, B.S. (1985) Opposing effects of striatonigral feedback pathways on midbrain dopamine cell activity. Brain Res. 333:271-284.

Gurski, M.R.; Hamilton, K.A. (1996) Effects of dopamine and fluphenazine on field potential amplitude in the salamander olfactory bulb. Exp Brain Res. 108:236-246.

Hardy, A.; Palouzier-Paulignan, B.; Duchamp, A.; Royet, J.P.; Duchamp-Viret, P. (2005) 5-Hydroxytryptamine action in the rat olfactory bulb: in vitro electrophysiological patch-clamp recordings of juxtaglomerular and mitral cells. Neuroscience 131:717-731.

Haydon, P.G.; McCobb, D.P.; Kater, S.B. (1984) Serotonin selectively inhibits growth cone motility and synaptogenesis of specific identified neurons. Science 226:561-564.

Haydon, P.G.; Zoran, M.J. (1989) Formation and modulation of chemical connections: evoked acetylcholine release from growth cones and neurites of specific identified neurons. Neuron 2:1483-1490.

Holmqvist, B.I.; Ekström, P. (1995) Hypophysiotrophic systems in the brain of the Atlantic salmon. Neuronal innervation of the pituitary and the origin of pituitary dopamine and nonapeptides identified by means of combined carbocyanine tract tracing and immunocytochemistry. J Chem Neuroanat. 8:125-145.

Jansen, K.; Fabro, C.; Artero, C.; Feuilloley, M.; Vaudry, H.; Fasolo, A.; Franzoni, M.F (1997) Characterization of pars intermedia connections in amphibians by biocytin tract tracing and immunofluorescence aided by confocal microscopy. Cell Tissue Res. 287:297-304.

Johnston, S.A.; Maler, L. (1992) Anatomical organization of the hypophysiotrophic systems in the electric fish, *Apteronotus leptorhynchus*. J Comp Neurol. 317:421-437.

Johnston, S.A.; Maler, L.; Tinner, B. (1990) The distribution of serotonin in the brain of *Apteronotus leptorhynchus*: an immunohistochemical study. J Chem Neuroanat. 3:429-465.

Kah, O.; Dulka, J.G.; Dubourg, P.; Thibault, J.; Peter, R.E. (1987) Neuroanatomical substrate for the inhibition of gonadotrophin secretion in goldfish: existence of a dopaminergic preoptico-hypophyseal pathway. Neuroendocrinology 45:451-458.

Kang, T.C.; Lee, J.C.; Choi, K.Y.; Park, S.K.; Jeong, Y.G.; Jo, S.M.; Won, M.H. (2001) Distribution of serotonin immunoreactivity in the main olfactory bulb of the Mongolian gerbil. Anat Histol Embryol. 30:117-120.

Kaslin, J.; Panula, P. (2001) Comparative anatomy of the histaminergic and other aminergic systems in zebrafish (*Danio rerio*). J Comp Neurol. 440:342-377.

Keverne, E.B.; Lévy, F.; Guevara-Guzman, R.; Kendrick, K.M. (1993) Influence of birth and maternal experience on olfactory bulb neurotransmitter release. Neuroscience 56:557-565.

Kosaka, T.; Kosaka, K.; Nagatsu, I. (1991) Tyrosine hydroxylase-like immunoreactive neurons in the olfactory bulb of the snake, *Elaphe quadrivirgata*, with special reference to the colocalization of tyrosine hydroxylase- and GABA-like immunoreactivities. Exp Brain Res. 87:353-362.

Lankford, K.L.; DeMello, F.G.; Klein, W.L. (1988) D1-type dopamine receptors inhibit growth cone motility in cultured retina neurons: evidence that neurotransmitters act as morphogenic growth regulators in the developing central nervous system. Proc Natl Acad Sci. 85:4567-4571.

Lauder, J.M.; Liu, J.; Devaud, L.; Morrow, A.L. (1998) GABA as a trophic factor for developing monoamine neurons. Perspect Dev Neurobiol. 5:247-259.

Lauder, J.M.; Wallace, J.A.; Krebs, H. (1981) Roles for serotonin in neuroembryogenesis. Adv Exp Med Biol. 133:477-506.

Linard, B.; Anglade, I.; Corio, M.; Navas, J.M.; Pakdel, F.; Saligaut, C.; Kah, O. (1996) Estrogen receptors are expressed in a subset of tyrosine hydroxylase-positive neurons of the anterior preoptic region in the rainbow trout. Neuroendocrinology 63:156-165.

Linard, B.; Bennani, S.; Saligaut, C. (1995) Involvement of estradiol in a catecholamine inhibitory tone of gonadotropin release in the rainbow trout (*Oncorhynchus mykiss*). Gen Comp Endocrinol. 99:192-196.

Liu, J.; Morrow, A.L.; Devaud, L.; Grayson, D.R.; Lauder, J.M. (1997) GABAA receptors mediate trophic effects of GABA on embryonic brainstem monoamine neurons in vitro. J Neurosci. 17:2420-2428.

Liu, Y.; Ishida, Y.; Shinoda, K.; Nakamura, S. (2003) Interaction between serotonergic and noradrenergic axons during axonal regeneration. Exp Neurol. 184:169-178.

Madtes, P.Jr.; Redburn, D.A. (1983) GABA as a trophic factor during development. Life Sci. 33:979-984.

Mathiasen, J.R.; Tomogane, H.; Voogt, J.L. (1992) Serotonin-induced decrease in hypothalamic tyrosine hydroxylase activity and corresponding increase in prolactin release are abolished at midpregnancy and by transplants of rat choriocarcinoma cells. Endocrinology 131:2527-2532.

Mattson, M.P. (1988) Neurotransmitters in the regulation of neuronal cytoarchitecture. Brain Res. 472:179-212.

McCobb, D.P.; Kater, S.B. (1988) Membrane voltage and neurotransmitter regulation of neuronal growth cone motility. Dev Biol. 130:599-609.

McLean, J.H.; Darby-King, A.; Sullivan, R.M.; King, S.R. (1993) Serotonergic influence on olfactory learning in the neonate rat. Behav Neural Biol. 60:152-162.

Medina, L.; Puelles, L.; Smeets, W.J. (1994) Ontogenesis of catecholamines systems in the brain of the lizard Gallotia galloti, in: W.J.A.J. Smeets, A. Reiner (Eds.), Phylogeny and development of catecholamine systems in the CNS of vertebrates, pp: 361-377; The Cambridge University Press.

Meek, J. (1999) The paraventricular organ of mormyrid fish: uptake or release of intraventricular biogenic amines? Eur J Morphol. 37:107-111.

Meek, J.; Joosten, H.W. (1989) Distribution of serotonin in the brain of the mormyrid teleost *Gnathonemus petersii*. J Comp Neurol. 281:206-224.

Melnikova, V.I.; Ugrumov, M.V.; Proshlyakova, E.V.; Calas, A.; Thibault, J. (2001) Tyrosine hydroxylase expression in differentiating neurons of the rat arcuate nucleus: stimulatory influence of serotonin afferents. Neural Plast. 8:271-284.

Menegola, E.; Broccia, M.L.; Di Renzo, F.; Massa, V.; Giavini, E. (2004) Effects of excess and deprivation of serotonin in vitro neuronal differentiation. In Vitro Cell Dev Biol Anim. 40:52-56.

Meredith, G.E.; Smeets, W.J. (1987) Immunocytochemical analysis of the dopamine system in the forebrain and midbrain of *Raja radiata*: evidence for a substantia nigra and ventral tegmental area in cartilaginous fish. J Comp Neurol. 265:530-548.

Northcutt, R.G. (1990) Visual pathways in elasmobranchs: organization and phylogenetic implications. J Exp Zool Suppl.5:97-107.

Northcutt, R.G.; Reiner, A.; Karten, H.J. (1988) Immunohistochemical study of the telencephalon of the spiny dogfish, *Squalus acanthias*. J Comp Neurol. 277:250-267.

Obrietan, K.; Gao, X.B.; Van Den Pol, A.N. (2002) Excitatory actions of GABA increase BDNF expression via a MAPK-CREB-dependent mechanism-a positive feedback circuit in developing neurons. J Neurophysiol. 88:1005-1015.

Owen, A.D.; Bird, M.M. (1997) Role of glutamate in the regulation of the outgrowth and motility of neurites from mouse spinal cord neurons in culture. J Anat. 191:301-307.

Parent, A.; Northcutt, R.G. (1982) The monoamine-containing neurons in the brain of the garfish, *Lepisosteus osseus*. Brain Res Bull. 9:189-204.

Petrova, E.S.; Otelli, V.A. (2007) Serotonin is involved in the regulation of histogenetic processes in rat embryonic neocortex. Bull Exp Biol Med. 143:372-375.

Pflieger, J.F.; Clarac, F.; Vinay, L. (2002) Postural modifications and neuronal excitability changes induced by a short-term serotonin depletion during neonatal development in the rat. J Neurosci. 22:5108-5117.

Pickel, V.M.; Joh, T.H.; Chan, J.; Beaudet, A. (1984) Serotoninergic terminals: ultrastructure and synaptic interaction with catecholamine-containing neurons in the medial nuclei of the solitary tracts. J Comp Neurol. 225:291-301.

Pinganaud, G.; Clairambault, P. 1979 The visual system of the trout *Salmo irideus gibb*. A degeneration and radioautographic study. J Hirnforsch. 20:413-431.

Pombal, M.A; Ruiz, Y; Rodríguez-Alonso, M; de Arriba, M.C; Costas, V; Álvarez, R; Megías, M. (2005) Developmental changes of the GABA-immunoreactive fibers in the lamprey spinal cord. Brain Res Bull. 66:371-375.

Reiner, A.; Anderson, K.D. (1990) The patterns of neurotransmitter and neuropeptide co-occurrence among striatal projection neurons: conclusions based on recent findings. Brain R Rev. 15:251-265.

Repérant, J.; Miceli, D.; Rio, J.P.; Peyrichoux, J.; Pierre J.; Kirpitchnikova E. (1986) The anatomical organization of retinal projections in the shark *Scyliorhinus canicula* with special reference to the evolution of the selachian primary visual system. Brain Res. 396:227-248.

Rieke, G.K. (1981) Movement disorders and lesions of pigeon brain stem analogues of basal ganglia. Physiol Behav. 26:379-384.

Rodríguez-Moldes, I.; Anadón, R. (1987) Aminergic neurons in the hypothalamus of the dogfish, *Scyliorhinus canicula L.* (Elasmobranch). A histofluorescence study. J Hirnforsch.28:685-693.

Roberts, B.L; Maslam, S; Scholten, G; Smit, W. (1995) Dopaminergic and GABAergic cerebrospinal fluid-contacting neurons along the central canal of the spinal cord of the eel and trout. J Comp Neurol. 354:423-437.

Ruiz, Y; Pombal, M.A; Megías, M. (2004) Development of GABA-immunoreactive cells in the spinal cord of the sea lamprey, *P. marinus*. J Comp Neurol. 470:151-163.

Sas, E.; Maler, L.; Tinner, B. (1990) Catecholaminergic systems in the brain of a gymnotiform teleost fish: an immunohistochemical study. J Comp Neurol. 292:127-162.

Shim, S.H.; Kim, S.J.; Sugahara, K.; Sugita, S.; Tanaka, H. (2001) Immunohistochemical detection of tyrosine hydroxylase and concentrations of monoamines in the substantia nigra and hypothalamus of hereditary microphthalmic rats. Exp Anim. 50:445-449.

Sivam, S.P.; Krause, J.E.; Breese, G.R.; Hong, J.S. (1991) Dopamine-dependent postnatal development of enkephalin and tachykinin neurons of rat basal ganglia. J Neurochem. 56:1499-1508.

Smeets W.J.; Reiner, A. (1994) Catecholamines in the CNS of vertebrates: current concepts of evolution and functional significance, in: W.J.A.J. Smeets, A. Reiner (Eds.), Phylogeny and development of catecholamine systems in the CNS of vertebrates, pp: 463-478; The Cambridge University Press.

Smeets, W.J. (1981) Retinofugal pathways in two chondrichthyans, the shark *Scyliorhinus canicula* and the ray *Raja clavata*. J Comp Neurol. 195:1-11.

Sodhi, M.S.; Sanders-Bush, E. (2004) Serotonin and brain development. Int Rev Neurobiol. 59:111-174.

Spencer, G.E.; Klumperman, J.; Syed, N.I. (1998) Neurotransmitters and neurodevelopment. Role of dopamine in neurite outgrowth, target selection and specific synapse formation. Perspect Dev Neurobiol. 5:451-467.

Spencer, G.E.; Lukowiak, K.; Syed, N.I. (2000) Transmitter-receptor interactions between growth cones of identified *Lymnaea* neurons determine target cell selection in vitro. J Neurosci. 20:8077-8086.

Spoerri, P.E. (1988) Neurotrophic effects of GABA in cultures of embryonic chick brain and retina. Synapse 2:11-22.

Stuesse, S.L.; Cruce, W.L. (1992) Distribution of tyrosine hydroxylase, serotonin, and leu-enkephalin immunoreactive cells in the brainstem of a shark, *Squalus acanthias*. Brain Behav Evol. 39:77-92.

Stuesse, S.L.; Cruce, W.L.; Northcutt, R.G. (1991b) Serotoninergic and enkephalinergic cell groups in the reticular formation of the bat ray and two skates. Brain Behav Evol. 38:39-52.

Stuesse, S.L.; Cruce, W.L.; Northcutt, RG. (1991) Localization of serotonin, tyrosine hydroxylase, and leu-enkephalin immunoreactive cells in the brainstem of the horn shark, *Heterodontus francisci*. J Comp Neurol. 308:277-292.

Stuesse, SL.; Cruce, W.L. (1991) Immunohistochemical localization of serotoninergic, enkephalinergic, and catecholaminergic cells in the brainstem and diencephalon of a cartilaginous fish, *Hydrolagus colliei*. J Comp Neurol. 309:535-548.

Sueiro, C. (2003) Estudio inmunohistoquímico de los sistemas gabaérgicos del sistema nervioso central de peces elasmobranquios y su relación con sistemas catecolaminérgicos y peptidérgicos. Doctoral Thesis. University Santiago de Compostela. Spain.

Tillet, Y. (1994) Catecholaminergic neuronal systems in the diencephalon of mammals, in: W.J.A.J. Smeets, A. Reiner (Eds.), Phylogeny and development of catecholamine systems in the CNS of vertebrates, pp: 207-236; The Cambridge University Press, Cambridge.

Trudeau, V.L.; Sloley, B.D.; Peter, R.E. (1993) GABA stimulation of gonadotropin-II release in goldfish: involvement of GABAA receptor, dopamine, and sex steroid. A J Physiol. 265:348-355.

Ubink, R.; Tuinhof, R.; Roubos, E.W. (1998) Identification of suprachiasmatic melanotrope-inhibiting neurons in *Xenopus laevis*: confocal laser-scanning microscopy study. J Comp Neurol. 397:60-68.

van Kesteren, R.E.; Spencer, G.E. (2003) The role of neurotransmitters in neurite outgrowth and synapse formation. Rev Neurosci. 14:217-231.

Veselkin, N.P; Batueva, I.V. (1999) Inhibition in the lamprey spinal cord. Ross Fiziol Zh Im I M Sechenova. 85:743-750.

Vigh, B; Vigh-Teichmann, I. (1992) Cytochemistry of CSF-contacting neurons and pinealocytes. Prog Brain Res. 91:299-306.

Vitalis, T.; Cases, O.; Passemard, S.; Callebert, J.; Parnavelas, J.G. (2007) Embryonic depletion of serotonin affects cortical development. Eur J Neurosci. 26:331-344.

Vuillez, P.; Pérez, S.C.; Stoeckel, M.E. (1987) Colocalization of GABA and tyrosine hydroxylase immunoreactivities in the axons innervating the neurointermediate lobe of the rat pituitary: an ultrastructural immunogold study. Neurosci Lett. 79:53-58.

Wagner, S.; Castel, M.; Gainer, H.; Yarom, Y. (1997) GABA in the mammalian suprachiasmatic nucleus and its role in diurnal rhythmicity. Nature 387:598-603.

Wai, M.S; Lorke, D.E; Zhang, A; Kung, H.F; Yew, D.T. (2007) Study of the spinal cords of the sturgeon *Acipenser schrenckii*, gar *Lepisosteus oculatus*, and goldfish *Carassius auratus* by morphological, immunohistochemical, and biochemical approaches. Microsc Res Tech. 70:1079-1090.

Wilson, D.A.; Sullivan, R.M. (1995) The D2 antagonist spiperone mimics the effects of olfactory deprivation on mitral/tufted cell odor response patterns. J Neurosci. 15:5574-5581.

Wirtshafter, D.; Sheppard, A.C. (2001) Localization of GABA(B) receptors in midbrain monoamine containing neurons in the rat. Brain Res Bull. 56:1-5.

Wolff, J.R.; Joó, F.; Kása, P. (1993) Modulation by GABA of neuroplasticity in the central and peripheral nervous system. Neurochem Res. 18:453-461.

Wullimann, M.F.; Northcutt, R.G. (1988) Connections of the corpus cerebelli in the green sunfish and the common goldfish: a comparison of perciform and cypriniform teleosts. Brain Behav Evol. 32:293-316.

Wullimann, M.F.; Northcutt, R.G. (1990) Visual and electrosensory circuits of the diencephalon in mormyrids: an evolutionary perspective. J Comp Neurol. 297:537-552.

Yan, W.; Wilson, C.C.; Haring, J.H. (1997) Effects of neonatal serotonin depletion on the development of rat dentate granule cells. Dev Brain Res. 98:177-184.

Yao, W.D.; Rusch, J.; Poo, M.; Wu, C.F. (2000) Spontaneous acetylcholine secretion from developing growth cones of *Drosophila* central neurons in culture: effects of cAMP-pathway mutations. J Neurosci. 20:2626-2637.

Young, S.H.; Poo, M.M. (1983) Spontaneous release of transmitter from growth cones of embryonic neurones. Nature 305:634-637.

Zhou, F.C.; Sari, Y.; Zhang, J.K. (2000) Expression of serotonin transporter protein in developing rat brain. Dev Brain Res. 119:33-45.

ABBREVIATIONS

Cb	cerebellum
Cc	central canal
CSF-c	cerebrospinal fluid contacting cell
Dh	dorsal horn
Di	diencephalon
DLL	dorsolateral longitudinal fascicle
fbt	basal telencephalic fascicle
fr	retroflexus fascicle
H	hypophysis
Ha	habenula
hht	hypothalamic-hypopheseal tract
IS	isthmus
LC	locus coeruleus
Mes	mesencephalon
MLF	medial longitudinal fascicle
OT	optic tectum
P	pallium
Pc	posterior commissure
Pi	pineal organ
Po	preoptic area
Pr	posterior recess
Pret	pretectum
Pro	posterior recess organ
PTN	posterior tubercle nucleus
PVO	paraventricular organ
R	Rathke's pouch
r1-r8	rhombomeres
RaC	raphe centralis superior nucleus
RaDa	raphe dorsalis anterioris nucleus
RaL	raphe linearis nucleus
RaM	raphe magnus nucleus
RaO	raphe obscurus nucleus
RaP	raphe pallidus nucleus
Ret	tegmental reticular groups
Rh	rhombencephalon
RO	nucleus reticularis pontis oralis
Rpo	preoptic recess
Sc	subcoeruleus
SCN	suprachiasmatic nucleus
Si	infundibuli saccus
SOT	supraoptic tract
SN	substantia nigra
Sp	subpallium
Spc	spinal cord
SV	saccus vasculosus
Syn	synencephalon
Td	dorsal thalamus
TPC	posterior commissure tract
TPOC	postoptic commissure tract
Tv	ventral thalamus
Vh	ventral horn
VMC	visceromotor column
VSC	viscerosensorial column
rVTA	rostral ventral tegmental area
cVTA	caudal ventral tegmental area
IIIr	oculomotor nerve root
Vr	trigeminal nerve root

Figure 1. Schematic representations of sagittal sections of brains of dogfish embryos at S30 showing the distribution of cells (circles) and fibers (thin lines) immunoreactive to GAD (red in **a** and **d**), TH (black in **b** and **d**), 5-HT (green in **c** and **d**). The diencephalic-mesencephalic and mesencephalic-rhombencephalic boundaries are represented by broken lines. The location of the exit of some cranial nerves (IIIr,Vr), and the tentative location of rhombomeres (r1-r8) are also shown. Scale bars: μm (100 μm).

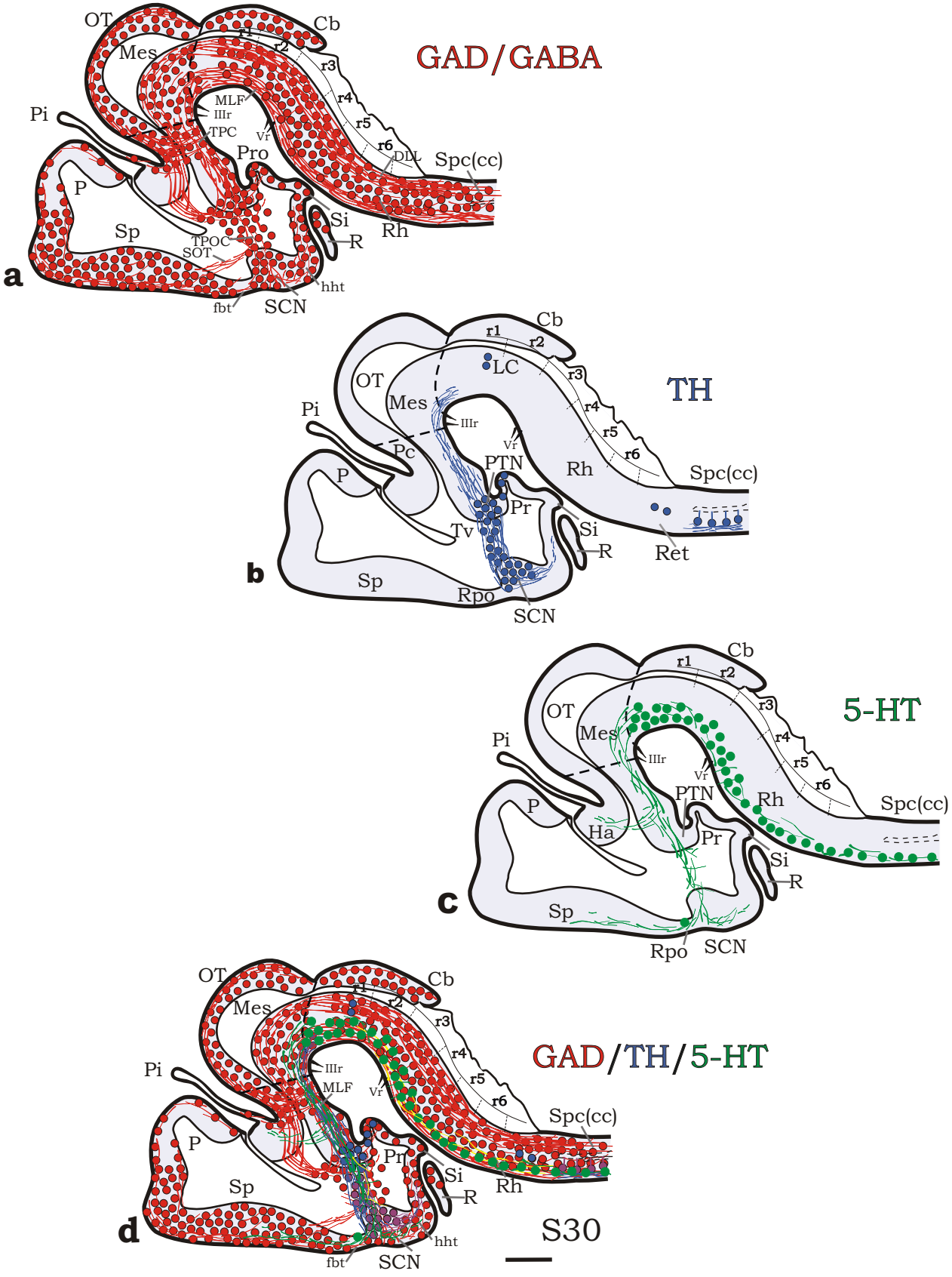
GAD/GABA
OT
Cb
Mes
r1
r2
r3
r4
r5
r6
MLF
IIIr
TPC
Vr
Pi
Pro
DLL
Spc(cc)
P
Si
Rh
Sp
TPOC
SOT
R
a
hht
fbt
SCN
TH
Cb
r1
r2
LC
OT
r3
Mes
r4
Pi
IIIr
r5
Vr
Pc
r6
PTN
Rh
Spc(cc)
P
Pr
Tv
Si
R
Ret
b
Sp
Rpo
SCN
5-HT
Cb
r1
r2
r3
OT
Mes
r4
Pi
IIIr
r5
Vr
r6
PTN
Rh
Spc(cc)
P
Ha
Pr
Si
R
c
Sp
Rpo
SCN
GAD/TH/5-HT
OT
Cb
Mes
r1
r2
r3
r4
Pi
IIIr
MLF
Vr
r5
r6
Spc(cc)
P
Pr
Si
Rh
Sp
R
d
hht
fbt
SCN
S30

Fig. 1

Figure 2. Sagittal (**A -H**) and transverse (**I**) sections throughout the brain (**A-H**) and spinal cord (**I**) of S30 embryos showing triple labeling with antibodies againt GAD, 5-HT and TH. **A.** Parasagittal section of the prosencephalon to show the co-distribution of GAD, 5-HT and TH immunoreactivity at the PTN (arrow). Numerous TH-ir cells were also seen at the suprachiasmatic nucleus, where they co-localize with GAD-ir cells and some 5-HT-ir ascending fibers (large arrow). Note the co-localization of some thin TH/GAD-ir fibers (arrows) that constituted the primordial hypothalamo-hypophyseal tract. **B.** Midsagittal section of the rostral prosencephalon to show TH-ir cells and GAD-ir and 5-HT-ir fibers in the PTN (arrowhead). Note the GAD-ir (arrow) and 5-HT-ir (thick arrow) fibers coursing through the basal prosencephalic tgmentum and dorsal hypothalamic walls. Also note some TH immunoreactivity in the suprachiasmatic nucleus populated by numerous GAD-ir cells and fibers (large arrow). **C**. Parasagittal section of the caudal prosencephalon to show the co-distribution of GAD, 5-HT and TH immunoreactivity at the PTN (arrowhead), as well as the GAD-/5-HT-ir fibers in the synencephalon (thick arrow). In the rhombencephalon, note some reticular formation 5-HT-ir cells (arrow) in the basal plate intermingled by the longitudinal GAD-ir fibers. **D**. Detail of the squared area in figure C to show the co-distribution of GAD, 5-HT and TH immunoreactivity at the PTN (arrowheads) but no co-localization. Note some GAD and TH immunoreactivity in some cells of the posterior recess organ (large arrow). **E.** Lateral sagittal section of the rostral prosencephalon to show co-distribution of GAD, 5-HT and TH immunoreactivity at the external walls of the PVO (arrowheads) and ventral thalamus (large arrow). **F**. Section of the caudal prosencephalon and rostral rhombencephalon to show co-distribution of GAD-ir, TH-ir (large arrow) and 5-HT-ir (thick arrow) fibers at the basal plate of the prosencephalic tegmentum, where GAD-ir and TH-ir fibers seemed to co-localize (large arrow). Note also the co-distribution of 5-HT-ir cells and longitudinal GAD-ir fibers in the basal plate (arrows); and GAD-/TH-ir cells (arrowhead) at the PTN. **G**. Section at the isthmic level to show GAD-ir cells (large arrows) at both alar and basal plate of the tegmentum, longitudinal TH-ir and 5-HT-ir fibers at the dorsal basal plate of the tegmentum, and also some 5-HT-ir cells (arrows) in the basal plate of the rostral rhombencephalon. Note that some longitudinal TH- and GAD-ir fibers seemed to co-localize (arrowheads). **H**. Midsagittal section at the caudal rhombencephalon and rostral spinal cord to show the co-distribution of the reticular formation 5-HT-ir cells (arrows) and GAD immunoreactivity (large arrow) at the basal plate, and also the co-localization of GAD-ir and TH-ir CSF-c cells (arrowheads) at the rostral spinal cord. **I**. Transverse section at the rostral spinal cord to show the co-distribution of TH-ir CSF-c cells (arrowhead), 5-HT-ir cells (arrow) and GAD-ir fibers (large arrow) ventrally to the central canal (star). Scale bars: 30µm (**D**, **I**); 60µm (**A-C**,**E-H**).

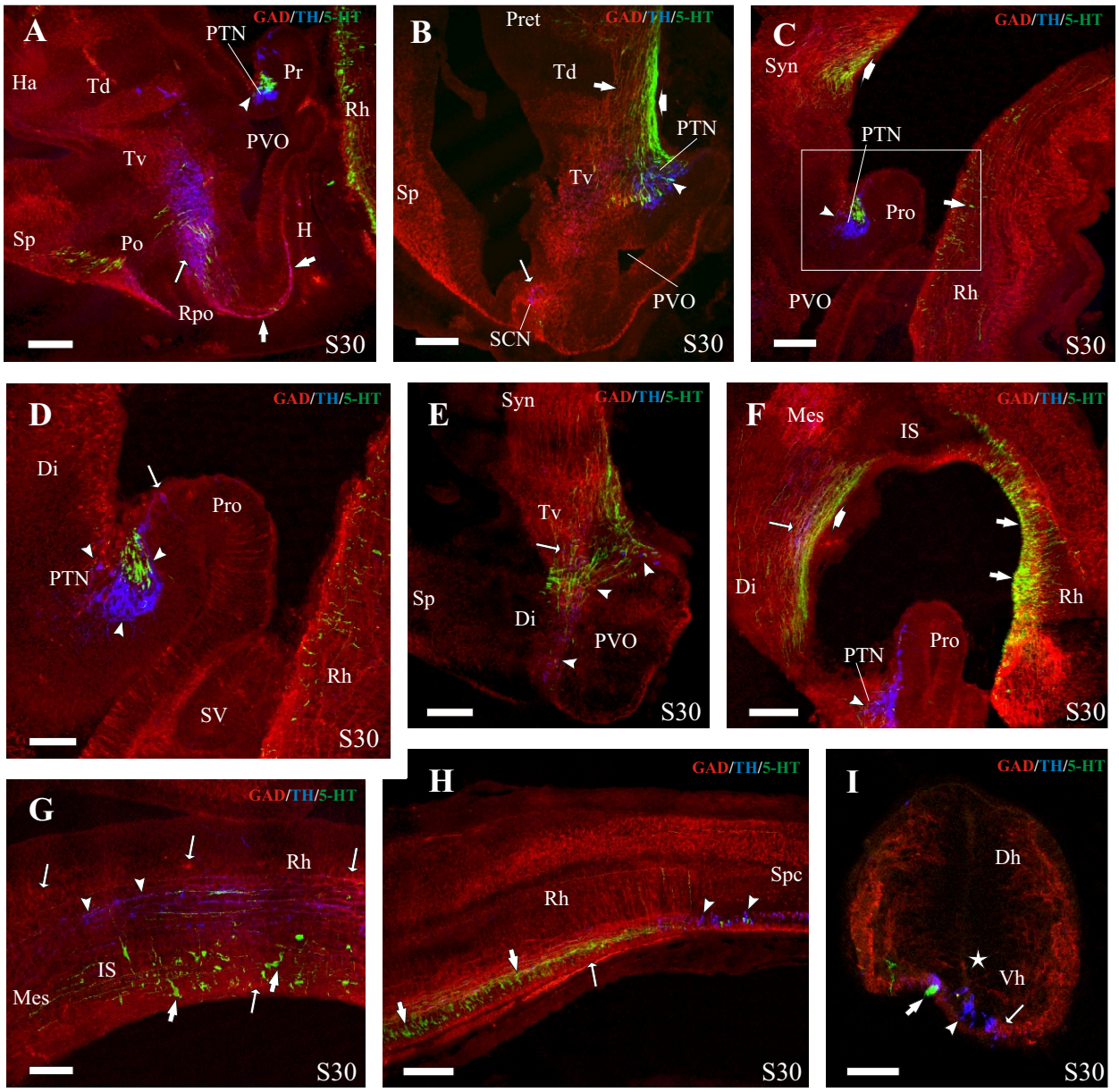
A
GAD/TH/5-HT
PTN
Pr
Ha
Td
Rh
PVO
Tv
Sp
Po
H
Rpo
S30
B
Pret
GAD/TH/5-HT
Td
PTN
Tv
Sp
PVO
SCN
S30
C
GAD/TH/5-HT
Syn
PTN
Pro
PVO
Rh
S30
D
GAD/TH/5-HT
Di
Pro
PTN
Rh
SV
S30
E
Syn
GAD/TH/5-HT
Tv
Sp
Di
PVO
S30
F
Mes
IS
GAD/TH/5-HT
Di
Rh
Pro
PTN
S30
G
GAD/TH/5-HT
Rh
IS
Mes
S30
H
GAD/TH/5-HT
Spc
Rh
S30
I
GAD/TH/5-HT
Dh
Vh
S30

Fig. 2

Figure 3. Sagittal (**A-N**) and transverse (**O,P**) sections through the brain (**A-N)** and spinal cord (**O-P**) of dogfish embryos at S31, showing double labeling cells and fibers immunoreactive to GAD (in red) and 5-HT (in green; **A-C,K,L**), to TH (in red) and 5-HT (in green; **D-J,M,N**), and also to TH (in red) and GAD (in green; **O,P**). A. Parasagittal section of the caudal telencephalon showing the co-distribution of GAD-ir cells and some ascending 5-HT-ir fibers (arrowheads) at the ventral intermediate zone. **B.** Parasagittal section of the rostral diencephalon showing co-distribution of fibers immunoreactive to 5-HT (arrows) and GAD coursing through the telencephalic fiber tract above the preoptic recess. **C.** Parasagittal section at the caudal diencephalon to show the ascending 5-HT-ir fibers (arrows) reaching the dorsal walls of the paraventricular organ. Note the abundant co-localization of fibers immunoreactive to GAD and 5-HT at the dorsal hypitalamic walls (arrowheads). **D** and **E.** Parasagittal section and detail (E) of the suprachiasmatic nucleus showing the massive 5-HT-ir innervation surrounding the TH-ir cells at this nucleus. Note also the same co-distribution pattern at the preoptic area in figure D. **F.** Panoramic midsagittal section showing the conspicuous ascending 5-HT-ir fibers that coursed from the rhombencephalic 5-HT-ir cell groups towards the basal telencephalon (arrowheads), innervating the TH-ir cells of the ventral thalamus and posterior tubercle. **G.** Sagittal detail of the caudal hypothalamus showing 5-HT-ir fiber innervation surrounding the TH-ir cells of the posterior tubercle. Note the co-distribution of both markers in some longitudinal fibers at the external walls of the posterior recess organ (arrowheads). **H.** Parasagittal detail of the basal hypothalamus showing some 5-HT-ir fibers (arrowhead) intermingled with the TH-ir fibers of the hypothalamic-hypophiseal tract (arrows). **I.** Sagittal section at the isthmic level showing some 5-HT-ir fiber innervation at the TH-ir cell groups of the ventral tegmental area. **J.** Sagittal section at the rostral rhombencephalon showing co-distribution of TH- and 5-HT-ir structures at the locus coeruleus and subcoeruleus. **K** and **L.** Midsagittal sections at the rostral (K) and caudal (L) rhombencephalon showing co-localization of longitudinal fibers immunorreactive to GAD and 5-HT at the ventral tegmental region (arrows), intermingled with some 5-HT-ir cells of the reticular formation. **M** and **N.** Panoramic and detail (N) sagittal sections at the viscerosensory column showing 5-HT-ir fibers and terminals grouped around the TH-ir perykaria (arrowheads). O. Transverse section of the rostral spinal cord showing co-localization of GAD and TH in the CSF-c cells (arrow) of the basal plate. (The central canal is indicated by the star). **P.** Detail of the spinal cord floor plate to show the co-localization of GAD and TH at some CSF-c cells (arrow) located ventral to the central canal (star) and at some longitudinal fibers (arrowhead) located ventrolaterally to the floor plate. Scale bars: 60μm (**A-D,I-M O**); 100μm (**F**); 30μm (**E,G**); 20μm (**N**,**P**).

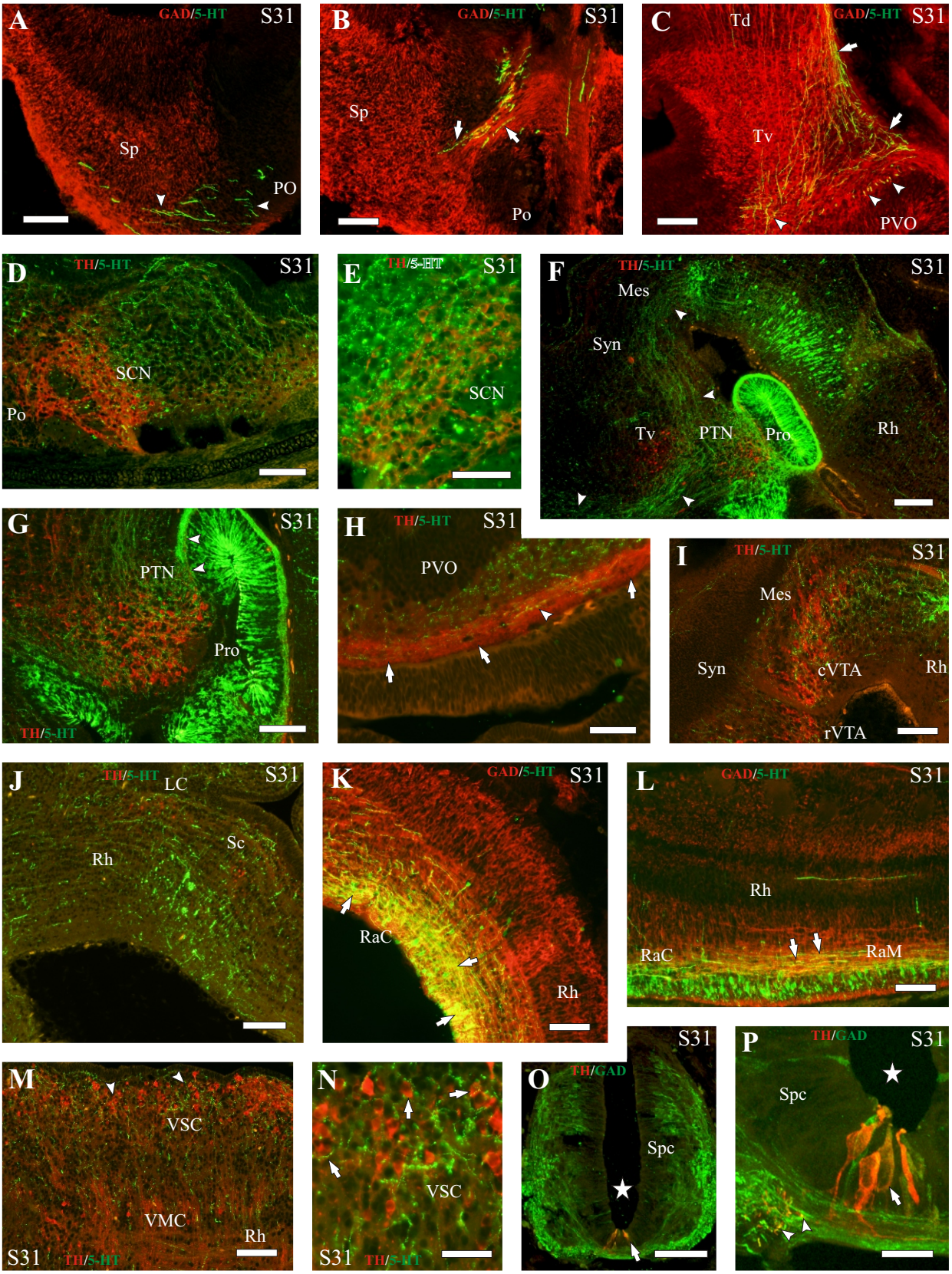
A
GAD/5-HT
S31
Sp
PO
B
GAD/5-HT
S31
Sp
Po
C
Td
GAD/5-HT
S31
Tv
PVO
D
TH/5-HT
S31
SCN
Po
E
TH/5-HT
S31
SCN
F
TH/5-HT
S31
Mes
Syn
Tv
PTN
Pro
Rh
G
S31
PTN
Pro
TH/5-HT
H
TH/5-HT
S31
PVO
I
TH/5-HT
S31
Mes
Syn
cVTA
Rh
rVTA
J
TH/5-HT
LC
S31
Sc
Rh
K
GAD/5-HT
S31
RaC
Rh
L
GAD/5-HT
S31
Rh
RaC
RaM
M
VSC
VMC
Rh
S31
TH/5-HT
N
VSC
S31
TH/5-HT
O
S31
TH/GAD
Spc
P
TH/GAD
S31
Spc

Fig. 3

Figure 4. Sagittal (**A-C,G,H,L**) and transverse (**D-F,I-K,M**) sections through the brain of dogfish juvenile, showing double immunofluorescence of cells and fibers TH-ir (in red) and 5-HT-ir (in green). **A.** Parasaggittal section of the caudal prosencephalon. The arrowheads indicate the co-localization of 5-HT-ir fibers and TH-ir structures at the main diencephalic TH-ir cell groups. **B.** Parasagittal section just caudal to the telencephalon showing the rich 5-HT-ir innervation surrounding the TH-ir cells of the several rostralmost diencephalic groups (arrowheads) and the profuse longitudinal 5-HT-ir fibers (arrows) that form the main ascending telencephalic pathway. **C.** Detail section of the caudal hypothalamus showing 5-HT-ir fibers and terminals surrounding TH-ir somata (arrows) at the posterior tubercle. Note also the co-localization of some TH- and 5-HT-ir fibers (arrowheads) at the external walls of the posterior recess organ. **D.** Transverse section of the paraventricular organ to show the co-localization of some transverse TH- and 5-HT-ir fibers that course through the external walls. Note that the few TH-ir cells observed in the paraventricular walls were intermingled among the numerous 5-HT-ir, but showing no co-localization. **E.** Detail section of the paraventricular walls showing some 5-HT-ir fiber terminals that contact the TH-ir pericaryon at the external walls. Note also the long TH-ir CSF-c cell process (arrowhead) that crosses transversally the 5-HT-ir cell layered wall to contact the ventricle. **F.** Transverse section at the caudal prosencephalon showing TH-ir cells of the substantia nigra and ventral tegmental groups densely innervated by 5-HT-ir fibers and terminals (arrows). **G.** Detail of the sagittal section at the isthmic region showing a rich 5-HT-ir innervation at the TH-ir cells (arrows) of the ventral tegmental area. Note the moderate TH-/5-HT-ir fiber density that surrounded the 5-HT-ir cells at the rostral rhombencephalon (arrowhead). Broken line indicates the isthmic boundary. **H.** Sagittal section of the rostral rhombencephalon showing the co-distribution of TH- and 5-HT-ir cells at the subcoeruleus nucleus. Note also the rich density of TH- and 5-HT-ir cells at the surrounding areas. **I** and **J.** Details of a transverse section at the rostral rhombencephalic level to show numerous immunoreactive fibers to TH and 5-HT at the central grey area (arrows in fig. I) and lateral to the dorsal midline intermingled with the 5-HT-ir cells of the subcoeruleus group (arrowheads in figs. I and J). **K.** Transveres section at caudal rhombencephalic levels showing co-distribution of the reticular TH-ir cells (arrowhead) located laterally and the 5-HT-ir cells of the reticular formation (arrows) at the midline and ventrolaterally regions of the tegmentum. **L.** Sagittal section through the caudal rhombencephalon showing a dense arborization of 5-HT-ir fibers and terminals over the TH-ir cells of the viscerosensory column (arrows). Note the conspicuous vertical and longitudinal TH-ir tracts (arrowheads) that coursed through the tegmentum. **M.** Transverse section showing co-distribution of reticular TH-ir and the reticular formation 5-HT-ir cells at the obex level. Note some TH-ir fibers surrounding the 5-HT-ir cells (arrow) at the ventral midline. Scale bars: 100µm (**A)**; 60µm (**B,F,G,I,L**); 30µm (**C-E,H,J,K,M**).

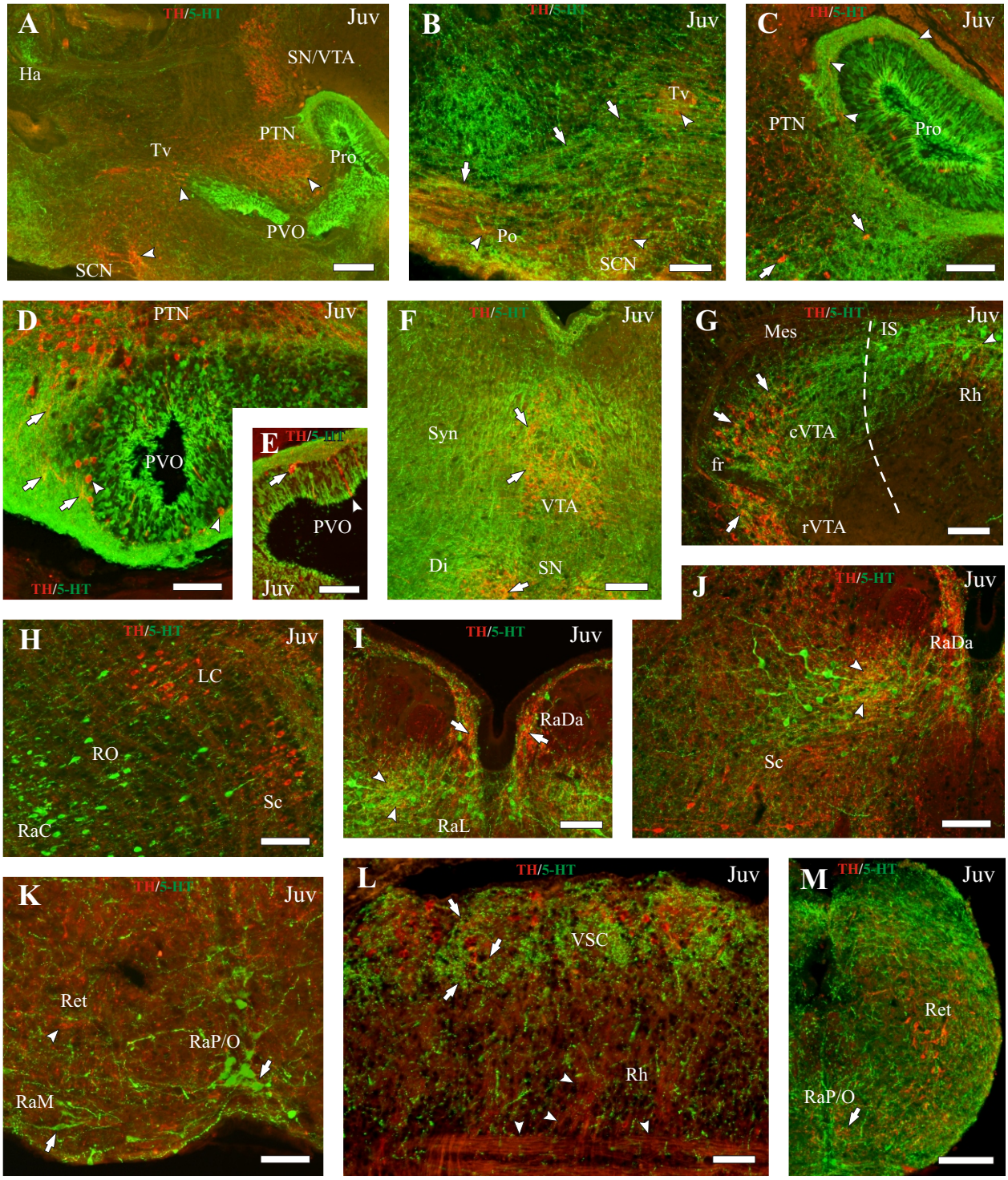
A
TH/5-HT
Juv
Ha
SN/VTA
PTN
Tv
Pro
PVO
SCN
B
TH/5-HT
Juv
Tv
Po
SCN
C
TH/5-HT
Juv
PTN
Pro
D
PTN
Juv
PVO
TH/5-HT
E
TH/5-HT
PVO
Juv
F
TH/5-HT
Juv
Syn
VTA
Di
SN
G
TH/5-HT
Juv
Mes
IS
Rh
cVTA
fr
rVTA
H
TH/5-HT
Juv
LC
RO
Sc
RaC
I
TH/5-HT
Juv
RaDa
RaL
J
TH/5-HT
Juv
RaDa
Sc
K
TH/5-HT
Juv
Ret
RaP/O
RaM
L
TH/5-HT
Juv
VSC
Rh
M
TH/5-HT
Juv
Ret
RaP/O

Fig. 4

RESUMEN Y CONCLUSIONES

RESUMEN Y CONCLUSIONES

Este trabajo se centra en el sistema nervioso central de peces cartilaginosos (condríctios) porque a pesar de la importancia que tiene este grupo de vertebrados desde el punto de vista de la evolución de los gnatóstomos, se le ha prestado muy poca atención en comparación con los peces óseos. Tradicionalmente se ha considerado a los teleósteos, representantes de los peces óseos modernos y de todos los peces con mandíbulas (gnatóstomos). El presente estudio creemos que contribuye a demostrar que los peces cartilaginosos presentan características neuroanatómicas específicas y que el análisis de las diferencias (y también de las similitudes) entre los peces óseos y cartilaginosos contribuye al conocimiento de la evolución del sistema nervioso central de vertebrados. Como objeto de este estudio hemos elegido una especie de elasmobranquio, la pintarroja o melgacho (*Scyliorhinus canicula*) por ser una especie muy accesible, ya que se encuentra a lo largo de toda la costa de Europa y es una de las pocas especies de elasmobranquios de la que se puede obtener cualquier estadio de desarrollo en cualquier época del año. Además, nuestro grupo de investigación lleva varios años estudiando distintos aspectos de la anatomía del sistema nervioso de esta especie, siendo considerada un modelo representativo del grupo de elasmobranquios.

En este trabajo, estudiamos la distribución en el sistema nervioso central de la pintarroja de los sistemas gabaérgico y monoaminérgico (catecolaminérgico y serotoninérgico) durante los sucesivos estadios de desarrollo. En general los estudios comparativos acerca del sistema nervioso central entre vertebrados son objeto de enorme interés por posibles implicaciones en diversas afecciones neurodegenerativas, vasculares o tras algún tipo de trauma. Pero además, la caracterización del origen y distribución de los grupos neuronales a lo largo del desarrollo embrionario y etapas maduras supone una aportación básica y fundamental para un completo entendimiento de la evolución del sistema nervioso de vertebrados. En este trabajo hemos estudiado la organización de los sistemas gabaérgico, catecolaminérgico y serotoninérgico desde el período embrionario a la etapa adulta así como su relación con el patrón segmentario.

Para ello, hemos utilizado técnicas inmunohistoquímicas que detectan el marcaje de anticuerpos específicos para el ácido γ-amino butírico (GABA) y su enzima de síntesis la glutamato descarboxilasa (GAD), la tirosina hidroxilasa (TH, el enzima limitante de la síntesis de dopamina) y la serotonina (5-HT). Además, para estudiar la relación entre estos tres sistemas hemos utilizado técnicas inmunofluorescentes que identifican la presencia de los distintos anticuerpos en una misma sección histológica gracias al uso simultáneo de varios marcadores fluorescentes. Todos los experimentos cumplen la normativa europea sobre experimentación animal.

Esta memoria se divide en cuatro capítulos, de los cuales los tres primeros se refieren al estudio de los sistemas gabaérgico, catecolaminérgico y serotoninérgico respectivamente, durante el desarrollo embrionario y etapa juvenil del SNC de pintarroja, mientras que el cuarto capítulo constituye un estudio comparado de la relación entre estos tres sistemas.

CAPÍTULO 1

Desarrollo del sistema gabaérgico en el sistema nervioso central de pintarroja

Este capítulo describe el desarrollo del sistema gabaérgico en el cerebro y médula espinal de pintarroja (*Scyliorhinus canicula*) desde estadios tempranos de desarrollo (estadio 22) hasta la etapa juvenil, utilizando anticuerpos contra el ácido γ-amino butírico (GABA) y su enzima de síntesis, el glutamato descarboxilasa (GAD). Hemos observado la presencia de células gabaérgicas en estadios muy tempranos de desarrollo (estadio 22), al igual que ha sido observado en mamíferos, reforzando la idea del papel de GABA como factor neurotrófico o como neurotransmisor excitatorio, antes de desempeñar su función inhibidora característica. Además, el desarrollo del sistema gabaérgico en pintarroja también se caracteriza por procesos de migración radial en gran parte del sistema nervioso central y migración tangencial en algunas regiones específicas (células gabaérgicas subpaliales hacia el palio; a partir del estadio 28) originando las diferentes capas encefálicas, similar a los procesos de migración radial y tangencial descritos en mamíferos; por la aparición temprana de las principales vías gabaérgicas a lo largo del eje longitudinal constituyendo el armazón básico de la

inervación del sistema nervioso central; y por la distribución segmentaria de las poblaciones gabaérgicas que demuestran un claro patrón neuromérico.

Las primeras poblaciones gabaérgicas en aparecer son las del área postóptica, tegmento sinencefálico (primordio del núcleo del fascículo longitudinal medial), rombencéfalo y médula espinal rostral (estadio 22). Células gabaérgicas aparecen temprano en el telencéfalo ventral (subpalio), área tegmental ventral y comisura posterior (estadio 23). En el estadio 24, se observan células gabaérgicas en el hipotálamo y tálamo ventral, mientras que en el estadio 25 aparecen en el techo óptico. Posteriormente, en el estadio 26, se observan células gabaergicas en el área preóptica, saco vasculoso, cerebelo y médula espinal. En esta última región las células gabaérgicas que se observan contactan con el líquido cefalorraquídeo (LCR-c). Además, en el estadio 27 aparecen células gabaérgicas en el órgano del receso posterior, tubérculo posterior, habénula y rombencéfalo (columna viscerosensorial). Las poblaciones más tardías en aparecer han sido observadas en el telencéfalo, tanto en el palio (estadio 28), como en el órgano pineal (estadio 30) y en el bulbo olfatorio (estadio 32). Algunas de estas poblaciones de células gabaérgicas no se observan en fases juveniles (tálamo ventral, area tegmental ventral y comisura posterior/pretecho) o en adultos (área preóptica, área postóptica, órgano del receso posterior, tubérculo posterior y techo óptico), presentando por ello una expresión transitoria.

En cuanto a la formación de los principales tractos de fibras gabaérgicas, hemos observado que en pintarroja el más temprano se forma a partir de células del primordio del núcleo del fascículo longitudinal medial (estadio 22) para formar el fascículo longitudinal medial (FLM) que recorre toda la placa basal de los tegmentos prosencefálico mesencefálico y rombencefálico, y cuya densidad de fibras se incrementa notablemente desde el estadio 23 al estadio 31. El FLM se continua rostralmente con el tracto de la comisura postóptica (TPOC; estadio 25) y se cruza con tres tractos transversales que cursan a nivel rostral del ístmo (estadio 24), en la comisura posterior/pretecho (TPC; estadio 24) y en la zona límitans intratalámica (DVDT; estadio 26). A lo largo del telencéfalo y del diencéfalo se observaron dos tractos longitudinales, cursando ventralmente (fascículo telencefálico basal; estadio 26) y dorsalmente (tracto supraóptico; estadio 30) a las paredes del receso preóptico. Caudalmente, en la placa alar del tegmento rombencefálico, aparece a partir del estadio 26 un tracto longitudinal de fibras gabaérgicas (fascículo longitudinal dorsolateral DLL; estadio 26) paralelo al

FLM y que inerva todo el tegmento dorsal. Estos grupos de tractos gabaérgicos que aparecen en etapas tempranas e intermedias del desarrollo, constituyen las principales vías de fibras sobre las que se desarrolla la inervación del sistema nervioso central maduro.

En general, el orden espacio-temporal de aparición de las diferentes poblaciones gabaérgicas en pintarroja es similar al descrito en otros grupos de vertebrados, indicando la importancia del GABA en la maduración temprana de las regiones encefálicas durante el desarrollo, así como un elevado grado de conservación del patrón de expresión de GABA entre el sistema nervioso central de vertebrados.

CAPÍTULO 2

Desarrollo del sistema catecolaminérgico en el sistema nervioso central de pintarroja

En este capítulo se describe el desarrollo del sistema catecolaminérgico en el sistema nervioso central de la pintarroja (*Scyliorhinus canicula*) mediante técnicas inmunohistoquímicas utilizando anticuerpos contra tirosina hidroxilasa (TH), desde el período embrionario a la etapa adulta. Las primeras células catecolaminérgicas (TH-ir) fueron observadas a partir del estadio 26 en el diencéfalo (primordio del tubérculo posterior, receso posterior y núcleo supraquiasmático) y en la médula espinal rostral (células TH-ir que contactan con el líquido cefalorraquídeo). Posteriormente, más células TH-ir se diferencian en el diencéfalo (tálamo ventral, estadio 28; órgano del receso posterior, estadio 30; área preóptica, estadio 31; órgano paraventricular y saco vasculoso, estadio 33), sinencéfalo/mesencéfalo (area tegmental ventral/substancia negra, estadio 31), rombencéfalo (locus coeruleus y formación reticular, estadio 30; subcoeruleus y columna viscerosensorial/motora, estadio 31), telencéfalo (palio, estadio 31; bulbo olfatório, estadio 32; y subpalio, estadio 33).

Las principales rutas ascendentes y descendentes de fibras catecolaminérgicas se originan a partir de la población de células TH-ir del tubérculo posterior y de sus poblaciones adyacentes (estadio 31). La densidad de fibras TH-ir aumenta progresivamente durante la última etapa del desarrollo, aunque la distribución observada en el estadio 32 es similar a la de juveniles y adultos, por lo que representa el estado de organización “madura” en el sistema nervioso central de pintarroja, excepto

en el telencéfalo en el cual la inervación ascendente no se observa hasta la etapa juvenil. En estos estadios tardíos de desarrollo, se observaron las primeras fibras hipotálamo-hipofisarias TH-ir cursando hacia el lóbulo neurointermedio de la hipófisis, mientras que la inervación catecolaminérgica del subpalio caudal se observa en juveniles por medio de fibras ascendentes longitudinales TH-ir de origen diencefálico. La secuencia de aparición espacio-temporal de células catecolaminérgicas en el encéfalo y en la médula espinal de pintarroja es similar al descrito en otros grupos de vertebrados, principalmente en mamíferos, aunque se han observado algunas variaciones entre anamniotas como la presencia, dependiendo del grupo, de poblaciones de células TH-ir en la región de la gris central, area tegmental ventral/substancia negra, saco vasculoso y palio, que están ausentes en el sistema nervioso central de peces óseos. Nuestros resultados también indican que las poblaciones de células catecolaminérgicas observadas durante el desarrollo embrionario de pintarroja presentan una organización segmentaria. Todo ello aporta conocimiento fundamental para caracterizar y comparar la evolución temprana del sistema catecolaminérgico entre elasmobranquios y tetrápodos, así como demuestra su elevado grado de conservación filogenética.

CAPÍTULO 3

Desarrollo del sistema serotoninérgico en el sistema nervioso central de pintarroja

En este capítulo pretendemos aportar conocimiento sobre el desarrollo evolutivo del sistema serotoninérgico en vertebrados mediante el estudio inmunohistoquímico del origen y la organización espacio-temporal de las poblaciones celulares y tractos de fibras serotoninérgicas en pintarroja, *Scyliorhinus canicula*. Hemos observado que el orden de aparición de las poblaciones de células inmunorreactivas a serotonina (5-HT-ir) del rombencéfalo y médula espinal (primero se originan los grupos rombencefálicos superiores y después los inferiores y los de la médula espinal) coincide con el orden descrito en otros vertebrados, aunque existen varias diferencias dentro del grupo de peces relacionadas con la formación de las poblaciones serotoninérgicas del prosencéfalo. En pintarroja, las primeras células serotoninérgicas fueron observadas a partir del estadio 26 en el rombencéfalo rostral (región ístmica), mientras que en los siguientes estadios las células 5-HT-ir aparecieron

en la médula espinal rostral (estadio 28) y en el resto del tegmento rombencefálico (estadio 29). Las últimas poblaciones serotoninérgicas en aparecer se localizan en el hipotálamo (estadio 31) y en el área preóptica (estadio 33) durante las etapas tardías del desarrollo. La organización "madura" de las poblaciones serotoninérgicas, que se caracteriza por la presencia de numerosas células 5-HT-ir en el hipotálamo (órgano paraventricular y órgano del receso posterior) y rombencéfalo (rafe superior e inferior) y algunas células 5-HT-ir en el área preóptica y médula espinal, se establece en los últimos estadios del desarrollo embrionario (estadio 33). También hemos observado que algunas células 5-HT-ir de los primeros grupos rafeales presentan una migración mediolateral, originando los distintos grupos serotoninérgicos de la formación reticular, siguiendo estos grupos un patrón segmentario en su organización. La presencia transitoria de células 5-HT-ir ha sido observada en el órgano pineal (estadio 31), en la región pretectal (estadio 32) y en la habénula (estadio 34), mientras que células 5-HT-ir que contactan con el líquido cefalorraquídeo se observaron en el área preóptica, en el órgano paraventricular, en el órgano del receso posterior y en el núcleo del rafe dorsal anterior.

En este estudio también se demuestra la existencia de dos fases (crecimiento y elongación de las principales rutas axónicas, y la posterior arborización de estas fibras, inervando masivamente ciertas regiones encefálicas) durante el desarrollo de la inervación serotoninérgica, y que son notablemente similares a las fases descritas en mamíferos. Las primeras fibras serotoninérgicas fueron observadas en el estadio 26, mientras que las principales rutas serotoninérgicas ascendentes y descendentes son reconocidas a partir del estadio 31. La organización de fibras serotoninérgicas desde el estadio 33 en adelante es similar a la observada en juveniles y adultos, caracterizada por una densa inervación serotoninérgica en la región hipotalámica y en el tegmento rombencefálico, moderada inervación serotoninérgica en los hemisferios telencefálicos y área preóptica, y escasa inervación serotoninérgica en el bulbo olfatorio, techo óptico y cerebelo.

El patrón de desarrollo de las células 5-HT-ir, así como de las principales rutas de fibras serotoninérgicas en pintarroja, son muy similares a lo observado en otros grupos de vertebrados, lo que indica un alto grado de conservación del sistema serotoninérgico central a lo largo de la filogenia de vertebrados y pone de manifiesto la importancia de los elasmobranquios para un mayor conocimiento de la evolución de este sistema.

CAPÍTULO 4

Co-distribución de los sistemas gabaérgico, catecolaminérgico y serotoninérgico en el sistema nervioso central de pintarroja

En este capítulo hemos tratado de reflejar la relación existente entre la organización de los tres sistemas de neurotransmisores estudiados (gabaérgico, catecolaminérgico y serotoninérgico) en el desarrollo y maduración del sistema nervioso central de pintarroja. En este estudio se han utilizado técnicas de doble y triple inmunofluorescencia en embriones de los estadios 30, 31 y en ejemplares juveniles, para caracterizar la distribución en simultáneo de los tres neuromarcadores estudiados (GAD, TH y 5-HT). Nuestros resultados demuestran que dichos neuromarcadores aparecen conjuntamente en ciertas regiones del sistema nervioso central, siendo esta co-distribución más evidente en el bulbo olfatorio, área preóptica, área postóptica, órgano paraventricular, núcleo del tubérculo posterior, área tegmental ventral, tegmento rombencefálico, columna viscerosensorial y médula espinal. Además hemos observado la co-expresión de TH y GAD en somas de neuronas del área preóptica, área postóptica, tálamo ventral y en células que contactan con el líquido cefalorraquídeo de la médula espinal y en fibras del tracto hipotálamo-hipofisario; de TH y 5-HT en fibras del órgano paraventricular y de GAD y 5-HT en las fibras longitudinales del tegmento rombencefálico.

Los resultados obtenidos indican que, aunque existen diferencias en la aparición espacio-temporal entre los tres sistemas estudiados, estos neurotransmisores clásicos están implicados en la morfogénesis del sistema nervioso central de la pintarroja, quizás jugando algún papel en el control en procesos como la proliferación, migración y diferenciación celular.

CONCLUSIONES

Del análisis detallado de los resultados de este estudio sobre el desarrollo de los sistemas gabaérgico, catecolaminérgico y serotoninérgico en el sistema nervioso central de pintarroja extraemos las siguientes conclusiones:

1. La presencia de células gabaérgicas desde estadios muy tempranos de desarrollo y antes del inicio de la sinaptogénesis, sostiene la idea de que el GABA pueda actuar como factor neurotrófico o neurotransmisor excitatorio antes de desempeñar su función inhibidora.

2. El orden de aparición de las poblaciones gabaérgicas en el sistema nervioso central de pintarroja es similar a lo observado en otros grupos de vertebrados, aunque existen diferencias relacionadas con la formación de las poblaciones gabaérgicas del tálamo ventral y techo óptico. La organización madura, caracterizada por un mayor número de somas en el telencéfalo y en el cerebelo, y en menor cantidad en el hipotálamo, rombencéfalo y médula espinal, se alcanza en estadios tardíos de desarrollo (S32).

3. Nuestra observación de neuronas gabaérgicas subpaliales migrando tangencialmente para colonizar el palio es la primera evidencia de que este proceso, que se creía una propiedad emergente en mamíferos, tiene lugar también en peces, lo que indica que las migraciones tangenciales de larga distancia para la formación del cerebro anterior o prosencéfalo aparecieron muy temprano en la evolución .

4. En las etapas tempranas de desarrollo tiene lugar la formación de la mayoría de las poblaciones celulares gabaérgicas, las cuales se originan mayoritariamente por procesos de migración radial que dan lugar a las diferentes capas del encéfalo y médula espinal de pintarroja.

5. Los principales tractos de fibras gabaérgicas aparecen en las etapas tempranas e intermedias del desarrollo embrionario, constituyendo el armazón básico sobre el que se desarrolla la inervación del sistema nervioso central de pintarroja.

6. La secuencia de aparición espacio-temporal de células catecolaminérgicas en el sistema nervioso central de pintarroja es básicamente similar a la descrita en otros grupos de vertebrados, principalmente en mamíferos, pero difiere de la de peces óseos y de ciclóstomos en cuanto a la presencia de células TH-ir en la gris central, área tegmental ventral/sustancia negra, saco vasculoso y telencéfalo dorsal. Esto indica la

inexactitud de las generalizaciones sobre la organización y desarrollo del encéfalo de peces basadas en resultados obtenidos a partir de un solo grupo.

7. Las principales rutas ascendentes y descendentes de fibras catecolaminérgicas se originan en estadios intermedios y tardíos de desarrollo a partir de las poblaciones diencefálicas, siendo determinantes para el desarrollo y maduración de la inervación catecolaminérgica en elasmobranquios.

8. El orden de aparición de las poblaciones 5-HT-ir así como de las principales rutas de fibras serotoninérgicas en pintarroja es similar a lo observado en otros grupos de vertebrados, aunque existen diferencias relacionadas con la formación de las poblaciones serotoninérgicas del prosencéfalo.

9. La comparación del desarrollo de los sistemas gabaérgico, catecolaminérgico y serotoninérgico muestra que el sistema gabaérgico tiene una aparición más temprana que los demás (estadio 22), siendo el sistema serotoninérgico el más tardío en madurar. Este resultado es similar a lo encontrado en la mayoría de vertebrados, lo que sugiere que el patrón de desarrollo de estos sistemas neuronales centrales representa una característica altamente conservada a lo largo de la evolución de vertebrados.

10. Los tres sistemas estudiados se distribuyen espacialmente durante el desarrollo embrionario siguiendo un patrón segmentario similar a lo observado en otros vertebrados. Así, las subdivisiones telencefálicas (palio y subpalio) se caracterizan por las diferencias en la organización del sistema gabaérgico, las diencefálicas, particularmente los prosómeros 1 a 3, por la organización de los sistemas gabaérgico y catecolaminérgico, mientras que las delimitaciones del istmo y de los diferentes rombómeros se relacionan estrechamente con la organización segmentaria de los tres sistemas.

11. Analizando simultáneamente los tres sistemas de neurotransmisores, hemos observado que estos aparecen mayoritariamente en las mismas regiones del sistema nervioso central de pintarroja, siendo esta co-distribución más evidente en el bulbo olfatorio, regiones prosencefálicas basales, tegmento mesencefálico y rombencefálico, columna viscerosensorial y médula espinal. Además, se ha observado co-localización de estos marcadores en algunas poblaciones neuronales y en determinados tractos de fibras. Estos resultados demuestran que dichos neurotransmisores clásicos están implicados conjuntamente en los procesos básicos del desarrollo del sistema nervioso central de pintarroja de forma similar a lo descrito en otros grupos de vertebrados.